

PDF hosted at the Radboud Repository of the Radboud University Nijmegen

The following full text is a publisher's version.

For additional information about this publication click this link.

<http://hdl.handle.net/2066/18735>

Please be advised that this information was generated on 2017-12-05 and may be subject to change.

**Characterization of the molecular environment
of the protein tyrosine phosphatase PTP-BL**

Characterization of the molecular environment of the protein tyrosine phosphatase PTP-BL

Een wetenschappelijke proeve op het gebied van
de Medische Wetenschappen

Proefschrift

ter verkrijging van de graad van doctor
aan de Katholiek Universiteit Nijmegen,
volgens besluit van het College van Decanen
in het openbaar te verdedigen op
woensdag 26 mei 1999
des namiddags om 1.30 uur precies

door

Edwin Pieter Johan Gerard Cuppen

geboren op 11 augustus 1970
te Boxmeer

Promotor: Prof. Dr. B. Wieringa

Co-promoter: Dr. W.J.A.J. Hendriks

Manuscriptcommissie: Prof. Dr. C.G. Figdor (UT)
Prof. Dr. C. van Os
Dr. J. den Hertog, Hubrecht Laboratorium, Utrecht

The studies described in this thesis were performed at the Department of Cell Biology of the Faculty of Medical Sciences, University of Nijmegen. This work was supported by a grant from the University of Nijmegen (KUN 100.099402)

Cuppen, Edwin

Characterization of the molecular environment of the protein tyrosine phosphatase PTP-BL.

ISBN 90-9012627-9

Cover: False color image of a large scale mating assay used to detect two-hybrid interactions in yeast.

Voor Ilze

Contents

	page
Chapter 1 General introduction	9
Chapter 2 A FERM domain governs apical, villi-like, confinement of PTP-BL in epithelial cells	27
Chapter 3 No evidence for involvement of mouse protein tyrosine phosphatase-BAS-like/Fas-associated phosphatase-1 in Fas-mediated apoptosis	49
Chapter 4 PDZ motifs in PTP-BL and RIL bind to internal protein segments in the LIM domain protein RIL	65
Chapter 5 Zyxin-related protein-1 (ZRP-1) interacts with PDZ motifs in the adaptor protein RIL and the protein tyrosine phosphatase PTP-BL	91
Chapter 6 Identification and molecular characterization of BP75, a novel bromodomain-containing protein	115
Chapter 7 The mouse orthologue of the <i>Drosophila</i> tumor suppressor and Rho-kinase homologue Warts interacts with protein tyrosine phosphatase PTP-BL	137
Chapter 8 The PTP-BL multiprotein complex: All actin' together? Model and future outlook	159
Summary / Samenvatting	167
Acknowledgments	175
Curriculum vitae	176
Publications	177

Chapter 1

General introduction

General introduction

Edwin Cuppen

*Department of Cell Biology, Institute of Cellular Signalling, University of Nijmegen,
Adelbertusplein 1, 6525 EK Nijmegen, The Netherlands.*

Processes like cell proliferation, differentiation, and metabolic control in multicellular organisms rely on the interpretation of external and internal stimuli in complex signaling networks. The response of a specific cell depends on the nature of the wiring and intertwining of different signal transduction pathways that transfer information to the proper subcellular site(s), and on the type of signals received. Therefore, it may come as no surprise that mechanisms that organize this complex network require tight regulation of the enzymes involved. Deregulation of these mechanisms may lead to improper cell functioning and oncogenesis (Hunter, 1997; Ninfa and Dixon, 1994). In the past few years, there has been enormous progress in our understanding of the molecular basis and pathobiology of different signaling disorders. A variety of oncoproteins and tumor suppressor proteins has been identified and most of these were found to be enzymes, that normally regulate mitogenic signaling or that are involved in determining cell morphology and motility. Key players like the protein tyrosine kinases (PTKs) were found to be proto-oncogenes (Porter and Vaillancourt, 1998; Rodrigues and Park, 1994), and consequently, it has been assumed that the enzymes that antagonize PTK function, the protein tyrosine phosphatases (PTPs) may function as tumor suppressors. Next to signaling enzymes, also adapter and scaffold proteins and cytoskeletal components were identified, mainly as tumor suppressors or developmentally important proteins (Ben-Ze'ev, 1997; Hulsken et al., 1994; Tsukita et al., 1993). Instead of giving a comprehensive overview of all protein phosphorylation cascades I will focus here on a specific protein, PTP-BL, that has characteristics in common with both signaling enzymes and cell-structural proteins. PTP-BL is a member of the large family of protein tyrosine phosphatases (see Schaapveld et al., 1997 and Zhang, 1998 for an extensive review) and has similarities to several known tumor suppressors. Therefore it may play a role in regulating cell growth and differentiation.

1.1 PTP-BL

Gene sequences that are central to the work described in this thesis were initially cloned from mouse brain using degenerate primers that were based upon the highly conserved catalytic domain of known PTPs (Hendriks et al., 1995). Characterization of the novel 8 kb transcript revealed a large open reading frame encoding a protein with a predicted

molecular weight of 270 kDa. Because of its high overall homology with human PTP-BAS (Maekawa et al., 1994), this mouse protein was named PTP-BL, for PTP-BAS-like (Hendriks et al., 1995). PTP-BAS was identified as an alternatively spliced transcript from differentiated human basophils (Maekawa et al., 1994) and has also been named hPTP1E (Banville et al., 1994), PTPL1 (Saras et al., 1994) and FAP-1 (Sato et al., 1995), whereas PTP-BL is also known as RIP (Chida et al., 1995). The gene encoding PTP-BL was mapped to mouse chromosome 5E/F, and the human orthologue PTP-BAS is located on human chromosome region 4 at band q21.3 (Inazawa et al., 1996; van den Maagdenberg et al., 1996). This region of the genome is believed to contain putative tumor suppressor genes of relevance to several types of human cancers, including liver and ovarian cancers. Expression analysis using RNA in situ hybridization experiments shows a predominantly epithelial expression pattern for the PTP-BL transcript and characterization of the predicted polypeptide reveals that PTP-BL harbors several modular protein domains (Fig. 1; Hendriks et al., 1995). At the N-terminus, the protein contains a large domain that entails multiple consensus threonine, serine and tyrosine phosphorylation sites and is subject to extensive alternative splicing (Chida et al., 1995; E.C. unpublished observations). Since no obvious homology to known proteins or protein domains is apparent the function for this domain in PTP-BL remains completely elusive. The remaining 200 kDa of PTP-BL consists of a FERM domain, five PDZ motifs and finally the catalytic domain which distinguishes the molecule as a member of the family of protein tyrosine phosphatases. In the human homologue PTP-BAS/PTPL1/hPTP1E/FAP-1 a potential leucine zipper that may be involved in homo- or hetero-dimerization can be discerned just N-terminal of the FERM domain (Saras et al., 1994). However, in mouse PTP-BL several critical residues within this motif are lacking, making a simple role in protein association unlikely. The general characteristics of the FERM, PDZ and tyrosine phosphatase domains in PTP-BL, as well as their homology to similar domains in other cytoarchitectural and signaling molecules (Fig. 1) will be discussed in the following sections.

1.2 FERM domain

The FERM domain, that is also known as band 4.1-like domain, is a motif of about 300 amino acid residues originally identified in the protein band 4.1 that was isolated from human erythrocyte ghosts (Leto and Marchesi, 1984). The FERM domain of band 4.1 has been reported to bind in vitro ATP, phosphatidylinositol 4,5-biphosphate, and phosphatidylserine. It also binds to soluble proteins like calmodulin and p55. Furthermore, the FERM domain mediates the attachment of protein 4.1 to the plasma membrane by binding to the cytoplasmic domains of the transmembrane proteins glycophorin A, glycophorin C, band 3 and CD44 (for references see Chishti et al., 1998). Next to the N-terminal FERM domain, the band 4.1 protein contains a C-terminal actin-binding domain and is therefore thought to function as an important cross-linker between the plasma

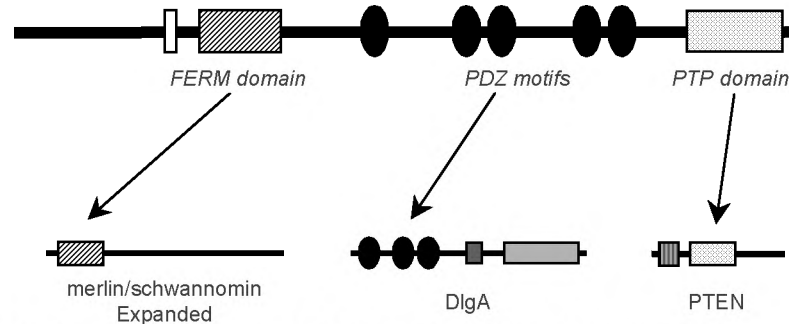


Figure 1: Schematic representation of PTP-BL and its homology to tumor suppressors.

Several modular protein domains with homology to known tumor suppressors can be discerned in PTP-BL. The C-terminal catalytic protein tyrosine phosphatase domain, that may counteract oncogenic tyrosine kinase activity, shows homology to the tumor suppressor and multi-specificity phosphatase PTEN. In the middle part of the protein five PDZ motifs are located, that are also found in the *Drosophila discs-large* tumor suppressor gene product, DlgA. The FERM domain is also found in the product of the neurofibromatosis type II (NF-2) gene product merlin/schwannomin and the *Drosophila* tumor suppressor Expanded. The large N-terminal domain displays no overt homologies to currently known protein sequences. Stippled box, PTP domain; black oval, PDZ motif; diagonal striped box, FERM domain; white box, putative leucine zipper; black box, SH3 domain; grey box, guanylate kinase domain; vertical striped box, tensin homology domain.

membranes and the actin cytoskeleton in red blood cells (Tsukita and Yonemura, 1997). Indeed, band 4.1 protein has been shown to be essential for maintaining the stability of the erythrocyte membrane and mutations in this protein are associated with human diseases causing forms of hereditary elliptocytosis (Conboy, 1993).

The FERM domain has now been identified in a large group of proteins that may function in the linkage of the cytoskeleton to the plasma membrane (Chishti et al., 1998). Evidence supporting this role comes from occurrence of FERM domains in a subfamily of membrane-associated proteins termed ezrin, radixin and moesin (the ERMs; hence the term FERM from F for 4.1, E for ezrin, R for radixin and M for moesin). The ERMs function as molecular linkers that can bind cell-surface transmembrane proteins such as CD44, CD43, ICAM-1 and ICAM-2, and the actin cytoskeleton via their N-terminal FERM and C-terminal actin binding domains, respectively. In addition, the N- and C-terminal halves of ERMs can bind to each other, resulting in homotypic and heterotypic head-to-tail oligomers (for review see Tsukita et al., 1997). Interestingly, FERM domains occur in multiple members of the family of protein tyrosine phosphatases, PTP-BAS/PTP1E/PTP-BL/RIP/PTPL1 (Banville et al., 1994; Chida et al., 1995; Hendriks et al., 1995; Maekawa et al., 1994; Saras et al., 1994), PTP-MEG (Gu et al., 1991), PTPH1 (Yang and Tonks, 1991), PTPD1 (Moller et al., 1994) and PTPD2/PEZ/PTP36 (Moller et al., 1994; Sawada et al., 1994; Smith et al., 1995), but here their function remains largely unknown. A possible

functional involvement of the FERM domain in growth control and differentiation can be deduced from its presence in the brain tumor suppressor neurofibromatosis 2, NF-2, (Rouleau et al., 1993; Trofatter et al., 1993) and in the *Drosophila* tumor suppressor expanded (Boedigheimer et al., 1993). Therefore, let us focus on the pathobiological significance of these proteins first.

Merlin/Schwannomin

Neurofibromatosis type 2 (NF2) is a disorder that occurs with a frequency of 1: 37000 and is characterized by the development of tumors derived from the central nervous system, like vestibular schwannomas, meningiomas, spinal schwannomas, ependymomas, and posterior lenticular opacities. The gene responsible for NF2 maps to the long arm of chromosome 22 and encodes a protein of 595 amino acids called merlin (Trofatter et al., 1993) or schwannomin (Rouleau et al., 1993) that is about 50% identical to the ERMs, with highest homology in the N-terminal FERM domain. Although merlin does not contain the C-terminal actin binding motif as it is found in the ERMs, the protein localizes to cortical actin structures and is particularly enriched in membrane ruffles (Gonzalez-Agosti et al., 1996). Reduction of merlin expression by antisense oligonucleotides reduces the adhesion and increases the proliferation of Schwann-like cells (Huynh and Pulst, 1996). In contrast overexpression of merlin inhibits growth of fibroblasts (Lutchman and Rouleau, 1995) and rat schwannoma cells (Sherman et al., 1997), clearly demonstrating its tumor suppressive capacity. Homozygous mutations at the mouse NF2 locus leads to embryonic failure immediately before gastrulation, indicating that merlin function is critical for normal differentiation at a very early stage in development (McClatchey et al., 1997). Mice heterozygous for a mutation in NF2 develop a range of highly metastatic tumors, this in contrast to the limited spectrum of benign tumors associated with NF2 in humans (McClatchey et al., 1998).

What is the molecular basis for merlin's tumor suppressive action and what is known about the role of the FERM domain therein? It has been demonstrated that the N-terminal half of merlin alone can inhibit growth and has an anti-Ras function, indicating that the FERM domain is essential for the expression of tumor-suppressing activity (Tikoo et al., 1994). Furthermore, a recent study showed that 7 out of 11 patients examined had a splicing abnormality that lead to absence of exon sequences that encode the FERM domain. Expression of these mutant proteins in a fibroblast cell line resulted in decreased adhesion and detachment from the substratum (Koga et al., 1998). Another report showed that the tumor suppressive action of merlin also depends on the presence of the C-terminal domain (encoded by exon 16) and merlin's ability to form inter- or intra-molecular interactions analogous as has been described for the ERMs (Sherman et al., 1997). These findings do not contradict, since for an inter- or intra-molecular interaction to occur both an intact FERM domain and the presence of the C-terminal binding domain are necessary. Finally, it

has been observed that inactivating mutations do occur in almost all exons (reviewed in Lutchman and Rouleau, 1996), suggesting that multiple determinants in merlin are important for its normal cellular function. Taken together, it can now be considered established that merlin may regulate membrane-cytoskeletal organization by inter- and intra-molecular interactions and thus forms a nodal factor in regulating cell growth and differentiation

Expanded

Genetic methods in *Drosophila* make it possible to identify negative regulators of cell proliferation by the overgrowth phenotype. The expanded gene (*ex*) was first identified by a spontaneous mutation that causes broad wings. Loss of function mutations in *ex* affect cell differentiation and proliferation of imaginal discs, which are composed of single epithelial layers, causing either hyperplasia or degeneration depending on the nature and developmental stage of the disc (Boedigheimer et al., 1993). Interestingly, overgrowth is not caused by prolonging the growth period as for mutations in many other genes, but is due to an increased proliferation rate during development (Boedigheimer et al., 1997). Furthermore, overexpression of *ex* leads to the opposite phenotype; a decrease in final cell number in the wing (Boedigheimer et al., 1997). The *ex* gene product Expanded, that has a similar overall organization as merlin/schwannomin, is present in the apical domain of the epithelial disc cells, overlapping precisely with the position of phosphotyrosine-containing proteins and presumably adherens junctions. Similar to the situation for merlin, Expanded lacks the C-terminal conserved actin-binding site found in other ERM proteins. This is consistent with data that suggest that Expanded does not function as a membrane-cytoskeletal linker in the way that ERM proteins generally do, but rather is involved in regulating a signaling pathway controlling cell proliferation. First, the presence of consensus SH3 binding sites in Expanded suggest that it functions in the recruitment or partitioning of cytosolic signaling enzymes or adaptor proteins. Secondly, if the protein would have a role in cross-connecting membrane and cytoskeletal proteins and growth regulation one would expect the N- or C-terminal domain to have a dominant negative effect by competing with endogenous binding partners. This, in turn, could result in overgrowth of imaginal discs, the similar phenotype as for loss of function mutants. In contrast to this expectation, overexpression of the N-terminal domain shows no phenotype and overexpression of the isolated C-terminal domain results in reduced cell proliferation, similar as for overexpression of the full-length Expanded protein (Boedigheimer et al., 1997). Further experiments are thus needed to reveal the mode of action of the FERM domain and clarify *ex*'s role in normal and aberrant growth behaviour.

1.3 PDZ motifs

PDZ motifs, formerly known as GLGF repeats (Cho et al., 1992) or Discs-large

Homologous Regions (DHRs) (Bryant et al., 1993), are small modular protein domains of about 90 amino acids, that were first identified in the post-synaptic density protein PSD-95 (Cho et al., 1992), the *Drosophila discs-large* tumor suppressor gene product DlgA (Woods and Bryant, 1991), and the tight junction component ZO-1 (Itoh et al., 1993). Nowadays, PDZ motifs have been identified in a very heterogeneous group of proteins in mammals, plants, yeast and bacteria (for review see Ponting et al., 1997). It is becoming clear that PDZ motifs mediate protein-protein interactions (Fanning and Anderson, 1996; Ranganathan and Ross, 1997; Saras and Heldin, 1996) and can associate with transmembrane proteins (Sheng, 1996), cytoskeletal components (Xia et al., 1997) and signal transduction enzymes (Ranganathan and Ross, 1997). PDZ-containing proteins have been implicated in the clustering of membrane proteins by binding to their C-terminal cytoplasmic tails (Gomperts, 1996). They also participate in the formation of submembranous protein networks (Fanning and Anderson, 1998) and function as scaffold proteins in organizing signal transduction pathways (reviewed in Tsunoda et al., 1998).

The crystal structure of the third PDZ motif from human Dlg reveals a modular structure consisting of a five-stranded antiparallel β -barrel flanked by three α -helices, that resembles the overall architecture as for the IRS-1 phosphotyrosine binding domain (PTB) (Morais Cabral et al., 1996). Another crystal structure, of the third PDZ motif from the synaptic protein PSD-95, in complex with its peptide ligand clearly illustrates the structural basis for C-terminal peptide recognition. A prominent hydrophobic pocket recognizes the terminal carboxylate group of the peptide and the selective recognition of the consensus peptide (T/S-x-V-*) is mediated by specific side chain interactions via an antiparallel β sheet with the β strand flanking the peptide-binding groove (Doyle et al., 1996). Although for several PDZ motifs a C-terminal consensus binding sequence has been deduced (Schepens et al., 1997; Songyang et al., 1997; Stricker et al., 1997; Wang et al., 1998), other binding modes have also been observed. Firstly, heteromeric PDZ-PDZ interactions have been observed for nNOS with PSD-95 and α 1-syntrophin (Brenman et al., 1996) and homomeric PDZ-PDZ interactions have been observed for the multi-PDZ-containing protein INAD (Xu et al., 1998). Interestingly, the PDZ motifs involved in these interactions are also able to recognize C-terminal peptides. For INAD, the PDZ-PDZ interaction does not prevent C-terminal peptide recognition, suggesting the presence of different binding interfaces (Xu et al., 1998). Contrasting with this, however, a peptide that specifically binds the α 1-syntrophin PDZ motif was found to compete with the PDZ-PDZ interaction with the nNOS PDZ motif, indicating binding to the same site (Gee et al., 1998). Secondly, PDZ motifs have also been found to recognize other internal protein sequences. For example, the third PDZ motif in INAD binds an internal S-T-V sequence in the TRP Ca²⁺-channel protein (Shieh and Zhu, 1996) and the PDZ motif in ALP associates with the second spectrin-like repeat in α -actinin-1 (Xia et al., 1997). Interestingly, the PDZ motif from syntrophin can

bind a short C-terminal peptide sequence as well as a similar internal peptide that is conformationally restricted by an intramolecular disulfide bond (Gee et al., 1998). Clearly, PDZ motifs are now well recognized as modular protein-protein interaction modules, that may display different modes of binding, potentially mediated by multiple interfaces on the globular PDZ motif. The presence of these motifs in a very heterogenous group of proteins (Ponting et al., 1997) suggests a general function for PDZ motifs in macromolecular organization. Moreover, the ubiquitous nature of PDZ domains in proteins with a (subcortical) membrane location can be of indirect help to obtain a better understanding of their general biological significance. What follows is a brief description of two illustrative examples of PDZ domain-bearing proteins.

Discs-large

Discs large (DlgA) (Woods and Bryant, 1991) was the first member identified of an increasingly important class of proteins called membrane-associated guanylate kinase homologues (MAGUKs), which are often concentrated at cell junctions and contain three PDZ domains, an SH3, a HOOK and a guanylate kinase (GUK) domain (Woods and Bryant, 1993). DlgA is located at the cytoplasmic face of septate junctions and is necessary for the formation of these junctions and maintenance of cell apico-basal polarity (Woods et al., 1996). DlgA is also required at neuromuscular junctions and epithelial septate junctions for signaling events controlling synaptic vesicle release and cell proliferation, respectively (Budnik et al., 1996; Woods and Bryant, 1991). Using deletion mutants, Hough et al. (1997) convincingly demonstrated which of the domains in DlgA are important for these functions. They showed that the HOOK domain is responsible for membrane targeting of the protein, but that the first two PDZ motifs are essential for septate junction localization. This is perfectly in line with the finding that these domains in mouse Dlg bind to the membrane-associated proteins ezrin and protein 4.1 (Lue et al., 1996). PDZ2 and PDZ3 were found to be required for growth regulation but not for epithelial structure, whereas the SH3 and HOOK domain are essential for both functional aspects (Hough et al., 1997). Thus far, no obvious function for the GUK domain, that lacks catalytic activity, has been found, although some data suggests that the GUK domain may act as a negative regulator, inhibiting the function of the rest of the protein in controlling cell proliferation (Hough et al., 1997).

InaD

Signal transduction in *Drosophila* photoreceptors involves several key steps: the absorption of a photon by the G protein-coupled receptor rhodopsin; the activation of rhodopsin of a member of the G_q class of heterotrimeric G protein; and subsequent activation of a phospholipase C β (PLC β). Activation of PLC β ultimately triggers the opening of cation channels, resulting in the depolarization of the photoreceptor cell. The predominant divalent

cation-permeability of the TRP class of light activated channels leads to a rapid influx of Ca^{2+} upon photoexcitation, which is the major signal for feedback regulation of the signaling process. An eye-specific isoform of protein kinase C (PKC) acts as the primary mediator of Ca^{2+} -dependent negative feedback regulation (reviewed in Ranganathan and Ross, 1997). INAD, a multivalent adapter protein consisting of five PDZ domains, is now recognized as the central player, that organizes this set of excitatory and regulatory visual transduction proteins into a single signaling complex in *Drosophila* photoreceptor neurons. Evidence for the INAD-driven formation of a multiprotein complex that organizes phototransduction signaling, began with the characterization of a *Drosophila* mutant, INAD (Inactivation no afterpotential D), that displays abnormal electrical responses in the retina (Shieh and Niemeyer, 1995). The mutant phenotype was found to be caused by a point mutation in the third PDZ motif of INAD, resulting in abolishment of interaction with the TRP Ca^{2+} -channel (Shieh and Zhu, 1996). Subsequent work showed that INAD binds TRP, PKC and PLC β via its third, fourth and fifth PDZ motif, respectively (Tsunoda et al., 1997), and recently it was demonstrated that also rhodopsin and another channel protein TRPL bind directly to INAD (Xu et al., 1998). In addition it was shown that PDZ motifs in INAD mediate homomultimerization of the complex (Xu et al., 1998). Taken together, INAD compartmentalizes all important components for photoreceptor signaling in a multiprotein complex, thereby allowing efficient and specific signal transduction and a rapid feedback mechanism. The recent identification of a putative human homolog of INAD (Philipp and Flockerzi, 1997) and the identification of other exclusively multi-PDZ proteins, such as the seven PDZ-domain protein GRIP (glutamate-receptor-interacting protein; Dong et al., 1997) and the eleven PDZ protein MUPP1 (multi PDZ containing protein-1; Ullmer et al., 1998), suggest a more general role for PDZ-containing proteins in organizing highly specialized signaling complexes or 'signalosomes'.

1.4 PTP domain

Protein tyrosine phosphorylation is a universal mechanism employed for the regulation of diverse cellular processes such as proliferation, differentiation, motility, cell-cell interactions, metabolism, gene transcription, and the immune response (Hunter, 1996). The propagation and termination of signaling events controlling these cellular processes are determined almost exclusively by the level of phosphorylation of different proteins in a cell. Changes in the degree of protein phosphorylation on a particular protein are regulated by two opposing enzyme activities: those catalyzed by the protein tyrosine kinases (PTKs), which covalently attach a phosphate group to a tyrosine residue within a protein, and the reverse activity of protein tyrosine phosphatases (PTPs). Ever since the discovery of PTPs it has been assumed that they may function as anti-oncogene or tumor suppressor proteins (Goldsmith and Koizumi, 1997; Hunter, 1995). Initially, this contention has been strengthened by the observation that treatment of cells with vanadate, a reasonably specific

PTP-inhibitor, results in an increase of phosphotyrosine-containing proteins and concomitantly in cellular transformation (Klarlund, 1985). Furthermore, overexpression of one of the earliest discovered PTP family members, the cytoplasmic protein tyrosine phosphatase PTP1B, in fibroblasts transformed by the *neu* oncogene significantly inhibited oncogenic transformation (Brown-Shimer et al., 1992). However, we now know that the initial conclusions drawn on basis of these results give a rather oversimplified picture of the true (patho)biological significance of PTPs.

The PTP family of proteins consist of receptor-like and non-transmembrane enzymes which share a high degree of homology in their 230-280 amino acids-large catalytic domains. Biochemical studies demonstrate that PTPs utilize a common mechanism for catalysis that involves the cysteine within the PTP signature motif ([I/V]HCXAGXXR[S/T]G) and a highly conserved aspartate. Crystal structure data reveal a very similar three-dimensional topology for different PTPs and have shed more light on the molecular basis of catalysis (for review see Barford et al., 1998). Regulation of phosphatase activity and specificity of ligand recognition is now believed to be mediated by the bewildering variety of protein domains that is present in PTPs, in addition to the catalytic domain (Fauman and Saper, 1996; Mauro and Dixon, 1994; Mourey and Dixon, 1994).

During the past decade we have witnessed a continuous increase in the number of known PTP-gene family members, their gene structure and their chromosomal location. So the question is justified whether this has also brought us more insight in the presumed role of this family of proteins in control of cell growth and behaviour? The general answer is no, and we now realize that each PTP may have a fully distinct cellular role. Although for example some PTPs have been mapped to chromosomal loci that are often deleted in specific types of tumors, or are able to counteract the transforming potential of oncogenic kinases in vitro (reviewed in Goldsmith and Koizumi, 1997), no specific PTP has been identified yet that behaves as a classical tumor suppressor in vivo. Recently, however, hope glimmered because a novel protein was identified, designated PTEN for Phosphatase and Tensin homologue deleted on chromosome Ten. This protein contains the typical phosphatase signature and is mutated at a considerable frequency in a wide range of human cancers (Li et al., 1997; Steck et al., 1997). Recombinant PTEN has been shown to dephosphorylate protein and peptide substrates phosphorylated on serine, threonine, and tyrosine residues in vitro, suggesting that it is a dual specificity phosphatase (Myers et al., 1997). Furthermore, PTEN has been shown to down-regulate integrin-mediated cell spreading and the formation of focal adhesions, and the protein was found to interact with the focal adhesion kinase FAK and to reduce its tyrosine phosphorylation (Tamura et al., 1998). However, to the surprise of many investigators, recent experiments indicated unequivocally, that PTEN also displays phosphoinositide 3-phosphatase activity (Maehama and Dixon, 1998) and that the regulation of PIP₃ levels in vivo is critical for its tumor suppressive function (Hopkin, 1998; Myers et al., 1998). Moreover, a mutation that was

found in two Cowden disease kindreds specifically ablates the ability of PTEN to recognize inositol phospholipids as a substrate, whereas its phosphatase activity was unaffected (Myers et al., 1998). From this, we can conclude that the quest for the first genuine PTP that acts as a tumor suppressor is still ongoing, and that one should also consider unanticipated substrates, like for example phospholipids, as possible targets for PTPs. Furthermore, since tyrosine phosphorylation plays an important regulatory role in a wide variety of cellular processes, normal PTP function may be involved in divergent processes like cell migration, cell morphology and immune response.

1.5 Scope and rationale of the work described in this thesis

The studies described in this thesis were aimed to obtain clues about the biological function of a specific protein tyrosine phosphatase, PTP-BL. Initially, most of our working hypotheses focussed on growth control regulation and subcellular compartmentalization as the protein contains many domains which also occur in tumor suppressor proteins. Therefore, important clues may be derived from a better understanding of the intracellular partitioning of the protein, and we used a combination of molecular and morphological approaches to follow PTP-BL's dynamic behaviour in cells *in vitro*. In Chapter 2 the study of the subcellular localization of PTP-BL and the protein determinants that govern its distribution dynamics are presented. Shortly after starting the thesis research, a potential biological function for PTP-BL in Fas-mediated apoptotic signaling was reported (Sato et al., 1995). We followed up on this result, and in Chapter 3 we show that there is, however, no evidence for such function in the mouse system. Next, to obtain additional cues on PTP-BL's biological function we started the characterization of the molecular environment of the molecule. Discovery of the nature and role of associating proteins in proteome networks often yields important clues for other protein components that act in the same network. We used yeast two-hybrid interaction cloning to identify proteins that can interact with PDZ motifs in PTP-BL. The same system was used to type the strength of the interactions and to delineate the actual protein domain segments involved. The identification of distinct protein partners, characterization of the observed interactions, and expression distribution studies of these proteins are presented in Chapters 4, 5, 6 and 7. In Chapter 8, a summary of converging results is given and a working model for PTP-BL function is proposed.

References

- Banville, D., Ahmad, S., Stocco, R., and Shen, S. H. (1994). A novel protein-tyrosine phosphatase with homology to both the cytoskeletal proteins of the band 4.1 family and junction-associated guanylate kinases. *J. Biol. Chem.* *269*, 22320-22327.
- Barford, D., Das, A. K., and Egloff, M.-P. (1998). The structure and mechanism of protein phosphatases: Insights into catalysis and regulation. *Annu. Rev. Biophys. Biomol. Struct.* *27*, 133-164.
- Ben-Ze'ev, A. (1997). Cytoskeletal and adhesion proteins as tumor suppressors. *Curr. Opin. Cell Biol.* *9*, 99-108.
- Boedigheimer, M., Bryant, P., and Laughon, A. (1993). Expanded, a negative regulator of cell proliferation in *Drosophila*, shows homology to the NF2 tumor suppressor. *Mech. Dev.* *44*, 83-84.
- Boedigheimer, M. J., Nguyen, K. P., and Bryant, P. J. (1997). Expanded functions in the apical cell domain to regulate the growth rate of imaginal discs. *Dev. Genet.* *20*, 103-110.
- Brenman, J. E., Chao, D. S., Gee, S. H., McGee, A. W., Craven, S. E., Santillano, D. R., Wu, Z., Huang, F., Xia, H., Peters, M. F., Froehner, S. C., and Brecht, D. S. (1996). Interaction of nitric oxide synthase with the postsynaptic density protein PSD-95 and alpha1-syntrophin mediated by PDZ domains. *Cell* *84*, 757-767.
- Brown-Shimer, S., Johnson, K. A., Hill, D. E., and Bruskin, A. M. (1992). Effect of protein tyrosine phosphatase 1B expression on transformation by the human neu oncogene. *Cancer Res.* *52*, 478-482.
- Bryant, P. J., Watson, K. L., Justice, R. W., and Woods, D. F. (1993). Tumor suppressor genes encoding proteins required for cell interactions and signal transduction in *Drosophila*. *Dev. Suppl.*, 239-249.
- Budnik, V., Koh, Y., Guan, B., Hartmann, B., Hough, C., Woods, D., and Gorczyca, M. (1996). Regulation of synapse structure and function by the *Drosophila* tumor suppressor gene *dlg*. *Neuron* *17*, 627-640.
- Chida, D., Kume, T., Mukoyama, Y., Tabata, S., Nomura, N., Thomas, M. L., Watanabe, T., and Oishi, M. (1995). Characterization of a protein tyrosine phosphatase (RIP) expressed at a very early stage of differentiation in both mouse erythroleukemia and embryonal carcinoma cells. *FEBS Lett.* *358*, 233-239.
- Chishti, A. H., Kim, A. C., Marfatia, S. M., Lutchnan, M., Hanspal, M., Jindal, H., Liu, S.-C., Low, P. S., Rouleau, G. A., Mohandas, N., Chasis, J. A., Conboy, J. G., Gascard, P., Takakuwa, Y., Huang, S.-C., Benz, E. J., Bretscher, A., Fehon, R. G., Gusella, J. F., Ramesh, V., Solomon, F., Marchesi, V. T., Tsukita, S., Tsukita, S., Arpin, M., Louvard, D., Tonks, N. K., Anderson, J. M., Fanning, A. S., Bryant, P. J., Woods, D. F., and Hoover, K. B. (1998). The FERM domain: a unique module involved in the linkage of cytoplasmic proteins to the membrane. *Trends Biochem. Sci.* *23*, 281-282.
- Cho, K.-O., Hunt, C. A., and Kennedy, M. B. (1992). The rat brain postsynaptic density fraction contains a homolog of the *Drosophila* discs-large tumor suppressor protein. *Neuron* *9*, 929-942.
- Conboy, J. G. (1993). Structure, function and molecular genetics of erythroid membrane skeletal protein 4.1 in normal and abnormal red blood cells. *Semin. Hematol.* *30*, 58-73.
- Dong, H., O'Brien, R. J., Fung, E. T., Lanahan, A. A., Worley, P. F., and Huganir, R. L. (1997). GRIP: a synaptic PDZ domain-containing protein that interacts with AMPA receptors. *Nature* *388*, 279-284.
- Doyle, D. A., Lee, A., Lewis, J., Kim, E., Sheng, M., and MacKinnon, R. (1996). Crystal structures of a complexed and peptide-free membrane protein-binding domain: molecular basis of peptide recognition by PDZ. *Cell* *85*, 1067-1076.
- Fanning, A. S., and Anderson, J. M. (1998). PDZ domains and the formation of protein networks at the plasma membrane. *Curr. Top. Microbiol. Immunol.* *228*, 209-233.
- Fanning, A. S., and Anderson, J. M. (1996). Protein-protein interactions: PDZ domain networks. *Curr. Biol.* *6*, 1385-1388.

- Fauman, E. B., and Saper, M. A. (1996). Structure and function of the protein tyrosine phosphatases. *Trends Biochem. Sci.* *21*, 413-417.
- Gee, S. H., Sekely, S. A., Lombardo, C., Kurakin, A., Froehner, S. C., and Kay, B. K. (1998). Cyclic peptides as non-carboxyl-terminal ligands of syntrophin PDZ domains. *J. Biol. Chem.* *273*, 21980-21987.
- Goldsmith, B. A., and Koizumi, S. (1997). Protein tyrosine phosphatases: Positive and negative regulation of proliferation. *Int. J. Oncol.* *11*, 825-834.
- Gomperts, S. N. (1996). Clustering membrane proteins: It's all coming together with the PSD-95/SAP90 protein family. *Cell* *84*, 659-662.
- Gonzalez-Agosti, C., Xu, L., Pinney, D., Beauchamp, R., Hobbs, W., Gusella, J., and Ramesh, V. (1996). The merlin tumor suppressor localizes preferentially in membrane ruffles. *Oncogene* *13*, 1239-1247.
- Gu, M., York, J. D., Warshawsky, I., and Majerus, P. W. (1991). Identification, cloning, and expression of a cytosolic megakaryocyte protein-tyrosine-phosphatase with sequence homology to cytoskeletal protein 4.1. *Proc. Natl. Acad. Sci. USA* *88*, 5867-5871.
- Hendriks, W., Schepens, J., Bachner, D., Rijss, J., Zeeuwen, P., Zechner, U., Hameister, H., and Wieringa, B. (1995). Molecular cloning of a mouse epithelial protein-tyrosine phosphatase with similarities to submembranous proteins. *J. Cell. Biochem.* *59*, 418-430.
- Hopkin, K. (1998). A surprising function for the PTEN tumor suppressor. *Science* *282*, 1027 - 1030.
- Hough, C. D., Woods, D. F., Park, S., and Bryant, P. J. (1997). Organizing a functional junctional complex requires specific domains of the *Drosophila* MAGUK discs large. *Genes Dev.* *11*, 3242-3253.
- Hulsken, J., Behrens, J., and Birchmeier, W. (1994). Tumor-suppressor gene products in cell contacts: the cadherin-APC-armadillo connection. *Curr. Opin. Cell Biol.* *6*, 711-716.
- Hunter, T. (1997). Oncoprotein networks. *Cell* *88*, 333-346.
- Hunter, T. (1995). Protein kinases and phosphatases: the yin and yang of protein phosphorylation and signaling. *Cell* *80*, 225-36.
- Hunter, T. (1996). Tyrosine phosphorylation: Past, present and future. *Biochem. Soc. Trans.* *24*, 307-327.
- Huynh, D. P., and Pulst, S. M. (1996). Neurofibromatosis 2 anti-sense oligodeoxynucleotides induce reversible inhibition of schwannomin synthesis and cell adhesion in STS26T and T98G cells. *Oncogene* *13*, 73-84.
- Inazawa, J., Ariyama, T., Abe, T., Druck, T., Ohta, M., Huebner, K., Yanagisawa, J., Reed, J. C., and Sato, T. (1996). PTPN13, a fas-associated protein tyrosine phosphatase, is located on the long arm of chromosome 4 at band q21.3. *Genomics* *31*, 240-242.
- Itoh, M., Nagafuchi, A., Yonemura, S., Kitani-Yasuda, T., Tsukita, S., and Tsukita, S. (1993). The 220-kD protein colocalizing with cadherins in non-epithelial cells is identical to ZO-1, a tight junction-associated protein in epithelial cells: cDNA cloning and immunoelectron microscopy. *J. Cell Biol.* *121*, 491-502.
- Klarlund, J. K. (1985). Transformation of cells by an inhibitor of phosphatases acting on phosphotyrosine in proteins. *Cell* *41*, 707-717.
- Koga, H., Araki, N., Takeshima, H., Nishi, T., Hirota, T., Kimura, Y., Nakao, M., and Saya, H. (1998). Impairment of cell adhesion by expression of the mutant neurofibromatosis type 2 (NF2) which lack exons in the ERM-homology domain. *Oncogene* *17*, 801-810.
- Leto, T. L., and Marchesi, V. T. (1984). A structural model of human erythrocyte protein 4.1. *J. Biol. Chem.* *259*, 4603-4608.
- Li, J., Yen, C., Liaw, D., Podsypanina, K., Bose, S., Wang, S. I., Puc, J., Miliaresis, C., Rodgers, L., McCombie, R., Bigner, S. H., Giovanella, B. C., Ittmann, M., Tycko, B., Hibshoosh, H., Wigler, M. H., and Parsons, R. (1997). PTEN, a putative protein tyrosine phosphatase gene mutated in human brain, breast, and prostate cancer. *Science* *275*, 1943-1947.
- Lue, R. A., Brandin, E., Chan, E. P., and Branton, D. (1996). Two independent domains of hDlg are sufficient for subcellular targeting: the PDZ1-2 conformational unit and an alternatively spliced

- domain. *J. Cell Biol.* *135*, 1125-1137.
- Lutchman, M., and Rouleau, G. A. (1995). The neurofibromatosis type 2 gene product, schwannomin, suppresses growth of NIH 3T3 cells. *Cancer Res.* *55*, 2270-2274.
- Lutchman, M., and Rouleau, G. A. (1996). Neurofibromatosis type 2: a new mechanism of tumor suppression. *Trends Neurosci.* *19*, 373-377.
- Maehama, T., and Dixon, J. E. (1998). The tumor suppressor, PTEN/MMAC1, dephosphorylates the lipid second messenger, phosphatidylinositol 3,4,5-triphosphate. *J. Biol. Chem.* *273*, 13375-13378.
- Maekawa, K., Imagawa, N., Nagamatsu, M., and Harada, S. (1994). Molecular cloning of a novel protein-tyrosine phosphatase containing a membrane-binding domain and GLGF repeats. *FEBS Lett.* *337*, 200-206.
- Mauro, L. J., and Dixon, J. E. (1994). 'Zip codes' direct intracellular protein tyrosine phosphatases to the correct cellular 'address'. *Trends Biochem. Sci.* *19*, 151-155.
- McClatchey, A. I., Saotome, I., Mercer, K., Crowley, D., Gusella, J. F., Bronson, R. T., and Jacks, T. (1998). Mice heterozygous for a mutation at the NF2 tumor suppressor locus develop a range of highly metastatic tumors. *Genes Dev.* *12*, 1121-1133.
- McClatchey, A. I., Saotome, I., Ramesh, V., Gusella, J. F., and Jacks, T. (1997). The NF2 tumor suppressor gene product is essential for extraembryonic development immediately prior to gastrulation. *Genes Dev.* *11*, 1253-1265.
- Moller, N. P. H., Moller, K. B., Lammers, R., Kharitonenkow, A., Sures, I., and Ullrich, A. (1994). Src kinase associates with a member of a distinct subfamily of protein-tyrosine phosphatases containing an ezrin-like domain. *Proc. Natl. Acad. Sci. USA* *91*, 7477-7481.
- Morais Cabral, J. H., Petrosa, C., Sutcliffe, M. J., Raza, S., Byron, O., Poy, F., Marfatia, S. M., Chishti, A. H., and Liddington, R. C. (1996). Crystal structure of a PDZ domain. *Nature* *382*, 649-652.
- Mourey, R. J., and Dixon, J. E. (1994). Protein tyrosine phosphatases: characterization of extracellular and intracellular domains. *Curr. Opin. Genet. Dev.* *4*, 31-39.
- Myers, M. P., Pass, I., Batty, I. H., Kaay, J. v. d., Stolarov, J. P., Hemmings, B. A., Wigler, M. H., Downes, C. P., and Tonks, N. K. (1998). The lipid phosphatase activity of PTEN is critical for its tumor suppressor function. *Proc. Natl. Acad. Sci. USA* *95*, 13513-13518.
- Myers, M. P., Stolarov, J. P., Eng, C., Li, J., Wang, S. I., Wigler, M. H., Parsons, R., and Tonks, N. K. (1997). P-TEN, the tumor suppressor from human chromosome 10q23, is a dual-specificity phosphatase. *Proc. Natl. Acad. Sci. USA* *94*, 9052-9057.
- Ninfa, E. G., and Dixon, J. E. (1994). Protein tyrosine phosphatases in disease processes. *Trends Cell Biol.* *4*, 427-430.
- Philipp, S., and Flockerzi, V. (1997). Molecular characterization of a novel human PDZ domain protein with homology to INAD from *Drosophila melanogaster*. *FEBS Lett.* *413*, 243-248.
- Ponting, C. P., Phillips, C., Davies, K. E., and Blake, D. J. (1997). PDZ domains: targeting signaling molecules to sub-membranous sites. *BioEssays* *19*, 469-479.
- Porter, A. C., and Vaillancourt, R. R. (1998). Tyrosine kinase receptor-activated signal transduction pathways which lead to oncogenesis. *Oncogene* *16*, 1343-1352.
- Ranganathan, R., and Ross, E. M. (1997). PDZ domain proteins: Scaffolds for signaling complexes. *Curr. Biol.* *7*, R770-R773.
- Rodrigues, G. A., and Park, M. (1994). Oncogenic activation of tyrosine kinases. *Curr. Opin. Genet. Dev.* *4*, 15-24.
- Rouleau, G. A., Merel, P., Lutchman, M., Sanson, M., Zucman, J., Marineau, C., Hoang-Xuan, K., Demczuk, S., Desmaze, C., Plougastel, B., Pulst, S. M., Lenoir, G., Bijlsma, E., Fashold, R., Dumanski, J., de Jong, P., Parry, D., Eldrige, R., Aurias, A., Delattre, O., and Thomas, G. (1993). Alteration in a new gene encoding a putative membrane-organizing protein causes neurofibromatosis type 2. *Nature* *363*, 515-521.
- Saras, J., Claesson Welsh, L., Heldin, C. H., and Gonez, L. J. (1994). Cloning and characterization of PTPL1, a protein tyrosine phosphatase with similarities to cytoskeletal-associated proteins. *J. Biol. Chem.* *269*, 24082-24089.

- Saras, J., and Heldin, C.-H. (1996). PDZ domains bind carboxy-terminal sequences of target proteins. *Trends Biochem. Sci.* *21*, 455-458.
- Sato, T., Irie, S., Kitada, S., and Reed, J. C. (1995). FAP-1: a protein tyrosine phosphatase that associates with Fas. *Science* *268*, 411-415.
- Sawada, M., Ogata, M., Fujino, Y., and Hamaoka, T. (1994). cDNA cloning of a novel protein tyrosine phosphatase with homology to cytoskeletal protein 4.1 and its expression in T-lineage cells. *Biochem. Biophys. Res. Commun.* *203*, 479-484.
- Schaapveld, R. Q. J., Wieringa, B., and Hendriks, W. (1997). Receptor-like protein tyrosine phosphatases: alike and yet so different. *Mol. Biol. Rep.* *24*, 247-262.
- Schepens, J., Cuppen, E., Wieringa, B., and Hendriks, W. (1997). The neuronal nitric oxide synthase PDZ motif binds to -G(D,E)XV* carboxyterminal sequences. *FEBS Lett.* *409*, 53-56.
- Sheng, M. (1996). PDZs and receptor/channel clustering: rounding up the latest suspects. *Neuron* *17*, 575-578.
- Sherman, L., Xu, H.-M., Geist, R. T., Saporito-Irwin, S., Howells, N., Ponta, H., Herrlich, P., and Gutmann, D. H. (1997). Interdomain binding mediates tumor growth suppression by the NF2 gene product. *Oncogene* *15*, 2505-2509.
- Shieh, B. H., and Zhu, M. Y. (1996). Regulation of the TRP Ca²⁺ channel by INAD in *Drosophila* photoreceptors. *Neuron* *16*, 991-998.
- Shieh, B.-H., and Niemeyer, B. (1995). A novel protein encoded by the InaD gene regulates recovery of visual transduction in *Drosophila*. *Neuron* *14*, 201-210.
- Smith, A. L., Mitchell, P. J., Shipley, J., Gusterson, B. A., Rogers, M. V., and Crompton, M. R. (1995). Pez: a novel human cDNA encoding protein tyrosine phosphatase- and ezrin-like domains. *Biochem. Biophys. Res. Commun.* *20*, 359-365.
- Songyang, Z., Fanning, A. S., Fu, C., Xu, J., Marfatia, S. M., Chishti, A. H., Crompton, A., Chan, A. C., Anderson, J. M., and Cantley, L. C. (1997). Recognition of unique carboxyl-terminal motifs by distinct PDZ domains. *Science* *275*, 73-77.
- Steck, P. A., Pershouse, M. A., Jasser, S. A., Yung, W. K. A., Lin, H., Ligon, A. H., Langford, L. A., Baumgard, M. L., Hattier, T., Davis, T., Frye, C., Hu, R., Bradley, S., Teng, D. H. F., and Tavtigian, S. V. (1997). Identification of a candidate tumour suppressor gene, MMAC1, at chromosome 10q23.3 that is mutated in multiple advanced cancers. *Nature Genetics* *15*, 356-362.
- Stricker, N. L., Christopherson, K. S., Yi, B. A., Schatz, P. J., Raab, R. W., Dawes, G., Bassett, D. E., Bredt, D. S., and Li, M. (1997). PDZ Domain of Neuronal Nitric Oxide Synthase Recognizes Novel C Terminal Peptide Sequences. *Nature-Biotechnology* *15*, 336-342.
- Tamura, M., Gu, J., Matsumoto, K., Aota, S., Parsons, R., and Yamada, K. M. (1998). Inhibition of cell migration, spreading, and focal adhesions by tumor suppressor PTEN. *Science* *280*, 1614-1617.
- Tikoo, A., Varga, M., Ramesh, V., Gusella, J., and Maruta, H. (1994). An anti-Ras function of neurofibromatosis type 2 gene product (NF2/merlin). *J. Biol. Chem.* *269*, 23387-23390.
- Trofatter, J. A., MacCollin, M. M., Rutter, J. L., Murrell, J. R., Duyao, M. P., Parry, D. M., Eldridge, R., Kley, N., Menon, A. G., Pulaski, K., Haase, V. H., Ambrose, C. M., Munroe, D., Bove, C., Haines, J. L., Martuza, R. L., MacDonald, M. E., Seizinger, B. R., Short, M. P., Buckler, A. J., and Gusella, J. F. (1993). A novel moesin-, ezrin-, radixin-like gene is a candidate for the neurofibromatosis 2 tumor suppressor. *Cell* *72*, 791-800.
- Tsukita, S., Itoh, M., Nagafuchi, A., Yonemura, S., and Tsukita, S. (1993). Submembranous junctional plaque proteins include potential tumor suppressor molecules. *J-Cell-Biol* *123*, 1049-53.
- Tsukita, S., and Yonemura, S. (1997). ERM (ezrin/radixin/moesin) family: from cytoskeleton to signal transduction. *Curr. Opin. Cell Biol.* *9*, 70-75.
- Tsukita, S., Yonemura, S., and Tsukita, S. (1997). ERM proteins: head-to-tail regulation of actin-plasma membrane interaction. *Trends Biochem. Sci.* *22*, 53-58.
- Tsunoda, S., Sierralta, J., Sun, Y., Bodner, R., Suzuki, E., Becker, A., Socolich, M., and Zuker, C. S. (1997). A multivalent PDZ-domain protein assembles signaling complexes in a G-protein-coupled

- cascade. *Nature* **388**, 243-249.
- Tsunoda, S., Sierralta, J., and Zuker, C. S. (1998). Specificity in signaling pathways: assembly into multimolecular signaling complexes. *Curr. Opin. Genet. Dev.* **8**, 419-422.
- Ullmer, C., Schmuck, K., Figge, A., and Lubbert, H. (1998). Cloning and characterization of MUPP1, a novel PDZ domain protein. *FEBS Lett.* **424**, 63-68.
- van den Maagdenberg, A. M., Olde Weghuis, D., Rijss, J., Merckx, G. F., Wieringa, B., Geurts van Kessel, A., and Hendriks, W. J. (1996). The gene (PTPN13) encoding the protein tyrosine phosphatase PTP-BL/PTP-BAS is located in mouse chromosome region 5E/F and human chromosome region 4q21. *Cytogenet-Cell-Genet* **74**, 153-5.
- Wang, S., Raab, R. W., Schatz, P. J., Guggino, W. B., and Li, M. (1998). Peptide binding consensus of the NHE-RF-PDZ-1 domain matches the C-terminal sequence of cystic fibrosis transmembrane conductance regulator (CFTR). *FEBS Lett.* **427**, 103-108.
- Woods, D. F., and Bryant, P. J. (1991). The discs-large tumor suppressor gene of *Drosophila* encodes a guanylate kinase homolog localized at septate junctions. *Cell* **66**, 451-464.
- Woods, D. F., and Bryant, P. J. (1993). ZO-1, DlgA and PSD-95/SAP90: homologous proteins in tight, septate and synaptic cell junctions. *Mech. Dev.* **44**, 85-89.
- Woods, D. F., Hough, C., Peel, D., Callaini, G., and Bryant, P. J. (1996). Dlg protein is required for junction structure, cell polarity, and proliferation control in *Drosophila* epithelia. *J. Cell Biol.* **134**, 1469-1482.
- Xia, H., Winokur, S. T., Kuo, W.-L., Altherr, M. R., and Brecht, D. S. (1997). Actinin-associated LIM Protein: Identification of a Domain Interaction between PDZ and Spectrin-like Repeat Motifs. *J. Cell Biol.* **139**, 507-515.
- Xu, X.-Z. S., Choudhury, A., Li, X., and Montell, C. (1998). Coordination of an array of signaling proteins through homo- and heteromeric interactions between PDZ domains and target proteins. *J. Cell Biol.* **142**, 545-555.
- Yang, Q., and Tonks, N. K. (1991). Isolation of a cDNA clone encoding a human protein-tyrosine phosphatase with homology to the cytoskeletal-associated proteins band 4.1, ezrin, and talin. *Proc. Natl. Acad. Sci. USA* **88**, 5949-5953.
- Zhang, Z.-Y. (1998). Protein-tyrosine phosphatases: Biological function, structural characteristics, and mechanism of catalysis. *Crit. Rev. Biochem. Mol. Biol.* **33**, 1-52.

Chapter 2

A FERM domain governs apical, villi-like, confinement of PTP-BL in epithelial cells

Edwin Cuppen, Mietske Wijers, Jan Schepens, Jack Fransen, Bé Wieringa, and Wiljan Hendriks.

A FERM domain governs apical, villi-like, confinement of PTP-BL in epithelial cells

Edwin Cuppen, Mietske Wijers, Jan Schepens, Jack Fransen, Bé Wieringa, and Wiljan Hendriks.

Department of Cell Biology, Institute of Cellular Signalling, University of Nijmegen, Adelbertusplein 1, 6525 EK Nijmegen, The Netherlands.

Summary

PTP-BL is a cytosolic multidomain protein tyrosine phosphatase that shares homologies with several submembranous and tumor suppressor proteins. Here we show, by transient expression of modular protein domains of PTP-BL in epithelial MDCK cells, that presence of a FERM domain in the protein is both necessary and sufficient for its targeting to the apical side of epithelial cells. Furthermore, immunoelectron microscopy on stable expressing MDCK pools, that were obtained using an EGFP-based cell sorting protocol, revealed that FERM domain containing fusion proteins are enriched in villi and have a typical submembranous location at about 10-15 nm from the plasma membrane. Immunofluorescence microscopy suggested colocalization of the FERM domain moiety with the membrane-cytoskeleton linker ezrin. However, at the electron microscopy level this colocalization can not be confirmed nor can we detect a direct interaction by immunoprecipitation assays. Fluorescence recovery after photobleaching (FRAP) experiments show that PTP-BL confinement is based on a dynamic steady state and that complete redistribution of the protein may occur within 20 minutes. Our observations suggest that relocation is mediated via a cytosolic pool, rather than by lateral movement. Finally, we show that PTP-BL phosphatase domains are involved in homotypic interactions, as demonstrated by yeast two-hybrid assays. Both the highly restricted subcellular compartmentalization and its specific associative properties may provide the appropriate conditions for regulating substrate specificity and catalytic activity of this member of the PTP family.

Introduction

Reversible phosphorylation of proteins on tyrosine residues is a key event in the regulation of various cellular processes, such as proliferation, differentiation, cell motility, cell-cell interactions, metabolism, gene transcription, and the immune response (Hunter, 1996). Proper initiation, propagation and termination of the signaling cascades involved are thus

critically dependent on the mode of action of individual members of the large families of protein tyrosine kinases (PTKs) and protein tyrosine phosphatases (PTPs) (Hunter, 1998; Ninfa and Dixon, 1994). It is now well established that receptor PTKs are activated by an intermolecular mechanism upon ligand-induced dimerization (Lemmon and Schlessinger, 1994). Cytoplasmic PTKs, on the other hand, are activated by both intra- and intermolecular mechanisms (Thomas and Brugge, 1997). Much less is known regarding the processes that antagonize the effects of PTKs or, for that matter, the functional activation of PTPs. Recent data suggest that for PTPs similar mechanisms as for PTKs do exist (reviewed in Weiss and Schlessinger, 1998). For example, ligand-induced dimerization of an epidermal growth factor-receptor-CD45 chimera was found to inhibit PTP activity and TCR signaling (Majeti et al., 1998). The crystal structure of the first membrane-proximal PTP domain of the receptor-type RPTP α gives structural support for a model in which enzyme inhibition is the consequence of dimerization, by showing that the active site cleft in the subunits is blocked by protruding loops of the opposing domain (Bilwes et al., 1996). Structural data on the RPTP μ membrane proximal PTP domain, however, show that this model might not be universally applicable (Hoffmann et al., 1997). Also, for the cytosolic PTP SHP-2, for example, it was shown that N-terminal SH2 domains are involved in blocking its catalytic site in an intramolecular interaction (Hof et al., 1998).

Importantly, also targeting of the enzyme to highly restricted subcellular micro-compartments may control PTP activity and substrate specificity. In this light, the existence of a variety of modular protein domains in cytosolic PTPs, that may function as 'zip codes' by directing the protein to the correct cellular 'address' (Mauro and Dixon, 1994), is intriguing. Candidate domains that may regulate activity and specificity are particularly abundant in the large cytosolic protein tyrosine phosphatase PTP-BL (Hendriks et al., 1995) or RIP (Chida et al., 1995), which is the mouse homologue of human PTP-BAS/PTPL1/PTP1E/FAP-1 (Banville et al., 1994; Maekawa et al., 1994; Saras et al., 1994; Sato et al., 1995). The approximately 250 kDa protein, that is expressed mainly in epithelia (Hendriks et al., 1995; Cuppen et al., 1998; Thomas et al., 1998), harbors a large N-terminal domain with no obvious homology to other proteins except for a potential leucine zipper (Saras et al., 1994), followed by a FERM domain, five PDZ motifs and a C-terminal PTP domain (see also Fig. 2). Outside its natural context, the PTP-BL phosphatase domain has a high rate of activity with a rather promiscuous substrate specificity (Cuppen et al., 1998; Hendriks et al., 1995). For example, a PTP-BL phosphatase domain-GST fusion protein is able to completely eliminate the extensive phosphorylation of endogenous proteins by the activated tyrosine kinase present in *E.Coli* TKX-1 cells (E.C., unpublished observations). Obviously, a regulatory mechanism must be involved in imposing the proper restrictions on PTP-BL's catalytic activity at endogenous sites. The modular domains, like the PDZ and FERM motifs that are present in PTP-BL, may provide this function in vivo.

PDZ motifs are small protein modules that mediate protein-protein interactions (Fanning

and Anderson, 1996; Ranganathan and Ross, 1997; Saras and Heldin, 1996) and can associate with transmembrane proteins (Sheng, 1996), cytoskeletal components (Xia et al., 1997) and signal transduction enzymes (Ranganathan and Ross, 1997). Indeed, several proteins that interact with PTP-BL PDZ motifs have been identified (Cuppen et al., 1998; Saras et al., 1997; E.C. submitted), but thus far no clues as to explain PTP-BL's subcellular localization in vivo have been identified.

The FERM domain in PTP-BL is a segment commonly found in a family of peripheral membrane proteins that function as membrane-cytoskeleton linkers (Chishti et al., 1998). This family includes erythrocyte protein 4.1, ezrin, radixin and moesin, but also the tumor suppressors Expanded and merlin and the protein tyrosine phosphatases PTP-MEG, PTPH1, PTPD1 and CDEP. The FERM domain in erythrocyte protein 4.1 binds a wide variety of molecules including ATP, PIP₂, phosphatidylserine, calmodulin, p55, glycophorin A, glycophorin C, Band 3 and CD44 (see Chishti et al., 1998 for references). Ezrin, radixin and moesin (ERMs) also function as molecular linkers that connect cell-surface transmembrane proteins to the actin cytoskeleton. The ERM subfamily members contain a C-terminal actin binding site and their N-terminal FERM domain associates with transmembrane molecules like CD44, CD43, ICAM-1 and ICAM-2 (Tsukita et al., 1997). Furthermore, the N-terminal FERM domain can associate with the C-terminal domain in an intra- or intermolecular manner. Intramolecular association would block the binding sites for transmembrane proteins and actin, and may be regulated via phosphorylation on tyrosine or threonine residues and by PIP₂ levels (Tsukita et al., 1997). The role of FERM domains in PTPs remains largely unknown, although, recently the PTPD1 FERM domain was found to associate with KIF1C, a new kinesin-like protein on ER-Golgi-like structures. However, although KIF1C is phosphorylated on tyrosine residues the physiological relevance of this modification is as yet enigmatic (Dorner et al., 1998).

Here we show, using immunofluorescence and immunoelectron microscopy, that the FERM domain in PTP-BL is necessary and sufficient for targeting the protein to the apical side of the cell, where it localizes at a typical, fixed distance from the cell membrane. Furthermore, fluorescence recovery after photobleaching (FRAP) experiments using EGFP-tagged proteins in living cells show that PTP-BL localization is dynamic. Also, two-hybrid experiments suggest a homotypic interaction of the catalytic PTP-BL phosphatase domain. We suggest that subcellular targeting of PTP-BL to a highly restricted microcompartment within the cell, together with a dimerization-induced shift in activity, may be an important determinant in confining its specificity and activity.

Results

Necessity for cellular confinement of PTP-BL catalytic activity

The importance of regulation of PTP activity becomes evident when the catalytic domain of PTP-BL is expressed as an isolated moiety in COS-1 cells, separated from the rest of the

molecule (as in construct BL-PTP, Fig. 2). Typical cellular protrusions are observed (Fig. 1A), that are not found in cells expressing the full-length protein. To demonstrate that the observed morphological effect is indeed due to PTP-BL's phosphatase activity only, a catalytically impaired mutant was constructed in which the critical aspartate residue is changed into an alanine (Flint et al., 1997). Introduction of the BL-PTP-DA mutant into COS-1 cells did not result in the typical protrusions as observed for the core PTP domain (Fig. 1B). Thus, PTP-BL sequences that precede the catalytic domain harbor regulatory potential that shield against dephosphorylating activity at ectopic sites.

The FERM domain in PTP-BL is sufficient for apical localization

The restricted localization of PTP-BL at the apical side of epithelia (Cuppen et al., 1998) suggests that subcellular targeting may contribute to the confinement of enzyme activity. To study the routing potential of PTP-BL's modular protein domains, we transiently expressed either full-length or truncated PTP-BL proteins (schematically shown in Fig. 2) in the epithelial MDCK cell line. Expression of full-length PTP-BL resulted in an apical location of the protein (Fig. 3A), nicely in line with the endogenous apical localization in epithelia observed in vivo (Cuppen et al., 1998). No canine PTP-BL could be detected in the MDCK cells by our antiserum, which was generated against protein of mouse origin. Strikingly, PTP-BL is not distributed homogeneously at the apical membrane but is seen in a rather typical punctuate pattern, reminiscent of a villi-like localization (Fig. 3A).

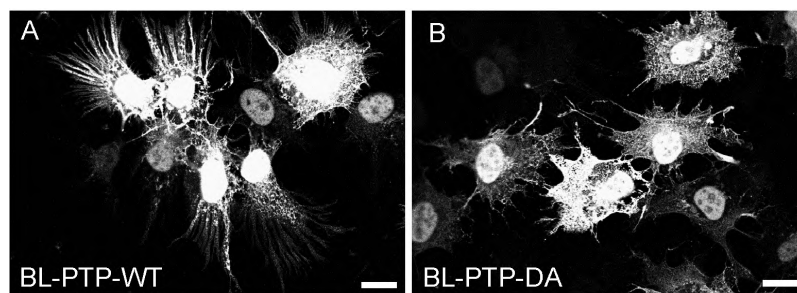


Figure 1: Overexpression of PTP domain of PTP-BL induces morphological changes in COS-1 cells. COS-1 cells were transiently transfected with an expression construct encoding VSV-tagged wild-type phosphatase domain of PTP-BL (A) or a catalytic mutant thereof (B). Expression of the tagged protein was detected using the monoclonal α -VSV antibody. Expression of the wild-type PTP domain induces typical cellular protrusions that are not seen in transfectants carrying the catalytically impaired mutant. Bars, 10 μ m.

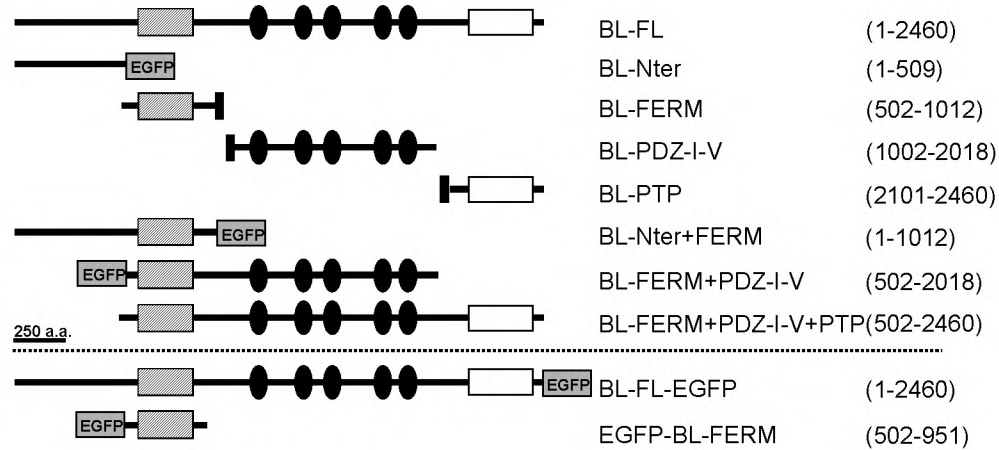


Figure 2: Overview of the PTP-BL expression constructs used.

Schematic representation of PTP-BL and the modular protein domains that can be discerned. Indicated are the protein segments, as they are produced in transient and stable (below dashed line) expression studies. In parentheses, the numbers corresponding to the first and last a.a. positions in the PTP-BL (Genbank accession Z32740) segment are shown. The gray and black box indicate the presence of an EGFP and VSV-G tag, respectively. Dashed box; FERM domain, black ovals; PDZ motifs, open box; PTP domain.

Next, we expressed VSV-G or EGFP epitope-tagged versions of the different modular domains of PTP-BL as shown in Fig. 2. When expressed as separate molecular entities, the N-terminus (Fig. 3B), the five PDZ motifs (Fig. 3D) and the PTP domain (Fig. 3E) are localized throughout the cytosol, whereas the FERM domain (Fig. 3C) shows the same apical punctuate localization as observed for full-length PTP-BL. The addition of flanking domains, i.e. the N-terminus (Fig. 3F) or the PDZ motifs (Fig. 3G), or the PDZ motifs and the catalytic PTP domain (Fig. 3H), does not alter this localization. These results clearly show that the FERM domain is both necessary and sufficient for the apical, villi-like localization of full-length PTP-BL. Expression of the FERM domain of human PTPD1 (a.a. 1-339, Genbank accession 2493260), which is 49% homologous to the FERM domain in PTP-BL, reveals a completely different, diffuse cytosolic localization pattern (data not shown), illustrating target specificity among distinct FERM domains.

Generation of stable expressing MDCK pools

To study the subcellular localization of PTP-BL in more detail, we started immuno-electron microscopy studies. Unfortunately, our antibodies against PTP-BL appeared unsuitable for this technique, excluding the direct visualization of endogenous PTP-BL in cell lines or tissues. Therefore, we decided to make use of epitope-tagged PTP-BL, also because the previous experiment had ruled out any effect by the tag on the PTP-BL localization. To

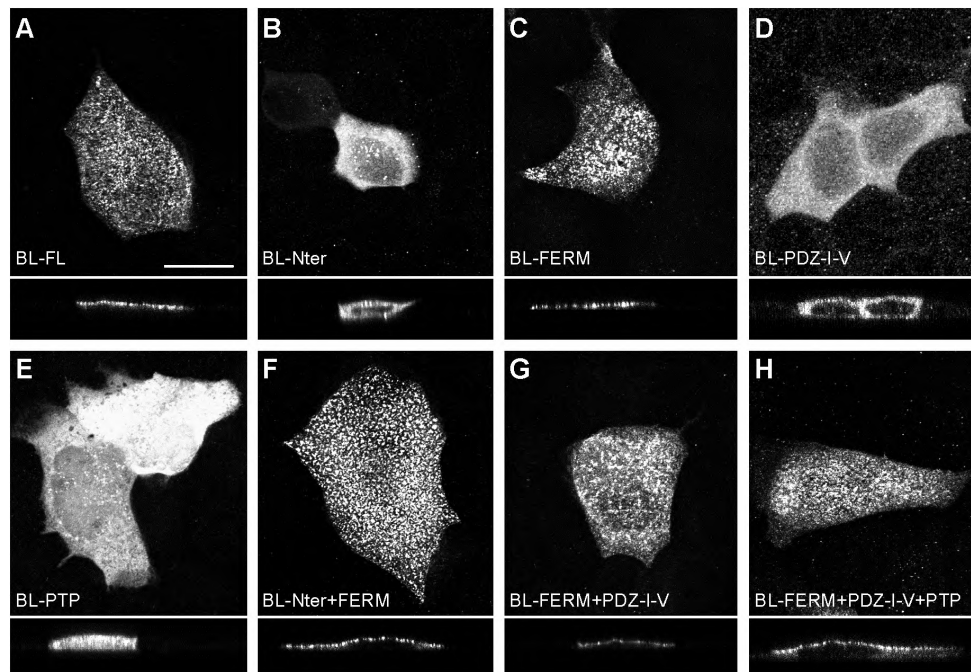


Figure 3: Apical targeting of PTP-BL is mediated by the FERM domain. Full length PTP-BL and truncated epitope-tagged modular protein domains (as shown in Fig. 2) were transiently expressed in MDCK cells and the subcellular localization was determined in confluent cultures by immunofluorescence assays and detection using confocal microscopy. The upper part of each panel represents merges of 8 to 10 horizontal optical sections and the lower part shows a vertical section through the cell. Full length PTP-BL (A) localizes apically showing a typical punctuate pattern. The N-terminus (B), the protein segment encompassing the five PDZ motifs (D) and the catalytic domain (E) localize throughout the whole cytosol, whereas the FERM domain alone (C) shows a similar localization as full length PTP-BL. The presence of flanking protein segments, like the N-terminus (F), the PDZ motifs (G) or PDZ motifs and PTP domain (H), next to the FERM domain, has no effect on the subcellular localization. Bar, 10 μ m.

overcome both the consistently low transfection efficiencies for full-length PTP-BL and the loss of transient expression during the process of polarization, we set out to generate stable expressing cell lines. Conventional attempts to accomplish this goal, using different types of vectors and epithelial cell lines, failed for unknown reasons (E.C., Derick G. Wansink, unpublished observations). We therefore adapted to the use of EGFP-tagged fusion proteins and fluorescence activated cell sorting to enrich for expressing cells. Pools of stably transfected (G418 resistant) MDCK cells were analyzed using flow cytometry (Fig. 4A) and EGFP-fluorescent cells were separated and expanded prior to subjecting them to another round of cell sorting. Starting with a pool MDCK cells in which 25% of the cells

showed detectable levels of wild-type EGFP, we obtained a mixed population consisting for 99% of high expressors after the two rounds of sorting (Figs 4A and B). The same procedure was used to obtain pools of MDCK cells that either express EGFP-tagged versions of full-length PTP-BL (BL-FL-EGFP) or of the PTP-BL FERM domain (EGFP-BL-FERM) (schematically shown in Fig.2). For EGFP-BL-FERM, we could readily obtain a population in which about 80% of cells express the fusion protein after two rounds of sorting, starting with a pool consisting for 25% of positive cells (Figs 4A and B). It is of note that the average EGFP-mediated fluorescence is much lower for the EGFP-BL-FERM expressing cells than for those containing the wild-type EGFP (Fig. 4A). Analysis of total cell lysates of both pools on Western blot shows that the proper proteins are made but that expression level of EGFP-BL-FERM is significantly lower than that for the unfused EGFP (Fig. 4C). In the case of full-length PTP-BL fused to EGFP, the percentage of fluorescent positive cells in the unsorted pool is very low (0.4%) when compared to the pools expressing EGFP or EGFP-BL-FERM (25%) (Figs 4A and B). Clearly, BL-FL-EGFP positive cells can be distinguished using flow cytometry (Fig. 4A), but the very weak EGFP-mediated fluorescence in these cells was undetectable using (confocal) fluorescence microscopy. Nevertheless, we were able to increase the percentage of positive cells to about 50% by using two rounds of sorting. The presence of the proper fusion protein was demonstrated by an immunofluorescence assay on fixed cells (not shown) and by Western blotting (Fig. 4C) using a polyclonal antiserum (α -GFP) recognizing the EGFP moiety in the fusion protein. Note that the lane containing BL-FL-EGFP required 10-fold longer exposure than the rest of the Western blot, illustrating that the expression of full-length PTP-BL is just at the threshold of detection. In retrospect, the very low percentage of positive cells in the pool of BL-FL-EGFP before sorting and the gradual loss of expression that was observed in the sorted pools (data not shown) provide an explanation for the failure to obtain stable cell lines expressing epitope-tagged PTP-BL using the more traditional approaches.

Subcellular localization of PTP-BL

Immunofluorescent monitoring of individual cells in the sorted MDCK pools show that the EGFP-tagged fusion proteins of BL-FL and the FERM domain have an identical subcellular localization, strongly resembling that of the untagged or VSV-tagged proteins (data not shown). Based on this observation we decided to use confluent, polarized cultures of the sorted MDCK pools for immuno-electron microscopy. The EGFP-tagged proteins were visualized in ultrathin cryosections using the rabbit polyclonal antiserum α -GFP and 10 nm gold-conjugated protein A. Interestingly, EGFP-BL-FERM specific label is almost uniquely found in the apical part of the cell (Fig. 5A), with an enrichment in villi-like protrusions (Fig. 5B). Some gold particles are found in the apical cytosolic region, but the majority is located regularly spaced at a fixed distance of about 10-15 nm from the apical membrane

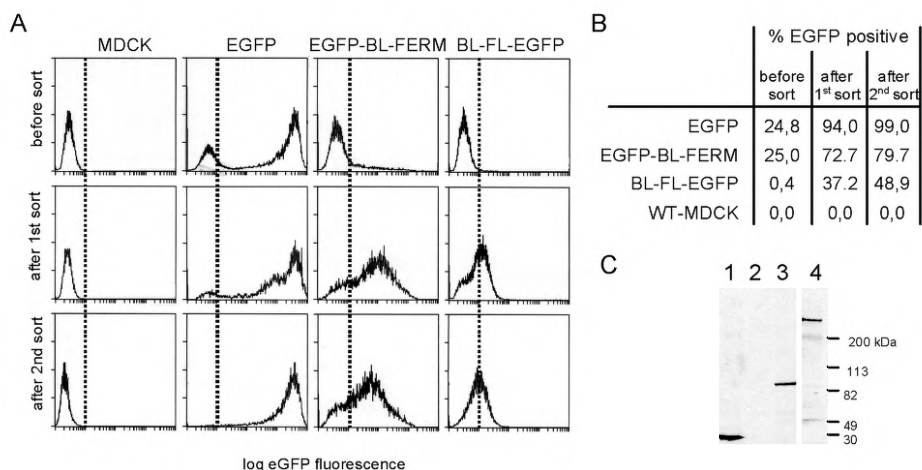


Figure 4: Analysis of MDCK pools stably expressing EGFP fusion proteins.

Flow-cytometric analysis of G418 resistant MDCK cells (A) transfected with expression constructs encoding wild type EGFP (second column), EGFP tagged FERM domain (EGFP-BL-FERM, third column) and EGFP tagged full-length PTP-BL (BL-FL-EGFP, fourth column), before sorting (first row), after one round of sorting and expansion (second row) and after two rounds of sorting and expansion (third row). As a control for the determination of endogenous fluorescence levels, untransfected MDCK cells were tested before each analysis (first column). The x-axis represents the fluorescence at 488 nm on a logarithmic scale in arbitrary units and on the y-axis the number of cells are indicated. The dotted lines indicate the fluorescence threshold for positive cells. (B) Numerical representation of the data shown in (A). After two rounds of sorting, pools of MDCK cells can be obtained, consisting of 99 % expressing cells for wild type EGFP and almost 80 and 50 % for EGFP-BL-FERM and BL-FL-EGFP, respectively. (C) Western blot analysis of the MDCK pools after two rounds of sorting. Expression of the proper EGFP fusion-protein was detected in total cell lysates using an antiserum that recognizes the EGFP moiety (α -GFP). The wild type EGFP protein (1) of 29 kDa and the EGFP fusion protein of FERM domain (3) of about 80 kDa are readily detectable (left panel), whereas detection of the full length PTP-BL fusion protein (4) (about 300 kDa) requires 10 times longer exposures, indicating a relative low expression level. As a control, a lysate of wild type MDCK cells (2) was loaded.

(Fig. 5A). No label was found at sites of cell-cell contact (not shown). For BL-FL-EGFP only a low level of labeling was found, again confirming our findings in cell extracts. Like for EGFP-BL-FERM, all immuno-gold label is found at a fixed distance from the apical membrane, although here no clear enrichment in villi was observed (Fig. 5C). In a proportion of the cells within any given preparation we could not detect any immunogold labeling, in keeping with the fact that a certain fraction of cells in the sorted pool is indeed EGFP-negative as determined by flow cytometry. This result also confirms the high specificity of the antiserum used.

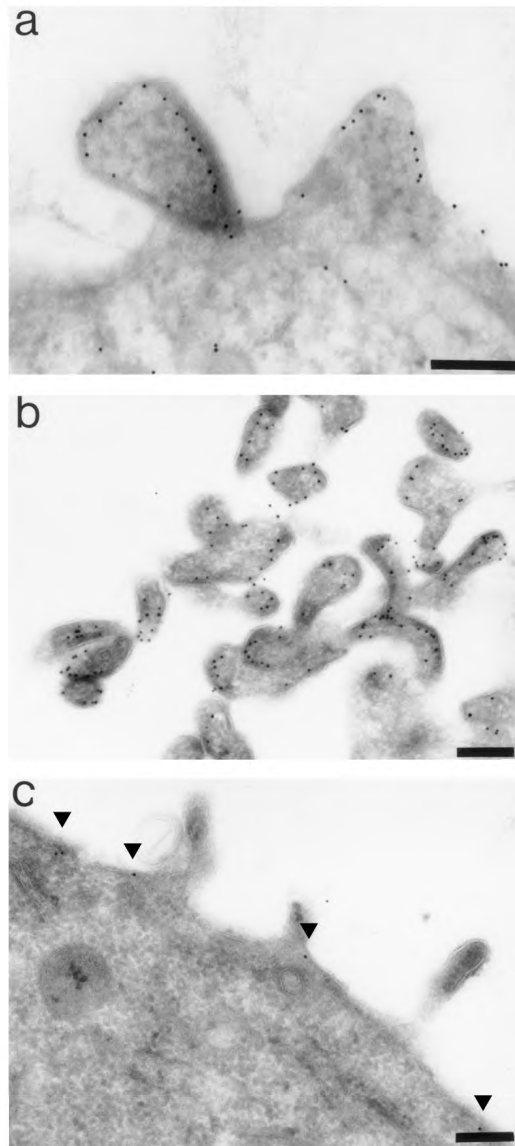


Figure 5: Ultrastructural immunolocalization of PTP-BL in transfected MDCK cells.

Sorted MDCK pools expressing EGFP fusion proteins of the FERM domain (A and B) and BL-FL (C) were used for immuno electron microscopy. Ultrathin cryosections were incubated with the polyclonal antiserum α -GFP and labeling was visualized using 10 nm gold particles, coupled to protein-A. The FERM domain of PTP-BL is localized exclusively in the apical compartment, where most label is found directly submembraneously at a typical fixed distance from the plasma membrane (A). Sections through the villi show enrichment in these structures (B). Although expression of full length PTP-BL is much lower, all labeling that is detected is located at the apical plasma membrane (C). Bars, 0.2 μ m.

No direct interaction of the FERM domain of PTP-BL with ezrin

The subcellular localization of PTP-BL shown here is reminiscent of that described for the FERM domain containing protein ezrin (Berryman et al., 1993). Because also heterooligomers of ezrin with other members of the FERM protein family have been reported (Berryman et al., 1995), we analyzed whether there could be a potential direct interaction between PTP-BL and ezrin. Immunofluorescent labeling of endogenous ezrin (Fig. 6B) in MDCK cells transiently expressing EGFP tagged BL-FERM (Fig. 6A) shows a typical

villi-like pattern for both proteins. Overlay of both pictures shows that the PTP-BL FERM domain colocalizes with ezrin at identical cellular structures although labeling intensities do not completely correlate. Similar data were obtained for full-length PTP-BL (not shown). To confirm these observations at the ultrastructural level we next used immuno-gold double labeling on ultrathin cryosections of cells in the sorted MDCK pools. To this end we used 5-nm gold to visualize ezrin and 10-nm gold for EGFP-BL-FERM (Fig. 6C). Clearly, both proteins are present in the same villi, but no extensive colocalization is observed. Since this can be due to putative steric hindrance of the immunochemicals, we additionally tested for the presence of PTP-BL and ezrin in the same multiprotein complex by co-immunoprecipitation of EGFP-BL-FERM or BL-FL-EGFP with ezrin and vice versa. For this, we used extracts prepared from the sorted MDCK pools, but there was no coordinate pull-down of both proteins under the experimental conditions used, so we must conclude that there is no evidence for a direct association between the PTP-BL FERM domain and ezrin (data not shown).

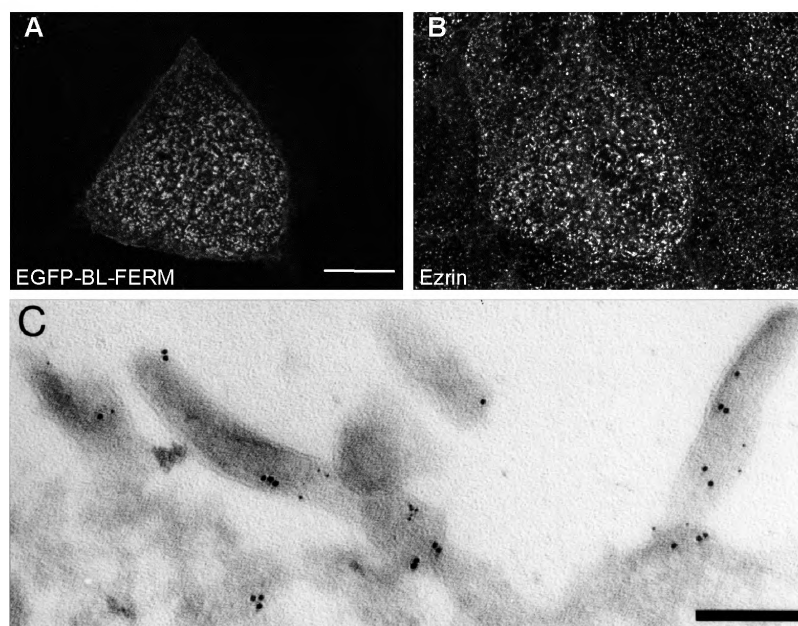


Figure 6: PTP-BL colocalizes with ezrin at the light microscopy level but not at the electron microscopy level.

Endogenous ezrin was detected in MDCK cells (B), transiently expressing an EGFP fusion protein of the FERM domain of PTP-BL. EGFP-mediated fluorescence for the FERM domain (B) overlaps with ezrin labeling in a punctate villi-like pattern. Bar, 10 μ m. (C) Immuno-gold double labeling for ezrin and EGFP-BL-FERM on ultrathin cryosections of the sorted MDCK pool. Endogenous ezrin and the FERM domain of PTP-BL are visualized with 5 nm and 10 nm gold particles, respectively. Coexpression of both proteins in the same villi is evident, but no direct colocalization is detected. Bar, 0.2 μ m.

PTP-BL dynamics

To find out whether the observed apical localization represents a stable or a dynamic distribution fluorescence recovery after photobleaching (FRAP) was used to study PTP-BL mobility dynamics in living cells. MDCK cells, transiently transfected with expression constructs encoding EGFP-tagged fusion proteins, were examined using a confocal laser scanning microscope. An initial image was captured before photobleaching. Next, part of the cell was photobleached for 10 seconds by exposure to the 488-nm laser line at full power. An averaged image was obtained immediately after photobleaching followed by a series of images with intervals of 2 minutes. For EGFP-BL-FERM, the bleaching procedure resulted in complete loss of the EGFP signal in the bleached area, whereas the EGFP-mediated fluorescence in the rest of the cell was unaffected (Fig. 7A, second frame). Within several minutes, EGFP-BL-FERM began to reappear to detectable levels in the bleached area, whereas the EGFP signal in the rest of the cell decreases. After 15 to 20 minutes about equal EGFP intensities were reached in both areas. Note that EGFP-BL-FERM reoccurs homogenous through the bleached area and does not start at the edges of the bleached region. To exclude the possibility that the reoccurrence of the EGFP-BL-FERM fluorescence was due to spontaneous fluorescence recovery or novel protein synthesis, a complete cell was bleached and monitored for EGFP labeling. No photobleaching recovery was observed for up to 30 minutes, clearly showing that the effect observed is due to exchange of fusion protein while the GFP bleaching itself is irreversible.

Identical experiments were performed with EGFP-tagged fusion proteins containing the N-terminus or the five PDZ motifs of PTP-BL, next to the FERM domain. No influence of

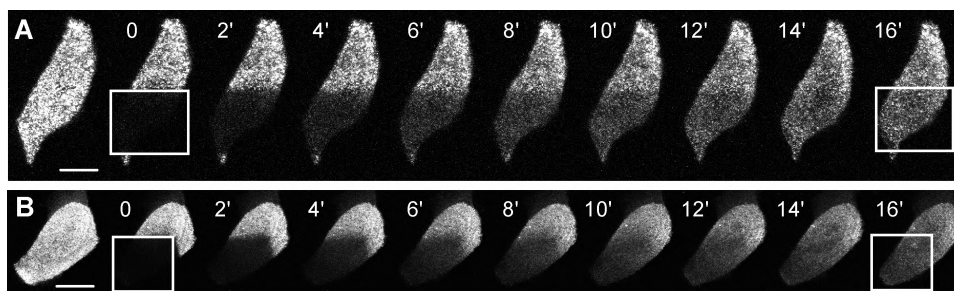


Figure 7: Fluorescence recovery after photobleaching (FRAP) reveals a dynamic cytoplasmic PTP-BL pool.

MDCK cells transiently expressing EGFP tagged versions of the FERM domain of PTP-BL (A) or full-length PTP-BL (B) were used to study the protein dynamics in living cells. Before photobleaching an image, consisting of 6 horizontal confocal sections, was acquired (first frame). Next, a region of about 1/3 of the cell (indicated by the white square) was photobleached, directly followed by the collection of images with intervals of 2 minutes. Already after 2 minutes recovery of fluorescence is evident in the bleached area, whereas almost complete redistribution is seen after 15 to 20 minutes. Bars, 10 μ m.

protein regions flanking the FERM domain in PTP-BL on the kinetics was observed. Moreover, EGFP-tagged full-length PTP-BL (EGFP-BL-FL) behaves with similar dynamics as EGFP-BL-FERM (Fig. 7B).

Homodimerization as a means to regulate PTP-BL phosphatase activity

The FRAP results and the immunoelectron microscopy findings points to the existence of a dynamic pool of cytosolic PTP-BL molecules in addition to a population of submembranous molecules which can be found at a distance of 10-15 nm from the cell membrane. Bearing in mind the morphological effects of unrestricted PTP-BL enzyme activity (Fig. 1A), the question arises whether the protein is being “captured” in two different activity-states in these distinct microenvironments. To answer this question it is important to characterize the type of intra- and intermolecular interactions in which PTP-BL is involved. For this, we used the different protein domains of PTP-BL (BL-Nter, BL-FERM, BL-PDZ-I-V and BL-PTP) as baits in the two-hybrid interaction trap and tested whether they could engage in an interaction with the PTP domain of PTP-BL (Table 1). No interaction was detectable for BL-Nter, BL-FERM and BL-PDZ-I-V, arguing against a direct role for these domains in regulating PTP-BL's catalytic activity. Also, the testing of single PDZ motifs did not reveal an interaction. However, we did observe a weak but significant homophilic interaction for the PTP-BL PTP domain (Table 1). This interaction is not affected by a mutation in the catalytic domain (PTP-DA) and therefore not dependent on enzymatic performance. Similar as for CD45 and RPTP α (Bilwes et al., 1996; Majeti et al., 1998), dimerization of the catalytic domain may thus result in inactivation of phosphatase activity.

Table 1. Two-hybrid interaction trap assays to test for interactions between the modular domains of PTP-BL with its catalytic domain.

	BL-PTP-WT	BL-PTP-DA	pJG4-5
BL-Nter	-	-	-
BL-FERM	-	-	-
BL-PDZ-I-V	-	-	-
BL-PTP	+	+	-
pEG202	-	-	-

Baits (left column) and preys (top row) combinations were tested for interaction as determined by growth on leucine deficient plates and β -galactosidase activity on X-gal plates. Empty bait (pEG202) and prey (pJG4-5) were used as controls. +, interaction (blue colonies after 5 days); -, no interaction (no blue colonies after 8 days).

Discussion

Relatively little is known about the biological function and substrate specificity of individual members of the family of PTPs. In part this is due to the difficulty in generating PTP overexpressing cell lines. Also in the case of PTP-BL only very low levels of overexpression could be achieved in transient assays or when generating stable expressing pools using EGFP-mediated cell sorting. Intriguingly, we found it impossible to generate stable expressing MDCK cells for catalytically impaired mutants of PTP-BL using the same strategy (E.C. unpublished observations). This suggests a dominant effect of the mutations, probably caused by substrate trapping (Flint et al., 1997), and points to an essential role for PTP-BL in cell survival or proliferation. In contrast to these *in vitro* data, ablation of PTP-BL catalytic activity in transgenic mice shows no overt effects (Thomas et al., 1998).

Although several PTPs have been shown to exhibit extremely stringent substrate specificity *in vivo*, *in vitro* most PTPs display only modest amino acid sequence specificity using phosphopeptides as substrates (reviewed in Zhang, 1998). We found that in COS-1 cells overexpression of the catalytic domain of PTP-BL results in dramatic changes in cell morphology (Fig. 1). Almost certainly the formation of prominent membrane protrusions is not a natural response with relevance for normal cellular behavior, but the observations do stress the importance of tight control of enzymatic activity of the phosphatase domain. Strikingly, in our experiments we did not see these effects when full-length PTP-BL was overexpressed in COS-1 cells, suggesting that elements regulating enzyme activity and/or specificity are present in the intact protein. The identification and characterization of these elements forms therefore one of the main aims in our study. We here demonstrate that the FERM domain is the primarily responsible element for apical targeting of PTP-BL in polarized epithelial cells (Fig. 3). FERM domains in band 4.1, ezrin, radixin and moesin bind to transmembrane proteins like CD44, CD43, ICAM-1 and 2 (Yonemura et al., 1998). If the PTP-BL FERM domain has the same properties and therefore engages in the same type of molecular association, it would explain in part the submembranous localization of PTP-BL. Unfortunately, direct evidence for this hypothetical model is lacking at present. Moreover, another phosphatase, PTPD1, associates with the microtubule motor protein KIF1C via its FERM domain and localizes to ER-Golgi like subcellular structures (Dorner et al., 1998), precluding on the variability in binding properties that FERM domains may display.

Furthermore, it is of note that that the FERM domains in ezrin, radixin, moesin and merlin can engage in intra- or intermolecular binding with C-terminal domains in these proteins, thereby forming either monomers or concatamers (reviewed in Tsukita et al., 1997). This is particularly interesting, as the villi-like appearance of PTP-BL localization is reminiscent of that of ezrin. This notion triggered us to study a potential direct interaction between the BL-FERM domain and ezrin but we were unable to obtain supportive evidence for this model by co-immunoprecipitation from stable expressing MDCK pools. Also, data from

immunoelectron microscopy suggest that PTP-BL is not incorporated in the structures containing head-to-tail ezrin oligomers at the plasma membrane (Tsukita et al., 1997). At present we cannot exclude association of PTP-BL with other ERM family members.

So although the precise composition of the structure in which PTP-BL is embedded remains enigmatic, the typical subcellular localization pattern, at a constant distance from the cell membrane, that is observed for BL-FERM (Fig. 5) does provide strong evidence for it being a component of a highly organized, probably membrane- or cyto-skeletal linked, structure. FRAP experiments, however, show that PTP-BL is redistributed through the cell within 20 minutes (Fig. 7). These observations may either indicate that PTP-BL is highly mobile or that the PTP-BL-containing structures are constantly formed and degraded. Although the fluorescent signal in the bleached area reoccurs in the same typical punctuate pattern as before photobleaching, we cannot conclude from our data whether the individual spots represent still the same villi-like structures or are ones that are newly formed. The identical kinetics for BL-FERM and BL-FL in the FRAP experiments even leaves open the possibility that a large multiprotein complex, including previously described PTP-BL associated proteins, relocates in the cell.

Several clues about the mechanism of relocation of PTP-BL are obtained from the FRAP experiments. Firstly, we noted that the reoccurrence of fluorescence does not start at the borders of the bleached area, but rather results from a gradual increase of signal that is equally distributed throughout the entire surface. These observations argue against lateral movement as the dominant event. Rather it suggests a mechanism of relocation whereby a soluble pool in the cytosol is involved in replenishing the bleached pool of proteins. Indeed, in our ultrastructural analyses some immuno-gold labeling is observed in the apical cytosol for EGFP-BL-FERM and these signals could potentially represent protein that is in transit between the cytosolic and subcortical pools. In addition, preliminary FRAP results indicate slower relocation of catalytically impaired mutants, suggesting that reversible tyrosine phosphorylation may play a role in the dynamics of the exchange process. This is also supported by the observation that the FERM domain of PTP-BL is phosphorylated on tyrosine residues *in vivo* (E.C. unpublished observations).

If PTP-BL relocates dynamically between different sites, it would, at least temporarily, be released from its microenvironmental constraints. It seems therefore appropriate to expect that alternative regulatory principles are subjected on the enzyme while at different sites. One example of a mechanism involved in fine-tuning of enzymatic activity is found in SHP-2 where an intramolecular interaction between SH2 and PTP domains regulates the catalytic activity (Hof et al., 1998). Using two-hybrid interaction analysis we found no evidence in support of intramolecular interactions within the full-length PTP-BL polypeptide. Instead, we did observe a weak homotypic interaction for the catalytic PTP domain in our two hybrid assays (Table 1). This lends support to a model in which PTP-BL is subject to regulation as proposed for RPTP α (Bilwes et al., 1996) and RPTP σ (Wallace

et al., 1998), where homo- or heterotypic interactions between PTP domains may inhibit enzymatic activity by blocking the catalytic cleft. Also, there may be similarities to the ligand-induced dimerization of an EGFR-CD45 chimeric receptor which inhibited CD45 PTP function and TCR signal transduction (Majeti et al., 1998). Interestingly, in the human homologue of PTP-BL, PTPL1, a potential leucine zipper that could serve as dimerization motif can be discerned (Saras et al., 1994) but this motif is not conserved in mouse. Finally, intermolecular interactions mediated by proteins that have been found to interact with PDZ motifs in PTP-BL, like the small adapter protein RIL (Cuppen et al., 1998), the zyxin-related protein ZRP-1 (E.C., unpublished data) and PARG-1 (a protein with a GTPase activating domain specific for Rho, Saras et al., 1997), could also play a role in clustering and activity-determination of PTP-BL molecules. Especially, RIL is a strong candidate. Its C-terminal LIM domain can interact with both the second and the fourth PDZ motif of PTP-BL, apparently via different interaction interfaces, enabling di- or even multimerization of PTP-BL. Interestingly, the N-terminal PDZ motif of RIL itself is competing for the same binding site and, thus, might cause dissociation of such a complex. Furthermore, since RIL is phosphorylated on tyrosine *in vivo* and is a substrate for PTP-BL (Cuppen et al., 1998), additional regulation of RIL functioning in PTP-BL aggregation is very well possible. The same line of reasoning could be followed for the role of ZRP-1, which also colocalizes with F-actin structures (Cuppen et al., unpublished).

In summary, based upon its subcellular localization and the predicted properties of its associated proteins, a role for PTP-BL in (re-)organization of the cortical (actin) cytoskeleton in or near villi, is suggested. Most likely, its function is dictated by compartmentational constraints regulated by its FERM domain. Additionally, PTP activity may be (down-) regulated by homotypic association of the catalytic domains, perhaps induced by proteins that can interact with the PDZ motifs in PTP-BL. Clearly, future experiments will be necessary to validate this model.

Acknowledgments

We thank Arie Pennings for help with flow cytometric analysis and cell sorting, Dr. Reiner Lammers for kindly providing us with PTPD1 FERM domain cDNA, Dr. Roger Brent and colleagues for providing two-hybrid vectors and yeast strains and Dr. Paul Mangeat for generously providing the α -ezrin antiserum.

Materials and Methods

Expression plasmid constructions - The cDNA restriction fragments encoding segments of PTP-BL (Genbank accession number Z32740) as indicated in Fig. 2 were subcloned in pEGFP vectors (Clontech) or in modified versions of the eukaryotic expression vector pSG5 (Green et al., 1988). In the pSG5 vector we have introduced an in-frame VSV-G epitope tag sequence to allow the production of fusion-proteins that can be detected with the α -VSV monoclonal antibody P5D4. Furthermore, we introduced either an initiator AUG codon or a stop codon for proper start or termination of translation (see also Cuppen et al., 1998). BL-PDZ-I-V and BL-PTP were tagged at their N-terminal end, whereas BL-FERM is tagged at its C-terminus. A single point mutation at amino acid 2344, aspartate to alanine, was introduced in BL-PTP by PCR using synthetic oligonucleotides, resulting in the catalytic mutant BL-PTP-DA. The BL-Nter and the BL-Nter-FERM constructs were tagged C-terminally with EGFP by subcloning into the pEGFP-N3 vector (Clontech), whereas BL-FERM+PDZ-I-V and EGFP-BL-FERM were tagged N-terminally by subcloning into the pEGFP-C1 vector (Clontech). BL-FERM+PDZ-I-V+PTP was expressed as an untagged protein from the pSG5 vector. Full-length PTP-BL cDNA, including its 3'-UTR, was inserted into pEGFP-N3, allowing the production of untagged PTP-BL (BL-FL). Subsequently, this construct was modified by PCR to generate a PTP-BL-EGFP fusion construct (BL-FL-EGFP). To this end, we introduced a XhoI site at the position of the stop codon, thereby removing the 3'-UTR including the stop codon, before introducing the EGFP moiety. Detailed cloning information can be obtained from the authors upon request.

Antibodies - The affinity-purified polyclonal antiserum α -BL-PDZ-I directed against the first PDZ motif of PTP-BL and the monoclonal α -VSV antibody P5D4 have been described elsewhere (Cuppen et al., 1998; Kreis, 1986). The polyclonal antiserum directed against ezrin was a kind gift of Dr. Paul Mangeat (Montpellier, France). The polyclonal antiserum α -GFP was obtained by immunizing a rabbit with a GST-EBFP (Enhanced Blue Fluorescent Protein) fusion protein (Cuppen et al., submitted). The resulting antiserum was found to recognize also the widely used EGFP (Enhanced Green Fluorescent Protein) in Western blotting, immunofluorescence and immunoprecipitation experiments with high specificity.

Tissue culture and transient cell transfection - COS-1 cells were cultured in DMEM/10% fetal calf serum (FCS). For each assay, 1.5×10^6 cells were electroporated at 0.3 kV and 125 μ F using the Bio-Rad GenePulser with a 4-mm electroporation cuvette, in 200 μ l of phosphate-buffered saline (PBS) containing 10 μ g of plasmid DNA. Cells were seeded in 24 wells plates on 14-mm diameter glass coverslips coated with poly-L-lysine, cultured for 24 hours in DMEM/10% fetal calf serum and subsequently used for immunofluorescence analysis. MDCK cells (type II, a kind gift of K. Ekroos, Heidelberg, Germany) were cultured in DMEM/10% FCS. Prior to transfection, cells were seeded onto 14-mm diameter glass coverslips (Menzel-Gläser, Germany) in 24 wells cell culture plates. Transfection mix was made by adding 0.3 μ g plasmid DNA to 2 μ g DAC-30 (Eurogentec, Seraing Belgium) in 150 μ l OptiMEM (Gibco BRL, Gaithersburg, MD) and incubating for 30 minutes at room temperature. After replacing the culture medium on the cells (30-70% confluency) with 150 μ l fresh DMEM/10% FCS, the transfection mix (150 μ l) was added to the cells. Following a 5-hour incubation at 37°C the medium was replaced with fresh DMEM/10% FCS and incubation was prolonged overnight. The cells were subsequently used for immunofluorescence analysis.

Immunofluorescence - Cells were fixed for 10 minutes in 2% paraformaldehyde in PHEM buffer (60 mM Pipes, 25 mM Hepes pH 6.9, 10 mM EGTA, 2 mM MgCl₂) and permeabilized with 0.5% Nonidet P-40 in PBS for 5 minutes. At further steps, solutions are prepared in PBS, cells were thoroughly rinsed in PBS between stages, and incubations were performed at room temperature. Free aldehyde groups were quenched for 10 minutes in 0.1 M glycine. 50 μ l of affinity-purified rabbit α -BL-PDZ-I (1:200 dilution, Cuppen et al., 1998), rabbit polyclonal α -GFP (1:1000 dilution), rabbit polyclonal α -ezrin (1:5000 dilution) or mouse monoclonal α -VSV (P5D4, ascites fluid; 1:1000 dilution) was used for a 1 hour incubation with primary antibody. Subsequent incubation was for 1

hour with 50 μ l of FITC- or Texas Red-conjugated AffiniPure Goat anti-rabbit or Goat anti-mouse IgG (10 μ g/ml; Jackson ImmunoResearch Laboratories, Inc., West Grove, PA). Finally, coverslips were rinsed in PBS and water and mounted on glass slides by inversion over 5 μ l Mowiol mountant (Sigma Chemical Co.). Cells were examined using an MRC1000 confocal laser-scanning microscope (Bio-Rad).

Generation of stable expressing pools - MDCK cells were grown in 6-wells plates and transfected at 50-70% confluency. Transfection mix was made by adding 1.5 μ g AflIII digested (EGFP-based) plasmid DNA to 10 μ g DAC-30 (Eurogentec, Seraing Belgium) in 750 μ l OptiMEM (Gibco BRL). The mixture was incubated for 30 minutes at room temperature and then added to the wells containing cells in 750 μ l fresh DMEM/10% FCS. Following a 5-hour incubation at 37°C the medium was replaced with fresh DMEM/10% FCS and incubation was prolonged overnight. Cells were transferred to a T75 culture flask and after 6 hours selection for neomycin-resistant cells was applied (450 μ g/ml G418). Cells were grown under selection for 10-12 days and replated in T25 or T75 culture flasks (depending on the amount of colonies) when colonies became too large. Cells from one T75 culture flask (70% confluent) were collected in 1 ml PBS and used for fluorescence activated cell sorting. EGFP-mediated fluorescence was detected using the FITC-filter set on the flow cytometer (Coulter) and 2000 to 10000 positive cells were sorted, collected in 5 ml DMEM/10%FCS (without G418 selection), and reseeded in a T25 culture flask. After expansion to confluency in a T75 culture flask, cells were subjected to another round of cell sorting. Expression of the proper EGFP-fusion protein was checked by Western blotting. For this, a confluent layer of MDCK cells in a 24-well plate was lysed in 100 μ l sample buffer (50 mM Tris-HCl, pH 6.8, 100 mM dithiothreitol, 2% SDS, 0.1% bromophenol blue, 10% glycerol) and boiled for 5 minutes. Protein samples (20 μ l) were resolved by SDS-PAGE on a gradient polyacrylamide gel (4 to 15%), and transferred to nitrocellulose membranes (Hybond-C+, Amersham). Blots were blocked using 5% nonfat dry milk in TBST (10 mM Tris-HCl, pH 7.5, 150 mM NaCl, 0.05% Tween 20). One hour incubations with primary (5.000 x diluted α -GFP) and secondary (10.000 x diluted peroxidase-conjugated goat anti-rabbit IgG (Pierce)) antibody and subsequent washes were done in TBST at room temperature. Labeled bands were visualized using freshly prepared chemiluminescent substrate (100 mM Tris-HCl, pH 8.5, 1.25 mM p-coumaric acid (Sigma), 0.2 mM luminol (Sigma), and 0.009 % H₂O₂) and exposure to radiography films (X-omat, Kodak).

Immuno-electron microscopy - Ultrastructural localization studies were performed on sorted pools of stable expressing MDCK cells that were grown on polycarbonate filter (Transwell, 0.4 μ m, Costar) for five days. Cells were fixed with 1% paraformaldehyde (PFA) in PHEM buffer (60 mM Pipes, 25 mM Hepes pH 6.9, 10 mM EGTA, 2 mM MgCl₂) for 1 hour, and stored until use in 1% PFA. Filters were stacked in 10% gelatin and fixed in 1% PFA for 24 hours. Ultrathin cryosectioning was performed as described before (Fransen et al., 1985). Sections were incubated with the polyclonal antiserum α -GFP (1:1000 dilution), followed by a rabbit polyclonal serum against mouse IgG (Dako A/S, Glostrup, Denmark) and protein A complexed to 10 nm gold particles (Fransen et al., 1985). For simultaneous detection of EGFP-tagged protein and endogenous ezrin, sections were first incubated with the polyclonal antiserum against ezrin (1:200) and Protein A complexed to 5 nm gold particles. This was followed by a second incubation with biotinylated anti-GFP (1:100), streptavidin and biotinylated BSA complexed to 10 nm gold particles (Komuves and Heath, 1992). Electron microscopy was performed with a JEOL 1010 electron microscope operating at 80 kV.

Fluorescence recovery after photobleaching (FRAP) - FRAP studies were performed using transiently transfected MDCK cells (see above) that were grown for 24 hours on 24-mm diameter glass coverslips (Menzel Gläser). Cells were cultured and measured in DMEM without phenol red (Gibco) in the presence of 10% fetal calf serum, and analyzed in a temperature-controlled chamber using a MRC1000 confocal laser scanning microscope (BioRad). An initial image (composed of 6 optical sections) was acquired, and a selected area was photobleached for 10 seconds using the 488-nm line of the krypton/argon laser at full power (5 mW). Immediately after the bleaching process, images (composed of 6 optical sections) were collected at 2 minutes intervals.

Interaction trap assay - Plasmid DNAs and the yeast strain used for the interaction trap assay were generously provided by Dr. Roger Brent and colleagues (Massachusetts General Hospital, Boston, MA) and used as described (Gyuris et al., 1993). Construction of the bait plasmids BL-FERM (also named BL-band 4.1), BL-PDZ-I-V and BL-PTP is described elsewhere (Cuppen et al., 1998). The bait BL-Nter (a.a. 1 to 509) and the prey BL-PTP (a.a. 2101-2460) constructs were generated by introducing appropriate restriction fragments of full-length PTP-BL (Genbank accession number Z32740) in the pEG202 and pJG4-5 plasmid, respectively. For the prey construct BL-PTP-DA the insert from the pSG-based expression construct VSV-BL-PTP-DA (see above) was introduced into the pJG4-5 vector. For detection of two-hybrid interactions, bait and prey plasmids were transfected in yeast strain EGY48 containing the LacZ reporter plasmid pSH18-24. Interactions were validated by growth and blue coloring on minimal agar-plates lacking histidine, tryptophan, uracil and leucine, and containing 2% galactose, 1% raffinose and 80 µg/ml X-gal, buffered at pH 7.0.

References

- Banville, D., Ahmad, S., Stocco, R. and Shen, S. H. (1994). A novel protein-tyrosine phosphatase with homology to both the cytoskeletal proteins of the band 4.1 family and junction-associated guanylate kinases. *J. Biol. Chem.* *269*, 22320-22327.
- Berryman, M., Franck, Z. and Bretscher, A. (1993). Ezrin is concentrated in the apical microvilli of a wide variety of epithelial cells whereas moesin is found primarily in endothelial cells. *J. Cell Sci.* *105*, 1025-1043.
- Berryman, M., Gary, R. and Bretscher, A. (1995). Ezrin oligomers are major cytoskeletal components of placental microvilli: a proposal for their involvement in cortical morphogenesis. *J. Cell Biol.* *131*, 1231-1242.
- Bilwes, A. M., Hertog, J. d., Hunter, T. and Noel, J. P. (1996). Structural basis for inhibition of receptor protein-tyrosine- α phosphatase by dimerization. *Nature* *382*, 555-559.
- Chida, D., Kume, T., Mukoyama, Y., Tabata, S., Nomura, N., Thomas, M. L., Watanabe, T. and Oishi, M. (1995). Characterization of a protein tyrosine phosphatase (RIP) expressed at a very early stage of differentiation in both mouse erythroleukemia and embryonal carcinoma cells. *FEBS Lett.* *358*, 233-239.
- Chishti, A. H., Kim, A. C., Marfatia, S. M., Lutchman, M., Hanspal, M., Jindal, H., Liu, S.-C., Low, P. S., Rouleau, G. A., Mohandas, N. et al. (1998). The FERM domain: a unique module involved in the linkage of cytoplasmic proteins to the membrane. *Trends Biochem. Sci.* *23*, 281-282.
- Cuppen, E., Gerrits, H., Pepers, B., Wieringa, B. and Hendriks, W. (1998). PDZ motifs in PTP-BL and RIL bind to internal protein segments in the LIM domain protein RIL. *Mol. Biol. Cell* *9*, 671-683.
- Dorner, C., Ciossek, T., Muller, S., Moller, N. P. H., Ullrich, A. and Lammers, R. (1998). Characterization of KIF1C, a new kinesin-like protein involved in vesicle transport from the Golgi apparatus to the endoplasmic reticulum. *J. Biol. Chem.* *273*, 20267-20275.
- Fanning, A. S. and Anderson, J. M. (1996). Protein-protein interactions: PDZ domain networks. *Curr. Biol.* *6*, 1385-1388.
- Flint, A. J., Tiganis, T., Barford, D. and Tonks, N. K. (1997). Development of substrate trapping mutants to identify physiological substrates of protein tyrosine phosphatases. *Proc. Natl. Acad. Sci. USA* *94*, 1680-1685.
- Fransen, J. A. M., Ginsel, L. A., Hauri, H. P., Sterchi, E. and Blok, J. (1985). Immunoelectronmicroscopical localization of a microvillus membrane disaccharidase in the human small-intestinal epithelium with monoclonal antibodies. *Eur. J. Cell Biol.* *38*, 6-15.
- Green, S., Issemann, I. and Sheer, E. (1988). A versatile in vivo and in vitro eukaryotic expression vector for protein engineering. *Nucl. Acids Res.* *16*, 369.
- Gyuris, J., Golemis, E., Chertkov, H. and Brent, R. (1993). Cdi1, a human G1 and S phase protein

- phosphatase that associates with Cdk2. *Cell* *75*, 791-803.
- Hendriks, W., Schepens, J., Bächner, D., Rijss, J., Zeeuwen, P., Zechner, U., Hameister, H. and Wieringa, B. (1995). Molecular cloning of a mouse epithelial protein-tyrosine phosphatase with similarities to submembranous proteins. *J. Cell. Biochem.* *59*, 418-430.
- Hof, P., Pluskey, S., Dhe-Paganon, S., Eck, M. J. and Shoelson, S. E. (1998). Crystal structure of the tyrosine phosphatase SHP-2. *Cell* *92*, 441-450.
- Hoffmann, K. M., Tonks, N. K. and Barford, D. (1997). The crystal structure of domain 1 of receptor protein-tyrosine phosphatase mu. *J. Biol. Chem.* *272*, 27505-17508.
- Hunter, T. (1996). Tyrosine phosphorylation: Past, present and future. *Biochemical Society Transactions* *24*, 307-327.
- Hunter, T. (1998). The Croonian Lecture 1997. The phosphorylation of proteins on tyrosine: its role in cell growth and disease. *Philos. Trans. R. Soc. Lond. B. Biol. Sci.* *353*, 583-605.
- Komuves, L. G. and Heath, J. P. (1992). Uptake of maternal immunoglobulins in the enterocytes of suckling piglets: improved selection with a streptavidin-biotin bridge gold technique. *J. Histochem. Cytochem.* *40*, 1637-1646.
- Kreis, T. E. (1986). Microinjected antibodies against the cytoplasmic domain of vesicular stomatitis virus glycoprotein block its transport to the cell surface. *EMBO J.* *5*, 931-941.
- Lemmon, M. A. and Schlessinger, J. (1994). Regulation of signal transduction and signal diversity by receptor oligomerization. *Trends Biochem. Sci.* *19*, 459-463.
- Maekawa, K., Imagawa, N., Nagamatsu, M. and Harada, S. (1994). Molecular cloning of a novel protein-tyrosine phosphatase containing a membrane-binding domain and GLGF repeats. *FEBS Lett.* *337*, 200-206.
- Majeti, R., Bilwes, A. M., Noel, J. P., Hunter, T. and Weiss, A. (1998). Dimerization-induced inhibition of receptor protein tyrosine phosphatase function through an inhibitory wedge. *Science* *279*, 88-91.
- Mauro, L. J. and Dixon, J. E. (1994). 'Zip codes' direct intracellular protein tyrosine phosphatases to the correct cellular 'address'. *Trends Biochem. Sci.* *19*, 151-155.
- Ninfa, E. G. and Dixon, J. E. (1994). Protein tyrosine phosphatases in disease processes. *Trends Cell Biol.* *4*, 427-430.
- Ranganathan, R. and Ross, E. M. (1997). PDZ domain proteins: Scaffolds for signaling complexes. *Curr. Biol.* *7*, R770-R773.
- Saras, J., Claesson Welsh, L., Heldin, C. H. and Gonez, L. J. (1994). Cloning and characterization of PTPL1, a protein tyrosine phosphatase with similarities to cytoskeletal-associated proteins. *J. Biol. Chem.* *269*, 24082-24089.
- Saras, J., Franzen, P., Aspenstrom, P., Hellman, U., Gonez, L. J. and Heldin, C. (1997). A novel GTPase-activating protein for Rho interacts with a PDZ domain of the protein-tyrosine phosphatase PTPL1. *J. Biol. Chem.* *272*, 24333-24338.
- Saras, J. and Heldin, C.-H. (1996). PDZ domains bind carboxy-terminal sequences of target proteins. *Trends Biochem. Sci.* *21*, 455-458.
- Sato, T., Irie, S., Kitada, S. and Reed, J. C. (1995). FAP-1: a protein tyrosine phosphatase that associates with Fas. *Science* *268*, 411-415.
- Sheng, M. (1996). PDZs and receptor/channel clustering: rounding up the latest suspects. *Neuron* *17*, 575-578.
- Thomas, S. M. and Brugge, J. S. (1997). Cellular functions regulated by Src family kinases. *Annu. Rev. Cell Dev. Biol.* *13*, 513-609.
- Thomas, T., Voss, A. K. and Gruss, P. (1998). Distribution of a murine protein tyrosine phosphatase BL-beta-galactosidase fusion protein suggests a role in neurite outgrowth. *Dev. Dynamics* *212*, 250-257.
- Tsukita, S., Yonemura, S. and Tsukita, S. (1997). ERM proteins: head-to-tail regulation of actin-plasma membrane interaction. *Trends Biochem. Sci.* *22*, 53-58.
- Wallace, M. J., Fladd, C., Batt, J. and Rotin, D. (1998). The second catalytic domain of protein

- tyrosine phosphatase δ (PTP δ) binds to and inhibits the first catalytic domain of PTP σ . *Mol. Cell Biol.* *18*, 2608-2616.
- Weiss, A. and Schlessinger, J. (1998). Switching signals on or off by receptor dimerization. *Cell* *94*, 277-280.
- Xia, H., Winokur, S. T., Kuo, W.-L., Altherr, M. R. and Brecht, D. S. (1997). Actinin-associated LIM Protein: Identification of a Domain Interaction between PDZ and Spectrin-like Repeat Motifs. *J. Cell Biol.* *139*, 507-515.
- Yonemura, S., Hirao, M., Doi, Y., Takahashi, N., Kondo, T., Tsukita, S. and Tsukita, S. (1998). Ezrin/Radixin/Moesin (ERM) proteins bind to a positively charged amino acid cluster in the juxta-membrane cytoplasmic domain of CD44, CD43, and ICAM-2. *J. Cell Biol.* *140*, 885-896.
- Zhang, Z.-Y. (1998). Protein-tyrosine phosphatases: Biological function, structural characteristics, and mechanism of catalysis. *Crit. Rev. Biochem. Mol. Biol.* *33*, 1-52.

Chapter 3

No evidence for involvement of mouse protein tyrosine phosphatase-BAS-like / Fas-associated phosphatase-1 in Fas-mediated apoptosis

Edwin Cuppen, Shigekazu Nagata, Bé Wieringa, and Wiljan Hendriks.

Reprinted from

The Journal of Biological Chemistry, 1997, Vol. 272, 30215-30220,

with permission by The American Society for Biochemistry and Molecular Biology, Inc.

No evidence for involvement of mouse protein tyrosine phosphatase-BAS-like / Fas-associated phosphatase-1 in Fas-mediated apoptosis

Edwin Cuppen, Shigekazu Nagata*, Bé Wieringa, and Wiljan Hendriks.

*Department of Cell Biology and Histology, Institute of Cellular Signaling, University of Nijmegen, P.O. Box 9101, 6500 HB Nijmegen, The Netherlands and *Department of Genetics, Osaka University Medical School, 2-2 Yamada-oka, Suita, Osaka 565, Japan.*

Abstract

Recently, one of the PDZ domains in the cytosolic protein tyrosine phosphatase Fas-associated phosphatase-1 (FAP-1)/PTP-BAS was shown to interact with the C-terminal *tS-L-V* peptide of the human Fas receptor (Sato, T., Irie, S., Kitada, S., and Reed, J.C. (1995) *Science* 268, 411-415), suggesting a role for protein (de)phosphorylation in Fas signaling. To investigate whether this interaction is conserved in mouse, we performed yeast two-hybrid interaction experiments and transfection studies in mouse T cell lines. For the corresponding PDZ motif in the mouse homologue of FAP-1/PTP-BAS, PTP-BL, only an interaction with human but not with mouse Fas could be detected. Presence of the *tS-L-V* motif proper, which is unique for human Fas, rather than the structural context of its C-terminus, apparently explains the initially observed binding. To test for functional conservation of any indirect involvement of PTP-BL in Fas-mediated signaling, we generated T lymphoma cell lines stably expressing mouse or human Fas receptor with and without PTP-BL. No inhibitory effect of PTP-BL was observed upon triggering apoptosis using mouse or human Fas-activating antibodies. Together with the markedly different tissue expression patterns for PTP-BL and Fas receptor, our findings suggest that protein tyrosine phosphatase PTP-BL does not play a key role in the Fas-mediated death pathway.

Introduction

Many signaling pathways depend upon the reversible assembly of protein complexes to evoke temporally and spatially distinct effects. Small modular protein domains like Src homology 2 (SH2) and SH3 domains and phosphotyrosine-binding (PTB) domains, were found to play an important role in signal transduction cascades (Cohen et al., 1995; Lemmon et al., 1996; Pawson, 1995). Recently, it has become clear that PDZ motifs have a

similar role (Fanning and Anderson, 1996). PDZ motifs (acronym for postsynaptic density protein PSD-95, *Drosophila* discs-large tumor suppressor DlgA, and the tight junction protein ZO-1) are now identified in a wide variety of proteins in bacteria (Ponting, 1997) and lower and higher eukaryotes (Ponting and Phillips, 1995), many of which are localized at specific regions of cell-cell contact, such as tight, septate and synaptic junctions (Woods and Bryant, 1993). For example, PDZ motifs present in membrane-associated guanylate kinase (MAGUK) family members have been found to interact with the C-terminus of diverse transmembrane proteins (Sheng, 1996), thereby inducing clustering of these proteins at specialized cell-cell junctions (Gomperts, 1996). Recent experiments demonstrate that PDZ motifs from different types of proteins can recognize unique C-terminal peptide motifs (Schepens et al., 1997; Songyang et al., 1997; Yanagisawa et al., 1997). As these interactions have been identified by screenings of peptide libraries, the in vivo relevance for most of them remains to be demonstrated. PTP-BAS (Maekawa et al., 1994), also known as hPTP1E (Banville et al., 1994) and PTPL1 (Saras et al., 1994) in humans, is one of the few PDZ containing proteins known so far that contain an active catalytic protein domain, i.e. a C-terminal protein tyrosine phosphatase domain. Recently, this protein was found to directly associate via one of its PDZ motifs to the C-terminal regulatory domain of Fas and was termed FAP-1 for Fas-associating phosphatase-1 (Sato et al., 1995). This association points to a possible link between reversible tyrosine phosphorylation and the apoptotic death cascade mediated by Fas. Activation of the Fas receptor (Itoh et al., 1991), a member of the tumor necrosis factor receptor superfamily (Smith et al., 1994) induces very rapid physiological and morphological changes in many cell types (Nagata and Golstein, 1995). The Fas receptor itself does not contain a catalytic protein domain, but in the activated conformation it recruits several proteins to the death-inducing signaling complex (Peter et al., 1996) which can trigger several proteolytic cascades and signaling pathways (Nagata, 1997). Direct association of a protein tyrosine phosphatase could have important modulatory effects on Fas signaling, and indeed a correlation between FAP-1 expression and (partial) resistance to Fas-mediated apoptosis has been noted in the human system (Sato et al., 1995).

The second PDZ motif of the five PDZ motifs as present in FAP-1 (referred to as the third out of six PDZ motifs in Sato et al., 1995 and Songyang et al., 1997) and the C-terminal 15 amino acids of Fas were found to be necessary and sufficient for the observed direct association between FAP-1 and Fas (Sato et al., 1995). Indeed, screenings of oriented peptide libraries employing the second PDZ motif of FAP-1 revealed a consensus binding sequence of $t(S/T)-X-(V/I/L)$ (Songyang et al., 1997; Yanagisawa et al., 1997) that is present in the Fas C-terminus ($tS-L-V$).

Puzzled by the considerable sequence divergence displayed by the C-terminus of Fas (Fig. 1), we set out to study whether FAP-1's presumed role in Fas signaling was evolutionary conserved. We found that mouse Fas does not interact with the mouse homologue of PTP-

BAS/FAP-1, known as PTP-BL (Hendriks et al., 1995) or RIP (Chida et al., 1995). Furthermore, studies using transformed mouse cell lines failed to demonstrate any role for PTP-BL in the regulation of Fas-mediated signaling. Our results show that the interaction between the Fas receptor and PTP-BL is not conserved between mice and men.

Human:	F	R	N	E	I	Q	S	L	V	*
Mouse:	N	E	N	E	G	Q	C	L	E	*
Rat:	N	E	N	E	G	Q	S	L	E	*
Bovine:	L	Q	N	E	N	E	N	L	V	*
							T/Sx	V	*	

Figure 1: Sequence comparison of the Fas receptor C-terminus from different species.

The last 9 amino acids of human (GenBank accession number M67454), mouse (A46484), rat (JC2395) and bovine Fas receptor (U34794) are shown and aligned with the proposed PDZ binding motif ι (T/S)-X-V (asterisks indicate the C-terminus).

Results

No interaction between mouse Fas receptor and PTP-BL

The large difference between species that is obvious in the C-terminal Fas receptor sequence (Fig. 1) prompted us to test the interaction between Fas receptor and PTP-BL using the two-hybrid interaction trap (Gyuris et al., 1993). Baits were generated containing either the complete array of PDZ motifs or individual PDZ motifs of PTP-BL and were assayed for interaction with both mouse and human Fas C-termini. An interaction of the ensemble of five PDZ motifs of PTP-BL (BL-PDZ-I-V) with the human Fas receptor could be observed, but no interaction occurred with mouse Fas receptor (Fig. 2). Assays employing single PDZ motifs only revealed an interaction for BL-PDZ-II and human Fas receptor, but this was rather weak. No interaction of mouse Fas receptor with any of the PTP-BL PDZ motifs tested was observed, nor did any of the baits activate transcription of the β -galactosidase reporter in the presence of an empty prey vector (Fig. 1).

Finally, two non-related domains, the nNOS PDZ motif, found to recognize the C-terminal ι G-(D/E)-X-V motif (Schepens et al., 1997; Stricker et al., 1997) and the RIL PDZ motif (Cuppen et al., submitted), did not interact with mouse or human Fas receptor. Another motif, the second PDZ motif of PSD95/SAP90, known to recognize ι (T/S)-X-V (Kornau et al., 1995; Niethammer et al., 1996) did interact only with the human Fas receptor (not shown; Schepens et al., 1997).

Generation of stable PTP-BL and Fas transformants

To study any functional involvement of PTP-BL in Fas-mediated apoptosis, we generated stable transformants of the mouse T cell lymphoma WR19L cell line. This cell line does not express PTP-BL (Fig. 3 C) or endogenous Fas receptor as identical flow cytometric staining profiles were obtained with (Fig. 3 A) and without the primary anti-Fas antibody (not

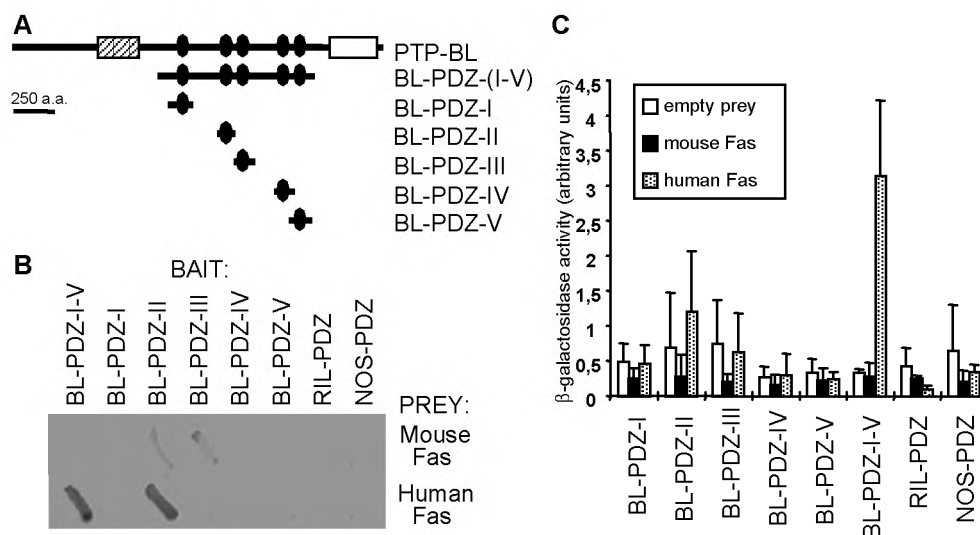


Figure 2: Two-hybrid analysis of the interaction between PTP-BL PDZ motifs and the C-terminus of mouse and human Fas receptor.

A) Schematic overview of the domain structure of PTP-BL and the protein domains used for the two-hybrid interaction analysis. B) X-gal assay plate for a two-hybrid interaction in yeast between PTP-BL PDZ motifs as baits and mouse or human Fas receptor C-termini as prey. C) Semi-quantitative analysis of the interaction strength between different PDZ motifs and mouse and human Fas receptor C-termini using the two-hybrid interaction trap. The interaction strength for mouse Fas receptor (black bar), human Fas receptor (gray bar) and empty prey vector (open bar) as a control, with the various PDZ baits, were determined by measuring the β -galactosidase activity in crude yeast lysates. Error bars indicate the standard deviation (n=5).

shown). Expression plasmids were introduced by electroporation and protein expression of Fas receptor and PTP-BL were analyzed by flow cytometric analysis and Western blotting, respectively. No endogenous Fas receptor could be detected in the wild-type WR19L cell line. Stable transformants were obtained expressing human Fas receptor in combination with (H20 and H25) or without (4B1) PTP-BL (Fig. 3A and C). Similarly transformants were generated expressing mouse Fas receptor with (M3 and M5) or without (2H2) PTP-BL (Fig. 3B and C). In addition a control line expressing PTP-BL only was generated (3C) (Fig. 3B and C). Transformants H20, H25 and M3, M5 express about equal amounts of surface-bound Fas receptor, as measured by flow cytometric analysis (Fig. 3A and B), but express different amounts of PTP-BL as determined by Western blotting (Fig. 3C).

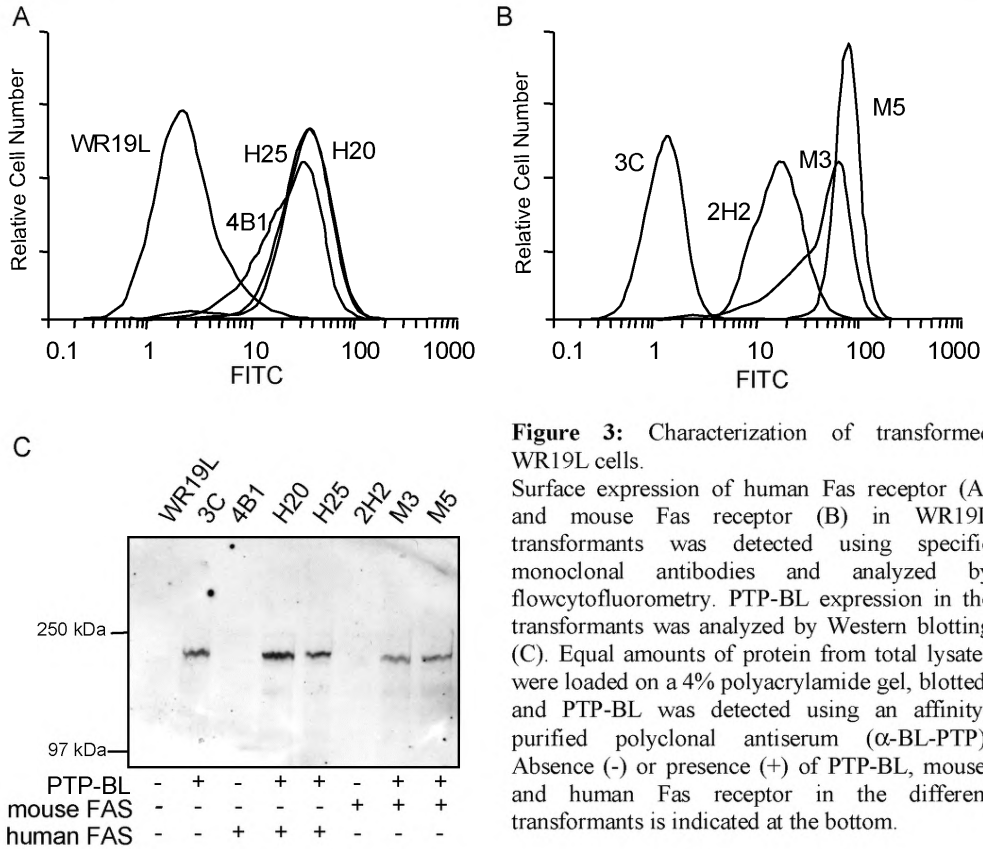


Figure 3: Characterization of transformed WR19L cells.

Surface expression of human Fas receptor (A) and mouse Fas receptor (B) in WR19L transformants was detected using specific monoclonal antibodies and analyzed by flowcytometry. PTP-BL expression in the transformants was analyzed by Western blotting (C). Equal amounts of protein from total lysates were loaded on a 4% polyacrylamide gel, blotted, and PTP-BL was detected using an affinity-purified polyclonal antiserum (α -BL-PTP). Absence (-) or presence (+) of PTP-BL, mouse, and human Fas receptor in the different transformants is indicated at the bottom.

Time response to antibody-induced Fas-mediated apoptosis

Apoptosis was triggered in the human Fas receptor transformants by adding monoclonal anti-Fas IgM (CH-11, 250 ng/ml) and apoptosis was measured at fixed time points by propidium iodide uptake and flow cytometric analysis. As expected, the wildtype cell line WR19L and the transformant that expresses PTP-BL only (3C), which both lack Fas receptor expression, do not undergo antibody-induced apoptosis (Fig. 4, A and B). The human Fas receptor-expressing transformant (4B1) undergoes rapid apoptosis, and within 8 hours over 95% of the cells have permeable membranes and take up propidium iodide, indicative for the onset of apoptosis. The transformants expressing in addition PTP-BL (H20 and H25) undergo rapid apoptosis also, although at a slightly slower pace. However, cell lines with and without PTP-BL are indistinguishable when the time points at 20 hours incubation are compared. Furthermore, no influence of the amount of PTP-BL protein expression is observed (H20 versus H25, Fig. 4A). These results indicate that PTP-BL expression has no major influence on human Fas-mediated apoptosis in mouse WR19L cells and doesn't protect against apoptosis.

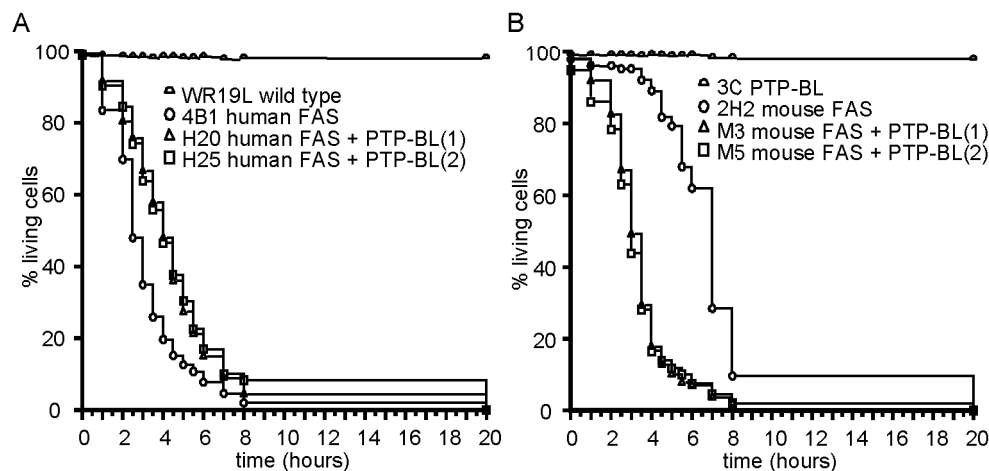


Figure 4: Time response curve of WR19L transformants upon antibody-induced Fas-mediated apoptosis.

Apoptosis mediated by the human Fas receptor (A) or the mouse Fas receptor (B) was induced by adding the monoclonal antibody CH-11 (250 ng/ml) or Jo2 (250 ng/ml) respectively. At fixed time-points cells were withdrawn and dead cells were stained by propidium iodide uptake and analyzed by flow cytometry.

A similar experiment was done with the mouse Fas receptor transformants by triggering apoptosis with the monoclonal antibody Jo2 (anti-mouse Fas). Apoptosis in the cell line expressing only mouse Fas receptor (2H2) is somewhat slower compared to human Fas mediated apoptosis. This difference may be explained by the lower surface expression of the mouse Fas receptor on 2H2 (Fig. 3B), or may be due to clonal variations or subtle differences in the way these two monoclonal antibodies induce apoptosis.

Compared with the cell line expressing only mouse Fas receptor (2H2), the transformants that express PTP-BL as well as mouse Fas receptor (M3 and M5) undergo apoptosis more rapidly (Fig. 4B), but at a rate comparable with the human Fas-mediated apoptosis (Fig. 4A). Again, comparison of the read-out upon overnight incubation of the transformants with apoptosis inducing antibody, revealed no effect of PTP-BL at all. Taken together these findings indicate that PTP-BL expression is not a significant modulatory factor in mouse or human Fas-mediated apoptosis.

Dose response to antibody-induced Fas-mediated apoptosis

Perhaps the impact of PTP-BL on Fas-mediated apoptosis is much more subtle than what was proposed for the human counterpart. Therefore, we tested for the influence of PTP-BL expression on dose-responsiveness by treating wildtype WR19L cells and its transformants overnight with increasing amounts of apoptosis inducing antibody. Even at the highest

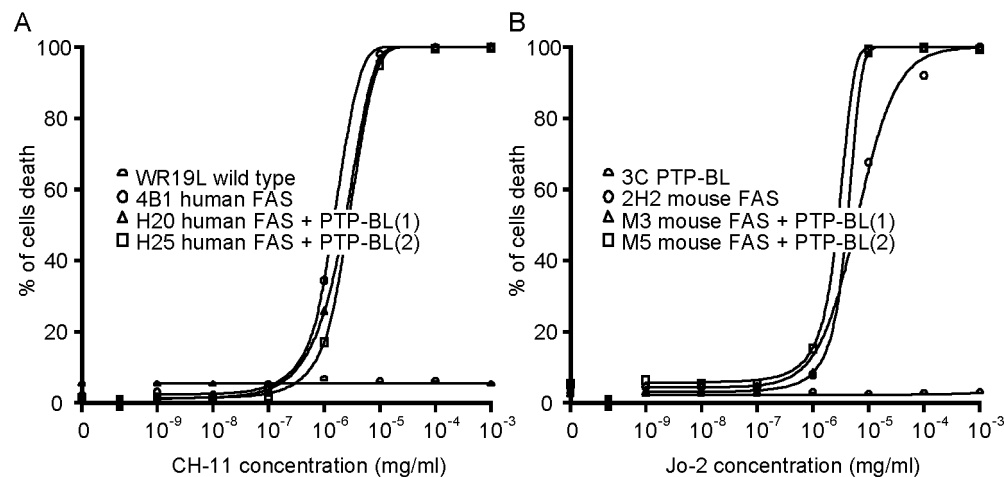


Figure 5: Dose response of WR19L transformants for antibody-induced Fas-mediated apoptosis. Apoptosis was induced in WR19L transformants expressing human Fas receptor (A) and mouse Fas receptor (B) by adding increasing amounts of monoclonal antibody (final concentration ranging from 10^{-9} to 10^{-3} mg/ml). After 20 hours dead cells were stained by propidium iodide uptake and analyzed by flow cytometry.

concentration of antibody tested, cells without Fas receptor are refractory to undergo apoptosis (Fig. 5A and B). The dose-dependent sensitivity for Fas-mediated apoptosis did not significantly differ between Fas receptor transformants with and without PTP-BL. Again, this argues against an inhibiting role of PTP-BL in Fas signaling. Moreover, the mouse Fas receptor expressing transformant seems to be slightly less sensitive without PTP-BL expression, even suggesting a small apoptosis-enhancing effect of PTP-BL.

Tissue expression patterns for PTP-BL and Fas receptor

A Northern blot of total RNA from several mouse tissues was used to determine the tissue distribution of both Fas receptor and PTP-BL. The obtained patterns are quite distinct (Fig. 6). Expression of Fas receptor is very high in lung and thymus and ubiquitously at a low level in all tissues examined. PTP-BL, on the contrary, is expressed at a high level in lung, kidney, testis, stomach, and skin (Fig. 6).

Discussion

It is now well-established that one of the functions of PDZ motifs is the recruitment of proteins via recognition-binding of their C-terminal domain (Gomperts, 1996; Songyang et al., 1997). The preferred motif in this domain has an extremely simple consensus structure (Saras and Heldin, 1996; Songyang et al., 1997). This raises the question how the cell can meet the criteria required for high specificity in binding-interaction, necessary to achieve

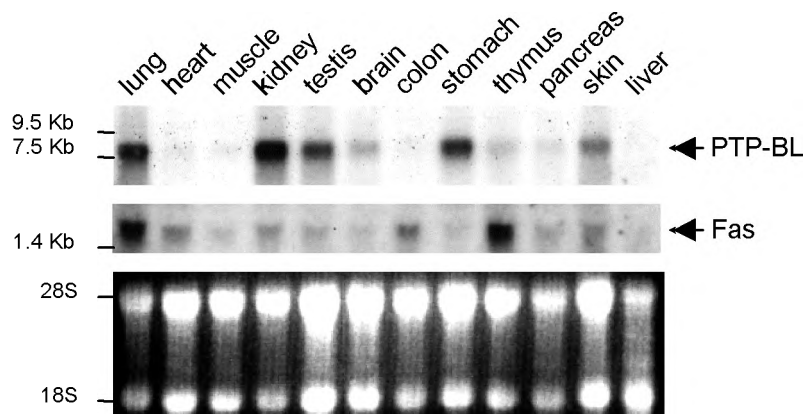


Figure 6: Tissue expression for PTP-BL and Fas receptor. Northern blot analysis of PTP-BL (upper panel) and Fas receptor (middle panel) mRNA expression in different mouse tissues. The lower panel shows an ethidium bromide staining as a control for RNA loading.

correct functioning of the cell signaling network. As a working hypothesis for the studies presented here, we assumed that there must be a strong evolutionary preference to conserve the optimal interaction-avidity between individual PDZ domains and their preferred substrate.

Interestingly, the protein tyrosine phosphatase PTP-BAS/FAP-1, which contains five PDZ motifs, was found to directly associate with the Fas receptor via its second PDZ motif. However, the C-terminus of the Fas receptor which is involved in this interaction, is not strongly conserved between species (Fig. 1). Furthermore, the amino acids demonstrated to be important for the interaction with PTP-BAS (Songyang et al., 1997; Yanagisawa et al., 1997) have been substituted in the mouse Fas receptor. To conserve the interaction, the second PDZ motif of the mouse homologue of PTP-BAS/FAP-1, PTP-BL, may have adapted to these changes. This is not very likely since this motif is very homologous between human (Maekawa et al., 1994) and mouse (Hendriks et al., 1995) (96 % identical) and bovine (GenBank accession number 915210) (98 % identical). Alternatively, the PTP-BL PDZ-II may be tolerant in peptide recognition, allowing different peptides to bind. This, however, would affect high specificity constraints necessary in signaling networks.

Our results show that PTP-BL does interact with the human Fas receptor, but fails to interact with the mouse Fas receptor. This indicates that specific peptide recognition is conserved between species and that changes, as found in the C-terminus of the Fas receptor abolishes the interaction. This last observation is in line with the tightly defined consensus motif for binding to the second PDZ domain of PTP-BAS/FAP-1, which was independently found to be *tS/TxV/I* (Songyang et al., 1997) or *tS/TxV/L/I* (Yanagisawa et al., 1997). Furthermore, none of the other PDZ motifs of PTP-BL does interact with the C-terminus of

the mouse Fas receptor, indicating that PTP-BL does not directly interact with the Fas receptor *in vivo*. This is corroborated by immunoprecipitation experiments, which failed to detect PTP-BAS/FAP-1 or an approximately 250 kDa protein in the unstimulated or stimulated Fas receptor-complex (Kischkel et al., 1995; Orlinick and Chao, 1996; Peter et al., 1996).

However, any indirect involvement of the tyrosine phosphatase PTP-BL in Fas signaling cannot be excluded, although even the basal question if tyrosine phosphorylation is involved in modulating Fas signaling is not answered yet. For tyrosine kinases as well as tyrosine phosphatases, both stimulatory and inhibitory effects on Fas-mediated apoptosis have been reported. For example, the protein tyrosine kinase Abl and the tyrosine phosphatase PTP-BAS/FAP-1 both were found to inhibit the process (McGahon et al., 1995; Sato et al., 1995), whereas another cytosolic tyrosine phosphatase, the hematopoietic cell phosphatase HCP/SHP-1, and the p59^{fyn} kinase seem to potentiate the apoptotic signal induced by Fas (Atkinson et al., 1996; Su et al., 1995). The involvement of HCP/SHP-1 remains controversial (Takayama et al., 1996). Furthermore, a rapid induction of tyrosine phosphorylation of multiple cellular proteins upon stimulation of Fas-mediated apoptosis is reported (Eischen et al., 1994). This phosphorylation as well as the apoptotic process could be blocked by inhibitors of protein tyrosine kinases in a concentration-dependent manner. Findings that a Jurkat cell variant, deficient in this elevation of tyrosine phosphorylation upon Fas-ligation, still does undergo apoptosis are contradictory to these findings (Janssen et al., 1996). Furthermore, the observed correlation between the levels of endogenous PTP-BAS/FAP-1 and resistance to Fas-mediated apoptosis in several cell lines (Sato et al., 1995), is not confirmed by others (Peter et al., 1996). Taken together, the involvement of tyrosine phosphorylation in general and certain protein tyrosine kinases and phosphatases in particular in Fas signaling remains controversial. The reported effects may be secondary downstream effects and might be cell type-specific.

Functional studies using our model system revealed no obvious role for the protein tyrosine phosphatase PTP-BL in the regulation of Fas-mediated apoptosis. A small inhibitory effect on Fas-mediated apoptosis was observed in transformants expressing human Fas receptor. In contrast, PTP-BL seems to enhance apoptosis in mouse Fas receptor expressing transformants. However, both effects are not dependent upon the expression level of PTP-BL, since transformants expressing equal amounts of Fas receptor on their surface, but expressing different amounts of PTP-BL, behave very similar. Clonal variations and differences in the amount of surface expression of Fas receptor for the transformants with and without PTP-BL, may partially account for the differences observed. Furthermore, the small inhibitory effect of PTP-BL on human Fas-mediated apoptosis may be caused by its capability to interact with the C-terminus of the human Fas receptor and thereby inhibiting the formation of a functional death-inducing signaling complex rather than its catalytic activity. This effect will not occur in the mouse system, because PTP-BL does not interact

with the mouse Fas receptor. Nevertheless, no influence of PTP-BL expression could be observed after overnight incubation with apoptosis-inducing antibodies, clearly demonstrating that PTP-BL can not (partially) protect from Fas-mediated apoptosis.

These results, combined with the different RNA expression patterns make an important role for PTP-BL in the regulation of Fas-mediated apoptosis in mouse very unlikely. In mouse the negatively regulatory C-terminus of the Fas receptor may bind other, so far unknown, proteins and perhaps in a PDZ-mediated fashion. Interestingly, we have observed that a deletion of the C-terminal region of human Fas potentiates Fas-induced apoptosis in mouse L929 cells (Itoh and Nagata, 1993). However, a similar deletion in mouse Fas did not show any effect (S.N., unpublished observations). Thus, the role of the Fas C-terminus in regulating the apoptotic process remains unclear. Furthermore, the target molecules for the PTP-BL PDZ motifs are still to be determined and will aid in elucidating its biological function.

Acknowledgments

We thank Cor Jacobs for help with flow cytometric analysis, Drs. R.L. Finley and R. Brent for providing the yeast two-hybrid interaction trap plasmids and yeast strain and Dr P. Anderson for the human Fas receptor cDNA.

Materials and Methods

Two-Hybrid Interaction Trap - Plasmid DNAs and the yeast strain used for the interaction trap assay were provided by Dr. Roger Brent and colleagues (Massachusetts General Hospital, Boston, MA) and used as described (Gyuris et al., 1993). The individual PDZ motifs of PTP-BL were cloned in the pEG202 bait vector by amplifying PTP-BL sequences using specific primers containing convenient restriction sites for cloning purposes. This results in LexA fusion proteins containing amino acids 1076-1177 (BL-PDZ-I), 1352-1450 (BL-PDZ-II), 1471-1601 (BL-PDZ-III), 1756-1855 (BL-PDZ-IV) and 1853-1946 (BL-PDZ-V) of PTP-BL. The C-terminal 60 residues of mouse Fas were cloned in the prey vector pJGBr2 by subcloning a 599 basepairs *PvuII* - *DraI* restriction fragment from pBOS-EA (Watanabe Fukunaga et al., 1992), and for the human Fas C-terminus (40 amino acids) this was done by subcloning a 120 basepairs *BglII* - *ApaI* restriction fragment from pCMV-hFAS (a kind gift of Dr. Anderson, Cambridge MA). Construction of the control baits is described elsewhere (Cuppen et al., submitted; Schepens et al., 1997)). Two-hybrid interactions were analyzed by plating yeast containing reporter, bait and prey constructs on minimal medium agar plates containing X-gal (5-bromo-4-chloro-3-indolyl β -D-galactopyranoside) and lacking tryptophane, histidine, uracil, and leucine and subsequent incubation at 30 °C for 4 days. The relative strength of two-hybrid interactions was determined by measuring the β -galactosidase activity in crude yeast lysates. For this, a single yeast colony was inoculated in 1.5 ml of minimal medium lacking histidine, tryptophan and uracil and containing 2% galactose and 1% raffinose. After overnight growth at 30 °C until the culture reached $OD_{600nm} \approx 1.0$, the cells were pelleted and resuspended in 0.2 ml of ice-cold buffer (0.1 M NaCl, 10 mM Tris-HCl pH7.0, 1 mM EDTA, 1 mM phenylmethylsulfonyl fluoride). About 100 μ l acid washed glass beads (425-600 μ m, Sigma) were added and the suspension was vortexed 6 times for 30 s alternated with 30-s incubations on ice. Lysates were centrifuged for 5 min with 14000 rpm at 4°C. Supernatants were transferred to fresh tubes and used for protein concentration determination

(Bradford, 1976). β -Galactosidase activity was measured by adding 10 μ l of lysate to 200 μ l of freshly prepared ONPG buffer (100 mM phosphate buffer pH 7.0, 1 mM MgCl₂, 10 mM KCl, 50 mM β -mercaptoethanol, 0.35 mg/ml o-nitrophenyl- β -D-galactopyranoside (Sigma)) in microtiter plates. Reactions were incubated at 30°C and the A_{420nm} was monitored for 1 h on a CERES UV900C MTP-photometer (Bio-Tek). The specific β -galactosidase activity (arbitrary units) was calculated using the initial linear part of the A_{420nm}/min curves and normalized for the protein concentration in the sample. Every sample was measured in duplicate and for each bait-prey combination, five independent colonies were assayed.

Cell lines and cell culture - Mouse T cell lymphoma WR19L cell line (ATCC TIB52) was grown in RPMI 1640 medium containing 10% fetal calf serum. Transformants expressing mouse or human Fas and PTP-BL were established by electroporation as described (Itoh et al., 1991). Briefly, 1×10^7 WR19L cells in 0.5 ml K-PBS (30.8 mM NaCl, 120.7 mM KCl, 8.1 mM Na₂PO₄, 1.46 mM KH₂PO₄) were cotransfected with 2.5 μ g/ml *PvuII* linearized pcDNA3 (Invitrogen) or pcDNA-BL (full-length PTP-BL cDNA (Hendriks et al., 1995) cloned in pcDNA3) and 25 μ g/ml *VspI* linearized pEF-F58 (Itoh et al., 1991) or pBOS-EA (Watanabe Fukunaga et al., 1992) by electroporation at 290 V with a capacitance of 960 μ F using a Gene Pulser (Bio-Rad). Cells were cultured in 40 ml of RPMI/10 % fetal calf serum in 96-well microtiter plates (0.1 ml/well) for 2 days and neomycin-resistant clones were then selected in medium containing G418 (900 μ g/ml). Cells were analyzed for PTP-BL and Fas receptor expression after 14 days of selection.

Western blot detection of PTP-BL - WR19L or derived transformed cells were lysed in buffer (10 mM Tris-HCl pH 8.0, 150 mM NaCl, 5 mM EDTA, 0.5% Nonidet P-40) for 1 h on ice and centrifuged for 10 min at 10,000 \times g. Amounts of lysate containing 25 μ g of protein were loaded in each lane of a 4 % (w/v) polyacrylamide mini-gel (BioRad) and following electrophoresis, proteins were blotted onto nitrocellulose (Amersham). The blot was blocked for 30 min in 5 % non-fat dry milk in PBST (PBS containing 0.05% Tween-20) and subsequently incubated for 1 h with affinity-purified polyclonal antibody directed against the C-terminal catalytic PTP domain of PTP-BL (Cuppen et al., submitted) in a one to thousand dilution in PBST containing 1% normal goat serum. After subsequent washings, the blot was incubated for 1 h with peroxidase-conjugated goat anti-rabbit (20,000 \times diluted, Pierce), washed and labeled bands were visualized using chemiluminescent substrate (Pierce) according to the manufacturer's instructions.

Flow cytometric analysis of surface-bound Fas receptor - Expression of Fas antigen was analyzed by incubating 5×10^5 cells in 100 μ l of IF buffer (PBS, 1% bovine serum albumine, 0.1% sodium azide) containing 0.5 μ g/ml hamster monoclonal antibody Jo2 (Ogasawara et al., 1993) for detection of mouse Fas or mouse monoclonal antibody CH-11 (Yonehara et al., 1989) for detection of human Fas, for 30 min on ice. The cells were washed twice with IF buffer and incubated with FITC-conjugated goat α -hamster-Ig (Jackson Immunoresearch, diluted 1:25 in IF buffer) or FITC-conjugated rabbit α -mouse-Ig (Dako, diluted 1:50 in IF buffer). Cells were washed and resuspended in 0.5 ml IF buffer and analyzed on a flow cytometer (Coulter).

Assay for apoptotic response - Mouse WR19L wild-type or transformed cells were seeded at 1×10^5 cells/ml in a 24-well tissue culture plate and cultured at 37°C. Cell death was induced by addition of anti-Fas monoclonal antibody (Jo2 for mouse Fas or CH-11 for human Fas expressing cells) to a final concentration ranging from 10^{-9} to 10^{-3} mg/ml. After incubation at 37°C for 1 to 20 hours, dead cells were stained by adding propidium iodide to a final concentration of 4 μ g/ml and incubating at room temperature for 10 min. The percentage of dead cells was determined by flow cytometric analysis (Coulter).

Northern blotting - Total RNA from several tissues was prepared using the guanidium isothiocyanate-phenol-chloroform extraction method (Chomczynski and Sacchi, 1987). Fifteen μ g RNA was loaded on a 1% formamide agarose gel, and after electrophoresis the RNA was transferred to nylon membrane according to standard procedures (Sambrook et al., 1989). Complete PTP-BL (Hendriks et al., 1995) and mouse Fas (Watanabe Fukunaga et al., 1992) cDNAs were radioactively labeled by random priming and used as probes for hybridization.

References

- Atkinson, E. A., Ostergaards, H., Kanes, K., Pinkoski, M. J., Caputo, A., Olszowy, M. W., and Bleackley, R. C. (1996). A physical interaction between the cell death protein Fas and the tyrosine kinase p59fynT. *J. Biol. Chem.* *271*, 5968-5971.
- Banville, D., Ahmad, S., Stocco, R., and Shen, S. H. (1994). A novel protein-tyrosine phosphatase with homology to both the cytoskeletal proteins of the band 4.1 family and junction-associated guanylate kinases. *J. Biol. Chem.* *269*, 22320-22327.
- Bradford, M. M. (1976). A rapid and sensitive method for the quantitation of microgram quantities of protein utilizing the principle of protein-dye binding. *Anal. Biochem.* *72*, 248-254.
- Chida, D., Kume, T., Mukoyama, Y., Tabata, S., Nomura, N., Thomas, M. L., Watanabe, T., and Oishi, M. (1995). Characterization of a protein tyrosine phosphatase (RIP) expressed at a very early stage of differentiation in both mouse erythroleukemia and embryonal carcinoma cells. *FEBS Lett.* *358*, 233-239.
- Chomczynski, P., and Sacchi, N. (1987). Single-step method of RNA isolation by acid guanidinium thiocyanate-phenol-chloroform extraction. *Anal. Biochem.* *162*, 156-159.
- Cohen, G. B., Ren, R., and Baltimore, D. (1995). Modular binding domains in signal transducing proteins. *Cell* *80*, 237-248.
- Eischen, C. M., Dick, C. J., and Leibson, P. J. (1994). Tyrosine kinase activation provides an early and requisite signal for Fas-induced apoptosis. *J. Immunol.* *153*, 1947-1954.
- Fanning, A. S., and Anderson, J. M. (1996). Protein-protein interactions: PDZ domain networks. *Curr. Biol.* *6*, 1385-1388.
- Gomperts, S. N. (1996). Clustering membrane proteins: It's all coming together with the PSD-95/SAP90 protein family. *Cell* *84*, 659-662.
- Gyuris, J., Golemis, E., Chertkov, H., and Brent, R. (1993). Cdi1, a human G1 and S phase protein phosphatase that associates with Cdk2. *Cell* *75*, 791-803.
- Hendriks, W., Schepens, J., Bachner, D., Rijss, J., Zeeuwen, P., Zechner, U., Hameister, H., and Wieringa, B. (1995). Molecular cloning of a mouse epithelial protein-tyrosine phosphatase with similarities to submembranous proteins. *J. Cell. Biochem.* *59*, 418-430.
- Itoh, N., and Nagata, S. (1993). A novel protein domain required for apoptosis. Mutational analysis of human Fas antigen. *J. Biol. Chem.* *268*, 10932-10937.
- Itoh, N., Yonehara, S., Ishii, A., Yonehara, M., Mizushima, S., Sameshima, M., Hase, A., Seto, Y., and Nagata, S. (1991). The polypeptide encoded by the cDNA for human cell surface antigen Fas can mediate apoptosis. *Cell* *66*, 233-43.
- Janssen, O., Lengel Janssen, B., Oberg, H. H., Robertson, M. J., and Kabelitz, D. (1996). Induction of cell death via Fas (CD95, Apo-1) may be associated with but is not dependent on Fas-induced tyrosine phosphorylation. *Immunol. Lett.* *49*, 63-69.
- Kischkel, F. C., Hellbardt, S., Behrmann, I., Germer, M., Pawlita, M., Krammer, P. H., and Peter, M. E. (1995). Cytotoxicity-dependent APO-1 (Fas/CD95)-associated proteins form a death-inducing signaling complex (DISC) with the receptor. *EMBO J.* *14*, 5579-5588.
- Kornau, H. C., Schenker, L. T., Kennedy, M. B., and Seeburg, P. H. (1995). Domain interaction between NMDA receptor subunits and the postsynaptic density protein PSD-95. *Science* *269*, 1737-1740.
- Lemmon, M. A., Ferguson, K. M., and Schlessinger, J. (1996). PH domains: diverse sequences with a common fold recruit signaling molecules to the cell surface. *Cell* *85*, 621-624.
- Maekawa, K., Imagawa, N., Nagamatsu, M., and Harada, S. (1994). Molecular cloning of a novel protein-tyrosine phosphatase containing a membrane-binding domain and GLGF repeats. *FEBS Lett.* *337*, 200-206.
- McGahon, A. J., Nishioka, W. K., Martin, S. J., Mahboubi, A., Cotter, T. G., and Green, D. R. (1995). Regulation of the Fas apoptotic cell death pathway by Abl. *J. Biol. Chem.* *270*, 22625-22631.
- Nagata, S. (1997). Apoptosis By Death Factor. *Cell* *88*, 355-365.
- Nagata, S., and Golstein, P. (1995). The Fas death factor. *Science* *267*, 1449-1456.

- Niethammer, M., Kim, E., and Sheng, M. (1996). Interaction between the C terminus of NMDA receptor subunits and multiple members of the PSD-95 family of membrane-associated guanylate kinases. *J. Neurosci.* *16*, 2157-2163.
- Ogasawara, J., Watanabe Fukunaga, R., Adachi, M., Matsuzawa, A., Kasugai, T., Kitamura, Y., Itoh, N., Suda, T., and Nagata, S. (1993). Lethal effect of the anti-Fas antibody in mice. *Nature* *364*, 806-809.
- Orlinick, J. R., and Chao, M. V. (1996). Interactions of cellular polypeptides with the cytoplasmic domain of the mouse Fas antigen. *J. Biol. Chem.* *271*, 8627-8632.
- Pawson, T. (1995). Protein modules and signalling networks. *Nature* *373*, 573-580.
- Peter, M. E., Kischkel, F. C., Hellbardt, S., Chinnaiyan, A. M., Krammer, P. H., and Dixit, V. M. (1996). CD95 (APO-1/Fas)-associating signalling proteins. *Cell Death Diff.* *3*, 161-170.
- Ponting, C. P. (1997). Evidence For PDZ Domains in Bacteria, Yeast, and Plants. *Prot. Sci.* *6*, 464-468.
- Ponting, C. P., and Phillips, C. (1995). DHR domains in syntrophins, neuronal NO synthases and other intracellular proteins. *Trends Biochem. Sci.* *20*, 102-103.
- Sambrook, J., Fritsch, E. F., and Maniatis, T. (1989). *Molecular Cloning: A laboratory manual*, 2nd Edition (Cold Spring Harbor, NY: Cold Spring Harbor Laboratory Press).
- Saras, J., Claesson Welsh, L., Heldin, C. H., and Gonez, L. J. (1994). Cloning and characterization of PTPL1, a protein tyrosine phosphatase with similarities to cytoskeletal-associated proteins. *J. Biol. Chem.* *269*, 24082-24089.
- Saras, J., and Heldin, C.-H. (1996). PDZ domains bind carboxy-terminal sequences of target proteins. *Trends Biochem. Sci.* *21*, 455-458.
- Sato, T., Irie, S., Kitada, S., and Reed, J. C. (1995). FAP-1: a protein tyrosine phosphatase that associates with Fas. *Science* *268*, 411-415.
- Schepens, J., Cuppen, E., Wieringa, B., and Hendriks, W. (1997). The neuronal nitric oxide synthase PDZ motif binds to -G(D,E)XV* carboxyterminal sequences. *FEBS Lett.* *409*, 53-56.
- Sheng, M. (1996). PDZs and receptor/channel clustering: rounding up the latest suspects. *Neuron* *17*, 575-578.
- Smith, A. C., Farrah, T., and Goodwin, R. G. (1994). The TNF receptor superfamily of cellular and viral proteins: activation, costimulation, and death. *Cell* *76*, 959-962.
- Songyang, Z., Fanning, A. S., Fu, C., Xu, J., Marfatia, S. M., Chishti, A. H., Crompton, A., Chan, A. C., Anderson, J. M., and Cantley, L. C. (1997). Recognition of unique carboxyl-terminal motifs by distinct PDZ domains. *Science* *275*, 73-77.
- Stricker, N. L., Christopherson, K. S., Yi, B. A., Schatz, P. J., Raab, R. W., Dawes, G., Bassett, D. E., Bredt, D. S., and Li, M. (1997). PDZ Domain of Neuronal Nitric Oxide Synthase Recognizes Novel C Terminal Peptide Sequences. *Nature Biotech.* *15*, 336-342.
- Su, X., Zhou, T., Wang, Z., Yang, P., Jope, R. S., and Mountz, J. D. (1995). Defective expression of hematopoietic cell protein tyrosine phosphatase (HCP) in lymphoid cells blocks Fas-mediated apoptosis. *Immunity* *2*, 353-362.
- Takayama, H., Lee, M. H., and Shirota Someya, Y. (1996). Lack of requirement for SHP-1 in both Fas-mediated and perforin-mediated cell death induced by CTL. *J. Immunol* *157*, 3943-3948.
- Watanabe Fukunaga, R., Brannan, C. I., Itoh, N., Yonehara, S., Copeland, N. G., Jenkins, N. A., and Nagata, S. (1992). The cDNA structure, expression, and chromosomal assignment of the mouse Fas antigen. *J. Immunol.* *148*, 1274-1279.
- Woods, D. F., and Bryant, P. J. (1993). ZO-1, DlgA and PSD-95/SAP90: homologous proteins in tight, septate and synaptic cell junctions. *Mech. Dev.* *44*, 85-89.
- Yanagisawa, J., Takahashi, M., Kanki, H., Yano-Yanagisawa, H., Tazunoki, T., Sawa, E., Nishitoba, T., Kamishohara, H., Kobayashi, E., Kataoka, S., and Sato, T. (1997). The molecular interaction of Fas and FAP-1. *J. Biol. Chem.* *272*, 8539-8545.
- Yonehara, S., Ishii, A., and Yonehara, M. (1989). A cell-killing monoclonal antibody (anti-Fas) to a cell surface antigen co-downregulated with the receptor of tumor necrosis factor. *J. Exp. Med.* *169*, 1747-1756.

Chapter 4

PDZ motifs in PTP-BL and RIL bind to internal protein segments in the LIM domain protein RIL

Edwin Cuppen, Herlinde Gerrits, Barry Pepers, Bé Wieringa, and Wiljan Hendriks.

Reprinted from

Molecular Biology of the Cell, 1998, Vol. 9, 671-683,

with permission by The American Society for Cell Biology.

PDZ motifs in PTP-BL and RIL bind to internal protein segments in the LIM domain protein RIL

Edwin Cuppen, Herlinde Gerrits, Barry Pepers, Bé Wieringa, and Wiljan Hendriks.

Department of Cell Biology and Histology, Institute of Cellular Signaling, University of Nijmegen, P.O. Box 9101, 6500 HB Nijmegen, The Netherlands.

Abstract

The specificity of protein-protein interactions in cellular signaling cascades is dependent on the sequence and intramolecular location of distinct amino acid motifs. We used the two-hybrid interaction trap to identify proteins that can associate with the PDZ motif-rich segment in the protein tyrosine phosphatase PTP-BL. A specific interaction was found with the LIM domain-containing protein RIL. More detailed analysis demonstrated that the binding specificity resides in the second and fourth PDZ motif of PTP-BL and the Lin-11, Isl-1, Mec-3 (LIM) domain in RIL. Immunohistochemistry on various mouse tissues revealed a submembranous colocalization of PTP-BL and RIL in epithelial cells. Remarkably, there is also an N-terminal PDZ motif in RIL itself that can bind to the RIL-LIM domain. We demonstrate here that the RIL-LIM domain can be phosphorylated on tyrosine *in vitro* and *in vivo* and can be dephosphorylated *in vitro* by the PTP domain of PTP-BL. Our data point to the presence of a double PDZ-binding interface on the RIL LIM domain and suggest tyrosine phosphorylation as a regulatory mechanism for LIM-PDZ associations in the assembly of multiprotein complexes. These findings are in line with an important role of PDZ-mediated interactions in the shaping and organization of submembranous microenvironments of polarized cells.

Introduction

Extracellular signals initiate signaling cascades within the cell by activating distinct receptor molecules on the cell surface. Signals are then propagated and amplified via specific cytosolic proteins or second messengers and ultimately are translated in specific cellular responses (Songyang and Cantley, 1995). Separate cascades in this complex signaling network depend on specific protein-protein interactions, which are mediated by different protein motifs like SH2, SH3, PID/PTB and PH domains (Cohen et al., 1995; Pawson, 1995; Lemmon et al., 1996). Reversible tyrosine phosphorylation plays an important regulatory role in signal transduction events (Hunter, 1995); for example, SH2 and PID/PTB interactions are critically dependent on this type of modification. The role of

protein tyrosine kinases in these processes has been studied extensively; target molecules have been identified and a broad range of cellular effects have been characterized. In contrast, relatively little is known about the role of protein tyrosine phosphatases (PTPs), although many different PTP family members have been isolated over the past years. PTPs contain one or two catalytic domains and a bewildering variety of protein motifs, which may serve to target the enzymes to restricted microcompartments and specific substrates within the cell (Mauro and Dixon, 1994). The current challenge is to obtain a better understanding of these features and identify subcellular compartments and binding proteins. Mouse PTP-BL (Hendriks et al., 1995) or RIP (Chida et al., 1995) is a large cytosolic PTP (Fig. 1A) containing a single catalytic tyrosine phosphatase domain and protein motifs which show similarities to both submembranous proteins and known tumor suppressor gene products. The human homologue of this protein has been termed PTP-BAS (Maekawa et al., 1994), hPTP1E (Banville et al., 1994), PTPL1 (Saras et al., 1994) and FAP-1 (Sato et al., 1995). Chromosomal localization of PTP-BAS placed the gene on 4q21, a region for which various cytogenetic abnormalities in human tumors have been reported (Inazawa et al., 1996; van den Maagdenberg et al., 1996). The PTP-BL polypeptide is split up in several distinct segments. Its N-terminus is subject to alternative splicing (Chida et al., 1995; our unpublished observations) and contains a putative leucine zipper motif (Saras et al., 1994), which may be involved in homo- or hetero-dimerization of the protein. This region is followed by a band 4.1-like domain, the common domain in the ezrin, radixin moesin family members, which is thought of as a linking segment between the actin cytoskeleton and the cell membrane (Tsukita et al., 1993). The band 4.1-like domain is also present in the product of the neurofibromatosis type 2 tumor suppressor gene, merlin or schwannomin, and in the *Drosophila melanogaster* tumor suppressor *expanded*, a protein involved in the control of cell proliferation in imaginal discs (Boedigheimer et al., 1993; Tsukita et al., 1993). At its very C-terminal end, PTP-BL harbors the tyrosine phosphatase domain that is catalytically active in vitro on artificial substrates (Hendriks et al., 1995), but in vivo substrates remain to be identified.

In between the band 4.1-like and the PTP domain PTP-BL contains five PDZ motifs. PDZ motifs, formerly referred to as GLGF repeats (Cho et al., 1992) or discs-large homologous regions (Woods and Bryant, 1993) were first identified as 90 amino acid (aa) repeats in PSD-95, DlgA and ZO-1. The *Drosophila* protein DlgA is the prototype of the family of membrane associated guanylate kinases. These proteins contain one or three N-terminal PDZ motifs, a SH3 motif and a guanylate kinase motif and are localized to specialized submembranous structures. DlgA is required for the maintenance of the septate junction structure, for the proper organization of the cytoskeleton and for apicobasal polarity of epithelial cells (Woods et al., 1996). Other members of this rapidly growing protein family were found to interact with the cytoplasmic tail (T/SxV) of Shaker-type K⁺ channels and of modulatory subunits (NR2) of NMDA-type glutamate receptors (Kim et al., 1995; Kornau

et al., 1995; Niethammer et al., 1996) and thus may play an important role in the clustering of membrane proteins (Garner, 1996; Gomperts, 1996). Recently, the molecular basis of the C-terminal peptide recognition by PDZ motifs was revealed by x-ray crystallography (Doyle et al., 1996). It appears that specific side chain interactions and a prominent hydrophobic pocket at the PDZ motif surface explain the selective recognition of the last four or five C-terminal residues of the target protein. The binding to C-terminal peptide motifs is mediated by an antiparallel interaction between β -strands and is reminiscent of the manner in which PID/PTB domains associate with phosphotyrosine-containing peptides (Doyle et al., 1996). In addition, it appears that PDZ motifs do not recognize exclusively C-terminal motifs. For example, the binding of the PDZ motif in INAD to the TRP Ca^{2+} channel is critically dependent on an interaction with an internal STV peptide (Shieh and Zhu, 1996). Furthermore, work on neuronal nitric oxide synthase (nNOS) suggests that specific PDZ motifs can recognize C-terminal peptide motifs as well as forming apparently homophilic associations with other PDZ motifs (Brenman et al., 1996; Stricker *et al.*, 1997; Schepens et al., 1997). Most recently, a PDZ motif in ALP (actinin-associated LIM protein) has been described that binds to the spectrin-like motifs of α -actinin-2 (Xia et al., 1997).

Our search for proteins that bind to the five PDZ motifs present in PTP-BL now provides evidence for yet another type of interaction that can be mediated by PDZ motifs. The second PDZ motif of PTP-BL as well as the PDZ motif of RIL (reversion induced LIM gene; Kiess et al., 1995) itself were found to bind specifically to the RIL LIM domain structure. The fourth PDZ motif of PTP-BL can also interact with RIL, but for this interaction to occur both the LIM domain and the proper C-terminus of RIL are necessary. Thus, along with PDZ-C-terminus and PDZ-internal peptides, PDZ-LIM interactions may contribute to the complex organization and dynamics of macromolecular assemblies at the cell cortex.

Results

The reversion-induced LIM-containing protein RIL interacts with PTP-BL PDZ motifs

Candidate proteins interacting with the five PDZ motifs of PTP-BL were obtained from a human G0-fibroblast cDNA library using BL-PDZ-(I-V) (Fig. 1A) as a bait in the yeast two-hybrid interaction trap (Gyuris et al., 1993). Sequence analysis showed that two independent but overlapping clones of 0.6 and 0.5 kb pairs encoding the C-terminal part of the human homologue of rat RIL were obtained (hRIL(164-330) and hRIL(188-330), respectively, Fig. 1B). RIL was originally identified as a gene which is down-regulated in H-Ras-transformed rat fibroblasts (Kiess et al., 1995). The RIL protein contains a single LIM domain at its C-terminus, which is a special double zinc finger motif implicated in protein-protein interactions in a broad range of polypeptides (reviewed by Dawid et al., 1995). The LIM domain is entirely present in our partial h-RIL cDNA clones (Figs. 1B and

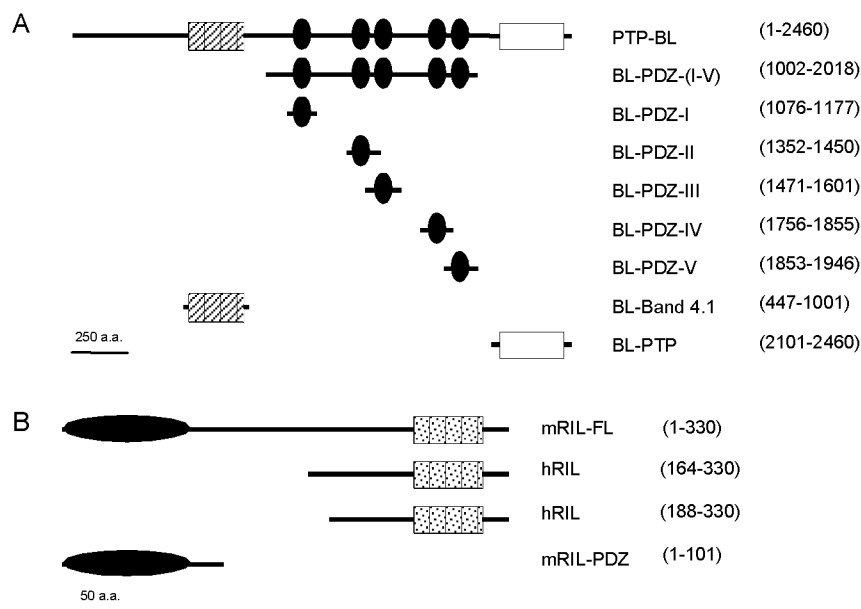


Figure 1: Schematic representation of the protein segments used in the two-hybrid interaction trap. Shown are the regions of PTP-BL (A) used as baits and the RIL segments [hRIL(164-330) and hRIL(188-330)] (B) as they were retrieved from the G0-fibroblast cDNA library and the RIL PDZ domain used as bait to assay for intramolecular interactions. In parentheses, the numbers corresponding to the first and last aa positions in the PTP-BL and RIL segments are shown. Band 4.1-like domain, hatched box; PTP, open box; PDZ motifs, black ovals; LIM domain, stippled box.

2). Comparison of the RNA in situ hybridization patterns of RIL (Kiess et al., 1995) and PTP-BL (Hendriks et al., 1995) revealed a conspicuous overlap in expression, implying that the interaction observed may indeed be of biological relevance.

To further study this interaction, a mouse fetal brain cDNA library was screened using the human 0.6 kb pair RIL cDNA insert as a probe. Two cDNAs of 1.2 and 1.5 kb pairs respectively, were obtained and their combined sequence (EMBL Nucleotide Sequence Database accession number Y08361) predicts an open reading frame resulting in a 330 aa polypeptide with a predicted molecular weight of 36,000 (Fig. 2). Transient expression of the cDNAs employing the pSG5 vector (Green, 1988) in COS-1 cells resulted in a protein product with an apparent molecular weight of 38,000. This is identical in size to endogenous RIL as detected on Western blots of several mouse tissue lysates by an affinity-purified polyclonal antiserum raised against the C-terminal half of human RIL (our unpublished results).

```

          10          20          30          40          50
mouse MTHSVTLRGP SPWGFRLVGG RDFSLLPLTIS RVHAGSKAAL AALCPGDLIQ
rat   ---A-----  -----  ---A-----  -----  -----S--
human -P-----  -----  ---A-----  -----S-  -----

          60          70          80          90          100
mouse AINGESTELM THLEAQNRIK GCHDHLTLSV SRPENKNWPS SPDD KAQAHR
rat   -----  -----  -----  -----  --N-
human -----  -----  -----  ---GRS---  A---S-----

          110         120         130         140         150
mouse IHIDPEFQDC SPATSRSSV SGISLEDNRS GLGSPYGQPP RLPVPHNGSS
rat   -----A--G -----I -----  -----  -----
human -----I--G -T-----P-G T-TGP--G-R S-----K-- CF-----

          160         ↓ 170         180         ↓ 200
mouse NEATLPAQMS ALHVSPPTSA DTARVLPRNR DCRVDLGSEV YRMLREPAEP
rat   --V--S--  -----P-- --P-I-----  -----
human -----  -----P-- -P-EA S-GA GS-----

          210         220         230         240         250
mouse TASEPKQSGS FRYLQGMLEA GEGGDRPGSG GPRNLKPAAS KLGAPLSGLQ
rat   A-----  -----  -----  -S-----  -----
human V-A-----  -----  -----W-P-- -----T--

          260         270         280         290         300
mouse GLPECTRCGH GIVGTIVKAR DKLYHPECFM CSDCGLNLKQ RGYFFLDERL
rat   -----  -----  -----  -----  -----
human -----C- -----E- -----  -----

          310         320         330
mouse YCENHAKARV KPPEGYDVVA VYPNAKVELV *
rat   -----  -----  -----
human --S-----  -----

```

Figure 2: Sequence alignment of RIL protein sequences from mouse, rat, and human. Protein sequences of mouse (acc.no. Y08361), rat (Kiess *et al.*, 1995, acc. no. X76454), and hRIL (Schaefer, unpublished, acc.no. X93510) were aligned using MULTALIGN. Aas identical to those of the mouse sequence are indicated with a dash. The PDZ motif is double underlined and the LIM domain is indicated by a single underline. Vertical arrows indicate the start positions of clones hRIL(164-330) and hRIL(188-330), which were originally identified in the two-hybrid interaction screening with the BL-PDZ-(I-V) bait. A potential tyrosine phosphorylation site is shaded.

Comparison of mouse, human and rat RIL sequences revealed a high species conservation (Fig. 2). The mouse peptide is 96 % identical to rat and 87 % to hRIL. Highest homologies were found at the N- and C-termini, suggesting a biological relevance for these regions. The C-terminal end brackets the LIM domain (aas 253-303), but in the N-terminus initially no conserved protein motif was discerned. Surprisingly, by performing more detailed database searches, we found that the N-terminal segment showed significant similarities to proteins known to contain PDZ motifs. This led to the identification of a previously undiscovered N-terminal PDZ motif (aas 4-84) in RIL (Fig. 3) that shows 40-45% homology to any of the three PDZ motifs of DlgA. It is most homologous to thus far unnoticed N-terminal PDZ motifs in CLP-36 (77%; Wang *et al.*, 1995) and enigma (67%; Wu and Gill, 1994). In the 150 aa spacer region between the PDZ motif and the LIM

```

DLG1      36 WLYEDIQLERGN-NSGLGFSTAGGTDNPH---IGTDTSYVTKLISCGAAAA
DLG2     150 PKVIEIDLKVG-GKGLGFSTAGGIGNQH---IPGDNGYVTKLTDGGRAQV
DLG3     482 REPRITITLQKG-PQGLGFNIVGGED-----GQGIYVVFILAGGPADL
consensus      V L      GLGF I GG D      V I L G A

RIL       1  MTHSVTLRGP--SPWGFRLVGGKDF-----SLPLITSRVHAGSKAAL

CLP36     1  MTTQQIVLQGP--GPWGFRLVGGKDF-----EQPLAISRVTFGSKAAI
enigma    1  MDSFKVVLKGP--APWGFRLQGGKDF-----NVPLSISRITFGGKAAQ
BL2     1353 GDTFEVELAKT-DGSLGLSVTGGVNT-----SVRHGGIVYKALIPKG-AAE
BL4     1759 EVELLITLKSE-KGSLGFIVTKGSG-----SIGCYVHDVIQD-PKKG
nNOS     13  PNVISVRLFKRVKVGGLGFLVKERVS-----KPPVITSDLRGG-AAE
BL1     1080 REITLVNKKKDPKHGLGFQIIGG-EKM----GRLDLGVFISAVTFGGPADL
BL3     1486 KIIFEVKLFKN-SSCLGFSSFSRE-DNLIP--EQINGSIVRVKLLFPQPAAE
BL5     1854 HLLPDITVTCH-GEELGFPLSGG-QGS-----PHGVVYISDINPRSAAV
LIMK1    160 HTVTLVSLPASHGKRGLSVSDPPHGGPPGCGTEHSHTVRVQGVDFGCMSPD

DLG1     -DGRISINDIIVSVND---VSVVDVPHASAVDALKKAGNVVKEVVK-RKRGTA 130
DLG2     -DGRISIGDKLIAVRTNGSEKNLENTHELAVATLKSITDKVTLIIG-KT-OHL 247
DLG3     -GSEIKRGDQLLSVNN---VNLTHATHEEAAQALKTSGGVVTLLAQYRP-BEY 570
Consensus G L  GD IL VNG      H EA  LK      V L L R E

RIL      --AALCPGDLIQAING---ESTELMTHLEAQNRIKKGCHDHLTISVS-RP-ENK 86

CLP36    --ANLCIGDLITATIDG---EDTSSMTHLEAQNRIKGCVDNMTITVS-RS-EQK 87
enigma   --AGVAVGDVWVLSIDG---ENAGSLTHLEAQNRIKACGERLSLGLS-RA-QPV 87
BL2     SDGRHKGDRVLAVNG---VSLEGATHKQAVETLRNTGQVHLLLE-KG-QVP 1444
BL4     -DGRKAGDRLLIKVND---TDVTNMTHTDAVNLLRAAPKTVRVLVVG-RILELP 1847
nNOS    QSGLIQAQDITLAVNG---RPLVDLSYDSALEVLRGIASETHVVLILRGPEGF 112
BL1     -DCLKPGDRLLISVNS---VSLEGVSHHAAVDILQNAPEVTLVVIS-QPKKP 1173
BL3     -SEKIDVGDVILKVN---APLKGLSQQDVISALRGTAPVSVLLC-RPAPGV 1581
BL5     -DGLQLLDIHYVNG---VSTQGMTLEDANRALDLSLPSVVLKVT-RDGCVP 1945
LIMK1   VKNSLHVGDRIILENG---TPIRNVPLDEIDLLIQETSRLLOITLE-HDPHDT 260

```

Figure 3: Multiple alignment of PDZ motifs.

The PDZ motif of mouse RIL is aligned with the PDZ motifs of *Drosophila* DlgA (DLG1, DLG2 and DLG3; acc.no. M73529), mouse PTP-BL (BL1 through 5; acc.no. Z32740), rat CLP36 (acc.no. U23769), human enigma (PIR:A55050), mouse nNOS (acc.no. D14552) and mouse LIMK1 (acc.no. X86569). The position number of the initial and last aa of the protein segments that were used are shown on either side of the sequence. Sequences presented below RIL are ordered by descending homology. Aas similar (score >0.7 in Dayhoff table (Schwartz and Dayhoff, 1979) in 9 of 13 sequences are shown on a gray background, and the most frequent aa at these positions is indicated in the consensus line. Aas identical in more than half of the sequences are indicated in white on a black background. Dashes represent sequence gaps.

domain of RIL, the identity between species is much lower and no protein motifs could be identified. Interestingly, a potential tyrosine phosphorylation site ([RK]-x(2,3)-[DE]-x(2,3)-Y) was found within the LIM domain (Y-274).

Both the second and fourth PTP-BL PDZ motif can interact with RIL

To narrow down the areas involved in the PTP-BL - RIL interaction, single BL-PDZ motifs were fused to the LexA bait (Fig. 1A) and assayed for an interaction with both the partial hRIL clone [hRIL(164-330)] and mRIL-FL in the yeast two-hybrid interaction trap (Fig. 4).

None of the baits used was able to activate transcription without prey (our unpublished results) or with an empty prey vector present (Fig. 4). For an interaction with hRIL(164-330) and mRIL-FL to occur the presence of the second (aas 1352-1450) or the fourth (aas 1756-1855) PDZ motif of PTP-BL was both necessary and sufficient. Furthermore, no interaction could be observed between RIL and the band 4.1-like domain or the PTP domain of PTP-BL (Fig. 4). This does not necessarily imply, however, that RIL is not a substrate for PTP-BL. Tyrosine phosphorylation levels are extremely low in yeast and proper phosphorylation of RIL may be a necessary prerequisite for such an interaction.

Interestingly, the interaction appears weaker if a single PDZ motif is used as a bait compared with the bait containing the five PDZ motifs [BL-PDZ-(I-V)]. This difference may be explained by the ability of BL-PDZ-(I-V) bait to bind more than one prey protein, leading to stronger transcription activation of the reporter and thereby to a higher β -galactosidase activity in this assay. Another explanation may be that the second and fourth PTP-BL PDZ motifs bind in a cooperative way to one RIL molecule, thereby stabilizing the interaction. Finally, BL-PDZ-(I-V) may form large aggregates through PDZ-PDZ interactions and recruit multiple, synergistically acting prey proteins to the complex. Therefore we tested whether the PDZ motifs of PTP-BL and RIL can mediate homotypic interactions. Because no evidence was found for this type of interactions (Table I), we may exclude the latter model as an explanation for our observations. Furthermore, our results

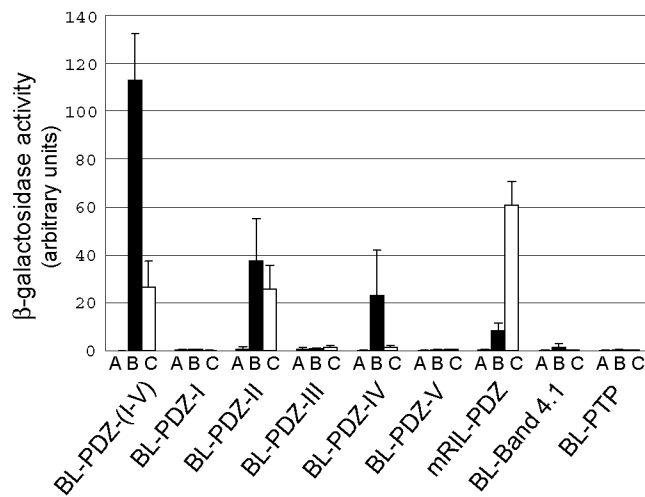


Figure 4: Determination of the relative strength of two-hybrid interactions.

β -galactosidase activities (arbitrary units) were measured in total lysates of yeast containing a LacZ-reporter plasmid. The yeast cells contained plasmids encoding baits as indicated below the bars, and the empty prey vector pJG4-5 (A, gray bars), hRIL(164-330) (B, filled bars), or mRIL-FL (C, open bars). Error bars indicate SD (n=5).

indicate that, in contrast to BL-PDZ-II, the interactions of BL-PDZ-(I-V) and BL-PDZ-IV with the mRIL-FL are significantly weaker than with the partial hRIL (Fig. 4). This effect is not caused by differences between mouse and human RIL sequences, because similar results were obtained with the partial mouse RIL clone [mRIL(209-330)], (Fig. 7). These data suggest the presence of a negatively regulating element located in the N-terminal part of RIL, which does not affect BL-PDZ-II binding.

Table 1: Two-hybrid interaction trap assays to test for PDZ-PDZ and LIM-LIM interactions

	BL-PDZ-(I-V)	RIL-PDZ	mRIL(209-330)
BL-PDZ-(I-V)	-	-	+
RIL-PDZ	-	-	+
mRIL(209-330)	+	+	-

Baits (top row) and preys (vertical row) were constructed and used as described in materials and methods. +, interaction (blue colonies after 3 d); -, no interaction (no blue colonies after 7 d).

RIL can be coprecipitated with BL-PDZ motifs

Although the two-hybrid interaction trap is a very powerful tool to identify potential partner proteins, interactions need to be confirmed in test systems that can provide the normal cellular environment of the molecules involved. Therefore, we have transiently coexpressed epitope-tagged PDZ motifs and RIL in mammalian epithelial cells (COS-1) as substrates for immunoprecipitation. Pull-down of the product of the partial RIL cDNA [hRIL(164-330)] was demonstrated for BL-PDZ-(I-V), BL-PDZ-II and BL-PDZ-IV (Fig. 5), confirming the results obtained in the yeast two-hybrid interaction trap. Again, no interaction between the band 4.1-like and the PTP domain of PTP-BL with RIL was observed. Strikingly, coprecipitation with single PDZ motifs (BL-PDZ-II and BL-PDZ-IV) is much less efficient than with BL-PDZ-(I-V). This is not a concentration effect because the amount of epitope-tagged PDZ motif present in the extracts, as determined by Western blotting, was comparable for all constructs used (our unpublished observations). The difference in the amount of coprecipitated RIL is significantly more than two-fold, excluding binding by BL-PDZ-(I-V) of two RIL molecules (via PDZ-II and PDZ-IV) as the only explanation for this phenomenon. Interestingly, we consistently observed very low concentration of mRIL-FL in our lysates (Fig. 8). This probably explains why coprecipitation of mRIL-FL was barely detectable (our unpublished observations). Preliminary observations indicate a rapid degradation of mRIL-FL, which in vivo may be an important regulatory element in RIL function.

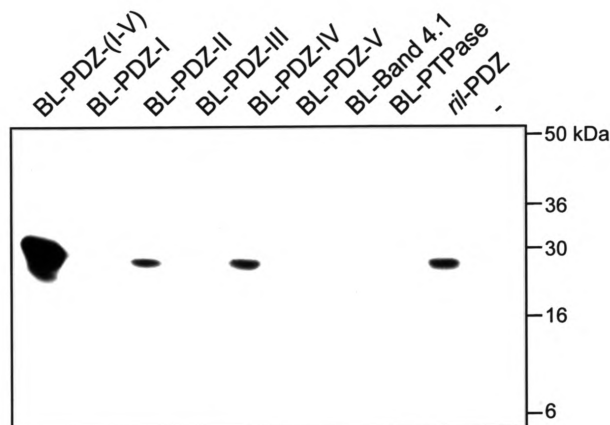


Figure 5: Coprecipitation of RIL with PDZ motifs. VSV epitope-tagged PDZ motifs of PTP-BL and RIL were transiently coexpressed in COS-1 cells with the C-terminal part of RIL, hRIL(164-330). α -VSV mAbs were used to immuno-precipitate the various PDZ motifs. Coprecipitated RIL was detected by Western blotting using a pAb (α -RIL) directed against the C-terminal part of hRIL. The labels on top refer to the protein segments outlined in Fig. 1 and the dash indicates mock-transfected cells.

PTP-BL and RIL colocalize in situ

To substantiate the biological relevance of the PTP-BL - RIL interaction we studied the tissue distribution and subcellular localization of these proteins by immunohistological assays (Fig. 6). Affinity-purified rabbit polyclonal antiserum against PTP-BL (α -BL-PDZ-I and α -BL-PTP) and hRIL (α -RIL) were used to detect the endogenous proteins. The results are in full agreement with those obtained by previous RNA in situ hybridization studies (Hendriks et al., 1995; Kiess et al., 1995). Expression of both proteins could be observed in various mouse epithelia. Detailed examination of lung cryosections revealed that the epithelium covering the bronchi expresses high amounts of both PTP-BL and RIL, whereas other parts of the lung show no detectable expression. PTP-BL and RIL are both expressed exclusively at the apical site of these epithelial cells. High expression levels were also found in the glandular part of the stomach and again both RIL and PTP-BL are consistently detected apically in all epithelial cell types studied. In corneal epithelium of mouse skin and in the non-glandular part of the stomach (our unpublished observations), both proteins are distributed in dot-like structures close to the cellular membrane, suggestive of a desmosome-like pattern. In fact, all near-membrane regions in the epidermis are positive for both PTP-BL and RIL except for the basement membrane of the basal cell layer which is negative for both proteins. The dermis and stratum corneum were found to be completely negative, whereas epithelia covering glands and hair follicles were again positive (our unpublished observations). Taken together, we may conclude that PTP-BL and RIL are

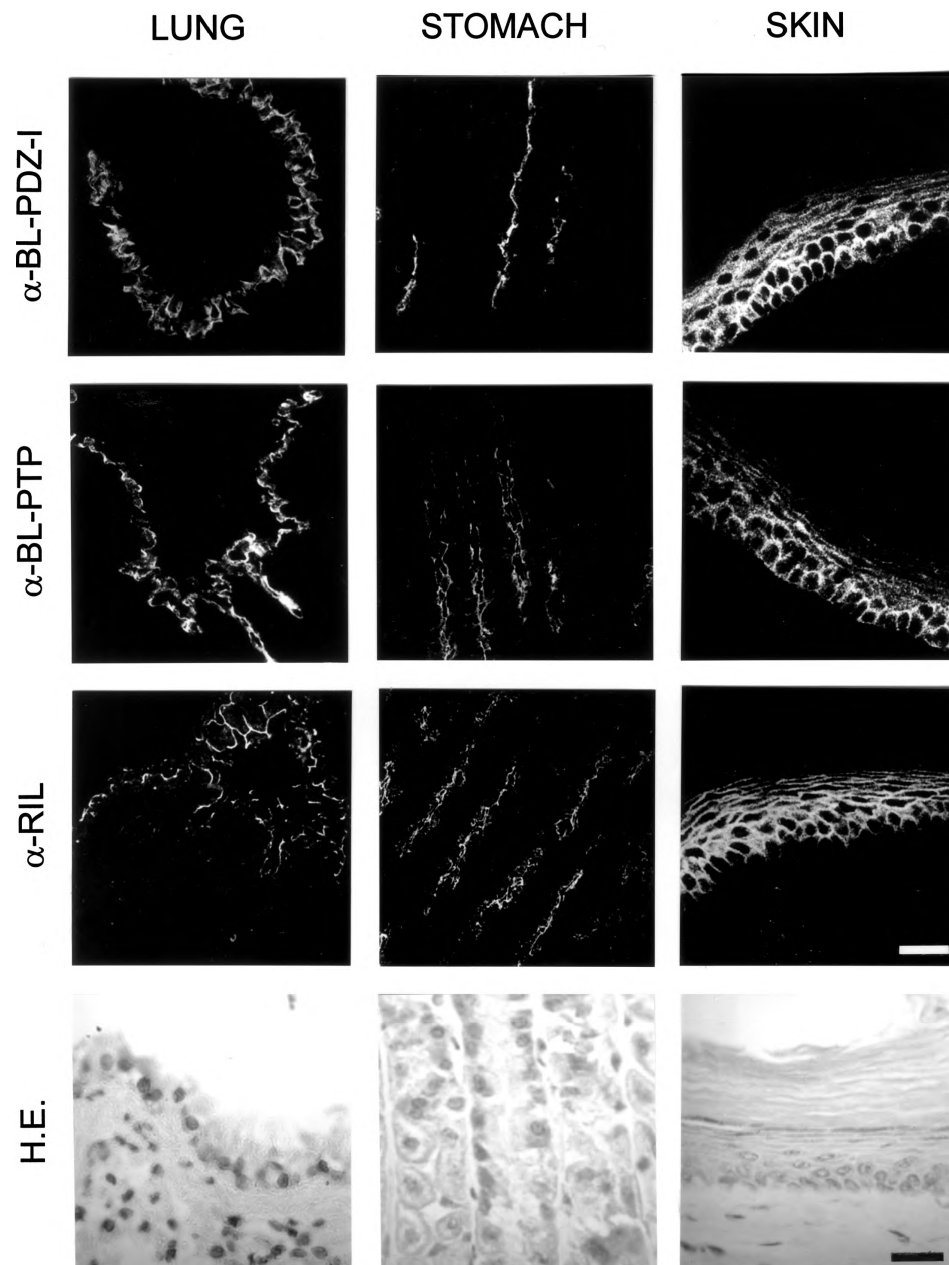


Figure 6: Colocalization of PTP-BL and RIL in mouse tissues. Visualization of the presence of PTP-BL and RIL proteins mouse lung, stomach, and skin was done using immunofluorescence labeling with affinity-purified pAb directed against PTP-BL (α -BL-PDZ-I and α -BL-PTP) and RIL (α -RIL). Corresponding hematoxylin/eosin-stained sections (HE) are shown for comparison. Bars, 25 μ m.

coexpressed apically in all polarized epithelial cell types studied so far, where they may play a role in the establishment or maintenance of the polarized phenotype of these cells.

The RIL LIM domain is necessary for interaction with PTP-BL PDZ motifs

Having shown the possibility for PTP-BL and RIL to interact *in vivo*, we next studied the molecular basis of their association. To determine the minimal region in RIL necessary for an interaction with the PTP-BL PDZ motifs, a series of N- and C-terminally truncated RIL peptides was used as a prey in the interaction trap along with BL-PDZ-II and BL-PDZ-IV as baits (Fig. 7). For BL-PDZ-II the entire RIL LIM-domain, including flanking N-terminal and C-terminal sequences, is needed to enable a strong interaction. Further truncation towards the LIM domain resulted in a weaker but still significant interaction (as determined by β -galactosidase activity measurements of total yeast lysates; our unpublished results). It is important to note that deletion of the last four RIL residues [mRIL(209-326)] does not affect binding. This defines the minimal region of RIL necessary for interaction with BL-PDZ-II to the polypeptide stretch between aa positions 249 and 309, which is essentially the complete LIM domain (Fig. 7).

In the same way, the minimal region of RIL for BL-PDZ-IV interaction was determined and assigned to the complete segment between aas 249 and 330 (Fig. 7). In contrast to BL-PDZ-II, deletion of the C-terminal 21 residues or the last 4 residues of RIL resulted in the abolishment of any detectable interaction, indicating that these residues are most relevant for interaction with BL-PDZ-IV. However, the C-terminal 15 or 21 residues alone, which are 100% conserved between mouse and human, did not show any interaction (Fig. 7). These results indicate that both the LIM domain and the proper C-terminus are necessary for a strong BL-PDZ-IV interaction with RIL, clearly distinguishing this mode of interaction from that described for PDZ motifs with C-terminal peptides (Doyle et al., 1996) and also from the interaction between BL-PDZ-II with the RIL-LIM domain reported here.

Because C-terminal consensus binding sequences have been determined for PDZ-II and IV of PTP-BAS by screenings of oriented peptide libraries (Songyang et al., 1997), we looked for the presence of these motifs in the entire RIL molecule. The last four residues of RIL are -VELV and the consensus for PDZ-II and IV binding are -(E/V)(T/S)X(V/I) and -(I/Y/V)YYV, respectively, which should be considered a very weak match. Strikingly, there is an internal TIV motif within the first loop of the LIM domain. However, mutation of this TIV to GIQ did not affect the BL-PDZ-II or IV interaction with RIL (Fig. 7). This contrasts markedly with the INAD PDZ motif-binding characteristics to the 19-aa C-terminus of TRP, which contains an essential (S/T)XV motif (Shieh and Zhu, 1996).

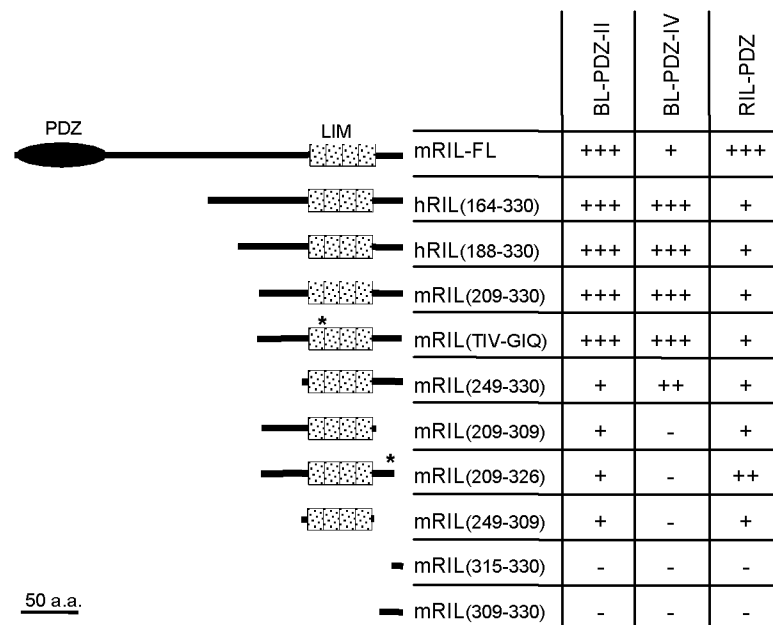


Figure 7: Analysis of PDZ-mediated interactions with truncated RIL peptides.

Schematic representation of the regions of RIL used as prey in the two-hybrid interaction trap are shown on the left. Interaction results using these constructs combined with BL-PDZ-II, BL-PDZ-IV and mRIL-PDZ as baits are represented by + and - signs. +++, very strong interaction (blue colonies within 2 d on X-gal assay plates); ++, interaction (blue colonies after 3 d); +, weak but detectable interaction (blue colonies after 4-6 d); -, no interaction detectable (no blue colonies after 7 d).

The RIL LIM domain is phosphorylated on tyrosines in vitro and in vivo and is an in vitro substrate for PTP-BL

Our results clearly indicated that the entire RIL LIM domain is necessary for the interaction with PTP-BL. This domain harbors a potential tyrosine phosphorylation site at position 274. To study whether the RIL LIM domain can be phosphorylated on tyrosines in vitro and may function as a substrate for PTP-BL, we induced GST-fusion proteins in TKX bacterial cells, which contain an inducible tyrosine kinase (Stratagene). No tyrosine phosphorylation of GST alone or GST-PDZ could be detected by Western blot analysis, whereas GST-RIL-LIM was phosphorylated on tyrosines in this bacterial system (Fig. 8A). The bands of lower molecular weight in the GST-RIL-LIM lane are most probably due to degradation of the fusion protein. Although there are several tyrosines within the GST-RIL-LIM sequence, only tyrosine 274 was predicted to be a substrate for tyrosine kinases by the PROSITE database. Therefore, we mutated this tyrosine to a phenylalanine (GST-RIL-LIM-Y-F). The tyrosine phosphorylation of the Y274F mutant fusion protein is markedly

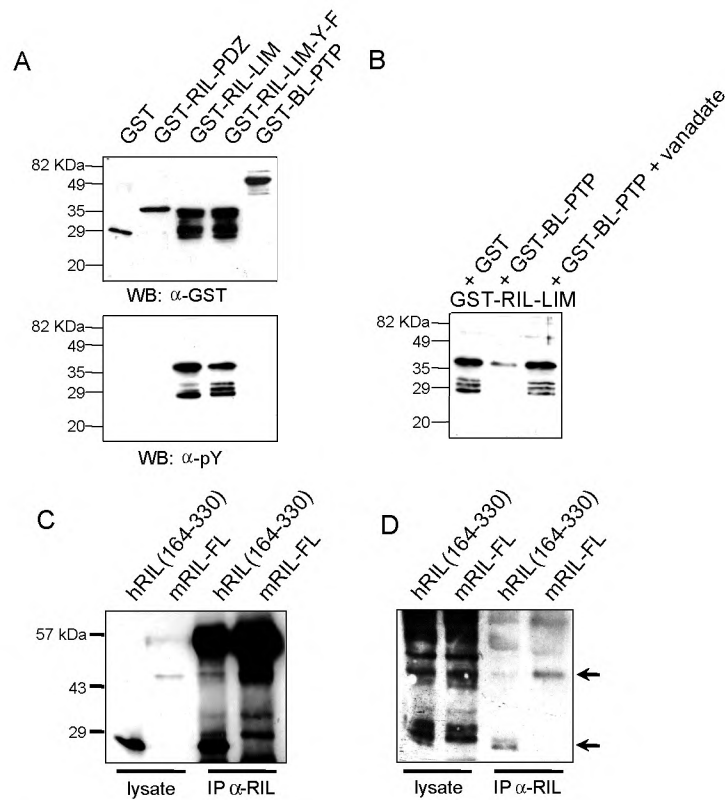


Figure 8: RIL is phosphorylated on tyrosines in vitro and in vivo and is an in vitro substrate for PTP-BL.

(A) GST-fusion proteins were purified from bacterial TKX cells expressing an inducible tyrosine kinase. Purified protein was detected by Western blotting using an anti-GST antibody (top panel) and analyzed for tyrosine phosphorylation using the phosphotyrosine specific antibody PY20 (bottom panel). Only GST-RIL-LIM (aas 209-330) is phosphorylated on tyrosines and mutation of tyrosine 294 to phenylalanine (GST-RIL-LIM-Y-F) clearly diminishes the phosphorylation level. (B) Purified phosphorylated GST-RIL-LIM was incubated for 15 min with purified GST or GST-BL-PTP (aas 2101-2460) and analyzed for its phosphotyrosine content. GST-BL-PTP can dephosphorylate the RIL-LIM domain, whereas GST alone does not affect the tyrosine phosphorylation. Furthermore, the specific tyrosine phosphatase inhibitor vanadate can completely inhibit the dephosphorylation by GST-BL-PTP. (C) COS-1 cells were transfected with an expression construct encoding the C-terminal half of RIL [hRIL(164-330)] or mRIL-FL. The presence of transiently expressed RIL in total cell lysates and anti-RIL immunoprecipitates was detected by Western blotting using anti-RIL antibody. (D) The tyrosine phosphorylation content of the same samples as depicted in C was determined by Western blotting using the phosphotyrosine-specific antibody PY20. Both the immunoprecipitated hRIL(164-330) and the mRIL-FL are found to be phosphorylated on tyrosine residues.

reduced (Fig. 8A), but other residues are phosphorylated as well in this bacterial system. The fact that tyrosine-phosphorylated GST-RIL-LIM can be dephosphorylated by addition of purified GST-BL-PTP, whereas GST alone had no effect (Fig. 8B), clearly demonstrates that the phosphorylated RIL-LIM domain is an *in vitro* substrate for PTP-BL. Moreover, the specific tyrosine phosphatase inhibitor vanadate can completely inhibit the tyrosine dephosphorylation by GST-BL-PTP (Fig. 8B).

To study this phosphorylation in a more physiological context, we immunoprecipitated the RIL LIM domain hRIL(164-330) and mRIL-FL from transiently overexpressing COS-1 cells that were treated for 15 min with vanadate. The presence of the RIL protein in the lysate and the immunoprecipitation was demonstrated by Western blotting and immunodetection using α -RIL antibodies (Fig. 8C). Tyrosine phosphorylation of both mRIL-FL and the RIL-LIM domain was demonstrated by incubating the Western blot with the phosphotyrosine specific antibody PY-20 (Fig. 8D).

An intra-molecular RIL PDZ - LIM interaction

Because RIL contains a PDZ motif itself (Figs. 2 and 3) the possibility of an intramolecular interaction between this N-terminal PDZ motif (aas 4-84) and the RIL C-terminus was studied. We tested aas 1-101 of RIL (mRIL-PDZ, Fig. 1B), containing the entire RIL-PDZ motif, for binding to mRIL-FL or the C-terminal part of RIL [hRIL(164-330)] using the two-hybrid interaction trap. Indeed, a significant interaction was observed, but in contrast to the findings with BL-PDZ-IV, the interaction is much stronger with the mRIL-FL than with the truncated protein (Fig. 4). This may be explained by the possibility of mRIL-FL to form linear multimers via PDZ-LIM interactions, recruiting multiple prey activation domains to one bait. The possibility of sequence differences between human and mouse RIL influencing the interaction was excluded using truncated mouse RIL [mRIL(209-330)] along with the mouse RIL PDZ motif, which gave the same results (Fig. 7). The testing of truncated C-terminal RIL peptides for their ability to interact with the RIL PDZ motif demonstrated weak but significant interactions for all constructs containing the LIM domain (Fig. 7). Interestingly, the RIL-PDZ motif interacts more strongly with the construct lacking the last four residues [mRIL(209-326)] than with mRIL(209-330), perhaps reflecting an inhibitory effect of these residues on RIL-PDZ binding. Again, the interaction between the RIL PDZ motif and the LIM domain could be confirmed by coprecipitation of the RIL C-terminus with epitope-tagged RIL-PDZ motif from transiently coexpressing COS-1 cells (Fig. 5). Because it has been shown that LIM domains can engage in homo- and heterodimerization (Feuerstein et al., 1994), we tested the ability of the RIL C-terminus (aas 209-330) containing the LIM domain including flanking sequences, to homodimerize using the two-hybrid interaction trap. No interaction was observed, by the use of experimental conditions in which RIL-PDZ or BL-PDZ-(I-V) interactions could be readily detected (Table 1).

Discussion

The protein tyrosine phosphatase PTP-BL contains in addition to its catalytic segment a band 4.1-like domain and five PDZ motifs, features that predict a restricted localization at submembranous or cytoskeletal structures within the cell (Ponting and Phillips, 1995; Tsukita et al., 1993). To obtain experimental evidence for this prediction and identify the individual protein constituents in the subcellular microenvironment, a two-hybrid screen was performed using the segment encompassing the five PDZ motifs of PTP-BL as a bait. An interacting protein was obtained that previously had been identified in rat as RIL, the product of a gene that is down-regulated in H-Ras transformed fibroblasts (Kiess et al., 1995). The interaction was confirmed by transfection experiments in COS-1 cells. Perhaps more importantly, the possible *in vivo* relevance of this interaction is firmly corroborated by the extensive overlap in RNA expression patterns in mouse (Hendriks et al., 1995; Kiess et al., 1995). Also the fact that both proteins are consistently localized at the same subcellular structures, such as the submembranous apical side of polarized epithelial cells, in mouse tissue sections (Fig. 6) supports our view that this interaction must have biological significance. Because PTP-BL is up-regulated by differentiation stimuli in mouse erythroleukemia and embryonal carcinoma (F9) cells (Chida et al., 1995) and RIL is downregulated in transformed cells (Kiess et al., 1995), it is tempting to speculate that the formation of PTP-BL-RIL complexes is a crucial aspect in the control of growth and differentiation of epithelial cells.

What could be the features that govern binding interaction and determination of PTP-BL-RIL location? The RIL protein contains a C-terminal LIM domain and, in addition, we identified a N-terminal PDZ motif (Fig. 3). We demonstrate that these motifs can mediate intermolecular and perhaps intramolecular associations because, like the second and fourth PTP-BL PDZ motif, the RIL PDZ motif can engage in binding to the RIL LIM domain (Figs. 4, 5 and 7). In view of results obtained in other studies (Kim et al., 1995; Kornau et al., 1995; Niethammer et al., 1996; Songyang et al., 1997) it is striking that ablation of the last four residues of RIL did not affect PDZ-II interaction and enhanced RIL-PDZ binding, whereas no PDZ-mediated interactions could be observed with the RIL C-terminus alone (Fig. 7). In contrast, for the BL-PDZ-IV binding there is dependence on the integrity of the C-terminus of RIL, but again not uniquely on the presence of the very last aa residues only. Random mutagenesis of the RIL-LIM domain confirms the above observations (our unpublished observations).

How can we reconcile these findings to the known properties of PDZ motifs? Thus far, one interaction mode for PDZ motifs has dominated the literature: recognition of a very short C-terminal sequence motif (Fanning and Anderson, 1996; Gomperts, 1996). The x-ray crystallographic structure of the third PDZ motif from the synaptic density protein PSD-95/SAP90 in the absence and presence of a binding peptide has recently been determined (Doyle et al., 1996) and provides a solid basis for our understanding of the recognition of

the T/SXV C-terminus as present in multiple channel and receptor subunits. That PDZ motifs are also able to bind to internal peptide segments has been inferred from studies on the PSD-95/SAP90 interaction with nNOS (Brenman et al., 1996; Schepens et al., 1997). An explanation for this was provided by assuming that not only a C-terminal sequence, but also an internal β -strand may interact with PDZ motifs in a similar manner (Harrison, 1996). This can indeed be witnessed in the crystal structure of the PDZ-III domain of hdlg, which displays a dimer mediated by β -strands in both molecules (Morais Cabral et al., 1996). Also, the binding of the INAD PDZ motif to the TRP store-operated channel deviates from the C-terminus rule. Although the interaction was localized to the 19-aa C-terminus of TRP, it appeared critically dependent on the presence of an internal STV motif (Shieh and Zhu, 1996). It has been proposed that alterations of residues within the carboxylate-binding loop of PDZ motifs could facilitate this binding of a peptide-internal segment (Fanning and Anderson, 1996). Strikingly, PDZ II and IV of PTP-BL and also the RIL PDZ motif share features with INAD, in that they contain a SLGI/F instead of a GLGF motif, and perhaps this represents a signature motif for domains with internal peptide-segment avidity. Further elaborating on an analogy to the INAD PDZ-TRP binding (Shieh and Zhu, 1996), an internal TIV peptide can be found within the first zinc-finger of the RIL-LIM domain. However, mutation of this peptide does not affect the interaction with PTP-BL, indicating that sequences outside this triplet are more important.

Taken together, the experimental data presented here provide compelling evidence for a novel type of protein-protein interaction mediated by PDZ motifs and LIM domain structures, that is structurally different from the C-terminus recognition mode by other PDZ motifs. The sequences flanking the LIM domain, including the C-terminus, may be directly involved in binding (in the case of PDZ-IV) or they may be important for stabilizing the LIM domain structure. Our results of course do not exclude that the PDZ motifs of PTP-BL can engage in more classical interactions or interactions with proteins other than RIL. For example, screening of an oriented peptide library with PDZ-II of the human homolog of PTP-BL, PTP-BAS, revealed the consensus C-terminal target T/SxV/I (Songyang et al., 1997). This sequence is present in human Fas and indeed it has been shown that PDZ-II of PTP-BL can interact with human Fas (Sato et al., 1996, Saras et al., 1997a, Cuppen et al., 1997) but not with mouse Fas, as this has a different C-terminal end (Cuppen et al., 1997). However, the interaction was found to be 30- to 40-fold weaker than the binding to the RIL-LIM domain in our assays (Cuppen et al., 1997; Fig. 4). Also for nNOS two different binding modes have been described (Schepens et al., 1997) and even the presence of separate binding interfaces on the PDZ protein module can not be excluded. In fact, a coordinate involvement of different binding interfaces on both the PDZ and the RIL-LIM motifs is suggested by our findings. Coprecipitation of truncated forms of RIL from cell lysates is much more efficient for constructs containing the PTP-BL PDZ motifs II and IV together, than for those harboring a single PDZ motif (Fig. 5). This effect cannot just be

explained by the binding of two RIL molecules to a single PDZ-(I-V) peptide and one has to assume a cooperative or stabilizing effect resulting from the binding of two distinct PDZ motifs to one and the same LIM domain. Moreover, the observation that PDZ-II and PDZ-IV differ in their minimal requirements for interaction with RIL LIM sequences (Fig. 7) is in line with the presence of two binding interfaces in the LIM domain. This would explain why the binding of the RIL PDZ motif to the RIL LIM domain does attenuate the binding of the fourth but not the second PDZ motif of PTP-BL in the two-hybrid experiments (Fig. 4). The possibility of two interacting interfaces on a single LIM domain has also been put forward by Arber and Caroni (1996) and from structural data it can be deduced that distinct binding interfaces may reside in the two independent zinc finger modules, each with different aa composition of their loop (Hammarstrom et al., 1996; Perez Alvarado et al., 1996).

If the RIL-LIM domain can indeed bind two different PTP-BL molecules very large clusters could be formed. The unoccupied PDZ motifs of PTP-BL and RIL in this assembly may in turn interact with other proteins, thus generating even larger heterogeneous protein complexes in which the band 4.1-like domain of PTP-BL may be responsible for a proper submembranous localization. The ability of RIL to form an intramolecular PDZ-LIM interaction, inducing disassembly or rearrangements of the complex, could then function as a regulatory principle. It is also conceivable that the phosphorylation of tyrosine residues within the RIL LIM domain, which we have demonstrated to occur *in vitro* and *in vivo* (Fig. 8), may function as such a regulatory switch for clustering behavior. In addition, the tyrosine phosphatase domain of PTP-BL may be a determinant of the phosphorylation status of proteins in such a complex. The recent identification of a GTPase-activating protein for Rho, PARG, which can interact with the human homolog of PTP-BL (Saras et al., 1997b) and the colocalization of RIL with F-actin (our unpublished observations), implicate a role for such a multiprotein PTP-BL complex in actin-cytoskeleton dynamics.

The principle of PDZ-LIM-mediated interactions as demonstrated here could have widespread biological significance because, in addition to RIL, several other LIM domain-containing proteins, such as CLP-36, ALP, enigma, LIMK1 and LIMK2 also harbor PDZ motifs intramolecularly (Okano et al., 1995; Wang et al., 1995; Wu and Gill, 1994; Xia et al., 1997). If these proteins function as adapter molecules in bringing together diverse molecules in a defined but dynamic microenvironment at specialized submembranous or cytoskeletal structures, a disturbance of such structures could lead to pathological phenomena like tumorigenesis and developmental abnormalities. Indeed, LIMK1 (or Kiz-1), a serine/threonine kinase containing two N-terminal LIM domains followed by a single PDZ motif that is strongly expressed in brain, has been recently implicated in impaired visuospatial constructive cognition in the developmental disorder Williams syndrome (Frangiskakis et al., 1996). Also for PDZ-containing proteins, like DlgA (Bryant et al., 1993), Canoe (Miyamoto et al., 1995), Dsh (Theisen et al., 1994) and INAD (Shieh and

Zhu, 1996) in *Drosophila* and LIN-2 (Hoskins et al., 1996), LIN-7 (Simske et al., 1996) and PAR3 (Etemad Moghadam et al., 1995) in *Caenorhabditis elegans*, the severe impact of mutations on growth and differentiation has been documented. Further characterization of the exact topological and dynamic constraints that govern the interactive capacities of LIM and PDZ domains should therefore help us in understanding the molecular mechanisms underlying these defects.

Acknowledgments

We thank Drs. Finley and Brent for providing the yeast interaction trap plasmids and yeast strain and Dr. Claude Sardet for the human G0-fibroblast cDNA library. We gratefully acknowledge Drs. Anne Debant and Michel Streuli for making us familiar with the two hybrid interaction trap and for their kind hospitality during the initial phase of the project. This work was supported in part by a grant from the Dutch Cancer Society to W.H. and by a Dutch Cancer Society travel grant to H.G.

Materials and methods

Interaction-trap assay - Plasmid DNAs and the yeast strain used for the interaction-trap assay were provided by Dr. Roger Brent and colleagues (Massachusetts General Hospital, Boston, MA) and used as described (Gyuris et al., 1993). From 10^6 transformants of a human G0-fibroblast library (a kind gift of Dr. C. Sardet, Cambridge, MA) 12 clones were retrieved showing an interaction. Comparison of cDNA sequences with database entries were done using the BLAST program (Altschul et al., 1990). Two of the clones were found to represent overlapping RIL cDNAs. The sequence content and schematic representation of the various PTP-BL and RIL peptide regions used in the two-hybrid interaction trap are shown in Fig. 1. The single PTP-BL PDZ motifs were obtained by polymerase chain reaction (PCR) using specific primers with PTP-BL cDNA (European Molecular Biology Laboratory [EMBL] accession number Z32740, Hendriks et al., 1995) as template, and cloned in-frame in the pEG202 bait vector (Gyuris et al., 1993) using standard procedures. The band 4.1-like, PDZ-(I-V) and PTP domain of PTP-BL and the PDZ motif of RIL were introduced in the pEG202 vector by standard subcloning procedures. The deletion constructs of RIL (Fig. 7) were made by subcloning the appropriate restriction fragments [full-length mouse RIL (mRIL-FL), mRIL(209-330), mRIL(209-309), mRIL(249-309), mRIL(249-330) and mRIL(309-330)] or specific PCR fragments [mRIL(315-330), mRIL(209-326) and mRIL(TIV-GIQ)] of mouse RIL in-frame in the pJG4-5 prey vector (Gyuris et al., 1993). All constructs generated by PCR were checked for mutations by DNA sequencing. For two-hybrid interaction assays, plasmids were introduced in yeast strain EGY48 and tested for an interaction on minimal agarplates lacking histidine, tryptophan, uracil, and leucine, containing 2% galactose, 1% raffinose and 80 μ g/ml of 5-bromo-4chloro-3-indolyl- β -D-galactopyranoside (X-gal).

β -galactosidase activity assay - Determination of the relative strength of two-hybrid interactions was done by measuring the β -galactosidase activity in crude yeast lysates. A single yeast colony was inoculated in 1.5 ml of minimum medium lacking histidine, tryptophan and uracil, containing 2% galactose and 1% raffinose and grown overnight until $OD_{600nm} \approx 1.0$. Cells were pelleted and resuspended in 0.2 ml ice-cold buffer (0.1 M NaCl, 10 mM Tris-HCl pH7.0, 1 mM EDTA, 1 mM phenylmethyl-sulfonyl fluoride). About 100 μ l acid washed glass beads (425-600 μ m, Sigma

Chemical, St. Louis, MO) were added and the suspension was vortexed six times for 30 s alternated with 30-s incubations on ice. Lysates were centrifuged for 5 min with 14,000 rpm at 4°C. Supernatants were transferred to fresh tubes and used for protein concentration determination (Bradford, 1976). β -Galactosidase activity was measured by adding 10 μ l lysate to 200 μ l freshly prepared ONPG buffer (100 mM phosphate buffer pH 7.0, 1 mM MgCl₂, 10 mM KCl, 50 mM β -mercaptoethanol, 0.35 mg/ml O-nitrophenyl- β -D-galactopyranoside, Sigma) in microtiter plates. Reactions were incubated at 30°C and the OD_{420nm} was monitored for 1 h on a CERES UV900C MTP-photometer (Bio-Tek, Winooski, VT). The specific β -galactosidase activity (arbitrary units) was calculated using the initial linear part of the OD_{420nm}/min curves and corrected for the protein concentration of the sample.

Isolation and sequencing of mouse RIL cDNAs - The 0.6 kbp hRIL(164-330) insert, encoding the C-terminus of human RIL (hRIL), was isolated, labeled radioactively by random priming and used to screen a mouse brain λ -ZAPII cDNA phage library (Stratagene, La Jolla, CA) following standard procedures. Of 0.65×10^6 plaques, two were found to be positive for the RIL cDNA. These phages were plaque-purified and inserts were rescued as pBluescript SK⁻ plasmids according to the manufacturer's protocols. Nucleotide sequences were determined by double-stranded DNA dideoxy sequencing using T3 and T7 sequencing primers on rescued plasmids and derived subclones. The mRIL-FL cDNA sequence was compared with database entries using the BLAST program (Altschul et al., 1990). Alignments with RIL cDNAs from various species and other PDZ containing proteins were made using MULTALIGN, were adapted manually and homologies were calculated using DISTANCES (Program manual for Wisconsin Package, Version 8, Genetics Computer Group, Madison, WI).

Polyclonal antibodies (pAbs) - Restriction fragments encoding aas (amino acids) 1056-1284 (including PDZ-I) or aas 2101-2460 (including the PTP domain) of PTP-BL and the insert of hRIL(164-330), encoding the C-terminal half of hRIL, were cloned in appropriate pGEX prokaryotic expression vectors (Pharmacia, Piscataway, NJ). GST-fusion proteins were isolated (Frangioni and Neel, 1993) and used to immunize rabbits. Affinity-purified pAbs (α -BL-PDZ-I, α -BL-PTP and α -RIL, respectively) were obtained by applying whole serum to Affigel-15-immobilized (Bio-Rad, Richmond, CA) purified GST-fusion protein and eluting bound antibodies.

Transient expression and immunoprecipitation - Mouse PTP-BL and RIL protein parts were expressed from the eukaryotic expression vector pSG5 (Green et al., 1988), which was modified to generate an in frame VSV epitope tag for detection or immunoprecipitation of the produced peptide using the monoclonal anti-VSV antibody P5D4 and, if necessary, an initiator AUG codon or a stop codon. hRIL(164-330) was expressed from the eukaryotic expression vector pMT.HAtag, a modified pMT2 vector that contains an initiator AUG codon followed by a hemagglutinin (HA) epitope tag sequence immediately upstream of the cloning site (Serra Pages et al., 1995), and mRIL-FL was expressed from the pSG5 expression vector by cloning the mRIL-FL-3 cDNA, containing its own initiator AUG codon, in the multiple cloning site. COS-1 cells were cultured in DMEM/10% fetal calf serum. For each assay, 1.5×10^6 cells were electroporated at 0.3 kV and 125 μ F using the BioRad GenePulser with a 4 mm electroporation cuvette, in 200 μ l phosphate-buffered saline (PBS) containing 10 μ g of plasmid DNA. Cells were plated on a 10 cm dish and cultured for 48 h in DMEM/10% fetal calf serum. Cells were harvested by scraping in ice-cold PBS, pelleted by centrifugation (1000 rpm, 5 min) and lysed in 500 μ l of lysis buffer (50 mM Tris-HCl pH8.0, 150 mM NaCl, 5 mM EDTA, 0.5% Non-idet P-40, 1 mM PMSF, 10 μ g/ml aprotinin, 10 μ g/ml leupeptin and 10 μ g/ml pepstatin A). After a 1-h incubation on ice, the lysate was centrifuged for 10 min at 10,000xg at 4°C and the supernatant was cleared with 20 μ l protein-A Sepharose CL-4B (Pharmacia) for 2 h rotating at 4°C. After addition of monoclonal antibody (mAb) P5D4 (2 μ l ascites fluid) or pAb α -RIL (5 μ g affinity purified) and rotation for 2 h at 4°C, 30 μ l of Protein A-Sepharose CL-4B were added and incubation was prolonged overnight. The immunoprecipitates were washed 4 times with 0.5 ml lysis buffer and boiled for 5 min in 20 μ l 2x sample buffer (100 mM Tris-HCl pH6.8, 200 mM

dithiothreitol, 4% SDS, 0.2% bromophenol blue, 20% glycerol), and proteins were resolved on 12% polyacrylamide gels and transferred to nitrocellulose membranes by Western blotting. Blots were blocked using 5 % nonfat dry milk in 10 mM Tris-HCl (pH8.0), 150 mM NaCl, and 0.05% Tween-20 (TBST). Affinity-purified pAb α -RIL (1:1000 dilution) was used to detect coprecipitation of RIL protein and mAb PY-20 (Transduction Laboratories, 1 μ g/ml) to detect tyrosine phosphorylated proteins. Incubations with primary and secondary antibodies [Alkaline Phosphatase-conjugated AffiniPure goat anti-rabbit IgG (0.06 μ g/ml), Jackson ImmunoResearch Laboratories, West Grove, PA] and subsequent washes were done in TBST. Labeled bands were visualized using CPD Star chemiluminescence according to the manufacturer (Tropix, Bedford, MA).

Immunofluorescence Assay - Cryo-sections of unfixed tissues (6 μ m) were cut and mounted on Superfrost/Plus slides (Menzel Gläser, Germany). After thawing, sections were fixed for 5 min in cold methanol (-20°C) for α -BL-PDZ-I and α -BL-PTP or in 3% paraformaldehyde in PBS for α -RIL, and subsequently washed twice with PBS/0.05% Tween-20 (PBST). Tissue sections were incubated in affinity-purified pAb (diluted 1:200 in PBST) for 1 h at room temperature. in the presence of 1% normal swine serum, and washed three times for 5 min in PBST. Specific labeling was detected by subsequent incubation in fluorescein-conjugated swine anti-rabbit IgG (12 μ g/ml, Dako, Carpinteria, CA) in PBST for 1 h and washing in PBST. Sections were mounted in Mowiol (Sigma). Hematoxylin/eosin-stained sections were prepared according to standard histological procedures.

In vitro tyrosine phosphorylation and dephosphorylation assay - The plasmid encoding GST-BL-PTP (aas 2101-2460) was generated as described above. GST-RIL-PDZ (aas 1-101) and GST-RIL-LIM (aas 209 to 330) were made by subcloning restriction fragments of mRIL-FL in the appropriate pGEX vector. The tyrosine-to-phenylalanine mutant of the RIL-LIM domain, GST-RIL-LIM-Y-F (aas 209-330), was made by PCR using oligonucleotides harboring the desired mutation and GST-RIL-LIM as a template. The mutated sequence of GST-RIL-LIM-Y-F was confirmed by sequencing. GST-fusion proteins were produced in bacterial TKX cells according to the supplier's instructions (Stratagene). Cells were lysed by sonification in PBS containing protease inhibitors (1 mM PMSF, 10 μ g/ml aprotinin, 10 μ g/ml leupeptin and 10 μ g/ml pepstatin A) and GST-fusion proteins were purified using glutathione-Sepharose CL4B (Pharmacia) and analyzed on 12% polyacrylamide gels. Samples representing about 1 μ g of fusion protein were loaded on each lane and the presence of GST-fusion protein and tyrosine phosphorylation was detected by Western blotting using the mAbs 2F3 (α -GST) and PY-20 (α -P-tyr, Transduction Laboratories, Lexington, KY), respectively. For the dephosphorylation assay, 1 μ g of purified phosphorylated GST-RIL-LIM was incubated for 15 min at 37°C in PBS containing protease inhibitors with 0.1 μ g of purified GST-BL-PTP or, as a control, with 0.1 μ g of GST. As a specific protein tyrosine phosphatase inhibitor, NaVO₃ was used at a final concentration of 1 mM.

References

- Altschul, S. F., Gish, W., Miller, W., Myers, E. W., and Lipman, D. J. (1990). Basic local alignment search tool. *J. Mol. Biol.* 215, 403-410.
- Arber, S., and Caroni, P. (1996). Specificity of single LIM motifs in targeting and LIM/LIM interactions in situ. *Genes Dev.* 10, 289-300.
- Banville, D., Ahmad, S., Stocco, R., and Shen, S. H. (1994). A novel protein-tyrosine phosphatase with homology to both the cytoskeletal proteins of the band 4.1 family and junction-associated guanylate kinases. *J. Biol. Chem.* 269, 22320-22327.
- Boedigheimer, M., Bryant, P., and Laughon, A. (1993). *Expanded*, a negative regulator of cell proliferation in *Drosophila*, shows homology to the NF2 tumor suppressor. *Mech. Dev.* 44, 83-84.
- Bradford, M. M. (1976). A rapid and sensitive method for the quantitation of microgram quantities of protein utilizing the principle of protein-dye binding. *Anal. Biochem.* 72, 248-254.
- Brenman, J. E., Chao, D. S., Gee, S. H., McGee, A. W., Craven, S. E., Santillano, D. R., Wu, Z.,

- Huang, F., Xia, H., Peters, M. F., Froehner, S. C., and Brecht, D. S. (1996). Interaction of nitric oxide synthase with the postsynaptic density protein PSD-95 and alpha1-syntrophin mediated by PDZ domains. *Cell* *84*, 757-767.
- Bryant, P. J., Watson, K. L., Justice, R. W., and Woods, D. F. (1993). Tumor suppressor genes encoding proteins required for cell interactions and signal transduction in *Drosophila*. *Development, Suppl.* 239-49.
- Chida, D., Kume, T., Mukoyama, Y., Tabata, S., Nomura, N., Thomas, M. L., Watanabe, T., and Oishi, M. (1995). Characterization of a protein tyrosine phosphatase (RIP) expressed at a very early stage of differentiation in both mouse erythroleukemia and embryonal carcinoma cells. *FEBS Lett.* *358*, 233-239.
- Cho, K.-O., Hunt, C. A., and Kennedy, M. B. (1992). The rat brain postsynaptic density fraction contains a homolog of the *Drosophila* discs-large tumor suppressor protein. *Neuron* *9*, 929-942.
- Cohen, G. B., Ren, R., and Baltimore, D. (1995). Modular binding domains in signal transducing proteins. *Cell* *80*, 237-248.
- Cuppen, E., Nagata, S., Wieringa, B. and Hendriks, W. (1997). No evidence for involvement of mouse protein-tyrosine phosphatase-BAS-like / Fas-associated phosphatase-1 in Fas-mediated apoptosis. *J. Biol. Chem.* *272*, 30215-30220.
- Dawid, I. B., Toyama, R., and Taira, M. (1995). LIM domain proteins. *C. R. Acad. Sci.* *318*, 295-306.
- Doyle, D. A., Lee, A., Lewis, J., Kim, E., Sheng, M., and MacKinnon, R. (1996). Crystal structures of a complexed and peptide-free membrane protein-binding domain: molecular basis of peptide recognition by PDZ. *Cell* *85*, 1067-1076.
- Etemad Moghadam, B., Guo, S., and Kemphues, K. J. (1995). Asymmetrically distributed PAR-3 protein contributes to cell polarity and spindle alignment in early *C. elegans* embryos. *Cell* *83*, 743-52.
- Fanning, A. S., and Anderson, J. M. (1996). Protein-protein interactions: PDZ domain networks. *Curr. Biol.* *6*, 1385-1388.
- Feuerstein, R., Wang, X., Song, D., Cooke, N. E., and Liebhaber, S. A. (1994). The LIM/double zinc-finger motif functions as a protein dimerization domain. *Proc. Nat. Acad. Sci. USA* *91*, 10655-9.
- Frangioni, J. V., and Neel, B. G. (1993). Solubilization and purification of enzymatically active glutathione S-transferase (pGEX) fusion proteins. *Anal. Biochem.* *210*, 179-87.
- Frangiskakis, J.M., Ewart, A. K., Morris, C. A., Mervis, C. B., Bertrand, J., Robinson, B. F., Klein, B. P., Ensing, G. J., Everett, L. A., Green, E. D., Pröschel, C., Gutowski, N. J., Noble, M., Atkinson, D. L., Odelberg, S. J., and Keating, M. T. (1996). LIMK-1 hemizyosity implicated in impaired visuospatial constructive cognition. *Cell* *86*, 59-69.
- Garner, C. C. (1996). Synaptic proteins and the assembly of synaptic junctions. *Trends Cell Biol.* *6*, 429-433.
- Gomperts, S. N. (1996). Clustering membrane proteins: It's all coming together with the PSD-95/SAP90 protein family. *Cell* *84*, 659-662.
- Green, S., Issemann, I., and Sheer, E. (1988). A versatile in vivo and in vitro eukaryotic expression vector for protein engineering. *Nucleic Acids Res.* *16*, 369.
- Gyuris, J., Golemis, E., Chertkov, H., and Brent, R. (1993). Cdi1, a human G1 and S phase protein phosphatase that associates with Cdk2. *Cell* *75*, 791-803.
- Hammarstrom, A., Berndt, K. D., Sillard, R., Adermann, K., and Otting, G. (1996). Solution structure of a naturally-occurring zinc-peptide complex demonstrates that the N-terminal zinc-binding module of the Lasp-1 LIM domain is an independent folding unit. *Biochemistry* *35*, 12723-32.
- Harrison, S. C. (1996). Peptide-surface association: the case of PDZ and PTB domains. *Cell* *86*, 341-343.
- Hendriks, W., Schepens, J., Bachner, D., Rijss, J., Zeeuwen, P., Zechner, U., Hameister, H., and Wieringa, B. (1995). Molecular cloning of a mouse epithelial protein-tyrosine phosphatase with similarities to submembranous proteins. *J. Cell. Biochem.* *59*, 418-430.
- Hoskins, R., Hajnal, A. F., Harp, S. A., and Kim, S. K. (1996). The *C. elegans* vulval induction gene *lin-2* encodes a member of the MAGUK family of cell junction proteins. *Development* *122*, 97-

- 111.
- Hunter, T. (1995). Protein kinases and phosphatases: the yin and yang of protein phosphorylation and signaling. *Cell* *80*, 225-236.
- Inazawa, J., Ariyama, T., Abe, T., Druck, T., Ohta, M., Huebner, K., Yanagisawa, J., Reed, J. C., and Sato, T. (1996). PTPN13, a Fas-associated protein tyrosine phosphatase, is located on the long arm of chromosome 4 at band q21.3. *Genomics* *31*, 240-242.
- Kiess, M., Scharm, B., Aguzzi, A., Hajnal, A., Klemenz, R., Schwarte Waldhoff, I., and Schafer, R. (1995). Expression of RIL, a novel LIM domain gene, is down-regulated in Hras-transformed cells and restored in phenotypic revertants. *Oncogene* *10*, 61-68.
- Kim, E., Niethammer, M., Rothschild, A., Jan, Y. N., and Sheng, M. (1995). Clustering of Shaker-type K⁺ channels by interaction with a family of membrane-associated guanylate kinases. *Nature* *378*, 85-88.
- Kornau, H. C., Schenker, L. T., Kennedy, M. B., and Seeburg, P. H. (1995). Domain interaction between NMDA receptor subunits and the postsynaptic density protein PSD-95. *Science* *269*, 1737-1740.
- Lemmon, M. A., Ferguson, K. M., and Schlessinger, J. (1996). PH domains: diverse sequences with a common fold recruit signaling molecules to the cell surface. *Cell* *85*, 621-624.
- Maekawa, K., Imagawa, N., Nagamatsu, M., and Harada, S. (1994). Molecular cloning of a novel protein-tyrosine phosphatase containing a membrane-binding domain and GLGF repeats. *FEBS Lett.* *337*, 200-206.
- Mauro, L. J., and Dixon, J. E. (1994). 'Zip codes' direct intracellular protein tyrosine phosphatases to the correct cellular 'address'. *Trends Biochem. Sci.* *19*, 151-155.
- Miyamoto, H., Nihonmatsu, I., Kondo, S., Ueda, R., Togashi, S., Hirata, K., Ikegami, Y., and Yamamoto, D. (1995). *canoe* encodes a novel protein containing a GLGF/DHR motif and functions with *Notch* and *scabrous* in common developmental pathways in *Drosophila*. *Genes Dev.* *9*, 612-625.
- Morais Cabral, J. H., Petrosa, C., Sutcliffe, M. J., Raza, S., Byron, O., Poy, F., Marfatia, S. M., Chishti, A. H., and Liddington, R. C. (1996). Crystal structure of a PDZ domain. *Nature* *382*, 649-652.
- Niethammer, M., Kim, E., and Sheng, M. (1996). Interaction between the C terminus of NMDA receptor subunits and multiple members of the PSD-95 family of membrane-associated guanylate kinases. *J. Neurosci.* *16*, 2157-2163.
- Okano, I., Hiraoka, J., Otera, H., Nunoue, K., Ohashi, K., Iwashita, S., Hirai, M., and Mizuno, K. (1995). Identification and characterization of a novel family of serine/threonine kinases containing two N-terminal LIM motifs. *J. Biol. Chem.* *270*, 31321-31330.
- Pawson, T. (1995). Protein modules and signalling networks. *Nature* *373*, 573-580.
- Perez Alvarado, G. C., Miles, C., Michelsen, J. W., Louis, H. A., Winge, D. R., Beckerle, M. C., and Summers, M. F. (1994). Structure of the carboxy-terminal LIM domain from the cysteine rich protein CRP. *Nat. Struct. Biol.* *1*, 388-398.
- Perez Alvarado, G. C., Kosa, J. L., Louis, H. A., Beckerle, M. C., Winge, D. R., and Summers, M. F. (1996). Structure of the cysteine-rich intestinal protein, CRIP. *J. Mol. Biol.* *257*, 153-174.
- Ponting, C. P., and Phillips, C. (1995). DHR domains in syntrophins, neuronal NO synthases and other intracellular proteins. *Trends Biochem. Sci.* *20*, 102-103.
- Saras, J., Claesson Welsh, L., Heldin, C. H., and Gonez, L. J. (1994). Cloning and characterization of PTPL1, a protein tyrosine phosphatase with similarities to cytoskeletal-associated proteins. *J. Biol. Chem.* *269*, 24082-24089.
- Saras, J., Engström, U., Gonez, L.J. and Heldin, C. H., (1997a). Characterization of the interactions between PDZ domains of the protein-tyrosine phosphatase PTPL1 and the carboxyl-terminal tail of Fas. *J. Biol. Chem.* *272*, 20979-20981.
- Saras, J., Franzen, P., Aspenstrom, P., Hellman, U., Gonez, L. J. and Heldin, C.H., (1997b). A novel GTPase-activating protein for Rho interacts with a PDZ domain of the protein-tyrosine phosphatase PTPL1. *J. Biol. Chem.* *272*, 24333-24338.

- Sato, T., Irie, S., Kitada, S., and Reed, J. C. (1995). FAP-1: a protein tyrosine phosphatase that associates with Fas. *Science* *268*, 411-415.
- Schepens, J., Cuppen, E., Wieringa, B., and Hendriks, W. (1997). The neuronal nitric oxide synthase PDZ motif binds to -GDXV* carboxyterminal sequences. *FEBS Lett.* *409*, 53-56.
- Schwartz, R. M., and Dayhoff, M. O. (1979). In: Atlas of protein sequence and structure, M. O. Dayhoff, ed. (Washington D.C.: National Biomedical Research Foundation), pp. 353-358.
- Serra Pages, C., Kedersha, N. L., Fazikas, L., Medley, Q., Debant, A., and Streuli, M. (1995). The LAR transmembrane protein tyrosine phosphatase and a coiled-coil LAR-interacting protein co-localize at focal adhesions. *EMBO J.* *14*, 2827-2838.
- Shieh, B. H., and Zhu, M. Y. (1996). Regulation of the TRP Ca²⁺ channel by INAD in *Drosophila* photoreceptors. *Neuron* *16*, 991-998.
- Simske, J. S., Kaech, S. M., Harp, S. A., and Kim, S. K. (1996). LET-23 receptor localization by the cell junction protein LIN-7 during *C. elegans* vulval induction. *Cell* *85*, 195-204.
- Songyang, Z., and Cantley, L. Z. (1995). Recognition and specificity in protein tyrosine kinase mediated signalling. *Trends Biochem. Sci.* *20*, 470-475.
- Songyang, Z., Fanning, A. S., Fu, C., Xu, J., Marfatia, S. M., Chishti, A. H., Crompton, A., Chan, A. C., Anderson, J. M., and Cantley, L. C. (1997). Recognition of unique carboxyl-terminal motifs by distinct PDZ domains. *Science* *275*, 73-77.
- Stricker, N. L., Christopherson, K. S., Yi, B. A., Schatz, P. J., Raab, R. W., Dawes, G., Bassett, D. E., Bredt, D. S., and Li, M. (1997). PDZ Domain of neuronal nitric oxide synthase recognizes novel C-terminal peptide sequences. *Nature Biotech.* *15*, 336-342.
- Theisen, H., Purcell, J., Bennett, M., Kansagara, D., Syed, A., and Marsh, J. L. (1994). *dishevelled* is required during *wingless* signaling to establish both cell polarity and cell identity. *Development* *120*, 347-360.
- Tsukita, S., Itoh, M., Nagafuchi, A., Yonemura, S., and Tsukita, S. (1993). Submembranous junctional plaque proteins include potential tumor suppressor molecules. *J. Cell Biol.* *123*, 1049-1053.
- van den Maagdenberg, A. M., Olde Weghuis, D., Rijss, J., Merckx, G. F., Wieringa, B., Geurts van Kessel, A., and Hendriks, W. J. (1996). The gene (PTPN13) encoding the protein tyrosine phosphatase PTP-BL/PTP-BAS is located in mouse chromosome region 5E/F and human chromosome region 4q21. *Cytogenet. Cell Genet.* *74*, 153-155.
- Wang, H., Harrison Shostak, D. C., Lemasters, J. J., and Herman, B. (1995). Cloning of a rat cDNA encoding a novel LIM domain protein with high homology to rat RIL. *Gene* *165*, 267-271.
- Woods, D. F., and Bryant, P. J. (1993). ZO-1, DlgA and PSD-95/SAP90: homologous proteins in tight, septate and synaptic cell junctions. *Mech. Dev.* *44*, 85-89.
- Woods, D. F., Hough, C., Peel, D., Callaini, G., and Bryant, P. J. (1996). Dlg protein is required for junction structure, cell polarity, and proliferation control in *Drosophila* epithelia. *J. Cell Biol.* *134*, 1469-1482.
- Wu, R., Durick, K., Songyang, Z., Cantley, L. C., Taylor, S. S., and Gill, G. N. (1996). Specificity of LIM domain interactions with receptor tyrosine kinases. *J. Biol. Chem.* *271*, 15934-15941.
- Wu, R. Y., and Gill, G. N. (1994). LIM domain recognition of a tyrosine-containing tight turn. *J. Biol. Chem.* *269*, 25085-25090.
- Xia, H., Winokur, S.T., Kuo, W., Altherr, M.R. and Bredt, D.S., (1997). Actinin-associated LIM protein: Identification of a domain interaction between PDZ and spectrin-like repeat motifs. *J. Cell Biol.* *139*, 507-515.

Chapter 5

**Zyxin-Related Protein-1 (ZRP-1) interacts with PDZ motif in
the adaptor protein RIL and the protein tyrosine
phosphatase PTP-BL**

Edwin Cuppen, Anurhada de Leeuw, Bé Wieringa, and Wiljan Hendriks.

Zyxin-Related Protein-1 (ZRP-1) interacts with PDZ motifs in the adaptor protein RIL and the protein tyrosine phosphatase PTP-BL

Edwin Cuppen, Anuradha de Leeuw, Bé Wieringa, and Wiljan Hendriks.

Department of Cell Biology, Institute of Cellular Signalling, University of Nijmegen, Adelbertusplein 1, 6525 EK Nijmegen, The Netherlands.

Abstract

The small adaptor protein RIL consists of two segments, the C-terminal LIM and the N-terminal PDZ domain, which mediate multiple protein-protein interactions. The LIM domain binds to PDZ domains in the protein tyrosine phosphatase PTP-BL and can also interact with the N-terminal PDZ domain in RIL. Here, we describe and characterize the interaction of the PDZ domain with the zyxin-related protein ZRP-1, a protein containing three C-terminal LIM domains. The second LIM domain in ZRP-1 is sufficient for a strong interaction with RIL although also an interaction with the third LIM domain, including the proper C-terminus, is evident. ZRP-1 also interacts with the second out of five PDZ motifs in PTP-BL. For this interaction to occur both the third LIM domain and the proper C-terminus is necessary. RNA expression analysis revealed overlapping patterns of expression for ZRP-1, RIL and PTP-BL, most notably in tissues of epithelial origin. Furthermore, ZRP-1 can be co-precipitated with RIL and PTP-BL PDZ polypeptides and a striking co-localization of ZRP-1 and RIL with F-actin structures is evident in transfected epithelial cells. Taken together, PTP-BL, RIL and ZRP-1 may function as components of multiprotein complexes that are involved in the dynamics of specialized actin-based sub-cellular structures.

Introduction

It is becoming increasingly clear that multiprotein complexes, as found at cell-cell and cell-substratum contacts, are dynamic structures that function as important cellular signal transduction centers for relaying extra-cellular stimuli to cellular responses. Scaffold, anchoring and adaptor proteins (Pawson and Scott, 1997) play an important role in coordinating the assembly and dynamics of these complex structures, thereby defining the architecture of sub-cellular domains and the 'wiring' of signaling pathways. Small protein domains, like SH2, SH3, PH, LIM, WW, WD, PDZ and PTB domains (Bork et al., 1997),

are often found as modular building blocks mediating specific and dynamic interactions between the different components and cytoarchitectural elements of the cellular context. We are studying the protein tyrosine phosphatase PTP-BL (Hendriks et al., 1995) or RIP (Chida et al., 1995), which is the mouse homologue of human PTP-BAS (Maekawa et al., 1994), PTPL1 (Saras et al., 1994), PTP1E (Banville et al., 1994) and FAP-1 (Sato et al., 1995), as a potential organizer of specialized multiprotein complexes in polarized cells. PTP-BL is expressed mainly in epithelia where it localizes apically (Cuppen et al., 1998; Hendriks et al., 1995) and it has several characteristics that make it a potential scaffold protein (Fig. 1A). The protein harbors a FERM domain (Chishti et al., 1998), that may target the protein to its highly restricted sub-cellular site, and five PDZ motifs (Ponting, 1997). PDZ motifs themselves are small protein modules that mediate protein-protein interactions (Fanning and Anderson, 1996; Ranganathan and Ross, 1997; Saras and Heldin, 1996) and can associate with transmembrane proteins (Sheng, 1996), cytoskeletal components (Xia et al., 1997) and signal transduction enzymes (Ranganathan and Ross, 1997). The five PDZ motifs in PTP-BL may thus function as anchoring or scaffolding sites for other proteins, thereby enabling the formation of multiprotein complexes in which the phosphotyrosine phosphatase action of PTP-BL itself can be combined with potential downstream substrates, competitor signaling proteins and putative upstream regulatory molecules. Indeed, proteins that interact with PDZ motifs of PTP-BL have been identified. Saras and coworkers (Saras et al., 1997) identified a 160 kDa protein with Rho-GAP activity, PARG1, that binds to the fourth PTP-BL PDZ motif. We characterized a novel bromodomain-containing protein, BP75, that specifically interacts with the first PDZ motif (Cuppen et al., submitted) and found the small adaptor protein RIL (Kiess et al., 1995) to be a binding target for both the second and fourth PDZ motif of PTP-BL (Cuppen et al., 1998). RIL is down-regulated in H-Ras-transformed fibroblasts (Kiess et al., 1995) and basically consists of a C-terminal LIM domain, that is indispensable for interaction with PTP-BL, and an N-terminal PDZ motif, that can also interact with the RIL C-terminal LIM domain. LIM domain proteins form a widely diverged protein family which can be divided in three groups based upon their homologies and function (Dawid et al., 1998). Group 1 consists of homeodomain-containing LIM proteins that are primarily nuclear and implicated in transcriptional regulation. Group 2 represents the LIM-only proteins that may function in regulating group 1 proteins by LIM-LIM interactions. RIL belongs to the group 3 LIM-domain proteins, consisting of members that contain one or multiple C-terminal LIM domains. The members of this group are located primarily cytoplasmic and some, like zyxin, CRP and paxillin, are associated with the actin-based cytoskeleton. RIL is highly homologous to the PDZ/LIM proteins CLP-36 (Wang et al., 1995), ALP-1 (Xia et al., 1997) and enigma (Wu and Gill, 1994). Some binding partners have been identified for these proteins. LIM domains in enigma recognize tyrosine-containing motifs in the insulin receptor and the receptor tyrosine kinase Ret (Wu et al., 1996), and the PDZ motif in

actinin-associated LIM-protein, ALP-1, is found to interact with a spectrin-repeat in α -actinin-2 (Xia et al., 1997).

To identify additional components of the multiprotein complex containing PTP-BL and RIL, we searched for proteins that specifically interact with the PDZ motif of RIL. We here describe the identification and characterization of the LIM domain-containing protein zyxin-related protein 1, ZRP-1, also described as TRIP6 (Lee et al., 1995) and Opa-interacting protein, OIP1 (Williams et al., 1998). Interestingly, ZRP-1 was also identified in an interaction screening using the second PDZ motif of the human homologue of PTP-BL, hPTP1E (Genbank accession AF000974; Murthy, K.K., Shen, S.-H and Banville, D., unpublished results). This interaction is confirmed by our data and we here show that the LIM domains in ZRP-1 are important for interaction with the RIL and PTP-BL PDZ motifs. The potential role of these interactions in the architecture or dynamics of specialized sub-cellular actin-based structures will be discussed.

Results

ZRP-1 interacts with PDZ motifs in RIL and PTP-BL

Candidate proteins interacting with the PDZ motif of RIL were obtained from a human fetal brain cDNA library using RIL-PDZ (Fig. 1A) as a bait in the yeast two-hybrid interaction trap (Gyuris et al., 1993). From 0.5×10^6 transformants several interacting clones were identified. One of them, AL7 (Fig. 1B), encodes the C-terminal half of the LIM domain-containing zyxin-related protein-1 (ZRP-1; Genbank AF000974, Murthy, K.K., Shen, S.-H and Banville, D., unpublished results), also described as thyroid receptor interacting protein-6, TRIP6 (Lee et al., 1995) and Opa-interacting protein, OIP1 (Williams et al., 1998). ZRP-1 was submitted to the public database as a protein resulting from a two-hybrid screening using the second PDZ domain of the cytosolic protein tyrosine phosphatase hPTP1E as bait (Murthy, K.K., Shen, S.-H. and Banville, D., unpublished results). ZRP-1 is a 476 amino acid protein that contains three LIM domains in its C-terminal half. Interestingly, we recently found that the single C-terminal LIM domain of the protein RIL interacts with PDZ motifs in PTP-BL, the mouse homologue of hPTP1E (Cuppen et al., 1998). Therefore, we also used the five PDZ motifs of PTP-BL as a bait (BL-PDZ-I-V, Fig. 1A) and indeed an interaction with AL7 could be demonstrated (Fig. 1B). Subsequent testing of single PDZ motifs of PTP-BL showed that only the second PDZ motif of PTP-BL interacts with AL7 (data not shown), in line with the observations made for hPTP1E (Murthy, K.K., Shen, S.-H and Banville, D., unpublished results).

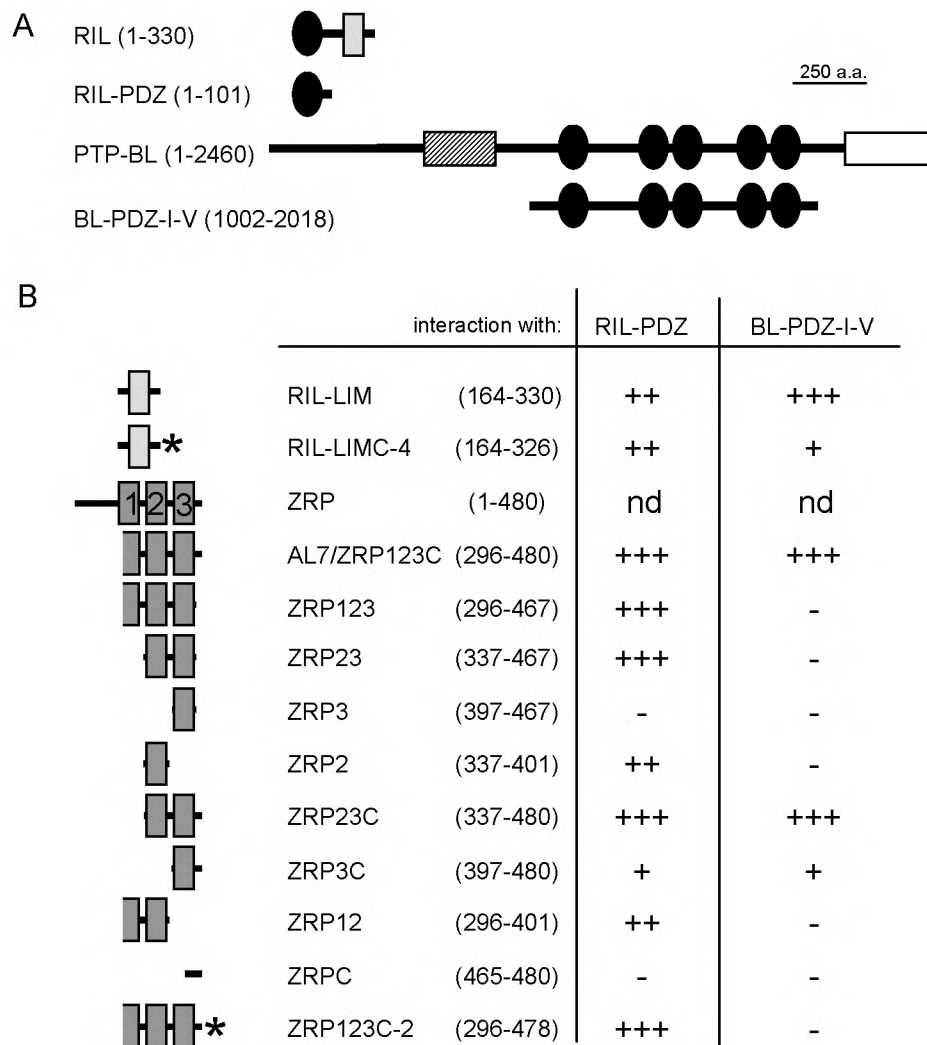


Figure 1: Schematic representation of the protein segments used in the two-hybrid interaction trap. Depicted are the RIL and PTP-BL proteins and their PDZ segments that were used as bait (A) in the two-hybrid interaction trap. Also the ZRP-1 and RIL segments represented in the prey constructs are shown (B). Numbers that correspond to the first and last a.a. positions in the PTP-BL (Z32740), RIL (Y08361) and mZRP-1 (AF097511) protein segments are shown in parentheses. Two hybrid interaction results with either RIL-PDZ or BL-PDZ-I-V are schematically indicated: +++, very strong interaction; ++, strong interaction; +, weak, but significant interaction; -, no interaction detectable; nd, not determined. FERM domain, hatched box; catalytic PTP domain, open box; PDZ motifs, black ovals; LIM domains, gray boxes.

Presence of LIM domains and the C-terminus of ZRP-1 have differential effects on binding to RIL and PTP-BL

To determine the requirements for binding to the RIL and PTP-BL PDZ motifs a series of deletion mutants of AL7 was constructed and tested using the interaction trap assay (Fig. 1B). None of the constructs used contained a complete first LIM domain, since this domain was only partially present in the original clone. For an interaction with the RIL-PDZ motif either the second LIM domain (ZRP2) or the third LIM domain together with the proper C-terminus (ZRP3C) of ZRP-1 are sufficient. Neither the C-terminus (ZRPC) nor the third LIM domain (ZRP3) alone can mediate the interaction with RIL-PDZ. Importantly, a conventional C-terminus recognition mode can be excluded because removal of the last two amino acids of ZRP-1 (ZRP123C-2) does not affect RIL-PDZ binding (Fig. 1B). Similarly, deletion of the last four residues in the RIL C-terminal half (RIL-LIMC-4) also has no effect on the interaction of this protein segment with the RIL-PDZ motif (Cuppen et al., 1998).

For an interaction with BL-PDZ-I-V to occur a C-terminal segment of ZRP-1 that includes the third LIM domain and the proper C-terminus (ZRP3C) is essential. Presence of the second LIM domain (ZRP23C) does enhance the interaction strength, whereas removal of either the LIM domain (ZRPC) or the proper C-terminus (ZRP3) totally abolishes the interaction. In contrast to the situation as for RIL-PDZ, deletion of the last two amino acids (ZRP123C-2) from the originally identified clone, completely destroys the interaction with BL-PDZ-I-V (Fig. 1B). Using only the second PDZ motif of PTP-BL as bait, the same results as for BL-PDZ-I-V were obtained (not shown).

Identification and characterization of full-length mouse ZRP

Sequence information on human ZRP-1 was used to screen public EST databases for mouse homologues. An EST clone with Genbank database accession number W58878 was found to contain the complete open reading frame encoding mouse ZRP-1 (mZRP-1), but part of the 5' untranslated region was lacking. The insert of this EST clone was completely sequenced and assigned the database accession number AF097511 by Genbank. Comparison of mouse and human ZRP-1 (AF000974) reveals 76% and 86% identity at the nucleotide and amino acid level, respectively (Fig. 2A). The C-terminal part of the protein,

Figure 2: (facing page) Comparison of mouse ZRP-1 with related peptide sequences.

The mouse ZRP-1 (M-ZRP-1; AF097511) protein sequence is shown, aligned with its human homologue (H-ZRP-1; AF000974) (A) and with the homologous LIM domain-containing proteins human LPP (U49957) and mouse zyxin (Q62523) (B). Single horizontal black lines indicate the LIM domains and the zinc-coordinating residues are marked by vertical black lines. The protein segment corresponding to the functional nuclear export signal in zyxin (Nix and Beckerle, 1997) is double underlined. The black arrowhead points to the beginning of the human ZRP-1 segment as present in clone AL7. Identical residues in two or three sequences are shown in black on a gray background or in white on a black background, respectively. Gaps are indicated by dashes (-).

```

                *           20           *           40           *           60           *           80           *           100
M-ZRP-1 : MSGPTWLPFKQPEFSRLPQGRSLFRGALGFPTAHGATLQPHFRVNFCLPEPEHCYQPPGVFEDRGTWVGSHTPQRLQGLFPDRGIIIRFGSLDAEIDSL
H-ZRP-1 : MSGPTWLPFKQPEFARAPQGRAIRPGTGPFPFANGAALQPHFRVNFCLPSEHCYQAPGGPFEDRGPANVGSHTVQLHTQGLPADRGGLRFGSLDAEIDL

                *           120          *           140          *           160          *           180          *           200
M-ZRP-1 : TSMLADLDGGRSHAPRRPDRQAFEAFFFFHAYRGGSLKPSGGAVPTMPLPASHYGGPTPASYATASTPAGPAFPVQVKVAQPVVRCGLPRRGASQASGFLP
H-ZRP-1 : STTLAKLNGGRGHASRRPDRQAYEPPFPAYRTGSLKPN----FASPLPASPYPGGPTPASYTTASTPAGPAFPVQVKVAQPVVRCGPFRRGASQASGFLP

                *           220          *           240          *           260          *           280          *           300
M-ZRP-1 : GPHFPLTGRGEVWGAGYRSHREPQGVPEGPGSVHIFAGGGRRGGHEPQGLGQPPPEELERLTKKLVHDMSHPPSGEYFGRCGGCGEDVVGDGAGVVAL
H-ZRP-1 : GPHFPLPGRGEVWGPYRSQREPFGAKKEAAAGVSGPAGRGRGGHEGQVFLSQPPELDRLTKKLVHDMNHPPSGEYFGQCGGCGEDVVGDGAGVVAL

                *           320          *           340          *           360          *           380          *           400
M-ZRP-1 : DRVFHIGCFVCSSTCRAQLRGQHFYAVERRAYCESCYVATLEKCSSTCSEPIILDRILRAMGKAYHPGCTFCVVCHRGLDGIPTVDATSQIHCIEDFHRKFA
H-ZRP-1 : DRVFHVGCFVCSSTCRAQLRGQHFYAVERRAYCEGCVATLEKCATCSQPIILDRILRAMGKAYHPGCTFCVVCHRGLDGIPTVDATSQIHCIEDFHRKFA

                *           420          *           440          *           460          *           480
M-ZRP-1 : FRCVCGGAIMPEPGQEEVTRIVALDRSFHIGCYKCEECGLLLSSEEGCQGCYPLDGHILCKACSAWRIQELSATVTDC
H-ZRP-1 : FRCVCGGAIMPEPGQEEVTRIVALDRSFHIGCYKCEECGLLLSSEEGCQGCYPLDGHILCKACSAWRIQELSATVTDC

M-ZRP-1 : -----
H-LPP : MSHPSWLPKSTGEPLGHVPAARMETHSFGNPSISVSTQQEPKKAFAVVAPEKPYNEPKQPGGEGDPLPPPPPLDD--SSALEPSISGNFP--EPPFLDEE : 97
M-ZYXIN : -----MAAPRPPPAISVSVSAPAFYAPQKKFAPVVAPEKPYNEPKQPGGEGDPLPPPPPLDD--SSALEPSISGNFP--EPPFLDEE : 81

M-ZRP-1 : -----MSGPTWLPFKQPEFSRLPQGRSLFRGALGFPTAHGATLQPHFRVNFCLPEPEHCYQPPGVFEDRGTWVGSHTPQRLQGLFPDRGIIIRFGSLDAEIDSL : 53
H-LPP : AFKVQGNPFGKTLERRSSLDAAIDSLTSLADLECSSEYKPRPPQSTGSSASPPVSTPVTGKRMVFNQPPPT--ATKKSILKQEPAPQAGPTP--- : 192
M-ZYXIN : GDDSEGALGGAFPPPPPMIEBPPFP--APLEEDIPSPFPPLLEEGGPEAPLQPLPQPRKVC SIDLEIDSLSSLLDDMTKNDFFKARVSSGYVPEP--- : 177

M-ZRP-1 : CYQPPGVFEDRGTWVGSHTPQRLQGLFPDRGIIIRFGSLDAEIDSLTSMMLADLDGGRSHAPRRPDRQAFEAFFFFHAYRGGSLKPSGGAVPTMPLPASHY : 153
H-LPP : -VADIGTLKQPPQEVPAASYTTASTSS--RPTFNQVQKSAQPSHYMAAESGGQIYSGPQGYNTQVFPVSGQCEPESTRGEMDYAYIIPPPGLQPEPGYGY : 289
M-ZYXIN : -VATPVPKPESTKEAPGGTAPLPPWK--TGS-----SSQPPQPPQKQV--QLHVQPAQKHFVQPPVSSANTQV--RCPLSQA-----PTAPKF : 257

M-ZRP-1 : GGPASPASYATASTPAGPAFPVQVKVAQPVVRCGLPRRGASQASGFLPQPHFPLTGRGEVWGAGYRSHREPQGVPEGPGSVHIFAGGGRRGGHEPQGLG : 253
H-LPP : A--ENQGRYREGYAAQPGYGGRRNDSDETYGQQGHENTWKREPGYTPPGAGNQNPFGMYPTGPKKTYITDPVSAFCAPPLQ--FKGHSGLGFPSSVAPS : 386
M-ZYXIN : A--EVAPKFTPVVSKFSPGAPSGPGQPI-----KKWCLRMPPSSVSTGSPQPPS--FTYAQQKPKLVQKQHPQPPPAQ--NQNQVRSPGGGGL--T : 344

M-ZRP-1 : QPPEELERLTKKLVHDMSHPPSGEYFGR--CGGCGEDVVGDGAGVVALDRVFHIGCFVCSSTCRAQLRGQHFYAVERRAYCESCYVATLEKCSSTCSEPI : 351
H-LPP : FREDELEHLLTKKLVHDMSHPPSGEYFGR--CARCENYVGGTGTCTAMDQVPHVDCTFCILINNKLRGQPFYAVKKAYPEPCYINTLEQCNVCKRPI : 484
M-ZYXIN : LKEVELEQLTQQLMDMSEHPQRSVAVNBSCKKQNPQLARAQPAVRAQGLLEHTCFECHOQQQQLGQQQFYSLECAPYCECCYTDLEKCNVCKRPI : 444

M-ZRP-1 : DRILRAMGKAYHPCFTCVVCHRGLDGIPTVDATSQIHCIEDFHRKFAAPRCVCGGAIMPEPGQEEVTRIVALDRSFHIGCYKCEECGLLLSSEEGCQGC : 451
H-LPP : DRILRAMGKAYHPCFTCVVCHRGLDGIPTVDAGGLLHCISDFHKKFAAPRCVCGGAIMPEPGQEEVTRIVALDRSFHIGCYKCEECGLLLSSEEGCQGC : 583
M-ZYXIN : DRILRAMGKAYHPCFTCVVCHRGLDGIPTVDQANQPSVPMYHKQYAPRCVCGGAIMPEPGQEEVTRIVALDRSFHIGCYKCEECGLLLSSEEGCQGC : 544

M-ZRP-1 : CMLDGHILCKACSAWRIQELSATVTDC : 480
H-LPP : CMLDGHILCKACNSARIRVLTAKASTDL : 612
M-ZYXIN : CMLDGHVLCRKKHSARAQT----- : 564

```

encompassing the three LIM domains, is almost completely conserved, whereas the N-terminus is less conserved and contains a small four amino acid insertion in mouse. Comparison of the predicted 51 kDa mZRP-1 polypeptide with entries in public protein databases revealed highest overall homology with the LIM domain-containing proteins lymphoma preferred partner (LPP; U49957) and the adhesion plaque protein zyxin (Q62523). Alignment of these proteins reveals very high homology in the region encompassing the three LIM domains (Fig. 2B). Also, the region N-terminal to the first LIM domain that in chicken zyxin corresponds to a nuclear export signal (Nix and Beckerle, 1997) is highly conserved. In contrast, the N-terminal half of mZRP-1 shows low overall homology with LPP and zyxin but, as in zyxin, this region is very rich in proline (19%) and glycine (15%).

mZRP-1 expression pattern

The observed interaction of ZRP-1 with RIL and PTP-BL can only be of biological significance when there is overlap in expression patterns. Previous studies have shown an epithelial expression pattern for PTP-BL (Cuppen et al., 1998; Hendriks et al., 1995) and

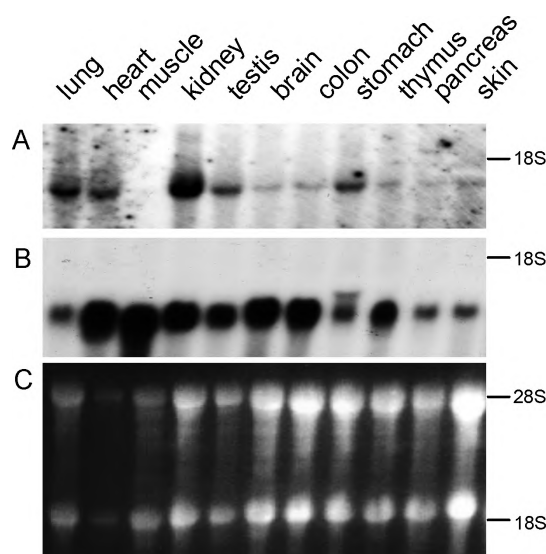


Figure 3: Tissue distribution of mZRP-1 messenger RNA.

Northern blot analysis of the mZRP-1 expression levels in total RNA isolated from different adult mouse tissues (A). As controls for RNA loading, hybridization results for the housekeeping gene GAPDH (B) as well as the ethidium bromide staining pattern of the gel (C) are shown. mZRP-1 is highly expressed in lung, heart, kidney, testis, and stomach. No expression is detected in skeletal muscle. The 28S and 18S ribosomal bands, corresponding to 4.6 and 1.9 kb transcript lengths, respectively, are indicated.

expression of RIL in various epithelia and different types of muscle (Kiess et al., 1995). The mZRP-1 cDNA was used to probe a Northern blot of total RNA from several different mouse tissues. A transcript of about 1.8 kb was detected that is highly expressed in kidney, stomach, lung, heart and testis, whereas low expression levels are found in brain, colon, thymus, pancreas and skin (Fig. 3). To further delineate the mZRP-1 expression pattern we used an antisense RNA probe for *in situ* hybridization on mouse embryo cryosections. mZRP-1 expression is found throughout development in all embryonic stages (10.5 dpc to 18.5 dpc) that were analyzed (Fig. 4 and data not shown). In 16.5 dpc embryos mZRP-1 is highly expressed in skin, lung, thymus, duodenum and the ependymal cell layer surrounding the ventricles in brain. High expression is also observed in the salivary glands, vibrissae, choroid plexus, blood vessel walls, oesophagus and midgut. Low levels of mZRP-1 mRNA are found in spinal cord, heart and liver (Fig. 4B). No positive signal was obtained using a mZRP-1 sense RNA probe (Fig. 4C). In summary, mZRP-1 is prominently expressed in epithelial and endothelial cell types and only low expression is found in neuronal and muscle cells. It is of note that high expression of mZRP-1 coincides with that of RIL and PTP-BL, most notably in the epithelium of the lung, the epidermis and the ependymal cell layer surrounding the ventricles in brain.

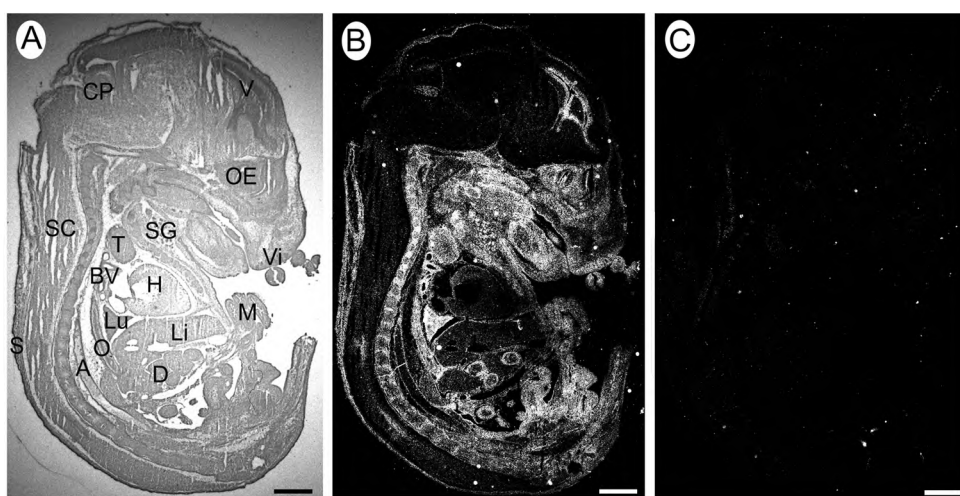


Figure 4: mZRP-1 mRNA *in situ* hybridization on 16.5 dpc mouse embryo sections. A bright field (A) and dark field images of parasagittal cryosections of 16.5 dpc mouse embryos hybridized with an antisense mZRP-1 RNA probe (B) and a sense mZRP-1 probe (C) are shown. High expression is evident in lung, skin, blood vessels, duodenum, salivary glands, vibrissae and the ependymal layer surrounding the ventricles in brain. A, abdominal aorta; BV, blood vessels; CP, choroid plexus; D, duodenum; H, heart; Li, liver; Lu, lung; O, oesophagus; OE, olfactory epithelium; S, skin; SC, spinal cord; T, thymus; Vi, vibrissae. Bars, 1 mm.

mZRP-1 co-precipitates with the RIL and PTP-BL PDZ motifs

To confirm the observed interaction in a more physiological surrounding, we co-transfected mammalian epithelial cells (COS-1) with expression constructs encoding an EGFP-mZRP fusion protein and VSV-G epitope-tagged versions of RIL-PDZ, the five PDZ motifs of PTP-BL, or the second PDZ motif of PTP-BL alone. All transiently expressed proteins are readily detected in the lysates by Western blotting (Figs. 5A and B). Pull-down of EGFP-mZRP was demonstrated for all PDZ constructs used, whereas the control (EGFP alone) remains negative (Fig. 5C). In the reciprocal experiment, co-precipitation of VSV-G epitope-tagged proteins with EGFP-mZRP could clearly be shown for the RIL PDZ motif, and to a lesser extend for the five PDZ motifs of PTP-BL (not shown). Unexpectedly in this experiment, we could not demonstrate co-precipitation of EGFP-mZRP and the second PTP-BL PDZ motif alone. Taken together, these findings confirm independently the results obtained in the yeast two-hybrid interaction trap.

Sub-cellular localization of RIL

We used an affinity-purified polyclonal antibody directed against RIL (Cuppen et al., 1998) to identify cell lines that express RIL endogenously and found that the human epidermoid

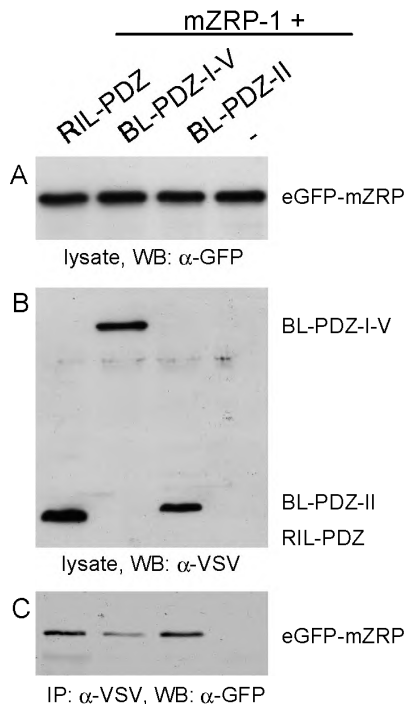


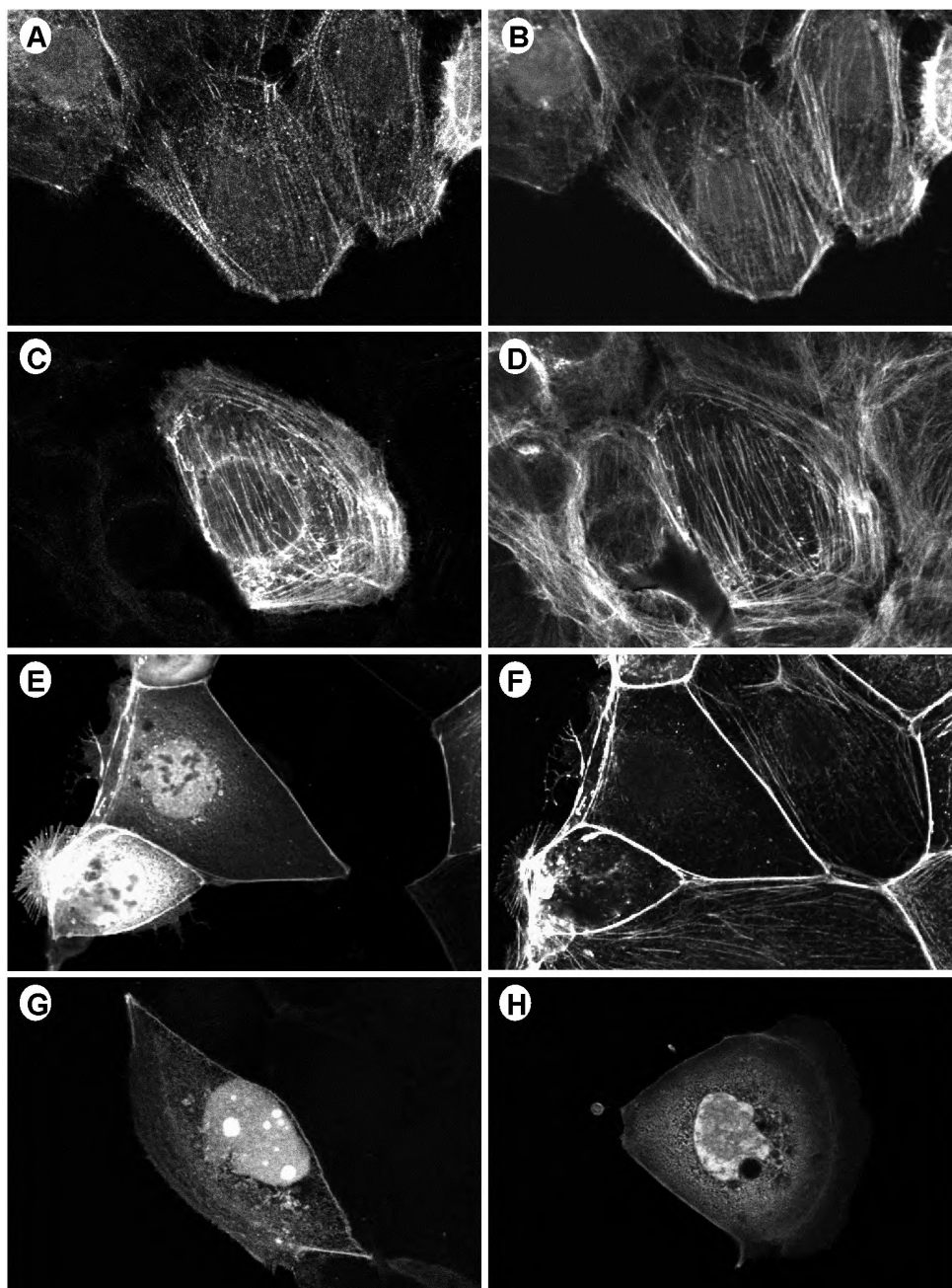
Figure 5: mZRP-1 co-precipitates with PDZ motifs of RIL and PTP-BL.

COS-1 cells are co-transfected with a construct encoding EGFP-tagged mZRP-1 and a construct encoding either VSV-tagged peptides of the RIL PDZ motif, the five PDZ motifs of PTP-BL (BL-PDZ-I-V) or the second PDZ motif of PTP-BL alone (BL-PDZ-II). As a control, empty vector (-) was co-transfected. Western blotting using an α -GFP antibody detects a single 80 kDa EGFP-mZRP fusion protein in the total cell lysates (A), whereas the α -VSV monoclonal antibody specifically detects the tagged PDZ motifs (B). After immunoprecipitation of the PDZ motifs, pull-down of EGFP-tagged mZRP-1 with the PDZ motifs is demonstrated (C). No pull-down of mZRP-1 is observed in lysates of COS cells co-transfected with empty vector.

carcinoma cell line A-431 expresses RIL at low but detectable levels. Clear co-localization of endogenous RIL with the filamentous actin stress-fibers is evident (Figs. 6A and B). To facilitate detection, RIL levels were increased artificially by transfection of full-length RIL in A-431 cells. Again, the same sub-cellular location and co-localization with F-actin was found (Figs. 6C and D) but now RIL staining was much more intensive, underscoring the specificity of the RIL polyclonal antiserum. In addition, weak perinuclear cytosolic staining for RIL is evident, which may be due to the high level of overexpression (note that endogenous RIL in neighboring untransfected cells is not visible under these sampling conditions, Fig. 6C). Likewise, in the human adenocarcinoma cell line Caco-2, endogenous RIL was barely detectable (not shown), but also here transfected RIL consistently co-localized with F-actin structures (Figs. 6E and F). In these cells, however, besides being localized at stress fibers, focal and cell-cell contacts, RIL was also present in the nucleus. Since RIL itself does not contain obvious motifs for direct F-actin binding, we tested whether either its PDZ or LIM domain could be responsible for (indirect) binding to F-actin structures. Transient expression of epitope-tagged RIL-PDZ and RIL-LIM protein segments showed that both domains were guided to F-actin containing cell-cell contacts. In addition, cytosolic staining and a typical nuclear localization with a distinct distribution pattern for each of the two segments, was observed (Figs. 6G and H).

Co-localization of mZRP-1 with RIL and F-actin

Next, to study the sub-cellular localization of mZRP-1 we transiently expressed the EGFP-mZRP fusion protein in Caco-2 cells. Because autofluorescence of EGFP signal was barely detectable, a biotinylated polyclonal antibody that recognizes EGFP in combination with a streptavidin-FITC conjugate was used to visualize the fusion protein. As shown in Fig. 7, panels A and B, a clear co-localization of mZRP-1 with F-actin at cell-cell contacts is evident. Also, mZRP-1 is found throughout the cytosol in a typical punctuate distribution pattern. Using antibodies against LAMP-1 and LAMP-2 (Carlsson et al., 1993) we could exclude co-localization with lysosomes for these structures (not shown). In the highest expressing cells the appearance of the speckles is most intense, suggesting that they result from overexpression and most likely represent aggregates of surplus EGFP-mZRP fusion protein. It is of note that formation of these aggregates is not caused by the EGFP moiety, since identical effects were observed for a cMyc epitope-tagged version of mZRP-1 (not shown). Also in transfected A-431 cells such aggregates have been observed next to the EGFP-mZRP decorated stress fibers (data not shown). When mZRP-1 and RIL are overexpressed simultaneously in Caco-2 cells, their co-localization with F-actin-containing structures at sites of cell-cell contacts and in lamellipodia remained evident (Figs. 7 C and D).



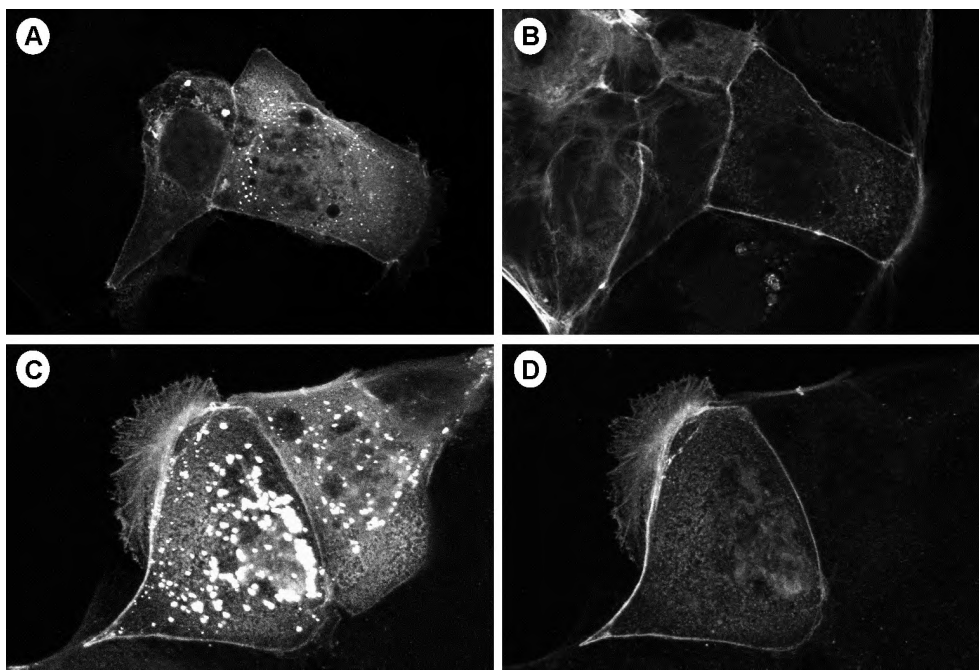


Figure 7: mZRP-1 co-localizes with F-actin and RIL

A construct encoding an EGFP-mZRP fusion protein was transfected in Caco-2 cells, alone (A, B) or together with a construct encoding full-length mouse RIL (C, D). mZRP-1 detection was enhanced using a biotinylated antibody directed against EGFP (A, C) and cells were double labeled with phalloidin-Texas Red for visualization of F-actin (B) or with α -RIL antibody for detection of overexpressed RIL (D). mZRP-1 localizes to F-actin-rich structures at cell-cell contacts but also typical dot-like structures, that may be overexpression artifacts, are observed. Also, weak cytosolic and nuclear staining is evident for mZRP-1.

Figure 6: (facing page) Subcellular localization of RIL in A-431 and Caco-2 cells.

Endogenous (A) and overexpressed RIL (C, E) is detected in untransfected A-431 cells (A, B) and A-431 (C, D) or Caco-2 (E, F) cells transfected with a construct encoding full-length mouse RIL. Cells were double labeled for F-actin using phalloidin-Texas Red (B, D, F). In A-431 cells endogenous RIL decorates stress fibers in a typical punctuate manner, as detected by an α -RIL polyclonal antibody. Overexpression of RIL in A-431 cells shows a similar co-localization with F-actin, but also weak cytosolic and nuclear staining is evident. In Caco-2 cells, that have less stress fibers than A-431 cells but do make cell-cell contacts, hardly any endogenous RIL can be detected (not shown). Transiently overexpressed RIL (E) co-localizes with the F-actin containing adhesion belt (F). Clearly, nuclear localization of the RIL protein can be seen in these cells (E). VSV-epitope-tagged peptides of both the RIL-PDZ motif (G) and the RIL-LIM domain (H) localize to stress fibers in A-431 cells (not shown) and to the adhesion belt in Caco-2 cells (G, H). Again, cytosolic and typical nuclear staining is evident.

Discussion

In our search for proteins that interact with the single, N-terminal PDZ motif of the small adaptor protein RIL, we identified a multiple LIM domain-containing protein termed zyxin-related protein-1 or ZRP-1. As the RIL-PDZ can also engage in binding to the single, C-terminal RIL-LIM domain, and, in turn, this latter domain can bind to the second and fourth PDZ motif of mouse protein tyrosine phosphatase PTP-BL (Cuppen et al, 1998) we tested whether the PDZ domains in RIL and PTP-BL or the LIM domains in ZRP-1 and RIL showed functional homology. Indeed, we and others found an association of ZRP-1 with the second PDZ motif in PTP-BL (Fig. 1) or its human counterpart hPTP1E (Genbank accession AF000974; Murthy, K.K., Shen, S.-H. and Banville, D., unpublished). Further support for a biological significance of these interactions comes from the demonstration of co-precipitation of mZRP-1 with RIL and PTP-BL PDZ motifs from lysates of transiently overexpressing cells (Fig. 5), from the overlap in cell-type specific distribution patterns (Figs. 3 and 4), and the sub-cellular localization studies (Fig. 7).

Characterization of the RIL and PTP-BL PDZ-mediated interactions using deletion mutants of ZRP-1 showed that these are critically dependent upon the presence and integrity of ZRP-1 LIM domains, but differ in the requirement of the proper C-terminus. PDZ motifs are best known as interactors which specifically recognize short C-terminal peptides (Saras and Heldin, 1996; Songyang et al., 1997). It is conspicuous, however, that both RIL and ZRP-1 C-terminal ends (-VELV* and -TTDC*, respectively) do not match the consensus C-terminal PDZ recognition site (-T/SxV*) (Songyang et al., 1997). Still, deletion of only the last four or two residues, respectively, dramatically affects the interaction with PTP-BL PDZ motifs (Fig. 1). The very same mutations, however, do not affect RIL-PDZ binding at all. This suggests that RIL PDZ and PTP-BL PDZ motifs mediate two different modes of interaction that are based on distinct mechanistic principles, namely internal and C-terminal binding. PDZ binding that is not based on C-terminus recognition has been described for other systems before. For example, binding of the third PDZ motif in INAD to the TRP Ca²⁺ channel is critically dependent on an internal STV peptide (Shieh and Zhu, 1996), its fifth PDZ motif binds an internal segment of phospholipase C- β (van Huizen et al., 1998), and the ALP-1 PDZ motif binds to an internal spectrin-like repeat in α -actinin-1 (Xia et al., 1997). Furthermore, homo- and heteromeric PDZ-PDZ interactions between the third and fourth motif in INAD (Xu et al., 1998) and the motifs in nNOS and α 1-syntrophin or PSD95 do occur (Brenman et al., 1996). Finally, dual specificity for both internal and C-terminal sequences by the same PDZ motif has been observed. The PDZ motifs in INAD, nNOS, α 1-syntrophin and PSD95 that are involved in the aforementioned PDZ-PDZ interactions are also able to recognize C-terminal peptides (Schepens et al., 1997; Stricker et al., 1997; Xu et al., 1998). The same situation holds for the second PDZ motif of PTP-BL, whose ability to recognize C-terminal T/SxV* peptides was demonstrated convincingly

(Cuppen et al., 1997; Saras et al., 1997; Sato et al., 1995; Songyang et al., 1997). It should be noted, however, that this binding is rather weak as compared to the interactions with the LIM domain containing segments of RIL and ZRP-1. Crystal structure analysis of PDZ motifs has uncovered the structural basis for C-terminal peptide recognition. A compact modular structure, formed by four β -sheets and two α -helices, creates a deep hydrophobic cleft that can harbor a short C-terminal peptide (Doyle et al., 1996; Morais Cabral et al., 1996). Thusfar, it is unclear whether polypeptide-internal interactions use the same interaction interface or whether other binding pockets exist on the globular PDZ motif. Data supporting the latter view comes from studies on INAD, showing that homo-multimerization via PDZ motifs does not prevent recognition of C-terminal targets by the same PDZ motifs (Xu et al., 1998). On the other hand, interaction with the nNOS PDZ motif seems to inhibit C-terminal peptide binding to the α 1-syntrophin PDZ motif (Gee et al., 1998), suggesting that – at least in some cases – there can be overlap or close proximity for the binding interfaces that mediate C-terminus recognition and PDZ motif dimerization. Thus, there is the possibility that the binding cleft in some PDZ motifs may be optimally tailored to receive both C-termini and internal peptides, whereas others may have two distinct binding interfaces, thus precluding interference by binding to different substrates. What could be the role of LIM domains in the RIL/PTP-BL/ZRP-1 interactions? One possibility is that LIM domains act passively in providing the conformational structure necessary for the recognition of internal peptide segments by PDZ motifs. Recent experiments indeed demonstrate that the syntrophin PDZ motif recognizes an internal peptide that is similar to its C-terminal consensus target only if it is conformationally constrained through intramolecular disulfide bond formation (Gee et al., 1998). Yet, another possibility is that LIM domains act as dimerization signals (Feuerstein et al., 1994), and mediate ZRP-1 and RIL interaction indirectly through the formation of dimers or multimers, thereby ‘concentrating’ the proper C-termini for efficient recognition by PDZ motifs. Data supporting such a model come from *in vitro* and two-hybrid experiments on syndecan binding to the PDZ protein syntenin, which indicate that at least dimers of the syndecan C-terminus are necessary for detectable interaction (Grootjans et al., 1997). Finally, LIM domains themselves may function as interaction interface for PDZ motifs. Next to homo- and heterophilic interactions (Curtiss and Heilig, 1998), LIM domains are found to interact with a variety of other domains (Dawid et al., 1998). For example, the LIM domain in LIMK1 interacts with the kinase domain in LIMK1 and 2 (Hiraoka et al., 1996), LIM domains in Enigma recognize tyrosine-containing motifs in receptor tyrosine kinases (Wu et al., 1996) and the N-terminal region of protein kinase C associates with LIM domains in ENH, Enigma and LIMK1 (Kuroda et al., 1996). Considering this diversity of interaction possibilities LIM domains may thus represent multifunctional interfaces, alike the situation with the members of the PDZ domain family.

We here demonstrate that endogenous and transfected RIL co-localizes with ZRP-1 at

specific F-actin rich structures, like stress fibers and cell-cell contacts. This is in keeping with the observation that several important LIM proteins have a role in adhesion-plaque and actin-microfilament organization (Beckerle, 1997; Dawid et al., 1998). The finding that epitope-tagged constructs of the PDZ and the LIM domain of RIL both reveal a similar localization was less well anticipated. Although many LIM proteins localize to F-actin and LIM domains have been found to be important for this localization (Arber and Caroni, 1996), no direct interaction of a LIM domains with F-actin has been shown thusfar. We can, therefore, most easily explain our findings by assuming that the routing and association of both artificially truncated RIL domains is determined via an interaction with endogenous full-length RIL (see also Cuppen et al., 1998). Ultimately, other components in the multiprotein complexes to which RIL molecules associate, may be responsible for targeting to the highly specialized sub-cellular sites. Interestingly, both ALP-1 and zyxin, that are highly homologous to RIL and ZRP-1, respectively, interact with the actin-binding protein α -actinin (Crawford et al., 1992; Xia et al., 1997). Could there thus be a direct role for ZRP-1 in the formation of F-actin rich structures? The ZRP-1 homologue zyxin has been implicated in the spatial control of actin filament assembly as well as in pathways important for cell differentiation (Beckerle, 1997). Both small GTPases like Rho and reversible tyrosine phosphorylation play an important role in these processes. For example, Vav, a guanine nucleotide exchange factor for small GTP-binding proteins in the Rho family, interacts directly with the proline-rich region of zyxin via its SH3 domain (Hobert et al., 1996). Furthermore, several SH3 domain-containing tyrosine kinases, such as the Src family members, co-localize with zyxin. We should be careful in extrapolating these findings, however, as the homology of ZRP-1 with zyxin in the proline-rich N-terminal half is rather limited. Still, it would be interesting to see whether this segment of ZRP-1 is indeed a target for proteins that contain domains known to recognize proline-rich regions, like SH3 (Sparks et al., 1996), WW/WWP (Chan et al., 1996; Chen and Sudol, 1995) or EVH1 modules (Niebuhr et al., 1998). Whatever, based on the findings reported here we can now postulate the (putative) combined presence of both a protein tyrosine phosphatase (i.e. PTP-BL) and a small GTPase activating protein with specificity for Rho (i.e. PARG1; (Saras et al., 1997)) within one large complex containing ZRP-1. Together with other recent findings this opens intriguing perspectives for explaining the dynamic behavior of the cortical actin cytoskeleton under normal and pathophysiological conditions.

One direct indication for ZRP-1 function in actin remodeling comes from the identification of ZRP-1 in a two-hybrid screening for proteins that interact with *Neisseria gonorrhoeae* OpaP, a member of a family of outer membrane proteins involved in gonococcal adherence to and invasion of human cells (Williams et al., 1998). Reorganization of the actin cytoskeleton is an important step in the invasion and spreading of bacteria in eukaryotic cells, and OpaP is likely to have a role in this process. Likewise, the similarity between the ZRP-1 homologues zyxin and ActA, the protein of *Listeria monocytogenes* that facilitates

host cell actin remodeling during infection and spread (Golsteyn et al., 1997) may be more than just coincidental. It should be stressed, therefore, that PTP-BL, RIL and mZRP-1 are localized in vivo at important sites of potential pathogen entry (Fig. 4; Cuppen et al., 1998). Besides the cytoskeleton-associated localization, also a nuclear location for mZRP-1 is evident in our transfection studies (Fig. 7). Again there is analogy with other members of the zyxin family, as the region homologous to the nuclear export signal in chicken zyxin (Nix and Beckerle, 1997) is indeed the only highly conserved region between zyxin and mZRP-1 outside the LIM domain area. It is, therefore, tempting to speculate that mZRP-1, like zyxin, shuttles between the nucleus and specific cytosolic sites for transducing signals between these compartments. Likewise, RIL and PTP-BL are also found in the nucleus, albeit at very low levels compared to their abundance in the cytosol (Fig. 6; Cuppen et al., submitted). Future studies should address the routing mechanism and physiological relevance of this phenomenon.

Taken together, our results show that LIM domains are important determinants in PDZ-mediated interactions that may shape signaling complexes containing PTP-BL, RIL and mZRP-1 that have the potential to be involved in regulating actin cytoskeleton dynamics at specialized subcellular sites.

Materials and Methods

Two-Hybrid Interaction Trap - Plasmid DNAs, the yeast strain EGY48 and the human fetal brain cDNA library used for the interaction-trap assay were kindly provided by Dr. Roger Brent and colleagues (Massachusetts General Hospital, Boston, MA) and used as described (Gyuris et al., 1993). The construction of RIL-PDZ and PTP-BL PDZ baits has been described previously (Cuppen et al., 1998). The deletion constructs of ZRP-1 were made by sub-cloning fragments, that were generated by PCR with human ZRP-1 as template, using synthetic oligonucleotides for introducing the appropriate stop codon and EcoRI and XhoI restriction sites. These fragments were cloned in-frame in the pJG4-5 prey vector and checked for mutations by DNA sequencing. For two-hybrid interaction assays plasmids were introduced in yeast strain EGY48 (*MATa trp1 ura3 his3 LEU2::pLexAop6-LEU2*) containing the plasmid pSH18-34, which includes the reporter *lacZ* gene, and tested for an interaction as detected by growth and blue coloring on minimal agar-plates lacking histidine, tryptophan, uracil and leucine, containing 2% galactose, 1% raffinose and 80 µg/ml X-gal, buffered at pH7.0.

Full-length mouse ZRP cDNA clones - Comparison of obtained prey cDNA sequences with database entries was done using the BLAST program (Altschul et al., 1997). Identification of a full-length mouse ZRP-1 cDNA clone was done by comparison of the 5'-end of the human ZRP-1 cDNA (Genbank accession number AF000974) with the EST sequences in the database of mouse specific IMAGE clones at the RZPD resource center (Berlin, Germany). One highly homologous mouse cDNA clone (W58878), that contains a start codon at the position anticipated from the human sequence, was ordered and sequenced completely.

RNA expression studies - Total RNA from several mouse (strain C57BL/6) tissues was prepared using the guanidium isothiocyanate-phenol-chloroform extraction method (Chomczynski and Sacchi, 1987). Fifteen µg RNA was loaded on a 1% formamide agarose gel and after electrophoresis the RNA was transferred to nylon membrane according to standard procedures (Sambrook et al., 1989). Complete mZRP-1 and GAPDH cDNAs were radioactively labeled by random priming and used as

probes for hybridization as described (Cuppen et al., 1997). RNA *in situ* hybridization on C57BL/6 mouse embryo cryosections was according to previously published protocols (Hendriks et al., 1995). To generate 'sense' and 'antisense' RNA probes the mZRP-1 cDNA (in the pT7T3D-Pac plasmid, Pharmacia) was linearized with NotI or EcoRI and used for *in vitro* transcription by T7 or T3 RNA Polymerase, respectively. Both probes were labeled with $\alpha^{35}\text{S}$ -UTP to a specific activity of $>10^9$ dpm/ μg .

Expression plasmid constructions - Full-length mouse RIL cDNA (Genbank accession number Y08361) was cloned in the multiple cloning site of the pSG5 expression vector (Green et al., 1988). The RIL-PDZ (Y08361, a.a. 1-101), RIL-LIM (Y08361, a.a. 209-330), BL-PDZ-I-V (Z32740, a.a. 1002-2018) and BL-PDZ-II (Z32740, a.a. 1352-1450) protein parts were expressed from a modified version of the eukaryotic expression vector pSG5, now containing an initiator AUG codon and an in-frame VSV-G epitope tag (see Cuppen et al., 1998) for detection or immunoprecipitation of the produced peptide using monoclonal antibody P5D4 (Kreis, 1986). The EGFP-mZRP fusion protein was expressed from the pEGFP-C1 vector (Clontech), by in-frame cloning of a XhoI - HindIII restriction fragment of the EST clone W58878 containing the complete mouse ZRP-1 cDNA sequence.

Antibodies - The affinity-purified polyclonal antibody α -RIL directed against the C-terminal half of RIL and the monoclonal α -VSV antibody P5D4 are described elsewhere (Cuppen et al., 1998; Kreis, 1986). The polyclonal antibody α -GFP was obtained by immunization of a rabbit with a GST-BFP (Blue Fluorescent Protein) fusion protein. The resulting antiserum was found to bind also to the widely used EGFP (Enhanced Green Fluorescent Protein) in Western blotting, immunofluorescence and immunoprecipitation experiments. For biotinylation, the Ig fraction was bound on a protein A-Sepharose column, eluted in 0.1 M glycine pH2.5, neutralized by addition of 1 M Tris-HCl pH7.5, and dialyzed against 50 mM NaHCO₃ pH8.5. The resulting antibody fraction was biotinylated using Immunopure Sulfo-NHS-LC-Biotin according to the manufacturer's instructions (Pierce Chemical Company, USA).

Immunoprecipitation and Western blotting - COS-1 cells were cultured in DMEM/10% fetal calf serum. For each assay, 1.5×10^6 cells were electroporated at 0.3 kV and 125 μF using the Bio-Rad Gene Pulser with a 4-mm electroporation cuvette, in 200 μl of phosphate-buffered saline (PBS) containing 10 μg of plasmid DNA. Cells were plated on a 10-cm dish and cultured for 24 h in DMEM/10% fetal calf serum. Cells were washed with cold PBS and lysed on plate with 550 μl ice-cold RIPA buffer (50 mM Tris, pH8.0, 100 mM NaCl, 1 mM EDTA, 1% NP-40, 0.1% SDS, 0.5% DOC, 1 mM PMSF and protease inhibitor cocktail (Boehringer)). After a 1-h incubation on ice, the lysate was centrifuged for 10 min at $10,000 \times g$ and 4°C , and 50 μl of the lysate was removed for later analysis of input protein levels on Western blot (see below). After addition of α -GFP (2 μl rabbit polyclonal antiserum) or α -VSV (2 μl ascites fluid of hybridoma P5D4) and 4-h rotation at 4°C , 50 μl of protein A-Sepharose CL-4B (Pharmacia) was added and incubation was prolonged overnight. The immunoprecipitates were washed four times with 1 ml RIPA lysis buffer and boiled for 5 min in 50 μl of sample buffer (100 mM Tris-HCl, pH6.8, 200 mM dithiothreitol, 4% SDS, 0.2% bromophenol blue, 20% glycerol). 15 μl of lysates and immunoprecipitates were resolved on 10 or 15% polyacrylamide gels and transferred to nitrocellulose membranes by Western blotting. Blots were blocked using 5% nonfat dry milk in 10 mM Tris-HCl (pH 8.0), 150 mM NaCl, and 0.05% Tween 20 (TBST). The mouse monoclonal α -VSV antibody P5D4 (10.000 x diluted ascites fluid) and the rabbit polyclonal α -GFP antibody (5000 x diluted total serum) were used to detect tagged-proteins in the lysates and immunoprecipitates. Incubations with primary and secondary (10.000 x diluted peroxidase-conjugated goat anti-mouse IgG or goat anti-rabbit IgG (Pierce)) antibodies and subsequent washes were done in TBST, as described elsewhere (Cuppen et al., 1998). Labeled bands were visualized using freshly prepared chemiluminescent substrate (100 mM Tris-HCl, pH8.5, 1.25 mM p-coumaric acid (Sigma), 0.2 mM luminol (Sigma), 0.009 % H₂O₂) and exposure to Kodak X-omat autoradiography films.

Cell transfection and Immunofluorescence - A-431 (ATCC: CRL-1555) and Caco-2 (ATCC: HTB-37) cells were cultured in DMEM/10% fetal calf serum. Prior to transfection, cells were seeded onto 14 mm diameter glass coverslips (Menzel-Gläser, Germany) in 24 wells cell culture plates. Transfection mix was made by adding 0.3 µg plasmid DNA to 2 µg DAC-30 (Eurogentec, Seraing Belgium) in 150 µl OptiMEM (Gibco BRL, Gaithersburg, MD) and incubating for 30 min at room temperature. After replacing the culture medium on the cells (30-70 % confluency) with 150 µl fresh DMEM containing 10% fetal calf serum, the transfection mix (150 µl) was added to the cells. Following a 5-h incubation at 37°C the medium was replaced with fresh DMEM containing 10% FCS and incubation was prolonged overnight. The cells were subsequently used for immunofluorescence analysis. Because the autofluorescent signal from the EGFP-mZRP fusion protein was rather weak, the signal was enhanced using the polyclonal antibody α -GFP. At further steps, solutions are prepared in PBS, cells were thoroughly rinsed in PBS between stages, and incubations were performed at room temperature. Cells were fixed for 10 min in 2% paraformaldehyde in PHEM buffer (60 mM Pipes, 25mM Hepes pH6.9, 10 mM EGTA, 2 mM MgCl₂) and permeabilized with 0.5% Nonidet P-40 for 5 min. Subsequently, free aldehyde groups were quenched for 10 min in 0.1 M glycine. 50 µl of affinity-purified rabbit α -RIL (1:10 dilution), rabbit polyclonal α -GFP (1:1000 dilution) or mouse monoclonal α -VSV (P5D4, ascites fluid; 1:1000 dilution) was used for the 1-h incubation with primary antibody. Subsequent incubation was for 45 min with 50 µl of FITC-conjugated AffiniPure Goat anti-rabbit or Goat anti-mouse IgG (10 µg/ml; Jackson ImmunoResearch Laboratories, Inc., West Grove, PA) and 2 units Texas Red-conjugated phalloidin (Molecular Probes). In cases where EGFP-mZRP and RIL are detected simultaneously, first the RIL protein was detected using the affinity-purified polyclonal α -RIL antibody and Texas Red-conjugated AffiniPure Goat anti-Rabbit (10 µg/ml; Jackson ImmunoResearch Laboratories, Inc., West Grove, PA). Subsequently, the EGFP-mZRP fusion protein was detected using biotinylated α -GFP (1:250 dilution) and streptavidin-FITC (2 µg/ml; Jackson ImmunoResearch Laboratories, Inc., West Grove, PA). Finally, coverslips were rinsed in PBS and water and mounted on glass slides by inversion over 5 µl Mowiol mountant (Sigma Chemical Co.). Cells were examined using an MRC1000 confocal laser scanning microscope (Bio-Rad).

References

- Altschul, S. F., Madden, T. L., Schaffer, A. A., Zhang, J., Zhang, Z., Miller, W., and Lipman, D. J. (1997). Gapped BLAST and PSI-BLAST: a new generation of protein database search programs. *Nucl. Acids Res.* *25*, 3389-3402.
- Arber, S., and Caroni, P. (1996). Specificity of single LIM motifs in targeting and LIM/LIM interactions in situ. *Genes Dev.* *10*, 289-300.
- Banville, D., Ahmad, S., Stocco, R., and Shen, S. H. (1994). A novel protein-tyrosine phosphatase with homology to both the cytoskeletal proteins of the band 4.1 family and junction-associated guanylate kinases. *J. Biol. Chem.* *269*, 22320-22327.
- Beckerle, M. C. (1997). Zyxin: zinc fingers at sites of cell adhesion. *Bioessays* *19*, 949-957.
- Bork, P., Schultz, J., and Ponting, C. P. (1997). Cytoplasmic signalling domains: the next generation. *Trends Biochem. Sci.* *22*, 296-298.
- Brenman, J. E., Chao, D. S., Gee, S. H., McGee, A. W., Craven, S. E., Santillano, D. R., Wu, Z., Huang, F., Xia, H., Peters, M. F., Froehner, S. C., and Brecht, D. S. (1996). Interaction of nitric oxide synthase with the postsynaptic density protein PSD-95 and alpha1-syntrophin mediated by PDZ domains. *Cell* *84*, 757-767.
- Carlsson, S. R., Lycksell, P. O., and Fukuda, M. (1993). Assignment of O-glycan attachment sites to the hinge-like regions of human lysosomal membrane glycoproteins lamp-1 and lamp-2. *Arch. Biochem. Biophys.* *304*, 65-73.
- Chan, D. C., Bedford, M. T., and Leder, P. (1996). Formin binding proteins bear WWp/WW domains

- that bind proline-rich peptides and functionally resemble SH3 domains. *EMBO J.* *15*, 1045-1054.
- Chen, H. I., and Sudol, M. (1995). The WW domain of yes-associated protein binds a proline-rich ligand that differs from the consensus established for Src homology 3 binding modules. *Proc. Natl. Acad. Sci. USA* *92*, 7819-7823.
- Chida, D., Kume, T., Mukoyama, Y., Tabata, S., Nomura, N., Thomas, M. L., Watanabe, T., and Oishi, M. (1995). Characterization of a protein tyrosine phosphatase (RIP) expressed at a very early stage of differentiation in both mouse erythroleukemia and embryonal carcinoma cells. *FEBS Lett.* *358*, 233-239.
- Chishti, A. H., Kim, A. C., Marfatia, S. M., Lutchnan, M., Hanspal, M., Jindal, H., Liu, S.-C., Low, P. S., Rouleau, G. A., Mohandas, N., Chasis, J. A., Conboy, J. G., Gascard, P., Takakuwa, Y., Huang, S.-C., Benz, E. J., Bretscher, A., Fehon, R. G., Gusella, J. F., Ramesh, V., Solomon, F., Marchesi, V. T., Tsukita, S., Tsukita, S., Arpin, M., Louvard, D., Tonks, N. K., Anderson, J. M., Fanning, A. S., Bryant, P. J., Woods, D. F., and Hoover, K. B. (1998). The FERM domain: a unique module involved in the linkage of cytoplasmic proteins to the membrane. *Trends Biochem. Sci.* *23*, 281-282.
- Chomczynski, P., and Sacchi, N. (1987). Single-step method of RNA isolation by acid guanidinium thiocyanate-phenol-chloroform extraction. *Anal. Biochem.* *162*, 156-159.
- Crawford, A. W., Michelsen, J. W., and Beckerle, M. C. (1992). An interaction between zyxin and actinin. *J. Cell Biol.* *116*, 1381-1393.
- Cuppen, E., Gerrits, H., Pepers, B., Wieringa, B., and Hendriks, W. (1998). PDZ motifs in PTP-BL and RIL bind to internal protein segments in the LIM domain protein RIL. *Mol. Biol. Cell* *9*, 671-683.
- Cuppen, E., Nagata, S., Wieringa, B., and Hendriks, W. (1997). No evidence for involvement of mouse protein-tyrosine phosphatase-BAS-like/Fas-associated Phosphatase-1 in Fas-mediated apoptosis. *J. Biol. Chem.* *272*, 30215-30220.
- Curtiss, J., and Heilig, J. S. (1998). DeLIMiting development. *Bioessays* *20*, 58-69.
- Dawid, I. B., Breen, J. J., and Toyama, R. (1998). LIM domains: multiple roles as adapters and functional modifiers in protein interactions. *Trends Gen.* *14*, 156-162.
- Doyle, D. A., Lee, A., Lewis, J., Kim, E., Sheng, M., and MacKinnon, R. (1996). Crystal structures of a complexed and peptide-free membrane protein-binding domain: molecular basis of peptide recognition by PDZ. *Cell* *85*, 1067-1076.
- Fanning, A. S., and Anderson, J. M. (1996). Protein-protein interactions: PDZ domain networks. *Curr. Biol.* *6*, 1385-1388.
- Feuerstein, R., Wang, X., Song, D., Cooke, N. E., and Lieberhaber, S. A. (1994). The LIM/double zinc-finger motif functions as a protein dimerization domain. *Proc. Natl. Acad. Sci. U.S.A.* *91*, 10655-10659.
- Gee, S. H., Sekely, S. A., Lombardo, C., Kurakin, A., Froehner, S. C., and Kay, B. K. (1998). Cyclic peptides as non-carboxyl-terminal ligands of syntrophin PDZ domains. *J. Biol. Chem.* *273*, 21980-21987.
- Golsteyn, R. M., Beckerle, M. C., Koay, T., and Friederich, E. (1997). Structural and functional similarities between the human cytoskeletal protein zyxin and the ActA protein of *Listeria monocytogenes*. *J. Cell Sci.* *110*, 1893-1906.
- Green, S., Issemann, I., and Sheer, E. (1988). A versatile in vivo and in vitro eukaryotic expression vector for protein engineering. *Nucl. Acids Res.* *16*, 369.
- Grootjans, J. J., Zimmerman, P., Reekmans, G., Smets, A., DeGeest, G., Durr, J., and David, G. (1997). Syntenin, a PDZ protein that binds syndecan cytoplasmic domains. *Proc. Natl. Acad. Sci. USA* *94*, 13683-13688.
- Gyuris, J., Golemis, E., Chertkov, H., and Brent, R. (1993). Cdi1, a human G1 and S phase protein phosphatase that associates with Cdk2. *Cell* *75*, 791-803.
- Hendriks, W., Schepens, J., Bachner, D., Rijss, J., Zeeuwen, P., Zechner, U., Hameister, H., and Wieringa, B. (1995). Molecular cloning of a mouse epithelial protein-tyrosine phosphatase with similarities to submembranous proteins. *J. Cell. Biochem.* *59*, 418-430.

- Hiraoka, J., Okano, I., Higuchi, O., Yang, N., and Mizuno, K. (1996). Self-association of LIM-kinase 1 mediated by the interaction between an N-terminal LIM domain and a C-terminal kinase domain. *FEBS Lett.* *399*, 117-121.
- Hobert, O., Schilling, J. W., Beckerle, M. C., Ullrich, A., and Jallal, B. (1996). SH3 domain-dependent interaction of Vav with the LIM domain protein, zyxin. *Oncogene* *12*, 1577-1581.
- Kiess, M., Scharm, B., Aguzzi, A., Hajnal, A., Klemenz, R., Schwarte Waldhoff, I., and Schafer, R. (1995). Expression of ril, a novel LIM domain gene, is down-regulated in Hras-transformed cells and restored in phenotypic revertants. *Oncogene* *10*, 61-68.
- Kreis, T. E. (1986). Microinjected antibodies against the cytoplasmic domain of vesicular stomatitis virus glycoprotein block its transport to the cell surface. *EMBO J.* *5*, 931-941.
- Kuroda, S., Tokunaga, C., Kiyohara, O., Konishi, H., Mizuno, K., Gill, G. N., and Kikkawa, U. (1996). Protein-protein interaction of zinc finger LIM domains with protein kinase C. *J. Biol. Chem.* *271*, 31029-31032.
- Lee, J. W., Choi, H. S., Gyuris, J., Brent, R., and Moore, D. D. (1995). Two classes of proteins dependent on either the presence or absence of thyroid hormone for interaction with the thyroid hormone receptor. *Mol. Endocrinol.* *9*, 243-254.
- Maekawa, K., Imagawa, N., Nagamatsu, M., and Harada, S. (1994). Molecular cloning of a novel protein-tyrosine phosphatase containing a membrane-binding domain and GLGF repeats. *FEBS Lett.* *337*, 200-206.
- Morais Cabral, J. H., Petrosa, C., Sutcliffe, M. J., Raza, S., Byron, O., Poy, F., Marfatia, S. M., Chishti, A. H., and Liddington, R. C. (1996). Crystal structure of a PDZ domain. *Nature* *382*, 649-652.
- Niebuhr, K., Ebel, F., Frank, R., Reinhard, M., Domann, E., Carl, U. D., Walter, U., Gertler, F. B., Wehland, J., and Chakraborty, T. (1998). A novel proline-rich motif present in ActA of *Listeria monocytogenes* and cytoskeletal proteins is the ligand for the EVH1 domain, a protein module present in the Ena/VASP family. *EMBO J.* *16*, 5433-5444.
- Nix, D. A., and Beckerle, M. C. (1997). Nuclear-cytoplasmic shuttling of the focal contact protein, Zyxin: A potential mechanism for communication between sites of cell adhesion and the nucleus. *J. Cell Biol.* *138*, 1139-1147.
- Pawson, T., and Scott, J. D. (1997). Signaling through scaffold, anchoring, and adaptor proteins. *Science* *278*, 2075-2080.
- Ponting, C. P. (1997). Evidence For PDZ Domains in Bacteria, Yeast, and Plants. *Prot. Sci.* *6*, 464-468.
- Ranganathan, R., and Ross, E. M. (1997). PDZ domain proteins: Scaffolds for signaling complexes. *Curr. Biol.* *7*, R770-R773.
- Sambrook, J., Fritsch, E. F., and Maniatis, T. (1989). *Molecular Cloning: A laboratory manual*, 2nd Edition (Cold Spring Harbor, NY: Cold Spring Harbor Laboratory Press).
- Saras, J., Claesson Welsh, L., Heldin, C. H., and Gonez, L. J. (1994). Cloning and characterization of PTPL1, a protein tyrosine phosphatase with similarities to cytoskeletal-associated proteins. *J. Biol. Chem.* *269*, 24082-24089.
- Saras, J., Engström, U., Gonez, L. J., and Heldin, C.-H. (1997). Characterization of the interactions between PDZ domains of the protein-tyrosine phosphatase PTPL1 and the carboxyl-terminal tail of Fas. *J. Biol. Chem.* *272*, 20979-20981.
- Saras, J., Franzen, P., Aspenstrom, P., Hellman, U., Gonez, L. J., and Heldin, C. (1997). A novel GTPase-activating protein for Rho interacts with a PDZ domain of the protein-tyrosine phosphatase PTPL1. *J. Biol. Chem.* *272*, 24333-24338.
- Saras, J., and Heldin, C.-H. (1996). PDZ domains bind carboxy-terminal sequences of target proteins. *Trends Biochem. Sci.* *21*, 455-458.
- Sato, T., Irie, S., Kitada, S., and Reed, J. C. (1995). FAP-1: a protein tyrosine phosphatase that associates with Fas. *Science* *268*, 411-415.
- Schepens, J., Cuppen, E., Wieringa, B., and Hendriks, W. (1997). The neuronal nitric oxide synthase PDZ motif binds to -G(D,E)XV* carboxyterminal sequences. *FEBS Lett.* *409*, 53-56.

- Sheng, M. (1996). PDZs and receptor/channel clustering: rounding up the latest suspects. *Neuron* *17*, 575-578.
- Shieh, B. H., and Zhu, M. Y. (1996). Regulation of the TRP Ca²⁺ channel by INAD in *Drosophila* photoreceptors. *Neuron* *16*, 991-998.
- Songyang, Z., Fanning, A. S., Fu, C., Xu, J., Marfatia, S. M., Chishti, A. H., Crompton, A., Chan, A. C., Anderson, J. M., and Cantley, L. C. (1997). Recognition of unique carboxyl-terminal motifs by distinct PDZ domains. *Science* *275*, 73-77.
- Sparks, A. B., Rider, J. E., Hoffmann, N. G., Fowlkes, D. M., Quilliam, L. A., and Kay, B. K. (1996). Distinct ligand preferences of Src homology 3 domains from Src, yes, Abl, cortactin, p53bp2, PLCgamma, Crk and Grb2. *Proc. Natl. Acad. Sci. USA* *93*, 1540-1544.
- Stricker, N. L., Christopherson, K. S., Yi, B. A., Schatz, P. J., Raab, R. W., Dawes, G., Bassett, D. E., Brecht, D. S., and Li, M. (1997). PDZ domain of neuronal nitric oxide synthase recognizes novel C-terminal peptide sequences. *Nat. Biotech.* *15*, 336-342.
- van Huizen, R., Miller, K., Chen, D. M., Li, Y., Lai, Z. C., Raab, R. W., Stark, W. S., Shortridge, R. D., and Li, M. (1998). Two distantly positioned PDZ domains mediate multivalent INAD-phospholipase C interactions essential for G protein-coupled signaling. *EMBO J.* *17*, 2285-2297.
- Wang, H., Harrison Shostak, D. C., Lemasters, J. J., and Herman, B. (1995). Cloning of a rat cDNA encoding a novel LIM domain protein with high homology to rat RIL. *Gene* *165*, 267-71.
- Williams, J. M., Chen, G. C., Zhu, L., and Rest, R. F. (1998). Using the yeast two-hybrid system to identify human epithelial cell proteins that bind gonococcal Opa proteins: intracellular gonococci bind pyruvate kinase via their Opa proteins and require host pyruvate for growth. *Mol. Microbiol.* *27*, 171-186.
- Wu, R., Durick, K., Songyang, Z., Cantley, L. C., Taylor, S. S., and Gill, G. N. (1996). Specificity of LIM domain interactions with receptor tyrosine kinases. *J. Biol. Chem.* *271*, 15934-15941.
- Wu, R. Y., and Gill, G. N. (1994). LIM domain recognition of a tyrosine-containing tight turn. *J. Biol. Chem.* *269*, 25085-25090.
- Xia, H., Winokur, S. T., Kuo, W.-L., Altherr, M. R., and Brecht, D. S. (1997). Actinin-associated LIM Protein: Identification of a Domain Interaction between PDZ and Spectrin-like Repeat Motifs. *J. Cell Biol.* *139*, 507-515.
- Xu, X.-Z. S., Choudhury, A., Li, X., and Montell, C. (1998). Coordination of an array of signaling proteins through homo- and heteromeric interactions between PDZ domains and target proteins. *J. Cell Biol.* *142*, 545-555.

Chapter 6

Identification and molecular characterization of BP75, a novel bromodomain-containing protein

Edwin Cuppen, Marco van Ham, Barry Pepers, Bé Wieringa, and Wiljan Hendriks.

Identification and molecular characterization of BP75, a novel bromodomain-containing protein

Edwin Cuppen, Marco van Ham, Barry Pepers, Bé Wieringa, and Wiljan Hendriks.

Department of Cell Biology and Histology, Institute of Cellular Signalling, University of Nijmegen, Adelbertusplein 1, 6525 EK Nijmegen, The Netherlands.

Abstract

PTP-BL is a multiple PDZ domain containing protein tyrosine phosphatase with a putative role in structuring the cytoarchitecture at apical submembranous sites in polarized epithelial cells. In a yeast two-hybrid screening for partner proteins, we identified a novel bromodomain-containing protein, BP75, that interacts uniquely with the first PDZ domain in PTP-BL via its C-terminal half. Besides the similarity to bromodomain proteins, BP75 displays overall homology to a hypothetical protein in *C. elegans* (C01H6.7) and to a novel domain in a putative DNA binding factor in yeast (YN92). Northern blot analysis revealed that BP75 mRNA is expressed in all tissues examined and RNA *in situ* hybridization experiments reveal thymus, lung, liver, colon and spinal cord as high expression sites. Transient transfection studies show that both BP75 and a PTP-BL deletion mutant consisting essentially of the first PDZ domain are located mainly in the nucleus, excluding the nucleoli, but also cytoplasmic localization is evident. Full-length PTP-BL, on the contrary, is predominantly localized in the cytoplasm, although some basal nuclear staining is observed. The described molecular interaction may reflect a mechanism of coupling submembranous signaling events and nuclear events.

Introduction

The accurateness of the signal transduction process, whereby extracellular signals evoke a specific cellular response, largely relies on mechanisms that regulate steps in the transmembrane transmission, and the integration or divergence of signaling pathways within the cytosol and nucleus. An important mechanism to achieve specificity in signaling is the use of scaffold, anchoring and adapter proteins (Pawson and Scott, 1997). Adapter proteins enable the recruitment of specific components to an activated signaling complex, as demonstrated by SH2 domain-containing proteins that bind to activated autophosphorylated receptor tyrosine kinases (Songyang et al., 1993). Anchoring proteins serve to direct an enzymatic activity to a particular subcellular site by confining the enzyme to the restricted microenvironment. This regulatory principle is used in the serine/threonine

phosphatases PP-1, PP-2A and PP-2B, where the catalytic subunits are bound to regulatory subunits that target the enzymatic complex to its proper subcellular location (Faux and Scott, 1996). Scaffold proteins are considered organizers of multiprotein complexes, creating 'signalosomes' with specialized functions at restricted microcompartments (Pawson and Scott, 1997). The scaffold proteins can be divided in two groups. One group of proteins functions as signaling pipelines by placing enzymes close to their substrates, increasing both speed and specificity of the signal transduction pathways involved. A well-known example is the yeast protein Ste5, that clusters the successive components of the MAPK cascade involved in the pheromone mating response (Herskowitz, 1995). The other group of scaffold proteins functions as organizers of cross-roads of signaling pathways by integrating and coupling components of different signaling cascades in a single 'signalosome'. This latter principle is used in the process of phototransduction in *Drosophila* photoreceptor cells, where the protein InaD clusters different types of enzymes and channels via PDZ-mediated interactions (Ranganathan and Ross, 1997). Here, clustering is used to regulate serine/threonine phosphorylation and lipid and calcium signaling from a single multiprotein complex (Tsunoda et al., 1997).

Protein modules like SH2, SH3, WW, LIM, WD, PTB, PH, and PDZ domains form the basal building blocks for scaffold, anchoring and adapter proteins, and play an important role in the architecture of signal transduction complexes (Bork et al., 1997). The mouse protein tyrosine phosphatase PTP-BL (Hendriks et al., 1995) or RIP (Chida et al., 1995), and the human homologue of this protein named PTP-BAS (Maekawa et al., 1994), PTPL1 (Saras et al., 1994), PTP1E (Banville et al., 1994) or FAP-1 (Sato et al., 1995), have several characteristics (Fig. 1) that make them potential organizers of signal transduction complexes. PTP-BL harbours five PDZ domains, small (about 90 a.a.) protein modules (Kennedy, 1995) that have now been identified in many members of a diverse group of proteins (Ponting, 1997) and can mediate protein-protein interactions (Fanning and Anderson, 1996; Ranganathan and Ross, 1997). PDZ domains associate with transmembrane proteins (Sheng, 1996), cytoskeletal components (Xia et al., 1997) and signal transduction enzymes (Ranganathan and Ross, 1997). The five PDZ domains in PTP-BL may thus enable the formation of large multiprotein complexes in which the phosphotyrosine phosphatase action of PTP-BL itself can be combined with potential downstream substrates, competitor signaling proteins and putative upstream regulatory molecules. Indeed, proteins that interact with PDZ domains of PTP-BL have already been described. Saras et al. (Saras et al., 1997) identified a 160 kDa protein with Rho-GAP activity, PARG1, that binds to PDZ-IV and our group has shown that the small adapter protein RIL (Kiess et al., 1995) can interact with both PDZ-II and IV of PTP-BL (Cuppen et al., 1998). Furthermore, the C-terminus of the apoptosis inducing Fas-receptor was found to bind the second PDZ domain in the human homologue of PTP-BL (Saras et al., 1997; Sato et al., 1995), but this interaction could not be confirmed in mouse (Cuppen et al.,

1997). The subcellular partitioning of the multiprotein complex that results from PTP-BL PDZ-mediated interactions may be further restricted due to the presence of a FERM domain in PTP-BL. FERM domains are found in the submembranous, cytoskeleton-associated proteins like ezrin, radixin, moesin, merlin and talin (Tsukita and Yonemura, 1997) and can bind transmembrane proteins like CD44, CD43 and ICAM-2 (Yonemura et al., 1998). This may explain why endogenous PTP-BL is located submembranously at the apical side of polarized epithelia (Cuppen et al., 1998).

Finally it is of note, that the C-terminal catalytic tyrosine phosphatase domain of PTP-BL can be involved in the reversible (de-)phosphorylation of associated proteins, thereby changing the dynamics of the multiprotein complex or the properties or activities of its constituents. We have found that the interacting molecule RIL is phosphorylated on tyrosines *in vitro* and *in vivo* and can be dephosphorylated by PTP-BL *in vitro* (Cuppen et al., 1998).

PTP-BL thus bears hallmarks of a scaffold protein that regulates the complex organization and dynamics of macromolecular assemblies at the cell cortex. To further identify the components of this complex we performed a two-hybrid screening for proteins that interact with the first PDZ domain of PTP-BL and identified a novel bromodomain-containing protein of about 75 kDa, BP75. The bromodomain, originally described as an evolutionary highly conserved 80 amino acid domain in human, *Drosophila* and yeast proteins (Haynes et al., 1992), is now defined as a conserved sequence of approximately 110 amino acids that is found in over 40 proteins, several of which are involved in transcriptional regulation (Jeanmougin et al., 1997). Our results suggest that BP75 may have a rather direct role in linking signaling events in the PTP-BL multiprotein complex and the nucleus.

Results

Identification of proteins that interact with PDZ-I of PTP-BL

Several candidate proteins interacting with the first PDZ domain of PTP-BL were identified in a HeLa cell cDNA library using BL-PDZ-I (Fig. 1A) as a bait in the yeast two-hybrid interaction trap (Gyuris et al., 1993). Four clones out of 0.9×10^6 transformants remained positive after reintroduction into freshly prepared yeast cells containing appropriate bait and reporter plasmids. Two clones, BP#3 and BP#6 with inserts of 1.2 and 1.1 kbp respectively, were found to represent independent cDNAs from the same messenger RNA (Fig. 1B). Comparison of the amino acid sequences of their predicted protein products with database entries did not reveal any similarity to known proteins. Furthermore, nucleotide database searches with the BP#3 cDNA insert showed only homology to expressed sequence tags (EST's) from various tissues, indicating that BP#3 encodes a novel ubiquitously expressed protein. Since PTP-BL is of mouse origin and the interacting clones were obtained from a human cDNA library, we isolated mouse cDNAs that are homologous to BP#3 (see below) and confirmed the two-hybrid interaction using the cDNA segment encoding the C-terminal

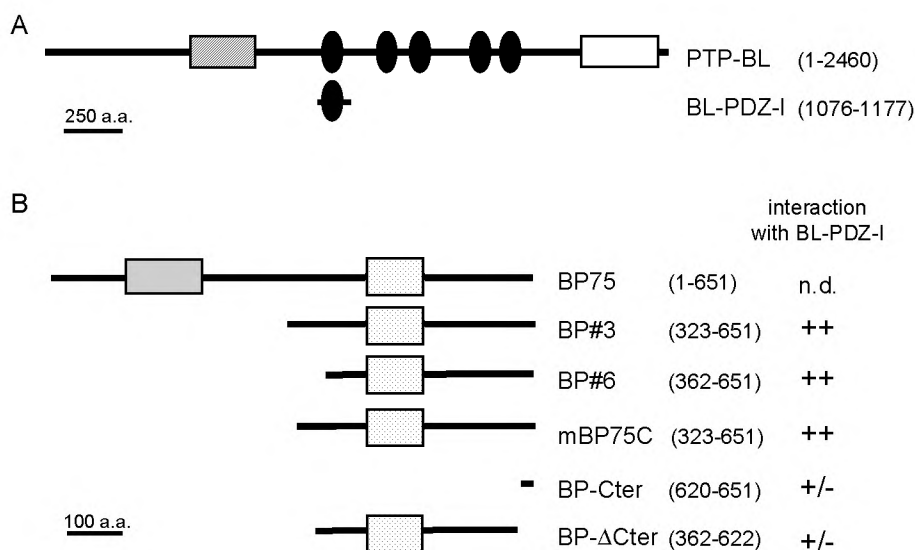


Figure 1: Schematic representation of the protein segments interacting in the two-hybrid trap. Depicted are (A) the PDZ-I segment of PTP-BL used as bait and (B) the BP75 segments retrieved from the HeLa cDNA library (BP#3 and BP#6) and used as deletion constructs. The numbers corresponding to the first and last a.a. positions in the PTP-BL (Z32740) and BP75 (AF084259) segments are shown in parentheses, followed by a quantitative interpretation of the two-hybrid interaction results with PDZ-I. ++, strong interaction; +/-, very weak interaction. Band 4.1 like domain, hatched box; PTP, open box; PDZ domains, black ovals; bromodomain, grey box; BYC-homology domain (see text), stippled box.

half of the mouse protein (mBP75C, Fig. 1B). To delineate the interacting interface more precisely, we subsequently tested deletion mutants of mBP75 (Fig. 1B). Deletion of the C-terminus (mBP-ΔCter) almost completely abolished the interaction, but presence of the C-terminus proper (mBP-Cter) is not sufficient for a strong interaction (Fig. 1B). None of the mBP75 constructs interacts with an empty bait or with other PDZ domains of PTP-BL (not shown). Furthermore, no interaction was observed with the PDZ domain of RIL, nNOS or the second PDZ domain of SAP90 (not shown).

Isolation and characterization of mouse BP75 cDNA clones

Sequence analysis of BP#3 and BP#6 cDNA inserts revealed that only partial sequence information of the encoded protein had been obtained. To acquire additional sequence data and at the same time have a more complete tool to study the biological function of the encoded protein, we searched for full-length cDNAs by screening a mouse fetal brain cDNA library using the human BP#3 cDNA insert as a probe. Two clones, with inserts of

1.8 and 2.4 kbp, respectively, were obtained. The 2361 bp insert of the longest cDNA (Genbank: AF084259) most probably represents a full-length cDNA since northern blot analysis revealed a transcript of about 2.5 kb in length (Fig. 5). The smaller cDNA was found to be identical to the last 1804 bp of this clone. Sequence analysis revealed a polyadenylation sequence located 18 bp upstream of the poly-A tract, and an open reading frame that specifies a 651 amino acid polypeptide (Fig. 2). The predicted protein has a molecular mass of about 75 kDa. In the complete putative protein we found a bromodomain (Haynes et al., 1992) and therefore termed it BP75 for bromodomain-containing protein of 75 kDa. The evolutionary highly conserved bromodomain spans about 110 amino acid residues and has now been identified in more than 40 different proteins (Jeanmougin et al., 1997). Database comparison and sequence alignment (Fig. 3A) reveal that the BP75 bromodomain displays the highest similarity to a bromodomain in a hypothetical *C.elegans* protein, C01H6.7 (Z71258, (Wilson et al., 1994)), and a human protein called peregrin or BR140 (JC2069, (Thompson et al., 1994)). Outside the BP75 bromodomain there is no clear similarity with any of the known bromodomain-containing proteins, nor any other known protein except for the C01H6.7 protein mentioned and a yeast protein called YN92 (see below). When the entire amino acid sequences of BP75 and C01H6.7 are aligned (Fig. 3B) it is evident that beside the bromodomain there is a second stretch of about 80 amino acids that is highly conserved. The sequence of this segment (Fig. 3C) is over 45% identical and almost 70% similar between *C.elegans* and mouse. This same segment is 21% identical and 34% similar to a region in YN92 (P53759) and we therefore will refer to this segment as BYC domain, for its presence in BP75, YN92 and C01H6.7. YN92 is a putative transcription regulatory protein from yeast, that contains a DNA binding Zn(2)-Cys(6) fungal-type binuclear cluster domain (Schjerling and Holmberg, 1996), for which no homology exists in BP75.

Analysis of BP75 using the PROSITE protein motif database predicts two consensus tyrosine phosphorylation sites (Fig. 2, underlined, a.a. 14 and 430), two partially overlapping bipartite nuclear localization signals (a.a. 66-83 and 80-97, (Dingwall and Laskey, 1991)) and several potential protein kinase C and casein kinase II phosphorylation sites. This suggests a nuclear localization for BP75, and indicates that the protein may be post-translational modified by both serine/threonine and tyrosine phosphorylation.

BP75, a novel bromodomain-containing protein

```

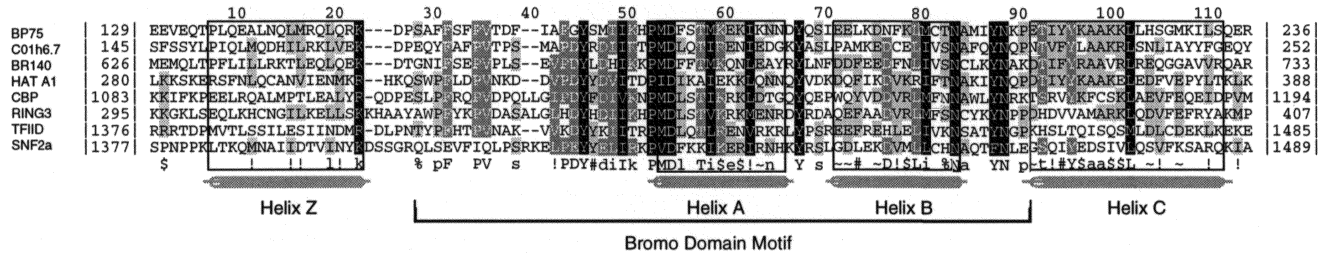
1 GAATTCGGCACGAGCTTCGGCCGCGTCCCGCGCGTGTGTTTTTTTTTCTCGTGAGGGACC
61 TCGCGCGCGCGCGCGTGCCTCCCTCCCTCGCTCGCGCGCGCGGCTCTCGCGGGCCCCGC
121 TCCCGCCCTCCGCTCGCTGCGCCCGCAACCGAAGCGCGCCGACCGCCCTGGCCCTGGCG
      M G K K H K K H K S 10
181 CGGGGGGGGGCTCTGGGGCCCCGTCCGACATGGGCAAGAAGCAAGAAGCACAAAGTCG
      D R H F Y E E Y V E K P L K L V L K V G 30
241 GACCCCACTTCTACGAGGAGTACGTGGAGAGCCCTGAAGCTGGTCTCAAAAGTCGGG
      G S E V T E L S T G S S G H D S S L F E 50
301 GGGAGCGAGGTACCGAGCTCTCCACGGGCGAGTCCGGGCGAGCTCCAGCCTCTTCGAA
      D R S D H D K H K D R K R K K R K K G E 70
361 GACAGAAGCGACCATGACAAACACAAAGACAGAAAACGAAAAGAGGAAAGGCGGAG
      K Q A P G E E K G R K R R R V K E D K K 90
421 AAGCAGCTCCCGGGGAGAGAGGGGAGAAAACGAGAGAGTCAAGGAGGATAAAAAAG
      K R D R D R A E N E V D R D L Q C H V P 110
481 AAGCGGATCGAGACCGTGCAGAGAATGAGGTGGACAGAGATCCAGTGTCTATCCCT
      I R L D L P P E K P L G T S S L A K Q E 130
541 ATAAGATTAGACTTACCTCCCTGAGAAGCCTCTTCAAGCTCCTAGCCAAACAGAAAGAA
      V E Q T P L O E A L N O L M R Q L O R K 150
601 GTAGAACAGACACCCCTTCAGGAAGCTTTGAATCAGCTCATGAGCAATTCGAAAGAAA
      D P S A P P S F P P V T D F I A P G Y S M 170
661 GACCCCACTTCTTCTTTCATTCCTGTGACGGATTTTATGGCCCTGGCTACTCCATG
      I I K H P M D F S T M K E K I K N N D Y 190
721 ATTATTAACACCCCAATGGATTTAGTACCATGAAAGAAAAGATCAAGAATAACGACTAC
      Q S I E E L K D N F K L M C T N A M I Y 210
781 CAGTCCATGAGAAGACTAAAGGATAA C T C A A G C T P A T G T G T A C T A A T G C A A T G T T T A C
      N K P E T I Y Y K A A K K L L H S G M K 230
841 AATAAGCCAGAGACCATTTTATAAAGCTGCAAAAGAGCTGTTGCACCTCAGGATGAAA
      I L S Q E E I Q S L K Q S I D F M S D L 250
901 ATTTTCAGTCAGGAGAGAAATTCAGAGCCTGAAGCAGATATAGACTTCATGTGAGACTTG
      Q K T R K Q K E R T D A C Q S G E D S G 270
961 CAGAAAACCGGAAGCAGAAAGAACGAAACAGATGCTGTGAGAGTGGGGAGGACAGCGGC
      C W Q R E R E D S G D A E T Q A F R S P 290
1021 TGCTGGCAGCGCAGAGGGGAAGACTCTGGAGATGCTGAACACAGCCCTTCAGAAAGCCCC
      A K D N K R K D K D V L E D K W R S S N 310
1081 GCTAAGACAAATAAAGAAAGACAAAGATGTGCTTGAAGACAAATGGAGAAGCAGCAAC
      S E R E H E Q I E R V V Q E S G G K L T 330
1141 TCAGAAAGGGAGCATGAGCAGATTGAGCGGTTTTCAGGAGTCCAGGAGCAAGCTAACAA
      R R L A N S Q C E F E R R K P D G T T T 350
1201 CGCGGGCTGGCAACAGTCACTGTAATTTGAAAGAGAAAACAGATGGGACACAACA
      L G L L H P V D P I V G E P G Y C P V R 370
1261 CTGGGGCTTCTCCATCCTGTGGATCCCATTTGGGGAGAGCCAGGCTACTGCCCTGTGAGA
      L G M T T G R L Q S G V N T L Q G F K E 390
1321 TTGGGGATGACAACTGGAAGACTGCAGTCTGGAGTGAACACTCTGCAGGGGTTCAAAGAG
      D K R N R V T P V L Y L N Y G P Y S S Y 410
1381 GATAAAGGAAACAGAGTAAACCCAGTATTATACTTGAATTTAGACCCCTCAGTCTTAT
      A P H Y D S T F A N I S K D D S D L I Y 430
1441 GCCCAATTAAGACTCTACATTTGCCAATATTAGCAAGATGATTCGATTTAATCTAC
      S T Y G E D S D L P N N F S I S E F L A 450
1501 TCAACATATGGGGAAGACTCTGACCTTCCAAACAAATTTACGATCTCTGAGTTTTGGCC
      T C Q D Y P Y V M A D S L L D V L T K G 470
1561 ACATGCCAAGATTAACCGTATGTTATGGCAGATAGTTTACTGGATGTTCTAACAAAAGGA
      G H S R S L Q D L D M S S P E D E G Q T 490
1621 GGACATTCAGGAGCCTGCAGGACTTGGACATGTCATCTCCTGAAGATGAAGGCCAGACC
      R A L D T A K E A E I T Q I E P T G R L 510
1681 AGAGCATTGGACACAGCAAAAGAGCAGAGATTACAAATAGAGCCAAAGGCGGTTTG
      E S S S Q D R L T A L Q A V T T F G A P 530
1741 GAGTCCAGCAGTCAGGACAGGCTCACAGCCTGCAAGCTGTAACCAACCTTTGGTGTCCA
      A E V F D S E E A E V F P Q R K L D E T 550
1801 GCTGAACTCTTTGACTCCGAAGAGGCTGAGGTGTTCCAGAGGAGCTGATGAGACGACA
      R L L R E L Q E A Q N E R L S T R P P P 570
1861 AGATTGCTCAGGGAGCTCCAGGAGGCAGAAATGAGCGACTGAGCACTAGGCTCCTCCC
      N M I C L L G P S Y R E M Y L A E Q V T 590
1921 AATATGATCTGTCTCCTGGTCTCTTACAGAGAAATGTACCTTGTGAAACAGTGACC
      N N L K E L T Q Q V T P G D V V S I H G 610
1981 AATAACCTCAAAGAACTCACAGCAAGTGACTCCAGGTGATGTTGTAAGCATAACAGGA
      V R K A M G I S V P S P I V G N S F V D 630
2041 GTGCGAAAAGCAATGGGATTTCTGTTCCCTTCCCCCATCGTGGGAAAACAGCTTCGTAGAT
      L T G E C E E P K E T S T A E C G P D A 650
2101 TTGACAGGAGAGTGTGAAGAACCTAAGGAGACCAGCTGCTGAGTGTGGCCCTGACGCG
      S * 651
2161 AGCTGAAGTACCTGGTATTTGATCTATTATGTACATAGTTTTTTCATTCTGAACCTGGA
2221 GGTGCTTTTCAGAGATATTAACATTTGTAATTTGTTTTAATTAAGCTTTGGACAGC
2281 TTCTTTTTAATGTTCCAAAGATTGGCCCTGTATTAGGAAATAAAGCTGAACCTGGGACTG
2341 TGAAAAAATAAAAAAAAAAAAAA

```

Figure 2: Complete cDNA and predicted amino acid sequence of mouse BP75.

The arrowheads (a.a. 323 and 362) indicate the start of the clones identified in the two-hybrid interaction trap (BP#3 and BP#6, respectively). The numbers to the left and right correspond to nucleotide and amino acid positions in the BP75 database entry (AF084259), respectively. The bromodomain and the BYC domain (for explanation see legend Fig. 3 and text) are shown on a dark and light grey background. Consensus tyrosine phosphorylation sites are shown underlined, the nuclear localization signal sequences are underlined with a dashed line and the polyadenylation sequence is doubly underlined.

A



BP75 interacts with the PTP-BL PDZ moiety when coexpressed in mammalian cells

To obtain independent evidence for the interaction between BP75 and PTP-BL, we cotransfected mammalian epithelial cells (COS-1) with an expression construct encoding Myc-epitope-tagged full-length BP75 and a construct encoding the five PDZ domains of PTP-BL (BL-PDZ-I-V), or, as a control, the empty expression vector. Specific coprecipitation of anti-Myc detectable full-length BP75 was demonstrated for BL-PDZ-I-V (Fig. 4) when using an antibody against BL-PDZ-I (Cuppen et al., 1998), confirming the results obtained in the yeast two-hybrid interaction trap.

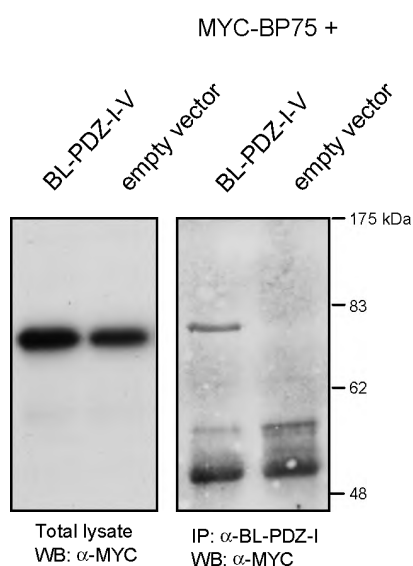


Figure 4: BP75 coprecipitates with PDZ domains of PTP-BL.

COS-1 cells were cotransfected with a construct encoding cMyc epitope-tagged BP75 and a construct encoding the five PDZ domains of PTP-BL (BL-PDZ-I-V) or empty vector as a control. Western blotting using a α -cMyc antibody detected a 75 kDa protein in the total cell lysates (left panel). After immunoprecipitation using a polyclonal antiserum directed against the first PDZ domain of PTP-BL (α -BL-PDZ-I) coprecipitation of cMyc epitope-tagged BP75 with the five PDZ domains of PTP-BL is shown (right panel). No coprecipitation of BP75 is observed in lysates of COS cells cotransfected with empty vector.

Figure 3: (facing page) Sequence comparison of the BP75 protein.

(A) The bromodomain of BP75 is shown, aligned with bromodomains from different proteins. The original 80 a.a. bromodomain motif (Haynes et al., 1992) and the secondary structure as predicted from a multiple alignment of 37 proteins (Jeanmougin et al., 1997) are indicated at the bottom. The aligned proteins are the hypothetical *C.elegans* protein C01H6.7 (Z71258), human peregrin or BR140 (JC2069), *Tetrahymena thermophila* Histone Acetyltransferase A (HAT A1, U47321), mouse CREB binding protein (CBP, P45481), mouse RING3 (D89801), human transcription initiation factor TFIID, 250 kDa subunit, (TAFII-250, P21675) and human SNF2 α (S45251). The numbers on the left and right of the peptides indicate the corresponding N and C-terminal amino acid positions in the database entry. Symbols used in the consensus sequence: \$, positive charge (K,R); !, (M,L,I,V); %, (S,T); #, (Y,F). Residues that are similar in at least half, two-third and all sequences are shown black on a grey background, white on a grey background and white on a black background, respectively. (B) The complete BP75 protein sequence was aligned with the predicted protein C01H6.7 from the *C.elegans* contig C01h6. Identical amino acids are shown on a black background and similar amino acids are indicated on a grey background. The bromodomain and BYC domain are single and double underlined, respectively. (C) Multiple alignment of the BYC domain of BP75 (AF084259), C01H6.7 (Z71258) and YN92 (P53749). Shading as depicted in A.

BP75 expression pattern

The observed interaction between BP75 and PTP-BL can only be of biological significance when both genes are coexpressed in at least some tissues. Therefore, the BP75 cDNA insert and full-length PTP-BL cDNA were used to probe a northern blot of total RNA from several different mouse tissues. As shown in Fig. 5A, a transcript of about 2.5 kb is highly expressed in all tissues examined, with the highest levels in lung, stomach and thymus. The 8.5 kb PTP-BL transcript has a more restricted expression pattern and is most abundant in lung, kidney, testis, stomach and skin. To further delineate the BP75 expression pattern we used an antisense BP75 RNA probe for *in situ* hybridization on mouse embryo cryosections. BP75 expression is found throughout development in all embryonic stages (10.5 dpc to 18.5 dpc) analysed (not shown). In 16.5 dpc embryos BP75 is ubiquitously expressed, with highest expression levels in thymus, lung, liver, colon and the spinal cord (Fig. 6B). Significant expression is also found in salivary glands, vibrissae and skin (Fig. 6B). No positive signal was obtained when a BP75 sense RNA probe was used (Fig. 6C).

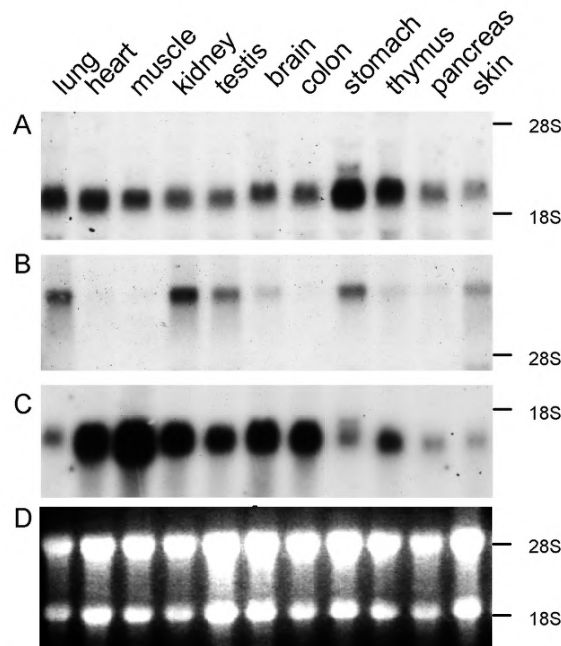


Figure 5: Tissue distribution of BP75 and PTP-BL.

Northern blot analysis of total RNA from mouse tissues for BP75 (A) and PTP-BL (B). As a control for RNA loading, levels of the housekeeping gene GAPDH (C) and rRNA bands in total RNA on an ethidium bromide-stained gel (D) were used. BP75 is expressed ubiquitously in all tissues examined, whereas PTP-BL is highly expressed in lung, kidney, testis, stomach and skin and to a lower level in brain and thymus.

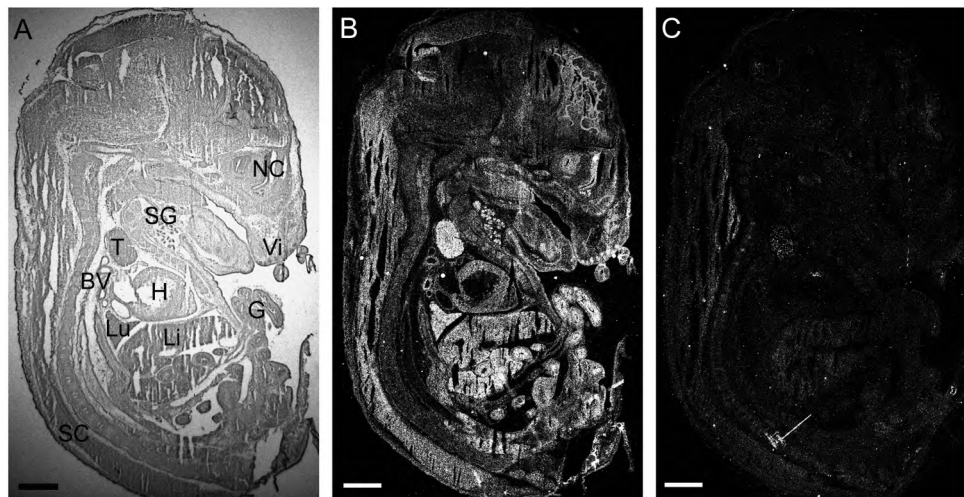


Figure 6: BP75 RNA *in situ* hybridization on 16.5 dpc mouse embryo sections.

A bright field image (A) and dark field images using an antisense BP75 RNA probe (B) and a sense BP75 probe (C) on 16.5 dpc mouse embryo cryosections are shown. BP75 is expressed throughout the whole embryo with highest expression in thymus, lung, liver, colon and the spinal cord. Furthermore, high expression is also observed in salivary glands, vibrissae and skin. BV, blood vessel; G, gut; H, heart; Li, liver; Lu, lung; NC, nasal cavity; SC, spinal cord; SG, salivary glands; Vi, vibrissae. Bars, 1 mm.

BP75 and PTP-BL protein localization

To study the subcellular distribution of both interactors, full-length cMyc epitope-tagged BP75 was expressed transiently in NIH 3T3 fibroblasts and MDCK cells together with either the first PTP-BL PDZ domain or full-length PTP-BL. Fluorescent double-labeling was performed using a mouse monoclonal antibody against the cMyc tag (9E10; Kari et al., 1986) and a rabbit polyclonal antibody directed against the first PDZ domain of PTP-BL (Cuppen et al., 1998). BP75 localizes predominantly to the nucleus in both fibroblast (Figs. 7A and C) and MDCK cells (Figs. 7E and G), as does BL-PDZ-I (Figs. 7B and F), although cytoplasmic staining is also evident in some cells. There is an interesting correlation between BP75 and BL-PDZ-I nuclear and cytoplasmic location in double transfected cells: in cells where BP75 is located in the cytoplasm also BL-PDZ-I is cytoplasmically localized. Furthermore, at higher magnification a typical distribution pattern that is indicative for a nucleoplasmic localization becomes obvious for both BP75 (Fig. 7A, insert) and BL-PDZ-I (Fig. 7B, insert). It is interesting to note that PTP-BL PDZ-I is the only domain out of seven PDZ domains tested by transient expression, that localizes to the nucleus (unpublished observations).

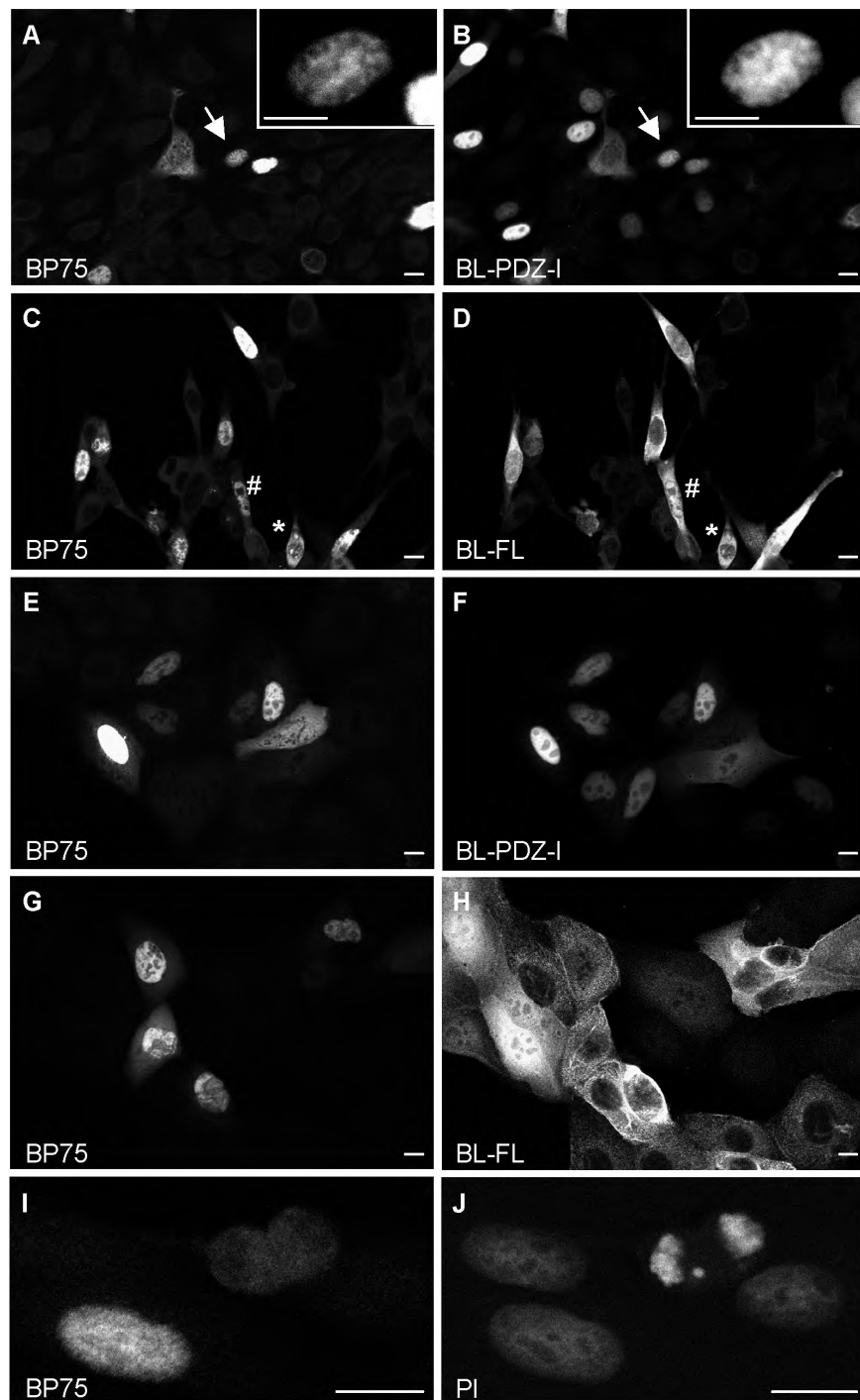
The BP75 localization hardly overlaps with that of the complete PTP-BL protein, although both cytoplasmic (Figs. 7C and D, cell indicated by #) and nuclear (Figs. 7C and D,

indicated by *) colocalization can occasionally be observed in fibroblasts. In MDCK cells PTP-BL is localized predominantly in a punctuate pattern at the apical side of the cell, corresponding to the microvilli-like membrane protrusions on these cells, but also nuclear staining is evident in some cells (Fig. 7H). Hardly any mitotic cells could be found that express BP75. However, the few cells observed showed very faint cytosolic staining, largely excluding the area of the chromosomes (Figs. 7I and J). These observations suggest that BP75 is degraded before or during mitosis.

Discussion

We report here on the identification of two independent clones encoding the C-terminal part of a novel bromodomain-containing protein, BP75, that specifically interact with the first PDZ domain of PTP-BL. In addition, several observations are described which have bearing on the restricted possibilities for this interaction and the limited overlap in both cell-type expression and subcellular distribution patterns of the putative partner proteins. These different issues need a further discussion in order to obtain a better appreciation of the complexity of PTP-BL biology and the role of the PTP-BL's distinct peptide domains. It is becoming increasingly clear that PDZ domains, as they occur in PTP-BL and a variety of other proteins (Ponting, 1997), are protein-protein interaction modules that generally bind to short C-terminal peptides (Saras and Heldin, 1996; Songyang et al., 1997). We found that the last 30 amino acids of BP75 are not sufficient for a strong interaction to occur (Fig. 1B). Still, the two-hybrid analysis shows that deletion of the last 29 amino acids of BP75 almost completely abolishes any detectable interaction. Taken together, this argues against a simple model in which PDZ domains uniquely engage in C-terminal peptide binding, also because the last three residues of BP75 (-DAS*) do not resemble any of the known consensus motifs for PDZ recognition (Songyang et al., 1997). Furthermore, screening of a two-hybrid random peptide library to identify a consensus C-terminal peptide target sequence for PTP-BL PDZ-I did not result in interacting peptides (E.C., M.v.H., unpublished work), whereas the same approach was successful for the neuronal NOS PDZ domain (Schepens et al., 1997). Perhaps BL-PDZ-I belongs to a subset of PDZ

Figure 7: (facing page) Confocal images of BP75 and PTP-BL localization in 3T3 and MDCK cells. cMyc-tagged BP75 was transiently coexpressed with the first PDZ domain of PTP-BL (A, B, E and F) or with full-length PTP-BL (C, D, G and H) in NIH 3T3 (A, B, C, and D) and MDCK cells (E, F, G and H). BP75 was detected using a monoclonal antibody against the cMyc-tag (A, C, E and G) and BL-PDZ-I and full-length PTP-BL were detected with a rabbit polyclonal antibody directed against PDZ-I (B, D, F and H). BP75 was detected in mitotic NIH 3T3 cells (I) and the DNA was stained with propidium iodide (J). The inserts in (A) and (B) show an enlargement of the cell indicated with an arrow. In cells coexpressing BP75 and PTP-BL, both cytoplasmic (*) and nuclear (#) colocalization is observed (C, D). The bars represent 10 μ m.



domains that is not capable of recognizing C-terminal peptide segments in isolation and requires accessory presence of other protein segments. Indeed, evidence is accumulating that internal peptide sequences may equally well serve as targets for recognition by PDZ domains. For example, the binding of the third PDZ domain in InaD to the TRP Ca²⁺ channel is critically dependent on an internal STV peptide (Shieh and Zhu, 1996), and the fifth InaD PDZ domain binds an internal segment of phospholipase C-β (van Huizen et al., 1998). Furthermore, the ALP-1 PDZ domain binds to an internal spectrin-like repeat in α-actinin-1 (Xia et al., 1997) and PTP-BL PDZ domains II and IV and the RIL PDZ domain require the C-terminal RIL LIM domain for interaction (Cuppen et al., 1998). A closer look at the critical residues in PTP-BL PDZ-I, that would govern C-terminal peptide binding analogous to the situation in the PSD95 PDZ domain (Doyle et al., 1996), did not reveal, however, a structural basis for assuming an impairment of such mode of interaction. So, there are arguments for both types of interactions to exist, and our findings are therefore most easily interpreted by assuming that combined internal and C-terminal information is required for a strong interaction of BP75 and PTP-BL PDZ-I. Interestingly, secondary structure prediction suggests the presence of coiled-coil elements in the C-terminal half of BP75 (a.a. 534-565) and perhaps dimerization via these structures may be a prerequisite for interaction with BL-PDZ-I.

The interaction identified in the yeast two-hybrid interaction trap was confirmed in an independent assay showing coimmunoprecipitation from transfected mammalian cells of BP75 with a protein segment encompassing the five PDZ domains of PTP-BL (Fig. 4). Unfortunately, we were unable to show an interaction between full-length proteins in this assay. Most likely, this is due to the very low PTP-BL protein levels that were obtained in our transfection studies. These and data from other experiments suggest that overexpression of the very large fully active PTP-BL protein conflicts with the cell's viability (E.C., Derick Wansink, unpublished work).

For the observed interaction to be of biological significance at least a partial overlap in expression pattern is required. Northern blot (Fig. 5) and RNA *in situ* hybridization analysis with BP75 and PTP-BL probes (Fig. 6; Hendriks et al., 1995) show that BP75 and PTP-BL are coexpressed in some, but not all, tissues. Clear coexpression can be observed in for example glandular epithelial cells, thymus and lung. The ubiquitous expression of BP75 mRNA suggests a structural or general function for the protein and perhaps this is modulated by PTP-BL in restricted tissues. In tissues where PTP-BL is not present, such as liver, other proteins may interact with BP75, but experimental evidence for this possibility is lacking.

Another aspect of our histological findings, the restricted occurrence of overlap in subcellular distribution between PTP-BL and BP75 is also enigmatic. Transfection studies, as shown in Fig. 7, reveal BP75 to have predominantly a nuclear location. This is in keeping with the presence of the bromodomain (Haynes et al., 1992; Jeanmougin et al.,

1997) and the bipartite nuclear localization signals in the product specified by the full-length mouse cDNA. The question whether there is also a role for the BYC domain (the conserved segment in BP75, YN92 and C01H6.7), with similarity to the putative transcriptional regulatory protein YN92 from yeast, is open for further study. If both the bromo- and the BYC domain are considered a key to function one might speculate that BP75 may have a role in regulation of chromatin structure and/or transcriptional activity.

Due to its secondary structure that consists of four α -helices the bromodomain has been proposed to mediate protein-protein interactions in the nucleus thereby influencing the assembly and/or activity of multiprotein complexes (Haynes et al., 1992; Jeanmougin et al., 1997). Indeed, GCN5, a putative transcriptional adapter in humans and yeast, was found to bind to DNA-dependent protein kinase holoenzyme via its bromodomain, resulting in phosphorylation of GCN5 and inhibition of its histone acetyltransferase activity (Barlev et al., 1998). Is there compatibility between the behaviour and putative role of BP75 and that of PTP-BL? For PTP-BL, we do know that it is localized mainly at the plasma membrane, although in some cells a nuclear localization can be observed in our experimental set-up. Interestingly, also low levels of endogenous PTP-BL have been found in nuclei of mouse keratinocytes (Derick Wansink, unpublished work) leaving open the possibility of BP75 and PTP-BL to physically interact. Of course, during mitosis there is ample opportunity for both proteins to interact, and maybe the low levels of BP75 in the cytoplasm and PTP-BL in the nucleus are indicative of a recently acquired post-mitotic state. Alternatively, it is possible that BP75 and/or PTP-BL shuttle between cytosol and the nucleus, coupling signal transduction processes at the cell cortex to nuclear events or vice versa. In this light it is interesting to note that Protein 4.1, which contains an FERM domain like PTP-BL, is also located both at the cell membrane and in the nucleus (Krauss et al., 1997). Furthermore, several other submembranous proteins like zyxin, ZO-1, β -catenin and plakophilins 2a and 2b are also found located in the nucleus (Behrens et al., 1996; Gottardi et al., 1996; Huber et al., 1996; Mertens et al., 1996; Nix and Beckerle, 1997). Conversely Br140, another primarily nuclear bromodomain-containing protein, was initially identified due to its copurification with an integrin (Thompson et al., 1994). Shuttling of proteins or protein-complexes between compartments may therefore form an important pathway for coupling submembranous signaling events to nuclear activity. External stimuli or the catalytic activity of enzymes like PTP-BL may regulate these processes. Interestingly, BP75 contains two consensus tyrosine phosphorylation sites and many potential serine and threonine phosphorylation sites that may regulate its properties in a reversible manner. Furthermore, since modulation of proteins by tyrosine phosphorylation and subsequent translocation into the nucleus is now seen as a general mechanism of transmitting signals from cell-surface to the nucleus (Karin and Hunter, 1995), the lack of coprecipitation of BP75 with full-length PTP-BL (Fig. 4) may also be due to direct or indirect modulation of the PDZ-BP75 interaction by the enzymatic activity of PTP-BL.

Clearly, to fully understand the importance of PTP-BL as a scaffold protein we require more knowledge about the biological processes PTP-BL is involved in. Knock-out mouse models could help us as they offer a clear view on the effect of PTP-BL deficiency. Recently, a gene trap insertion mutant has been described that displayed no obvious defects (Thomas et al., 1998). However, in the model presented by this group part of the scaffold function of PTP-BL might still be intact, because only the C-terminal half of the protein was deleted. Generation of additional animal and cellular models and the hunting of other binding partners may therefore be a good strategy to approach the biological function of PTP-BL.

Materials and Methods

Two-Hybrid Interaction Trap - Plasmid DNAs, the yeast strain EGY48 and the HeLa cell cDNA library used for the interaction-trap assay were kindly provided by Dr. Roger Brent and colleagues (Massachusetts General Hospital, Boston, MA) and used as described (Gyuris et al., 1993). The construction of the PTP-BL PDZ, RIL-PDZ, nNOS PDZ and SAP-PDZ baits has been described previously (Cuppen et al., 1998; Schepens et al., 1997). For two-hybrid interaction assays plasmids were introduced in yeast strain EGY48 (*MATa trp1 ura3 his3 LEU2::pLexAop6-LEU2*) containing the plasmid pSH18-34, which includes the reporter *lacZ* gene, and interactions were validated by growth and blue colouring on minimal agar-plates lacking histidine, tryptophan, uracil and leucine, which contain 2% galactose, 1% raffinose and 80 µg/ml X-gal, buffered at pH7.0. Comparison of candidate prey cDNA sequences with database entries was done using the BLAST program (Altschul et al., 1990). Mouse BP75 prey constructs containing the fragment corresponding to the shortest human prey insert (mBP75C, a.a. 323-651), the C-terminus of BP75 (BP-Cter, a.a. 620-651) and the C-terminal half of BP75 lacking the C-terminus (BP-ΔCter, a.a. 362-622), were generated by PCR using specific primers with either EcoRI or XhoI restriction enzyme recognition sites, using mouse full-length BP75 cDNA (AF084259) as a template. The resulting fragments were cloned in-frame in a EcoRI and XhoI digested pJG4-5 prey vector (Gyuris et al., 1993). All constructs generated by PCR were checked for absence of mutations by DNA sequencing.

Isolation and characterization of mouse BP75 cDNAs - The 1.2 kbp BP#3 insert was isolated, labelled radioactively by random priming and used to screen a mouse brain λ-ZAPIII cDNA phage library (Stratagene, La Jolla, CA) following standard procedures. Resulting phages were plaque-purified and inserts were rescued as pBluescript SK⁻ plasmids according to the manufacturer's protocols. Nucleotide sequences were determined by double-stranded DNA dideoxy sequencing using T3 and T7 sequencing primers on rescued plasmids and subclones derived thereof. Sequences were aligned with Multalin (Corpet, 1988) using the Blosum62 comparison table and annotated with Genedoc (shareware, version 2.2.005 (Nicholas and Nicholas, 1997)).

RNA expression studies - Total RNA from several tissues was prepared using the guanidium isothiocyanate-phenol-chloroform extraction method (Chomczynski and Sacchi, 1987). Fifteen µg RNA was loaded on a 1% formamide agarose gel and after electrophoresis the RNA was transferred to a nylon membrane (Hybond-N, Amersham) according to standard procedures. Complete mouse BP75, PTP-BL and GAPDH cDNAs were radioactively labelled by random priming and used as probes for hybridization as described (Cuppen et al., 1997). RNA *in situ* hybridization on mouse embryo cryosections was according to previously published protocols (Hendriks et al., 1995). To generate 'sense' and 'antisense' RNA probes, the mouse BP75 cDNA pBluescript-SK-based plasmid was linearized with XhoI and NotI, respectively, and used for *in vitro* transcription by T3 and T7 RNA

polymerase, respectively. Both probes were labelled with $\alpha^{35}\text{S}$ -UTP (400 Ci/mmol, Amersham) to a specific activity of $>10^9$ dpm/ μg .

Expression plasmid constructions - Restriction fragments encoding amino acid stretches 1056-1284 and 1002-2018 of PTP-BL (Z32740) encompassing PDZ-I and PDZ-I-V, respectively, were cloned into a modified version of the eukaryotic expression vector pSG5 (Green et al., 1988) that contains an initiator AUG codon at the multiple cloning site. A construct for the expression of an epitope-tagged version of mouse BP75 was generated as follows. Using a subcloned SmaI fragment of BP75 as template the 5'-end of the BP75 open reading frame was PCR amplified with a specific oligonucleotide (5'-CGAATTCATGGGCAAGAAGCACAAG-3', introducing an EcoRI site directly in front of the start codon) and the vector-specific T7 oligonucleotide. The resulting 0.2 kbp fragment was digested with EcoRI and XmaI and used together with a 1.9 kbp XmaI-XhoI restriction fragment of BP75 in a three-way ligation into the EcoRI-XhoI digested pMyc vector. pMyc is a pCDNA3-derived vector in which at the 5' end of the pCDNA3 (Invitrogen) multiple cloning site a synthetic DNA fragment was introduced that entails an initiator AUG codon followed by the cMyc-epitope tag and an EcoRI site. Full-length PTP-BL (Hendriks et al., 1995) was subcloned as a NotI-XhoI restriction fragment in pCDNA3.

Immunoprecipitation and Western blotting - COS-1 cells were cultured in DMEM/10% fetal calf serum. For each assay, 1.5×10^6 cells were electroporated at 0.3 kV and 125 μF using the Bio-Rad GenePulser with a 4-mm electroporation cuvette, in 200 μl of phosphate-buffered saline (PBS) containing 10 μg of supercoiled plasmid DNA. Cells were plated on a 10-cm dish and cultured for 24 h in DMEM/10% fetal calf serum. Cells were washed with cold PBS and lysed on plate with 550 μl ice-cold RIPA buffer (50 mM Tris, pH8.0, 100 mM NaCl, 1 mM EDTA, 1% NP-40, 0.1% SDS, 0.5% DOC, 1 mM PMSF and protease inhibitor cocktail (Boehringer)). After a 1 hour incubation on ice, the lysate was centrifuged for 10 min at $10,000 \times g$ at 4°C and proteins in 50 μl of the lysate were separated for further analysis. After addition of the polyclonal antibody α -BL-PDZ-I (affinity-purified, 50 x diluted; Cuppen et al., 1998) and overnight rotation at 4°C , 50 μl of protein A-Sepharose CL-4B (Pharmacia) were added and incubation was prolonged overnight. The Sepharose beads with immunobound proteins were washed four times with 1 ml RIPA lysis buffer and boiled for 5 min in 50 μl of 2x sample buffer (100 mM Tris-HCl, pH6.8, 200 mM dithiothreitol, 4% SDS, 0.2% bromophenol blue, 20% glycerol). Fifteen μl of lysates and immunobound proteins were resolved on 8% polyacrylamide gels and transferred to nitro-cellulose membranes by western blotting. Blots were blocked using 5% nonfat dry milk in 10 mM Tris-HCl (pH 8.0), 150 mM NaCl, and 0.05% Tween 20 (TBST). Cell culture supernatant of the α -cMyc hybridoma 9E10 (Kari et al., 1986) was used to detect coprecipitation of epitope-tagged BP75. Incubations with primary and secondary (1 hour, 10,000 x diluted peroxidase-conjugated goat anti-mouse IgG (Pierce)) and subsequent washes were done in TBST at room temperature. Labelled bands were visualized using freshly prepared chemiluminescent substrate (100 mM Tris-HCl, pH8.5, 1.25 mM p-coumaric acid (Sigma), 0.2 mM luminol (Sigma), and 0.009 % H_2O_2).

Cell transfection - Mouse embryonic fibroblasts (NIH 3T3) and MDCK type II cells (a kind gift of K. Ekroos, Heidelberg, Germany) were cultured in DMEM (Gibco BRL, Gaithersburg, MD), supplemented with 10% FCS (Zellbiologische Produkte GMBH, St.Salvator, Germany). Prior to transfection, cells were seeded onto 14 mm diameter glass coverslips (Menzel-Glaser, Germany) in 24 wells cell culture plates. Transfection mix was made by adding 0.3 μg supercoiled plasmid DNA to 2 μg DAC-30 (Eurogentec, Seraing Belgium) in 150 μl OptiMEM (Gibco BRL, Gaithersburg, MD) and incubating for 30 min at room temperature. After replacing the culture medium on the cells (at 30-50 % confluency) with 150 μl fresh DMEM containing 10% FCS, the transfection mix (150 μl) was added to the cells. Following a 5 hours incubation at 37°C the medium was replaced with fresh DMEM containing 10% FCS and incubation was prolonged overnight. Cells were subsequently used for immunofluorescence.

Immunofluorescence and Microscopy - All solutions are prepared in PBS and incubations were

performed at room temperature in the presence of 1% goat serum. Cells were fixed for 20 min in 2% paraformaldehyde, permeabilized with 0.5% Nonidet P-40, and then free aldehyde groups were quenched for 10 min in 0.1 M glycine. 50 μ l of a 1:2 dilution of monoclonal mouse α -cMyc (hybridoma culture supernatant, 9E10; Kari et al., 1986) and 1:50 dilution of affinity-purified polyclonal rabbit α -BL-PDZ-I (directed against the first PDZ domain of PTP-BL; Cuppen et al., 1998), was used for the 1 hour incubation with primary antibody. After thoroughly rinsing in PBS, cells were incubated for 5 min with the second antibodies, 50 μ l of a 1:75 dilution Texas Red-conjugated AffiniPure Goat anti-mouse IgG and 1:75 dilution Fluorescein-conjugated AffiniPure Goat anti-rabbit IgG (both from Jackson ImmunoResearch Laboratories, Inc., West Grove, PA). In cases where DNA was stained with propidium iodide (5 μ g/ml) the fluorescein-conjugated AffiniPure Goat anti-mouse IgG (Jackson ImmunoResearch Laboratories, Inc., West Grove, PA) was used as second antibody. Finally the coverslips were rinsed in PBS and water and mounted on slides by inversion over 5 μ l Mowiol mountant (Sigma Chemical Co.). Cells were examined using a confocal laser scanning microscope (MRC1000, Bio-Rad).

References

- Altschul, S. F., Gish, W., Miller, W., Myers, E. W., and Lipman, D. J. (1990). Basic local alignment search tool. *J. Mol. Biol.* *215*, 403-410.
- Banville, D., Ahmad, S., Stocco, R., and Shen, S. H. (1994). A novel protein-tyrosine phosphatase with homology to both the cytoskeletal proteins of the band 4.1 family and junction-associated guanylate kinases. *J. Biol. Chem.* *269*, 22320-22327.
- Barlev, N. A., Poltoratsky, V., Owen-Hughes, T., Ying, C., Liu, L., Workman, J. L., and Berger, S. (1998). Repression of GCN5 histone acetyltransferase activity via bromodomain-mediated binding and phosphorylation by the Ku-DNA-dependent protein kinase complex. *Mol. Cell. Biol.* *18*, 1349-1358.
- Behrens, J., Von Kries, J. P., Kuhl, M., Bruhn, L., Wedlich, D., Grosschedl, R., and Birchmeier, W. (1996). Functional interaction of b-catenin with the transcription factor LEF-1. *Nature* *382*, 638-642.
- Bork, P., Schultz, J., and Ponting, C. P. (1997). Cytoplasmic signaling domains: the next generation. *Trends Biochem. Sci.* *22*, 296-298.
- Chida, D., Kume, T., Mukoyama, Y., Tabata, S., Nomura, N., Thomas, M. L., Watanabe, T., and Oishi, M. (1995). Characterization of a protein tyrosine phosphatase (RIP) expressed at a very early stage of differentiation in both mouse erythroleukemia and embryonal carcinoma cells. *FEBS Lett.* *358*, 233-239.
- Chomczynski, P., and Sacchi, N. (1987). Single-step method of RNA isolation by acid guanidinium thiocyanate-phenol-chloroform extraction. *Anal. Biochem.* *162*, 156-159.
- Corpet, F. (1988). Multiple sequence alignment with hierarchical clustering. *Nucl. Acids Res.* *16*, 10881-10890.
- Cuppen, E., Gerrits, H., Pepers, B., Wieringa, B., and Hendriks, W. (1998). PDZ motifs in PTP-BL and RIL bind to internal protein segments in the LIM domain protein RIL. *Mol. Biol. Cell* *9*, 671-683.
- Cuppen, E., Nagata, S., Wieringa, B., and Hendriks, W. (1997). No evidence for involvement of mouse protein-tyrosine phosphatase-BAS-like/Fas-associated Phosphatase-1 in Fas-mediated apoptosis. *J. Biol. Chem.* *272*, 30215-30220.
- Dingwall, C., and Laskey, R. A. (1991). Nuclear targeting sequences--a consensus? *Trends Biochem. Sci.* *16*, 478-481.
- Doyle, D. A., Lee, A., Lewis, J., Kim, E., Sheng, M., and MacKinnon, R. (1996). Crystal structures of a complexed and peptide-free membrane protein-binding domain: molecular basis of peptide recognition by PDZ. *Cell* *85*, 1067-1076.
- Fanning, A. S., and Anderson, J. M. (1996). Protein-protein interactions: PDZ domain networks.

- Curr. Biol. *6*, 1385-1388.
- Faux, M. C., and Scott, J. D. (1996). More on target with protein phosphorylation: conferring specificity by location. Trends Biochem. Sci. *21*, 312-315.
- Gottardi, C. J., Arpin, M., Fanning, A. S., and Louvard, D. (1996). The junction-associated, ZO-1, localizes to the nucleus before the maturation and during the remodeling of cell-cell contacts. Proc. Natl. Acad. Sci. USA *93*, 10779-10784.
- Green, S., Issemann, I., and Sheer, E. (1988). A versatile in vivo and in vitro eukaryotic expression vector for protein engineering. Nucl. Acids Res. *16*, 369.
- Gyuris, J., Golemis, E., Chertkov, H., and Brent, R. (1993). Cdi1, a human G1 and S phase protein phosphatase that associates with Cdk2. Cell *75*, 791-803.
- Haynes, S. R., Dollard, C., Winston, F., Beck, S., Trowsdale, J., and Dawid, I. B. (1992). The bromodomain: a conserved sequence found in human, *Drosophila* and yeast proteins. Nucl. Acids Res. *20*, 2603.
- Hendriks, W., Schepens, J., Bachner, D., Rijss, J., Zeeuwen, P., Zechner, U., Hameister, H., and Wieringa, B. (1995). Molecular cloning of a mouse epithelial protein-tyrosine phosphatase with similarities to submembranous proteins. J. Cell. Biochem. *59*, 418-430.
- Herskowitz, I. (1995). MAP kinase pathways in yeast: for mating and more. Cell *80*, 187-197.
- Huber, O., Korn, R., McLaughlin, J., Oshugi, M., Herrmann, B. G., and Kemler, R. (1996). Nuclear localization of b-catenin by interaction with transcription factor LEF-1. Mech. Dev. *59*, 3-11.
- Jeanmougin, F., Wurtz, J., Le Douarin, B., Chambon, P., and Losson, R. (1997). The bromodomain revisited. Trends Biochem. Sci. *22*, 151-153.
- Kari, B., Lussenhop, N., Goertz, R., Wabuke-Bunoti, M., Radeke, R., and Gehrz, R. (1986). Characterization of monoclonal antibodies reactive to several biochemically distinct human cytomegalovirus glycoprotein complexes. J. Virol. *60*, 345-352.
- Karin, M., and Hunter, T. (1995). Transcriptional control by protein phosphorylation: signal transmission from the cell surface to the nucleus. Curr. Biol. *5*, 747-757.
- Kennedy, M. B. (1995). Origin of PDZ (DHR, GLGF) domains. Trends Biochem. Sci. *20*, 350.
- Kiess, M., Scharm, B., Aguzzi, A., Hajnal, A., Klemenz, R., Schwarte Waldhoff, I., and Schafer, R. (1995). Expression of ril, a novel LIM domain gene, is down-regulated in Hras-transformed cells and restored in phenotypic revertants. Oncogene *10*, 61-68.
- Krauss, S. W., Larabell, C. A., Locket, S., Gascard, P., Penman, S., Mohandas, N., and Chasis, J. A. (1997). Structural Protein 4.1 in the nucleus of human cells: dynamic rearrangements during cell division. J. Cell Biol. *137*, 275-289.
- Maekawa, K., Imagawa, N., Nagamatsu, M., and Harada, S. (1994). Molecular cloning of a novel protein-tyrosine phosphatase containing a membrane-binding domain and GLGF repeats. FEBS Lett. *337*, 200-206.
- Mertens, C., Kuhn, C., and Franke, W. W. (1996). Plakophilins 2a and 2b: constitutive proteins of dual location in the karyoplasm and desmosomal plaque. J. Cell Biol. *135*, 1009-1025.
- Nicholas, K. B., and Nicholas, J. H. B. (1997). Genedoc: a tool for editing and annotating multiple sequence alignments. Distributed by the author. [Http://www.cris.com/~ketchup/genedoc.shtml](http://www.cris.com/~ketchup/genedoc.shtml).
- Nix, D. A., and Beckerle, M. C. (1997). Nuclear-cytoplasmic shuttling of the focal contact protein, Zyxin: A potential mechanism for communication between sites of cell adhesion and the nucleus. J. Cell Biol. *138*, 1139-1147.
- Pawson, T., and Scott, J. D. (1997). Signaling through scaffold, anchoring, and adaptor
- Ponting, C. P. (1997). Evidence For PDZ Domains in Bacteria, Yeast, and Plants. Prot. Sci. *6*, 464-468.
- Ranganathan, R., and Ross, E. M. (1997). PDZ domain proteins: Scaffolds for signaling complexes. Curr. Biol. *7*, R770-R773.
- Saras, J., Claesson Welsh, L., Heldin, C. H., and Gonez, L. J. (1994). Cloning and characterization of PTPL1, a protein tyrosine phosphatase with similarities to cytoskeletal-associated proteins. J. Biol. Chem. *269*, 24082-24089.
- Saras, J., Engström, U., Gonez, L. J., and Heldin, C.-H. (1997). Characterization of the interactions

- between PDZ domains of the protein-tyrosine phosphatase PTPL1 and the carboxyl-terminal tail of Fas. *J. Biol. Chem.* *272*, 20979-20981.
- Saras, J., Franzen, P., Aspenstrom, P., Hellman, U., Gonez, L. J., and Heldin, C. (1997). A novel GTPase-activating protein for Rho interacts with a PDZ domain of the protein-tyrosine phosphatase PTPL1. *J. Biol. Chem.* *272*, 24333-24338.
- Saras, J., and Heldin, C.-H. (1996). PDZ domains bind carboxy-terminal sequences of target proteins. *Trends Biochem. Sci.* *21*, 455-458.
- Sato, T., Irie, S., Kitada, S., and Reed, J. C. (1995). FAP-1: a protein tyrosine phosphatase that associates with Fas. *Science* *268*, 411-415.
- Schepens, J., Cuppen, E., Wieringa, B., and Hendriks, W. (1997). The neuronal nitric oxide synthase PDZ motif binds to -G(D,E)XV* carboxyterminal sequences. *FEBS Lett.* *409*, 53-56.
- Schjerling, P., and Holmberg, S. (1996). Comparative amino acid sequence analysis of the C6 zinc cluster family of transcriptional regulators. *Nucl. Acids Res.* *24*, 4599-4607.
- Sheng, M. (1996). PDZs and receptor/channel clustering: rounding up the latest suspects. *Neuron* *17*, 575-578.
- Shieh, B. H., and Zhu, M. Y. (1996). Regulation of the TRP Ca²⁺ channel by INAD in *Drosophila* photoreceptors. *Neuron* *16*, 991-998.
- Songyang, Z., Fanning, A. S., Fu, C., Xu, J., Marfatia, S. M., Chishti, A. H., Crompton, A., Chan, A. C., Anderson, J. M., and Cantley, L. C. (1997). Recognition of unique carboxyl-terminal motifs by distinct PDZ domains. *Science* *275*, 73-77.
- Songyang, Z., Shoelson, S. E., Chaudhuri, M., Gish, G., Pawson, T., Haser, W. G., King, F., Roberts, T., Ratnofsky, S., and Lechleider, R. J. (1993). SH2 domains recognize specific phosphopeptide sequences. *Cell* *72*, 767-778.
- Thomas, T., Voss, A. K., and Gruss, P. (1998). Distribution of a murine protein tyrosine phosphatase BL-beta-galactosidase fusion protein suggests a role in neurite outgrowth. *Dev. Dynamics* *212*, 250-257.
- Thompson, K. A., Wang, B., Argraves, W. S., Giancotti, F. G., Schranck, D. P., and Ruoslahti, E. (1994). BR140, a novel zinc-finger protein with homology to the TAF250 subunit of TFIID. *Biochem. Biophys. Res. Comm.* *198*, 1143-1152.
- Tsukita, S., and Yonemura, S. (1997). ERM (ezrin/radixin/moesin) family: from cytoskeleton to signal transduction. *Curr. Opin. Cell Biol.* *9*, 70-75.
- Tsunoda, S., Sierralta, J., Sun, Y., Bodner, R., Suzuki, E., Becker, A., Socolich, M., and Zuker, C. S. (1997). A multivalent PDZ-domain protein assembles signaling complexes in a G-protein-coupled cascade. *Nature* *388*, 243-249.
- van Huizen, R., Miller, K., Chen, D. M., Li, Y., Lai, Z. C., Raab, R. W., Stark, W. S., Shortridge, R. D., and Li, M. (1998). Two distantly positioned PDZ domains mediate multivalent INAD-phospholipase C interactions essential for G protein-coupled signaling. *EMBO J.* *17*, 2285-2297.
- Wilson, R., Ainscough, R., Anderson, K., Baynes, C., Berks, M., Bonfield, J., Burton, J., Connell, M., Copsey, T., Cooper, J., Coulson, A., Craxton, M., Dear, S., Du, Z., Durbin, R., Favello, A., Fulton, L., Gardner, A., Green, P., Hawkins, T., Hillier, L., Jier, M., Johnston, L., Jones, M., Kershaw, J., Kirsten, J., Laister, N., Latreille, P., J., L., Lloyd, C., McMurray, A., Mortimore, B., O'Callaghan, M., Parsons, J., Percy, C., Rifken, L., Roopra, A., Saunders, D., Shownkeen, R., Smaldon, N., Smith, A., Sonnhammer, E., Staden, R., Sulston, J., Thierry-Mieg, J., Thomas, K., Vaudin, M., Vaughan, K., Waterston, R., Watson, A., Weinstock, L., Wilkinson-Sproat, J., and Wohldman, P. (1994). 2.2 Mb of contiguous nucleotide sequence from chromosome III of *C. elegans*. *Nature* *368*, 32-38.
- Xia, H., Winokur, S. T., Kuo, W.-L., Altherr, M. R., and Bredt, D. S. (1997). Actinin-associated LIM Protein: Identification of a Domain Interaction between PDZ and Spectrin-like Repeat Motifs. *J. Cell Biol.* *139*, 507-515.
- Yonemura, S., Hirao, M., Doi, Y., Takahashi, N., Kondo, T., Tsukita, S., and Tsukita, S. (1998). Ezrin/Radixin/Moesin (ERM) proteins bind to a positively charged amino acid cluster in the juxta-membrane cytoplasmic domain of CD44, CD43, and ICAM-2. *J. Cell Biol.* *140*, 885-896.

Chapter 7

The mouse orthologue of the *Drosophila* tumor suppressor and Rho-kinase homologue Warts interacts with protein tyrosine phosphatase PTP-BL

Edwin Cuppen, Bé Wieringa, and Wiljan Hendriks.

The mouse orthologue of the *Drosophila* tumor suppressor and Rho-kinase homologue Warts interacts with protein tyrosine phosphatase PTP-BL

Edwin Cuppen, Bé Wieringa, and Wiljan Hendriks.

Department of Cell Biology, Institute of Cellular Signaling, University of Nijmegen, P.O. Box 9101, 6500 HB Nijmegen, The Netherlands.

Abstract

PTP-BL is a large intracellular protein tyrosine phosphatase that functions as a molecular scaffold by binding other proteins via its five PDZ motifs. Here, we describe the identification and characterization of the mammalian orthologue of the *Drosophila* tumor suppressor warts, mWTS, that interacts specifically with the fourth PDZ motif in PTP-BL. The short C-terminal peptide stretch flanking the putative serine/threonine kinase domain of mWTS is sufficient for interaction, both in two-hybrid and co-immunoprecipitation experiments. Deletion of the last three residues (-VYV*) from this segment completely abolishes any detectable interaction, clearly illustrating C-terminal peptide recognition by the fourth PDZ motif of PTP-BL. The mWTS kinase domain is highly homologous to several cAMP dependent serine/threonine kinases, including kinases that are implicated in Rho-mediated signaling. Immunodetection reveals mWTS polypeptides of 80 and 175 kDa and shows that mWTS, like PTP-BL, localizes predominantly to the apical side of epithelial cells. Based upon its subcellular localization and characteristics of other components in the PTP-BL/mWTS supramolecular complex, we propose a potential role for PTP-BL in the remodeling of the apical actin cytoskeleton.

Introduction

Many of the cellular processes that are triggered by signaling cues involve the rearrangement of the actin-based cytoskeleton. Actin cytoskeletal remodeling can be controlled by members of the Rho family of Ras-like GTPases, which includes Rho, Rac and Cdc42 (Hall, 1998). In this process also the activation of proteins with enzymatic activity, like the tyrosine and serine/threonine kinases and phosphatases play an important role. For example, Rho activity appears poised to stimulate the tyrosine phosphorylation of several proteins, including focal adhesion kinase, p130 and paxillin (Flinn and Ridley, 1996; Seckl et al., 1995) and tyrosine kinase inhibitors have been shown to block Rho-

induced stress fiber assembly in response to lysophosphatidic acid (LPA) (Nobes et al., 1995). Furthermore, a tyrosine kinase-dependent mechanism, apparently involving Rho proteins, regulates activation of phospholipase D and synthesis of the second messenger PtdIns(4,5)P₂ in HEK-293 cells (Rumenapp et al., 1998). In turn, the cellular level of polyphosphoinositides may form a control element in cytoskeletal organization (Shibasaki et al., 1997). Clearly in these processes, there is also dependence on the level of phosphorylation of proteins that regulate the intrinsic activity of members of the Rho family of small GTPases. Vav, a Rho-GDP/GTP exchange factor (GEF) is tyrosine phosphorylated after TCR stimulation (Turner et al., 1997) and binding of Ras-GTPase-activating protein (GAP) p190 to RhoGAP p160 was found to depend on (tyrosine) phosphorylation of the latter (Bryant et al., 1995). Quite recently, a novel Rho-GAP, PARG1, was found to interact with a cytosolic protein tyrosine phosphatase, PTP-L1 (Saras et al., 1997), providing a potential direct link between tyrosine dephosphorylation, cytoskeletal dynamics and the Rho-signaling web.

We have been studying PTP-BL (Hendriks et al., 1995) (also known as RIP; Chida et al., 1995), the mouse orthologue of human PTP-L1 (also known as PTP-BAS, PTP-1E and FAP-1; Banville et al., 1994; Maekawa et al., 1994; Saras et al., 1994; Sato et al., 1995). This large submembranous protein of about 270 kDa (see Fig. 1) is predominantly expressed in epithelia (Cuppen et al., 1998; Hendriks et al., 1995) and contains a putative N-terminal leucine zipper motif (Saras et al., 1994) followed by a region with homology to the cytoskeleton-membrane linkers band 4.1, ezrin, radixin and moesin, recently named FERM domain (Chishti et al., 1998). This domain directs PTP-BL to the apical side of polarized cells, where it localizes at a typical fixed distance from the cell membrane (Cuppen et al., submitted). Between the FERM domain and the C-terminal protein tyrosine phosphatase (PTP) domain, five PDZ motifs are present. PDZ motifs are small protein modules that mediate protein-protein interactions (Fanning and Anderson, 1996; Ranganathan and Ross, 1997; Saras and Heldin, 1996) and can associate with transmembrane proteins (Sheng, 1996), cytoskeletal components (Xia et al., 1997) and signal transduction enzymes (Ranganathan and Ross, 1997). Several binding partners for the PDZ motifs in PTP-BL have already been identified and these suggest a potential role for the resulting multi-protein complex in regulating the actin-based cytoskeleton. Among the interactors are the Rho-GAP PARG1, which associates with the fourth PDZ motif in the human orthologue of PTP-BL (Saras et al., 1997), and the LIM domain proteins ZRP-1 (Cuppen et al., submitted) and RIL (Cuppen et al., 1998), which bind most strongly to the second and fourth PDZ domain. Both RIL and ZRP-1 colocalize with F-actin and thus may cluster with the structural and signaling components of the cytoskeleton, potentially in a similar way as their closest homologues ALP-1 (Xia et al., 1997) and zyxin (Crawford et al., 1992).

Here, we describe the characterization of the mouse orthologue of the *Drosophila* tumor

suppressor warts (WTS), a protein that emerged from two hybrid screening and specifically binds to the fourth PDZ motif in PTP-BL. Interestingly, mutations in *Drosophila* WTS cause apical hypertrophy of imaginal disc epithelial cells (Justice et al., 1995). Like dWTS mouse WTS is highly homologous to several cAMP dependent serine/threonine kinases, including kinases that are implicated in Rho-mediated signaling, and it localizes predominantly to the apical side of epithelial cells.

Results

Identification of proteins interacting with PTP-BL PDZ motifs

Candidate proteins interacting with the five PDZ motifs of PTP-BL were obtained from a human G0-fibroblast and a HeLa cDNA library, using BL-PDZ-I-V (Fig. 1A) as a bait in the yeast two-hybrid interaction trap (Gyuris et al., 1993). Sequence analysis showed that three clones, HG3 and HG5 from the HeLa library and HG21 from the fibroblast library, are independent but overlapping clones encoding short C-terminal peptides of 84, 32 and 71 amino acids, respectively (Fig. 1B). The interaction strength, as determined by blue coloring on X-gal assay plates, decreased with decreasing length of the encoded peptide. Comparison of the cDNA inserts and the encoded peptides with entries of nucleotide and protein databases initially revealed no clear homology to known proteins, indicating that HG3/5/21 cDNAs encode a novel protein.

The obtained clones are homologous to Drosophila WTS.

Next, by screening of expressed sequence tag (EST) databases, the HG3/5/21 inserts were found to be almost identical to a human EST (accession number: R75698) that was previously named DRES7 for *Drosophila*-Related Expressed Sequence-7 (Banfi et al., 1996). DRES sequences are defined as human EST sequences that are homologous to known *Drosophila* sequences implicated in mutant phenotypes. Interestingly, DRES7 shares homology with the *Drosophila* tumor suppressor warts (WTS). Comparison of the DRES7 cDNA sequence with the HG3/5/21 inserts revealed several point mutations and nucleotide deletions, probably representing sequence errors in the DRES7 cDNA sequence. Using the individually determined HG3/5/21 sequences, and the DRES7 sequence information from the database, we could, however, generate an open reading frame encoding a peptide (hWTS) of 187 amino acids (Fig. 2) which, as anticipated, is indeed highly homologous (56%) to the C-terminus of *Drosophila* WTS (dWTS). Clearly, DRES7 does not represent a full-length cDNA clone and therefore we used the 5'-end of the DRES7 cDNA sequence to search for EST's encoding N-proximal sequences. We identified one overlapping mouse EST (W81967) and sequenced this cDNA completely. The insert was found to be highly homologous to the human cDNA sequence in the coding region (79 % identical), but the 3'-UTR was much longer than for the human cDNA. The much shorter 3'-UTR for HG3/5/21 (not shown), is probably caused by alternative priming

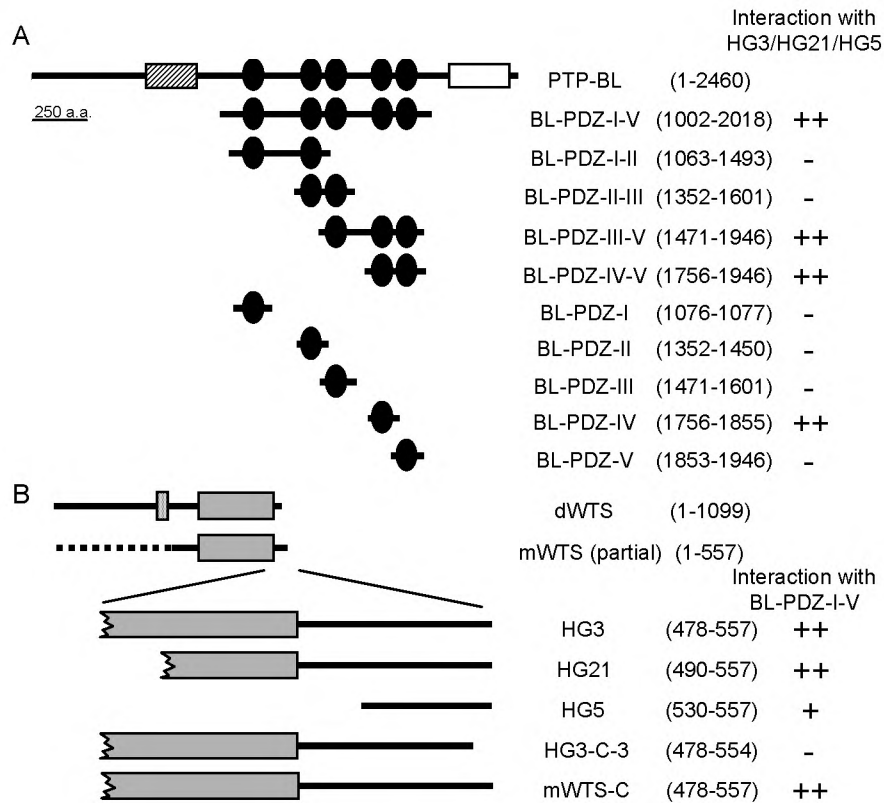


Figure 1: Schematic representation of the peptides used in the two-hybrid interaction trap. Shown are (A) the regions of PTP-BL used as baits and (B) the peptides as they were retrieved from the G0-fibroblast and HeLa cDNA library, compared with the available mouse and *Drosophila* WTS proteins. In addition, the mouse construct (mWTS-C) and the human construct lacking the last three amino acid residues (HG3-C-3) are shown. Between brackets, the corresponding first and last amino acid positions of the peptides in PTP-BL and mouse WTS (see also Fig. 2) are shown. Two hybrid interaction results with either HG3, HG21 or HG5 (A) or BL-PDZ-I-V (B) are schematically indicated: ++, very strong interaction; +, strong interaction; -, no interaction detectable. FERM domain, hatched box; catalytic PTP domain, open box; PDZ motifs, black ovals; serine/threonine kinase domain, gray box; poly-glutamine stretch, stippled box.

of reverse transcriptase during cDNA synthesis at an A-rich stretch in the human mRNA. Indeed, sequences homologous to the mouse 3'-UTR are present in the human EST library and these entries contain an A-rich stretch at the site corresponding to the 3'-end of the HG3/5/21 clones. Next, the 5'-end of the EST W81967 insert was used to screen a mouse brain cDNA-phage library. Two positive phages were isolated, mWTS#2 and mWTS#4, that extended the open reading frame as deduced from W81967 with 157 and 295 N-terminal amino acid residues, respectively. mWTS#4 contains the longest insert of about

3.3 kbp and an open reading frame of about 1.7 kbp. Northern blot analysis reveals a transcript of about 6.5 kb (Fig. 5), indicating that the obtained clones still are not full-length. Except for the stretch of the first 50 amino acids, the deduced peptide (mWTS) of 557 amino acids, is highly homologous to the C-terminal part of *Drosophila* WTS (72%) and spans the entire putative cAMP-dependent serine/threonine kinase domain (Fig. 2).

mWTS is the closest mammalian homologue of the *Drosophila* tumor suppressor warts

Comparison of the mWTS peptide with entries of protein databases revealed high homology with other members of the family of cAMP-dependent serine/threonine kinases (Fig. 3A). Alignment across the kinase domains of these proteins (Fig. 3B) shows that the mouse WTS kinase domain is 70% identical to the *Drosophila* WTS kinase domain and 49% to that in an uncharacterized *C.elegans* protein, T20F10.1, resulting from the *C.elegans* genome project (Wilson et al., 1994). In absence of sequence information for the entire kinase domain in the human WTS the most homologous human kinase domain present in currently existing databases is that found in the nuclear kinase Ndr. This protein, however, lacks the large N-terminal segment present in *Drosophila* WTS. The yeast protein ORB6, that is essential for maintenance of cell polarity and is involved in mitotic control, also lacks this region. Other homologues (all about 34 % identical in the kinase domain) include effectors of the small GTP-binding protein family Rho, like CDC42-binding kinase, ROCK-1, ROCK-2 and the myotonic dystrophy protein kinase (DMPK). These latter proteins are all characterized by an N-terminal kinase domain and a large C-terminal segment that can form coiled-coil structures. Furthermore, the kinase domains in these proteins all lack the large insertion between subdomains VII and VIII. Therefore, based on the structural similarities between mWTS and dWTS, i.e. the presence of structurally similar kinase domains flanked by very short C-terminal sequences, we suggest that the novel protein segment described here stems from the mouse orthologue of the *Drosophila* tumor suppressor warts.

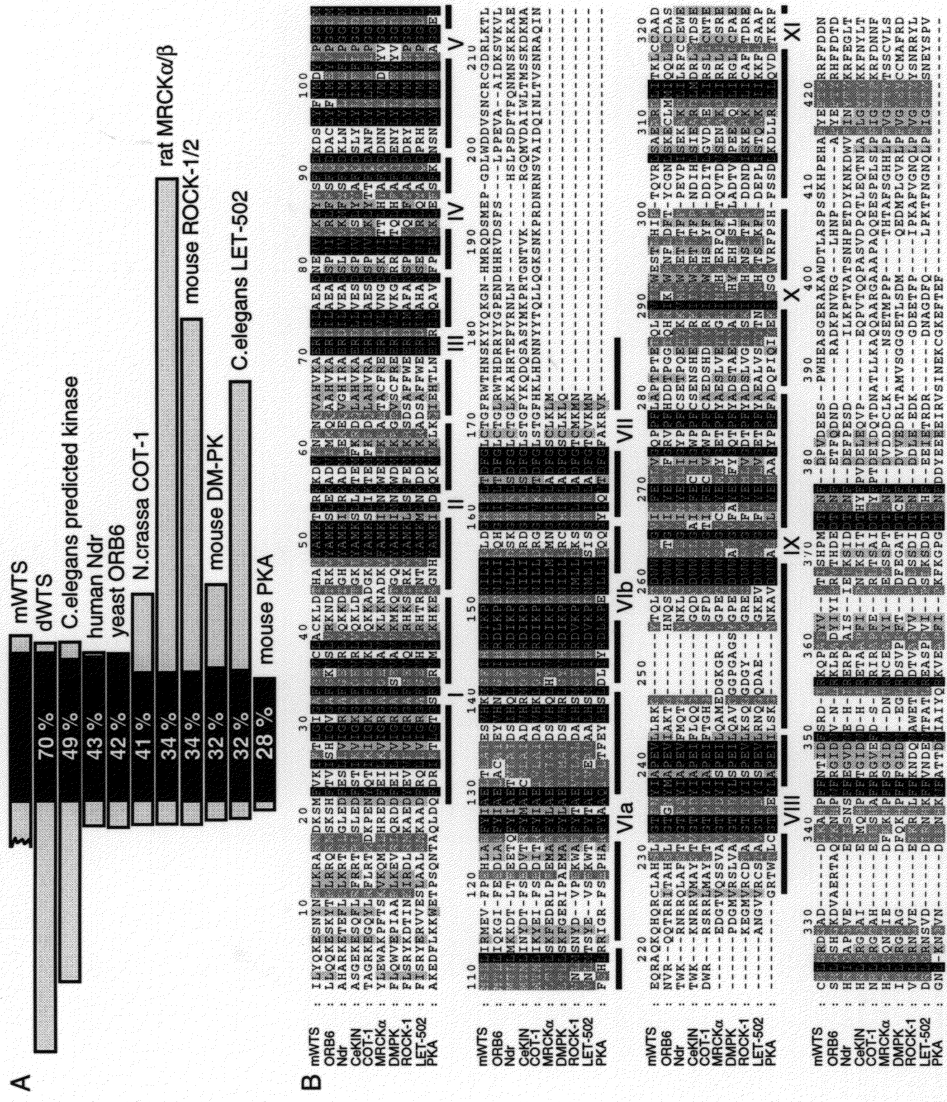
Figure 2: (facing page) Sequence alignment of the available mouse and human WTS protein sequences with the corresponding peptide segment in *Drosophila*.

The partial protein sequences of mouse and human WTS were aligned with *Drosophila* WTS (acc.no. A56155) using MULTALIGN. Black arrowheads indicate the start positions of clones HG3, HG21 and HG5, respectively, that were originally identified in the two-hybrid interaction screening with the BL-PDZ-I-V bait. The open arrowhead indicates the start of the EGFP-hWTS-C protein used for the coprecipitation assay (Fig. 4). Horizontal arrows mark the beginning and end of the kinase domain and a vertical arrow indicates the start of EST W81967. Amino acids conserved in all three species are shown white on a black background, whereas residues conserved in two species are indicated on a gray background. Gaps are indicated by dashes (-).

```

DWTS: 10 20 30 40 50 60 70 80 90 100
mWTS: SNLAPPPPAKYNNNSNTANSSGSGSGSTPTASSSTSCTKTKHAKSTSTPEKIKIKSKEEEEKERERKESESTRTRQSPSPQENENFEHEHTETENTNTATATISISYRYRRTRTYFYF
hwts: -EQYVDLDSLCTSVQQLRGSTEQDRSDKSHKAKAKDKKAGHDHDKKQQIIOOTTSSSSVVLVLVENEN------SRDRDERERKSKS------LSLSSPSPYKYKEREREHEHOHOHENENNTNTATATISISYRYRRTRTYFYF
-----
DWTS: 110 120 130 140 150 160 170 180 190 200
mWTS: QQLIIKEMEMHTHTVTVTPDPDOTOTIRIRRRRRKNKNESESNTNTIRIRKAKAMDMDSMSMPKPKIRIRPPQQSSSSFGFGETETVSVSKTKTDSDSMTMTSNSNHAHALVLVAKAKRTRTLALAEE
hwts: ELELLOLOEMEMMAMAILILCACAEEEEEMEMRRRRTITIYQYQESESNTNTIRIRKAKAMDMDSMSMPKPKIRIRPPQQSSSSFGFGETETVSVSKTKTDSDSMTMTSNSNHAHALVLVAKAKRTRTLALAEE
-----
DWTS: 210 220 230 240 250 260 270 280 290 300
mWTS: AADNDNWWVIVIYYSPSPQQKNKNVFVFYYNDNDYYIRIRGDGDMSMSLLLLIGIGTETEEEEEELELAFAFYYAEAEVCVCVDVDSKSKKEKEIRIRHRHRDPDPNINILRLRGHGHIKIKLDLDFGFGQQRGRGPTPTHSHS
hwts: LLNENEWWVIVIYYSPSPQQKNKNVFVFYYNDNDYYIRIRGDGDMSMSLLLLIGIGTETEEEEEELELAFAFYYAEAEVCVCVDVDSKSKKEKEIRIRHRHRDPDPNINILRLRGHGHIKIKLDLDFGFGQQRGRGPTPTHSHS
-----
DWTS: 310 320 330 340 350 360 370 380 390 400
mWTS: YYYENGSGSQQDSDSERER------EEYYENEN------PPPPTVVLRLRRMRMADADPRPRYYLALAHSHSVGVGHPHPNYNYLALAREREVEVERSRSYYIQIQCDCDYSYSVGVGVIVIEMEMLVLVQQPPPPLALANNSSPEPELL
hwts: YYYENGSGSQQDSDSERER------EEYYENEN------PPPPTVVLRLRRMRMADADPRPRYYLALAHSHSVGVGHPHPNYNYLALAREREVEVERSRSYYIQIQCDCDYSYSVGVGVIVIEMEMLVLVQQPPPPLALANNSSPEPELL
-----
DWTS: 410 420 430 440 450 460 470 480 490 500
mWTS: QQKYANANWEWEKKEHEHHTHTEPEPAEAESRSRETETDLDLIRIRQAQASASADDKKLGLGSS------VVEERSHSHDDEERKGKGLDLDFAFADRDRKKAPAPYYPEPEKKIPIPDSDSNNFDFDVDVDEEKLKL------RRSSNDNDSS------
hwts: QQKYANANWEWEKKEHEHHTHTEPEPAEAESRSRETETDLDLIRIRQAQASASADDKKLGLGSS------VVEERSHSHDDEERKGKGLDLDFAFADRDRKKAPAPYYPEPEKKIPIPDSDSNNFDFDVDVDEEKLKL------RRSSNDNDSS------
-----
DWTS: 510 520 530 540 550 560
mWTS: GGDDYY------DDOODRDRTFTFQQFEFEFTFTFRFRFDFDKKQQPP------EEPPERARAPGPGDADAEGEGAAAAGGGGQQPPYYVV------
hwts: DDLFLFTSTSNNKKEPEPEHEHFFYETFRFRFDFDGGGGPPFRFRKSKSGGAEASOSO------LLSSSS------LLSSSS------VVQQLELEGGGGPPYYVV
-----
DWTS: 1099
mWTS: 557
hwts: 187

```



Characterization of the interaction between PTP-BL and WTS

We used deletion mutants of the segment encompassing the five PDZ motifs of PTP-BL in the yeast two-hybrid interaction trap to identify the region mediating the interaction with WTS (Fig. 1A). All constructs containing the coding segment for the fourth PDZ motif resulted in a strong interaction with the proteins encoded by the three clones that were identified initially (Fig. 1A). In line with this, constructs lacking PDZ-IV-encoding sequences remained negative. These results clearly show that PDZ-IV is both necessary and sufficient for interaction. Since it is now well established that PDZ motifs can recognize short C-terminal peptide segments (Fanning and Anderson, 1996; Saras and Heldin, 1996; Songyang et al., 1997), we tested the importance of the C-terminus of WTS for the interaction with the PTP-BL PDZ motif. Indeed, deletion of the last three amino acids from the longest hWTS peptide (HG3-C-3) resulted in a complete loss of interaction with BL-PDZ-I-V (Fig. 1B) or BL-PDZ-IV alone (not shown). Although the last four amino acids (-PVYV*) are conserved between human and mouse, the preceding 20 amino acids are much less conserved (Fig. 2). Therefore, we also tested the observed interaction for peptides of murine origin only. As shown in Fig. 1, the mouse peptide stretch that corresponds to the HG3 peptide, mWTS-C, interacts strongly with BL-PDZ-I-V.

WTS C-terminus co-precipitates with PTP-BL PDZ motifs

To confirm the observed interaction in a more physiological surrounding, we co-transfected mammalian epithelial cells (COS-1) with expression constructs encoding EGFP fused to the last C-terminal 49 amino acids of hWTS and a VSV-G epitope-tagged version of the PTP-BL segment encompassing the five PDZ motifs. As a control, wild-type EGFP was co-transfected. By Western blotting we could readily detect all transiently expressed proteins

Figure 3: (facing page) Sequence comparison of mouse WTS and homologous proteins. The predicted amino acid sequences of mouse WTS, mWTS, the *Drosophila* tumor suppressor WTS, dWTS (A56155), a predicted kinase from *C.elegans*, CeKIN (T20F10.1, Z81594), human nuclear kinase Ndr (I38133), yeast ORB6 (O13310), *N. crassa* COT-1 (P38679), rat myotonic dystrophy kinase-related Cdc42-binding kinase, MRCK α (AF021935), mouse Rho-associated coiled-coil containing protein kinase p160, ROCK-1 (U58512), mouse myotonic dystrophy protein kinase, DMPK (P54265), *C. elegans* LET-502 (U85515) and the C- α subunit of mouse cAMP-dependent protein kinase, PKA (P05132) were compared using the MULTALIN program (Corpet, 1988). (A) The position of the putative catalytic domain is shown in black, and the percent amino acid identity of this region with the predicted mouse WTS protein is shown in white. (B) Multiple sequence alignment of the catalytic domains and the immediate flanking sequences of the proteins shown in (A). mWTS, a.a. 119-522; CeKIN, a.a. 481-871; Ndr, a.a. 68-452; ORB6, a.a. 72-464; COT-1, a.a. 215-619; MRCK α , a.a. 56-411; DMPK, a.a. 50-412; ROCK-1, a.a. 55-406; LET-502, a.a. 47-399; PKA, a.a. 23-351. The 11 subdomains that are highly conserved in the protein kinase family (Hanks et al., 1988) are underlined and designated by Roman numerals. Darkness of shading indicates the conservation of residues (black, 100% similar, dark grey, at least 80% similar, light grey, at least 60% similar). Gaps are represented by dashes.

in the supernatant of the lysates (Fig. 4). Both wild-type EGFP and the hWTS-C fusion protein are efficiently immunoprecipitated using the α -GFP polyclonal antibody. The VSV-tagged PDZ motifs are coprecipitated very efficiently with EGFP-hWTS-C, but not at all with wild-type EGFP as a control (Fig. 4). Co-immunoprecipitation experiments from cells in which single PTP-BL PDZ motifs were coexpressed with the WTS C-terminus confirmed that only the fourth PTP-BL PDZ motif is binding to hWTS (not shown). These findings independently confirm the results obtained in the yeast two-hybrid interaction trap.

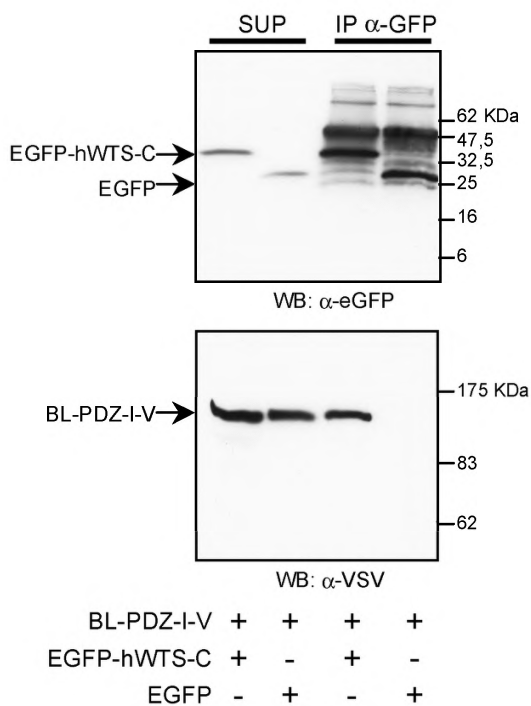


Figure 4: Coprecipitation of hWTS C-terminus with PTP-BL PDZ motifs.

VSV epitope-tagged PDZ motifs of PTP-BL (BL-PDZ-I-V) were transiently coexpressed in COS-1 cells with EGFP-tagged hWTS C-terminus (EGFP-hWTS-C) or as a control, wild-type EGFP. The presence of the EGFP- (upper panel) and VSV-tagged (lower panel) proteins in the supernatant of the lysate (sup, left two lanes) and in α -GFP immunoprecipitates (right two lanes) was detected by Western blot analysis of protein samples following size-separation on 15% (upper panel) and 8% (lower panel) SDS-PAGE gels. Coprecipitated PDZ motifs were detected only for EGFP-hWTS-C, whereas the EGFP control remains negative.

mWTS RNA and protein expression

The interaction of WTS with PTP-BL can only be of biological significance when there is overlap in expression patterns. Previous studies have shown an epithelial expression pattern for PTP-BL (Cuppen et al., 1998; Hendriks et al., 1995). To determine the tissue distribution of mouse WTS mRNA a Northern blot of total RNA from several different mouse tissues was probed with the partial mWTS cDNA. A transcript of about 6.5 kb was present in all tissues examined (Fig. 5). High mWTS mRNA levels are observed in lung, kidney, brain and stomach. In the latter organ also a smaller transcript of about 4 kb is detected (Fig. 5).

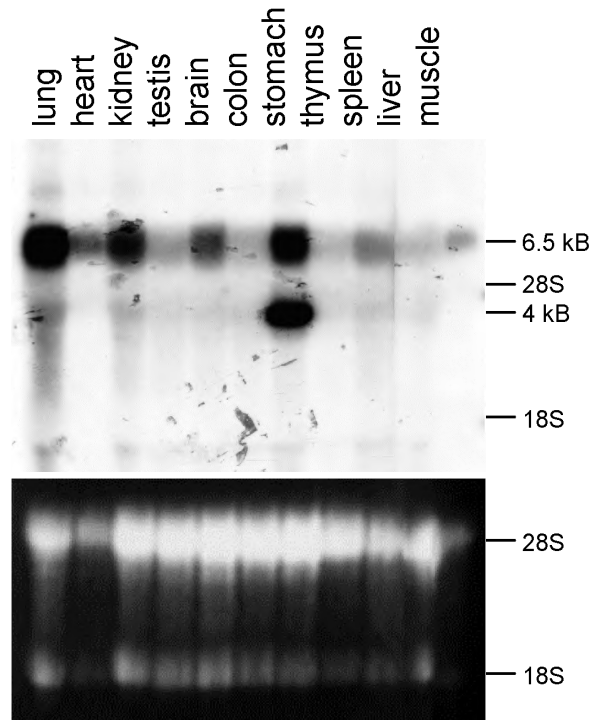


Figure 5: Tissue distribution of mWTS messenger RNA. Northern blot analysis of the mWTS expression levels in total RNA isolated from different adult mouse tissues (top panel). As a control for RNA loading, the ethidium bromide staining pattern of the gel is shown (bottom panel). mWTS is expressed in all tissues examined, with high levels in lung, kidney, brain, and stomach. The 28S and 18S ribosomal bands, corresponding to 4.6 and 1.9 kb transcript lengths, respectively, are indicated.

To study WTS protein expression and localization, a polyclonal antibody was raised against a GST-fusion protein containing the last 84 amino acids of human WTS (78% homologous to mouse WTS in this region). Resulting serum (α -WTS) was tested on lysates of COS-1 cells expressing an EGFP fusion protein harboring the last 49 amino acids of human WTS (EGFP-hWTS-C), or wild-type EGFP as a control. The α -WTS antibody specifically recognizes the EGFP-hWTS-C fusion protein, whereas no protein was detected in lysates from EGFP transfected cells or by the pre-immune serum (Fig. 6A). Next, the α -WTS antibody was used to detect endogenous protein in total lysates of several mouse tissues. No specific labeling of proteins was observed when the pre-immune serum was used (not shown). The α -WTS antibody recognizes proteins of 175 and 80 kDa (Fig. 6B). In brain and testis only the 175 kDa band is labeled, and a shorter exposure reveals the band to be a doublet, with highest intensity for the lower band. In thymus, spleen, lung and ovarium

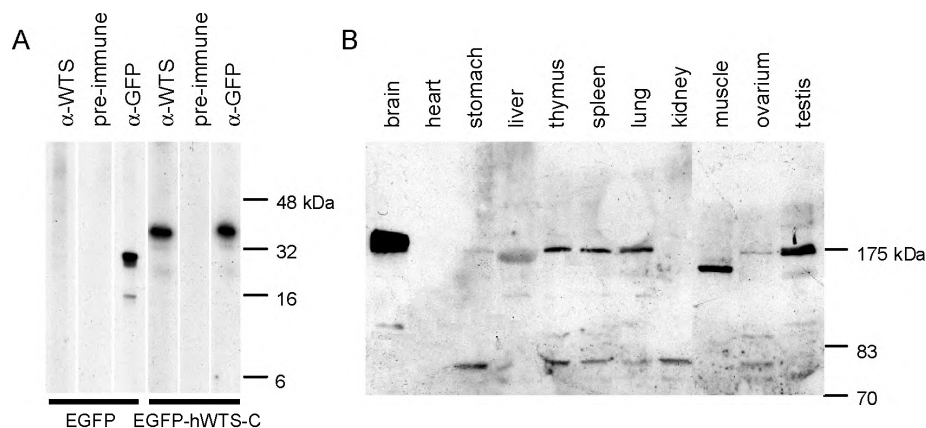


Figure 6: Tissue distribution of mWTS protein.

The polyclonal antiserum raised against a GST-fusion protein of the hWTS C-terminus was tested on lysates of COS-1 cells transiently expressing EGFP (A, left three lanes) or EGFP-hWTS-C (A, right three lanes). No protein was recognized using the pre-immune serum, whereas the α -WTS antiserum specifically recognizes the EGFP-hWTS peptide. As a control for protein expression, EGFP (fusion-)protein was detected using a polyclonal α -GFP antiserum. The α -WTS serum was used to detect endogenous WTS protein in total lysates of several mouse tissues (B). 80 and 175 kDa proteins are specifically recognized in several tissues, whereas in skeletal muscle a 160 kDa protein is detected.

both the 80 and the 175 kDa protein are expressed, whereas in stomach and kidney the 80 kDa protein is most prominent. In muscle, a single protein of about 160 kDa is detected.

mWTS in situ localization

The α -WTS antiserum was used to test the tissue distribution of WTS in mouse. In general, high expression is observed apically in simple epithelium, although also other cell types are found positive. High levels of WTS were found in colon epithelium (Fig. 7A) and in the epithelium covering the bronchii in lung (Fig. 7B). Most protein is localized apically, but also some basolateral staining is evident. In kidney, high expression is found in the the collecting tubules and the epithelium covering the renal pelvis (Fig. 7C). Expression of WTS in the non-glandular part of the stomach is very low, whereas high expression is found in the glandular epithelium. Here, the signal is most prominent at the apical side of the cells (Fig. 7D). In skeletal muscle, WTS localizes to submembranously along the fibers (Fig. 7E), and higher magnification also reveals a striated staining within the fibers (Fig. 7F). Furthermore, in heart a highly restricted localization of mWTS is observed at intercalated discs (not shown). In skin, only low expression is observed in stratified epithelium, but high expression is seen in glandular epithelium, i.e. sweat glands (Fig. 7G). In brain and testis, WTS is expressed ubiquitously (not shown). To monitor antiserum specificity, parallel sections were incubated with pre-immune serum, but no significant labeling was observed (not shown).

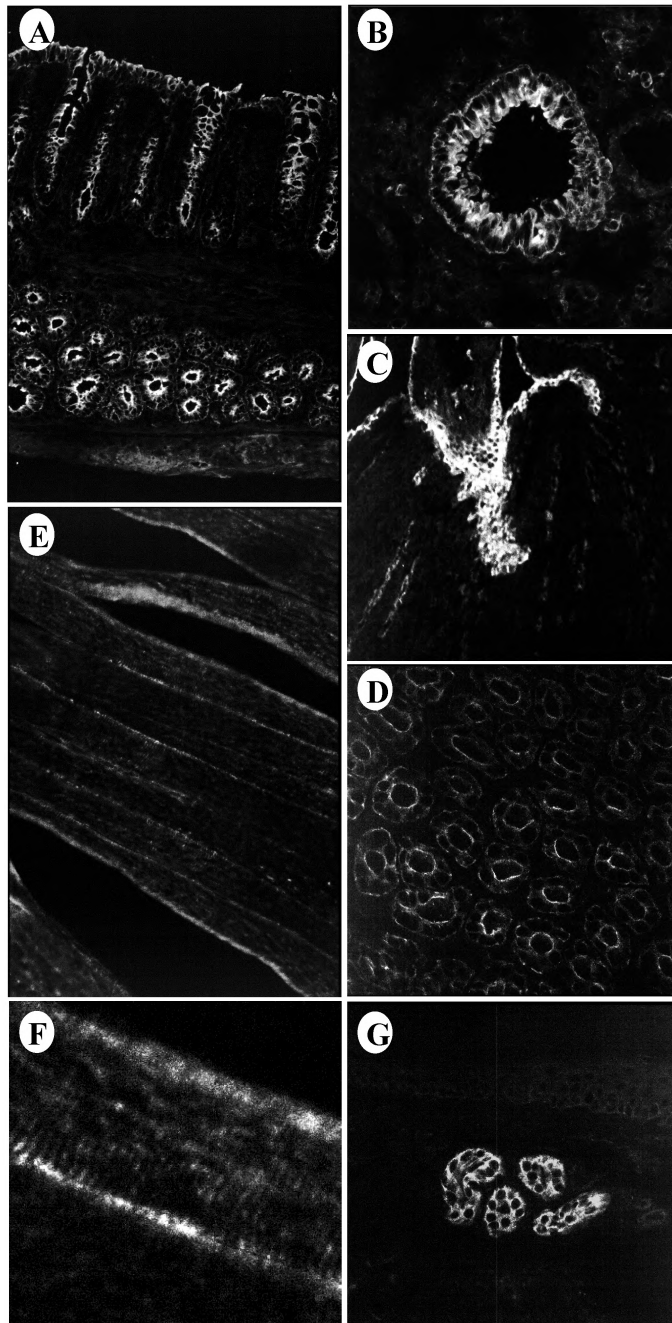


Figure 7: In situ protein expression of mouse WTS. The mWTS protein was visualized in cryosections of mouse colon (A), lung (B), kidney (C), stomach (D), skeletal muscle (E and F) and skin (footpad) (G) using immunofluorescence labeling with α -WTS polyclonal antiserum. mWTS is predominantly expressed in cells of epithelial origin, where it localizes apically. Furthermore, in skeletal muscle a submembranous staining is evident (E) and higher magnification (F) shows a striated staining pattern.

Discussion

In our search for proteins that interact with the PDZ motifs in PTP-BL, we identified three independent clones encoding the mammalian orthologue of the *Drosophila* tumor suppressor warts (also termed lats for large tumor suppressor; Xu et al., 1995), a serine/threonine kinase family member. Deletion studies show that the fourth PDZ motif in PTP-BL is necessary and sufficient for this strong interaction. The shortest WTS clone that was identified by two-hybrid screening encodes the last 32 amino acids C-terminal to the kinase domain. Ablation of the last three amino acids (-V-Y-V-*) completely abolished any detectable interaction. These results point to a classical PDZ-mediated interaction, involving a single PDZ motif and a C-terminal peptide sequence in the partner protein (Fanning and Anderson, 1998; Saras and Heldin, 1996). Indeed, screening of oriented peptide libraries had shown that short C-terminal peptides that together yield the consensus (I/Y/V)-**Y**-(**Y**-K)-(V/K/I)-* (residues in bold are preferred) are recognized by the fourth PDZ motif of the human orthologue of PTP-BL (referred to as PTPbas-5 in the paper by Songyang et al., 1997). Furthermore, two other binding targets have been described for this PDZ motif. First, the 150 kDa GTPase-activating protein for Rho, PARG1, was identified in pull-down experiments from cell lysates using PTP-BAS PDZ motifs as baits (Saras et al., 1997). A GST-PDZ-IV fusion protein was found to bind specifically to an immobilized peptide corresponding to the C-terminal four residues (-P-Q-F-V-*) of this protein. Secondly, the LIM domain-containing protein RIL can interact with both PDZ-II and PDZ-IV of PTP-BL (Cuppen et al., 1998). Deletion of the last four amino acids of RIL (-V-E-L-V-*) completely abolishes the interaction with PDZ-IV but has no influence on the interaction with PDZ-II. The merging of all C-termini that are now known to bind to PDZ-IV in PTP-BL, including the WTS C-terminus (-P-V-Y-V-*) described here, does not yield a clear consensus peptide sequence: -[P, V, I, Y]-[Q, V, E, Y]-[F, Y, L]-V-*. Only the valine at the -1 position is consistently present. Nevertheless, this motif produces no additional hits when used to scan the complete SwissProt and translated EMBL databases for potential binding proteins. Thus, although this target appears rather vague, one may expect the PTP-BL PDZ-IV motif to bind specifically and selectively to only a very small number of proteins in the proteome, including mWTS.

Intriguingly, although the C-terminal segment flanking the kinase domain is not overall evenly conserved between human, mouse and *Drosophila*, the last four amino acids are completely identical. This suggests that the PDZ-mediated interaction, which we show here for the mouse and human WTS peptide, might be functionally well preserved during evolution. This may also hold for behaviour which determines WTS's subcellular localization. Absence of WTS results in hyperproliferation as well as apical hypertrophy of imaginal disc epithelial cells and, therefore, *Drosophila* WTS was expected to localize at apical or apical-lateral epithelial cell margins (Watson, 1995). Indeed, we here show that mouse WTS is localized predominantly at the apical side of epithelial cells. This highly

specific localization may be mediated via the interaction with PTP-BL, which is targeted apically in epithelial cells by virtue of its FERM domain (Cuppen et al., submitted). Unfortunately, so far no *Drosophila* protein tyrosine phosphatase that resembles PTP-BL has been reported. It is of note, however, that PTP-BL shares homology with two other, non-PTP, *Drosophila* tumor suppressor gene products; Expanded and Discs-large (Boedigheimer et al., 1993; Hendriks et al., 1995; Woods and Bryant, 1991). Domains in these proteins may fulfill an accessory role in the assembly of submembranous supramolecular structures necessary for epithelial growth and homeostasis. Next to epithelial expression, there is also clear expression of mWTS in skeletal muscle, where PTP-BL is absent (Fig. 7). Strikingly, the mWTS protein in muscle has a molecular weight of about 160 kDa, slightly smaller than in other tissues. Also here it has a restricted localization, resulting in a both a submembranous and striated pattern. These observations suggest a specialized function for mWTS, like in epithelia. In brain and testes a single peptide of 175 kDa is recognized, whereas in lysates of stomach, thymus, spleen, lung and ovarium two peptides, of 80 and 175 kDa, are recognized by our antiserum. Although Northern blot analysis reveals a second, shorter transcript, this messenger is only expressed in stomach, and therefore makes alternative splicing unlikely as an explanation for the two protein products. Evidently, we cannot exclude that our antibody cross-reacts with other (homologous) proteins. To add further to the complexity of the situation, we would like to note that in testis and brain the 175 kDa band appears as a doublet, suggesting that mWTS may be subjected to post-translational modification.

What could be the biological role for WTS-PTP-BL interaction and WTS activity? Based on the high homology between the partial mouse WTS peptide, *Drosophila* WTS and other known kinases some speculative predictions can be made. Presence of the large insert between the conserved subdomains VII and VIII, as well as the C-terminal location of the kinase domain classify WTS, Ndr, COT-1, ORB6 and the putative *C. elegans* kinase as novel subgroup in the subfamily of serine/threonine kinases. Interestingly, when we omit Ndr-like proteins, which are a nuclear group of proteins (Millward et al., 1995), there is a great deal of convergence in the properties of these proteins. The COT-1 (colonial temperature sensitive-1) protein of *Neurospora* was identified by study of a temperature-sensitive mutant that causes compact colonial growth. Strains lacking COT-1 have a defect in hyphal tip elongation and a concomitant increase in hyphal branching (Yarden et al., 1992). The yeast ORB6 protein kinase functions in the control of cell morphology, maintaining a polarized actin cytoskeleton and promoting polarized growth, while delaying the onset of mitosis (Verde et al., 1998). Interestingly, *orb6* interacts genetically with *orb2*, which encodes the Pak1/Shk1 protein kinase, a component of the Ras1 and Cdc42-dependent signaling pathway. More distant homologues of WTS include Rho-associated coiled-coil-containing protein kinase-1 and 2 (ROCK-1/2; Leung et al., 1995; Matsui et al., 1996; Nakagawa et al., 1996), the Myotonic Dystrophy Protein kinase (Groenen and

Wieringa, 1998; Mahadevan et al., 1992), the Myotonic Dystrophy kinase-related CDC42-binding kinase (MRCK α/β ; Leung et al., 1998) and *C.elegans* LET-502 (Wissmann et al., 1997). ROCK-1/2 and MRCK α/β are effectors of small GTPases and are, like LET-502, among others implicated in phosphorylation of the myosin-binding subunit of myosin light chain (MLC) phosphatase, and MLC itself. Rho kinase may also regulate the cytoskeleton by phosphorylating the ezrin/radixin/moesin proteins (Matsui et al., 1998; Shaw et al., 1998).

Based on these similarities we would like to propose that mWTS acts in a Rho-mediated regulation of actin cytoskeleton remodeling. PTP-BL may act in this web as an apical submembranous scaffold protein, tethering both actin binding proteins, like ZRP-1 and RIL, and proteins, that are actively involved in actin-cytoskeleton modification, like PARG1 and mWTS. It is not known how exactly PTP-BL action on reversible tyrosine phosphorylation is merged here with the wide repertoire of Rho-mediated signaling. However, if the capture of the Rho inactivator (PARG1) and the (potential) Rho effector (mWTS) by the fourth PDZ domain in PTP-BL would be of some competitive nature, this opens an intriguing possibility for agonistic and antagonistic regulation of Rho-dependent signaling.

Materials and methods

Two-Hybrid Interaction Trap - Plasmid DNAs, the yeast strain EGY48 and the human fetal brain cDNA library used for the interaction-trap assay were kindly provided by Dr. Roger Brent and colleagues (Massachusetts General Hospital, Boston, MA) and used as described (Gyuris et al., 1993). The HeLa and the human G0 fibroblast libraries were generously provided by J. Gyuris (Massachusetts General Hospital, Boston, MA) and C. Sardet (MIT, Boston, MA). The construction of most of the PTP-BL PDZ baits has been described previously (Cuppen et al., 1998). BL-PDZ-I-II was made by subcloning a 1.3 kbp *Dra*I fragment from full-length PTP-BL in pEG202 and BL-PDZ-II-III, BL-PDZ-III-V and BL-PDZ-IV-V were generated by PCR, using synthetic oligonucleotides for introducing *Eco*RI and *Xho*I restriction sites, and cloned in-frame in the pEG202 bait vector. The prey HG3-C-3 (see below) was made by PCR, using the oligonucleotide 5'-CCCTCGAGTCAAGGCTGGCAGCCTTCAGT-3' in combination with a pJG4-5-vector specific primer, and HG3 as template. In the construct a premature stop codon and a *Xho*I restriction site were introduced. The prey construct encoding the mouse peptide corresponding to HG3 (mWTS-C) was made by PCR using the oligonucleotide 5'-GGGAATTCGTGGATGAAGAAAGCCCC-3' in combination with a T3 primer and the mouse EST clone W81967 as template, followed by subcloning of an *Eco*RI-*Xho*I restriction fragment of the resulting amplicon in the prey vector pJG4-5. All constructs made were checked for the absence of mutations by DNA sequencing. For two-hybrid interaction assays plasmids were introduced in yeast strain EGY48 (*MATa trp1 ura3 his3 LEU2::pLexAop6-LEU2*) containing the plasmid pSH18-34, which includes the reporter *lacZ* gene, and tested for an interaction as detected by growth and blue coloring on minimal agar-plates lacking histidine, tryptophan, uracil and leucine, containing 2% galactose, 1% raffinose and 80 μ g/ml X-gal, buffered at pH 7.0.

Identification of mouse WTS cDNAs - Comparison of the obtained human prey cDNA sequences with database entries was done using the BLAST program (Altschul et al., 1997). Identification of a

mouse WTS cDNA clone was done by comparison of the insert of HG3 with the EST sequences in the database of mouse specific IMAGE clones at the RZPD resource center (Berlin, Germany). One highly homologous mouse cDNA clone (W81967) from this collection was retrieved and sequenced completely. Next, the insert from this clone was isolated, labeled radioactively by random priming and used to screen a mouse brain λ -ZAPII cDNA phage library (Stratagene) following standard procedures. Out of 0.65×10^6 plaques, two were found positive for the mWTS cDNA. These phages were plaque-purified and inserts were rescued as pBluescript SK⁻ plasmids according to the manufacturer's protocols, and sequenced using specific oligonucleotides. The predicted polypeptide was compared with database entries using the BLAST program (Altschul et al., 1997). The available predicted protein sequence of mouse, human and *Drosophila* WTS and related kinase domains were aligned with Multalin (Corpet, 1988) using the blosum62 comparison table and annotated with Genedoc (shareware, version 2.2.005; Nicholas and Nicholas, 1997).

Antibodies - The complete insert of the HG3 prey (EcoRI-EcoRI-XhoI fragment) was subcloned in the prokaryotic expression vector pGEX-1N (Pharmacia), which was modified to generate a XhoI site 3' to the EcoRI site. GST-fusion protein of the C-terminal 84 amino acids was produced in *E. coli* DH5 α and isolated according to the supplier's instructions by binding to glutathione Sepharose beads (Pharmacia). The purified protein was used to immunize a rabbit. The rabbit polyclonal α -GFP (whole serum) and the mouse monoclonal α -VSV (P5D4, ascites) have been described elsewhere (Cuppen et al., submitted; Kreis, 1986).

Expression constructs - The eukaryotic expression construct for the C-terminus of hWTS (EGFP-hWTS-C) was made by subcloning an EcoRI-XhoI fragment from plasmid HG3 into the mammalian expression vector pEGFP-C2 (Clontech). Since the HG3 cDNA insert contains an internal EcoRI site, the resulting EGFP-fusion protein from this construct contains only the last 49 amino acids from human WTS (open arrowhead in Fig. 2). The expression construct encoding VSV-tagged PDZ-I-V (BL-PDZ-I-V) has been described elsewhere (Cuppen et al., 1998).

Immunoprecipitation experiments - COS-1 cells were cultured and transfected by electroporation as described previously (Cuppen et al., 1998). One day after transfection, cells were washed with cold PBS and lysed on plate with 550 μ l ice-cold RIPA buffer (50 mM Tris, pH 8.0, 100 mM NaCl, 1 mM EDTA, 1% NP-40, 0.1% SDS, 0.5% DOC, 1 mM PMSF and protease inhibitor cocktail (Boehringer)). After a 1-hour incubation on ice, the lysate was centrifuged for 10 minutes at $10,000 \times g$ at 4°C and proteins in 50 μ l of the lysate were separated for further analysis. After addition of the polyclonal antibody α -GFP (2 μ l complete serum) and overnight rotation at 4°C, 50 μ l of protein A-Sepharose CL-4B (Pharmacia) were added and incubation was prolonged overnight. The Sepharose beads with immunobound proteins were washed four times with 1 ml RIPA lysis buffer and boiled for 5 minutes in 50 μ l of sample buffer (100 mM Tris-HCl, pH 6.8, 200 mM dithiothreitol, 4% SDS, 0.2% bromophenol blue, 20% glycerol). Fifteen μ l of lysates and immunobound proteins were resolved on 15% and 8% polyacrylamide gels and transferred to nitrocellulose membranes by western blotting. Blots were blocked using 5% nonfat dry milk in 10 mM Tris-HCl (pH 8.0), 150 mM NaCl, and 0.05% Tween 20 (TBST). The polyclonal α -GFP (5.000 x diluted) was used to detect production and immunoprecipitation of the EGFP-fusion protein and the monoclonal α -VSV (10.000 x diluted ascites) was used to detect coprecipitated proteins. Incubations (1 hour) with primary and secondary antisera (10.000 x diluted peroxidase-conjugated goat anti-mouse or goat anti-rabbit IgG (Pierce)) and subsequent washes were done in TBST at room temperature. Labeled bands were visualized using freshly prepared chemiluminescent substrate (100 mM Tris-HCl, pH 8.5, 1.25 mM p-coumaric acid (Sigma), 0.2 mM luminol (Sigma), and 0.009% H₂O₂).

Northern blotting - Total RNA from several mouse (strain C57BL/6) tissues was prepared using the guanidium isothiocyanate-phenol-chloroform extraction method (Chomczynski and Sacchi, 1987). Fifteen μ g RNA was loaded on a 1% formamide agarose gel and after electrophoresis the RNA was transferred to nylon membrane (Hybond-N, Amersham) according to standard procedures. The complete cDNA insert of EST W81967 was radioactively labeled by random priming and used as probe for hybridization as described (Cuppen et al., 1998).

Western blotting - Protein lysates from several mouse (strain C57BL/6) tissues were made by mechanical disintegration of tissue in an equal volume (0.5 to 2 ml) of lysis buffer (50 mM Tris pH 8.0, 150 mM NaCl, 1 mM EDTA, 0.1 mM PMSF and containing protease inhibitor cocktail (Boehringer)). Next, detergents were added (final concentration 1% Nonidet P-40, 0.5% Na-DOC, 0.1% SDS) and the lysates were incubated at 4°C for 1 hour, followed by centrifugation for 30 minutes at 10,000 g and 4°C. The protein concentration in the supernatants was determined according to Bradford (Bradford, 1976). Fifty µg of protein was loaded per lane on a 8% polyacrylamide gel and transferred to nitrocellulose membrane (Hybond-C+, Amersham) by Western blotting. Blots were blocked and incubated with primary (α -WTS, total serum 5,000 x diluted) and secondary antibodies (peroxidase-conjugated goat anti-rabbit IgG (Pierce), 10,000 x diluted) as described above, followed by chemiluminescent detection.

Immunofluorescence assay - 6 µm cryo-sections of unfixed mouse (strain C57BL/6) tissues were cut and mounted on Superfrost/Plus slides (Menzel Gläser, Germany). After thawing, sections were fixed for 10 minutes in 2 % paraformaldehyde in PHEM buffer (60 mM Pipes, 25 mM Hepes pH 6.9, 10 mM EGTA, 2 mM MgCl₂). Subsequently, free aldehyde groups were quenched for 10 minutes in 0.1 M glycine in PBS and tissue sections were incubated in primary antibody (α -WTS or preimmune serum, 1000 x diluted in PBS, containing 1% goat serum) for 1 hour at room temperature. After washing three times for 10 minutes in PBS, specific labeling was detected by a 1-hour incubation in FITC-conjugated AffiniPure Goat anti-rabbit IgG (10 µg/ml in PBS containing 1% goat serum; Jackson ImmunoResearch Laboratories, Inc., West Grove, PA). Finally, sections were washed three times for 10 minutes in PBS, rinsed in water and mounted in Mowiol (Sigma Chemical Co.).

References

- Altschul, S. F., Madden, T. L., Schaffer, A. A., Zhang, J., Zhang, Z., Miller, W., and Lipman, D. J. (1997). Gapped BLAST and PSI-BLAST: a new generation of protein database search programs. *Nucl. Acids Res.* *25*, 3389-3402.
- Banfi, S., Borsani, G., Rossi, E., Bernard, L., Guffanti, A., Rubboli, F., Marchitello, M., Giglio, S., Goluccia, E., Zollo, M., Zuffardi, O., and Ballabio, A. (1996). Identification and mapping of human cDNAs homologous to *Drosophila* mutant genes through EST database searching. *Nature Gen.* *13*, 167-174.
- Banville, D., Ahmad, S., Stocco, R., and Shen, S. H. (1994). A novel protein-tyrosine phosphatase with homology to both the cytoskeletal proteins of the band 4.1 family and junction-associated guanylate kinases. *J. Biol. Chem.* *269*, 22320-22327.
- Boedigheimer, M., Bryant, P., and Laughon, A. (1993). Expanded, a negative regulator of cell proliferation in *Drosophila*, shows homology to the NF2 tumor suppressor. *Mech. Dev.* *44*, 83-84.
- Bradford, M. M. (1976). A rapid and sensitive method for the quantitation of microgram quantities of protein utilizing the principle of protein-dye binding. *Anal. Biochem.* *72*, 248-254.
- Bryant, S. S., Briggs, S., Smithgall, T. E., Martin, G. A., McCormick, F., Chang, J. H., Parsons, S. J., and Jove, R. (1995). Two SH2 domains of p120 Ras GTPase-activating protein bind synergistically to tyrosine phosphorylated p190 Rho GTPase-activating protein. *J. Biol. Chem.* *270*, 17947-17952.
- Chida, D., Kume, T., Mukoyama, Y., Tabata, S., Nomura, N., Thomas, M. L., Watanabe, T., and Oishi, M. (1995). Characterization of a protein tyrosine phosphatase (RIP) expressed at a very early stage of differentiation in both mouse erythroleukemia and embryonal carcinoma cells. *FEBS Lett.* *358*, 233-239.
- Chishti, A. H., Kim, A. C., Marfatia, S. M., Lutchman, M., Hanspal, M., Jindal, H., Liu, S.-C., Low, P. S., Rouleau, G. A., Mohandas, N., Chasis, J. A., Conboy, J. G., Gascard, P., Takakuwa, Y., Huang, S.-C., Benz, E. J., Bretscher, A., Fehon, R. G., Gusella, J. F., Ramesh, V., Solomon, F., Marchesi, V. T., Tsukita, S., Tsukita, S., Arpin, M., Louvard, D., Tonks, N. K., Anderson, J. M., Fanning, A. S., Bryant, P. J., Woods, D. F., and Hoover, K. B. (1998). The FERM domain: a

- unique module involved in the linkage of cytoplasmic proteins to the membrane. *Trends Biochem. Sci.* *23*, 281-282.
- Chomczynski, P., and Sacchi, N. (1987). Single-step method of RNA isolation by acid guanidinium thiocyanate-phenol-chloroform extraction. *Anal. Biochem.* *162*, 156-159.
- Corpet, F. (1988). Multiple sequence alignment with hierarchical clustering. *Nucl. Acids Res.* *16*, 10881-10890.
- Crawford, A. W., Michelsen, J. W., and Beckerle, M. C. (1992). An interaction between zyxin and actinin. *J. Cell Biol.* *116*, 1381-1393.
- Cuppen, E., Gerrits, H., Pepers, B., Wieringa, B., and Hendriks, W. (1998). PDZ motifs in PTP-BL and RIL bind to internal protein segments in the LIM domain protein RIL. *Mol. Biol. Cell* *9*, 671-683.
- Fanning, A. S., and Anderson, J. M. (1998). PDZ domains and the formation of protein networks at the plasma membrane. *Curr. Top. Microbiol. Immunol.* *228*, 209-233.
- Fanning, A. S., and Anderson, J. M. (1996). Protein-protein interactions: PDZ domain networks. *Curr. Biol.* *6*, 1385-1388.
- Flinn, H. M., and Ridley, A. J. (1996). Rho stimulates tyrosine phosphorylation of focal adhesion kinase, p130 and paxillin. *J. Cell Sci.* *109*, 1133-1141.
- Groenen, P., and Wieringa, B. (1998). Expanding complexity in myotonic dystrophy. *Bioessay* *20*, 901-912.
- Gyuris, J., Golemis, E., Chertkov, H., and Brent, R. (1993). Cdi1, a human G1 and S phase protein phosphatase that associates with Cdk2. *Cell* *75*, 791-803.
- Hall, A. (1998). Rho GTPases and the Actin Cytoskeleton. *Science* *279*, 509-514.
- Hanks, S.K., Quinn, A.M., and Hunter, T. (1998). The protein kinase family: Conserved features and deduced phylogeny of the catalytic domains. *Science* *242*, 42-52.
- Hendriks, W., Schepens, J., Bachner, D., Rijss, J., Zeeuwen, P., Zechner, U., Hameister, H., and Wieringa, B. (1995). Molecular cloning of a mouse epithelial protein-tyrosine phosphatase with similarities to submembranous proteins. *J. Cell. Biochem.* *59*, 418-430.
- Justice, R. W., Zilian, O., Woods, D. F., Noll, M., and Bryant, P. J. (1995). The *Drosophila* tumor suppressor gene warts encodes a homolog of human myotonic dystrophy kinase and is required for the control of cell shape and proliferation. *Genes Dev.* *9*, 534-546.
- Kreis, T. E. (1986). Microinjected antibodies against the cytoplasmic domain of vesicular stomatitis virus glycoprotein block its transport to the cell surface. *EMBO J.* *5*, 931-941.
- Leung, T., Chen, X.-Q., Tan, I., Manser, E., and Lim, L. (1998). Myotonic dystrophy kinase-related CDC42-binding kinase acts as a Cdc42 effector in promoting cytoskeletal reorganization. *Mol. Cell Biol.* *18*, 130-140.
- Leung, T., Manser, E., Tan, L., and Lim, L. (1995). A novel serine/threonine kinase binding the ras-related rhoA GTPase which translocates the kinase to peripheral membranes. *J. Biol. Chem.* *270*, 29051-29054.
- Maekawa, K., Imagawa, N., Nagamatsu, M., and Harada, S. (1994). Molecular cloning of a novel protein-tyrosine phosphatase containing a membrane-binding domain and GLGF repeats. *FEBS Lett.* *337*, 200-206.
- Mahadevan, M., Tsilfidis, C., Sabourin, L., Shutler, G., Amemiya, C., Jansen, G., Neville, C., Narang, M., Barcelo, J., O'Hoy, K., Leblond, S., Earle-MacDonald, J., Jong, P. J. d., Wieringa, B., and Korneluk, R. G. (1992). Myotonic dystrophy mutation: An unstable CTG repeat in the 3' untranslated region of the gene. *Science* *255*, 1253-1255.
- Matsui, T., Amano, M., Yamamoto, T., Chihara, K., Nakafuku, M., Ito, M., Nakano, T., Okawa, K., Iwamatsu, A., and Kaibuchi, K. (1996). Rho-associated kinase, a novel serine/threonine kinase, as a putative target for the small GTP-binding protein Rho. *EMBO J.* *15*, 2208-2216.
- Matsui, T., Maeda, M., Doi, Y., Yonemura, S., Amano, M., Kaibuchi, K., Tsukita, S., and Tsukita, S. (1998). Rho-kinase phosphorylates COOH-terminal threonines of Ezrin/Radixin/Moesin (ERM) proteins and regulates their head-to-tail association. *J. Cell Biol.* *140*, 647-657.
- Millward, T., Cron, P., and Hemmings, B. A. (1995). Molecular cloning and characterization of a

- conserved nuclear serine(threonine) protein kinase. *Proc. Natl. Acad. Sci. USA* *92*, 5022-5026.
- Nakagawa, O., Fujisawa, K., Ishizaki, T., Saito, Y., Nakao, K., and Narumiya, S. (1996). ROCK-I and ROCK-II, two isoforms of Rho-associated coiled-coil forming protein serine/threonine kinase in mice. *FEBS Lett.* *392*, 189-193.
- Nicholas, K. B., and Nicholas, J. H. B. (1997). Genedoc: a tool for editing and annotating multiple sequence alignments. Distributed by the author. [Http://www.cris.com/~ketchup/genedoc.shtml](http://www.cris.com/~ketchup/genedoc.shtml).
- Nobes, C. D., Hawkins, P., Stephens, L., and Hall, A. (1995). Activation of the small GTP-binding proteins rho and rac by growth factor receptors. *J. Cell Sci.* *108*, 225-233.
- Ranganathan, R., and Ross, E. M. (1997). PDZ domain proteins: Scaffolds for signaling complexes. *Curr. Biol.* *7*, R770-R773.
- Rumenapp, U., Schmidt, M., Olesch, S., Ott, S., Eichel-Streiber, C. v., and Jakobs, K. H. (1998). Tyrosine-phosphorylation-dependent and Rho-protein-mediated control of cellular phosphatidylinositol 4,5-bisphosphate levels. *Biochem. J.* *334*, 625-631.
- Saras, J., Claesson Welsh, L., Heldin, C. H., and Gonez, L. J. (1994). Cloning and characterization of PTPL1, a protein tyrosine phosphatase with similarities to cytoskeletal-associated proteins. *J. Biol. Chem.* *269*, 24082-24089.
- Saras, J., Franzen, P., Aspenstrom, P., Hellman, U., Gonez, L. J., and Heldin, C. (1997). A novel GTPase-activating protein for Rho interacts with a PDZ domain of the protein-tyrosine phosphatase PTPL1. *J. Biol. Chem.* *272*, 24333-24338.
- Saras, J., and Heldin, C.-H. (1996). PDZ domains bind carboxy-terminal sequences of target proteins. *Trends Biochem. Sci.* *21*, 455-458.
- Sato, T., Irie, S., Kitada, S., and Reed, J. C. (1995). FAP-1: a protein tyrosine phosphatase that associates with Fas. *Science* *268*, 411-415.
- Seckl, M., Morii, N., Narumiya, S., and Rozengurt, E. (1995). Guanosine 5'-3-O-(thio)triphosphate stimulates tyrosine phosphorylation of p125FAK and paxillin in permeabilized Swiss 3T3 cells. Role of p21rho. *J. Biol. Chem.* *270*, 6984-6990.
- Shaw, R. J., Henry, M., Solomon, F., and Jacks, T. (1998). RhoA-dependent phosphorylation and relocalization of ERM proteins into apical membrane/actin protrusions in fibroblasts. *Mol. Biol. Cell* *9*, 403-419.
- Sheng, M. (1996). PDZs and receptor/channel clustering: rounding up the latest suspects. *Neuron* *17*, 575-578.
- Shibasaki, Y., Ishihara, H., Kizuki, N., Asano, T., Oka, Y., and Yazaki, Y. (1997). Massive actin polymerization induced by phosphatidylinositol-4-phosphate 5-kinase in vivo. *J. Biol. Chem.* *272*, 7578-7581.
- Songyang, Z., Fanning, A. S., Fu, C., Xu, J., Marfatia, S. M., Chishti, A. H., Crompton, A., Chan, A. C., Anderson, J. M., and Cantley, L. C. (1997). Recognition of unique carboxyl-terminal motifs by distinct PDZ domains. *Science* *275*, 73-77.
- Turner, M., Mee, P. J., Walters, A. E., Quinn, M. E., Mellor, A. L., Zamoyska, R., and Tybulewicz, V. L. (1997). A requirement for the Rho-family GTP exchange factor Vav in positive and negative selection of thymocytes. *Immunity* *7*, 451-460.
- Verde, F., Wiley, D. J., and Nurse, P. (1998). Fission yeast orb6, a ser/thr protein kinase related to mammalian rho kinase and myotonic dystrophy kinase, is required for maintenance of cell polarity and coordinates cell morphogenesis with the cell cycle. *Proc. Natl. Acad. Sci. USA* *95*, 7526-7531.
- Watson, K. L. (1995). *Drosophila* WARTS - tumor suppressor and member of the myotonic dystrophy protein kinase family. *Bioessay* *17*, 673-676.
- Wilson, R., Ainscough, R., Anderson, K., Baynes, C., Berks, M., Bonfield, J., Burton, J., Connell, M., Copsey, T., Cooper, J., Coulson, A., Craxton, M., Dear, S., Du, Z., Durbin, R., Favello, A., Fulton, L., Gardner, A., Green, P., Hawkins, T., Hillier, L., Jier, M., Johnston, L., Jones, M., Kershaw, J., Kirsten, J., Laister, N., Latreille, P., J., L., Lloyd, C., McMurray, A., Mortimore, B., O'Callaghan, M., Parsons, J., Percy, C., Rifken, L., Roopra, A., Saunders, D., Shownkeen, R., Smaldon, N., Smith, A., Sonhammer, E., Staden, R., Sulston, J., Thierry-Mieg, J., Thomas, K.,

- Vaudin, M., Vaughan, K., Waterston, R., Watson, A., Weinstock, L., Wilkinson-Sproat, J., and Wohldman, P. (1994). 2.2 Mb of contiguous nucleotide sequence from chromosome III of *C.elegans*. *Nature* *368*, 32-38.
- Wissmann, A., Ingles, J., McGhee, J. D., and Mains, P. E. (1997). *Caenorhabditis elegans* LET-502 is related to Rho-binding kinases and human myotonic dystrophy kinase and interacts genetically with a homolog of the regulatory subunit of smooth muscle myosine phosphatase to affect cell shape. *Genes Dev.* *11*, 409-422.
- Woods, D. F., and Bryant, P. J. (1991). The discs-large tumor suppressor gene of *Drosophila* encodes a guanylate kinase homolog localized at septate junctions. *Cell* *66*, 451-464.
- Xia, H., Winokur, S. T., Kuo, W.-L., Altherr, M. R., and Brecht, D. S. (1997). Actinin-associated LIM Protein: Identification of a Domain Interaction between PDZ and Spectrin-like Repeat Motifs. *J. Cell Biol.* *139*, 507-515.
- Xu, T., Wang, W., Zhang, S., Stewart, R. A., and Yu, W. (1995). Identifying tumor suppressors in genetic mosaics: the *Drosophila* *lats* gene encodes a putative protein kinase. *Dev.* *121*, 1053-1063.
- Yarden, O., Plamann, M., Ebbole, D. J., and Yanofsky, C. (1992). *cot-1*, a gene required for hyphal elongation in *Neurospora crassa*, encodes a protein kinase. *EMBO J.* *11*, 2159-2166.

Chapter 8

The PTP-BL multiprotein complex: All actin' together?

- model and future outlook -

The PTP-BL multiprotein complex: All actin' together?

- model and future outlook -

Edwin Cuppen

*Department of Cell Biology, Institute of Cellular Signalling, University of Nijmegen,
Adelbertusplein 1, 6525 EK Nijmegen, The Netherlands.*

From the data presented in the preceding chapters we can now provide a provisional picture of the microenvironment where the protein tyrosine phosphatase PTP-BL is active. The highly restricted subcellular localization of PTP-BL combined with the properties of the proteins that interact with its PDZ domains point to a role in the submembranous microfilament-based cytoarchitecture, and/or the structural dynamics thereof. PTP-BL is most prominently expressed in polarized epithelia, where it is located almost exclusively at the apical side of the cell (Hendriks et al., 1995, and Chapter 4) due to targeting properties that reside within its FERM domain (Chapter 2). The presence of five PDZ motifs enable PTP-BL to function as a scaffold protein and organize submembranous multi-protein complexes. In the previous chapters several PTP-BL associating proteins have been discussed, namely the LIM domain-containing (adaptor-like) proteins RIL and ZRP-1, the mouse homologue of the *Drosophila* tumor suppressor Warts and member of the Rho-kinase family, mWTS and a GTPase activating protein with high activity towards Rho, PARG1 (reported by Saras et al., 1997). Most recently, we identified the proteoglycan syndecan-4 as a binding partner for the third PDZ motif in PTP-BL (E.C., unpublished observations).

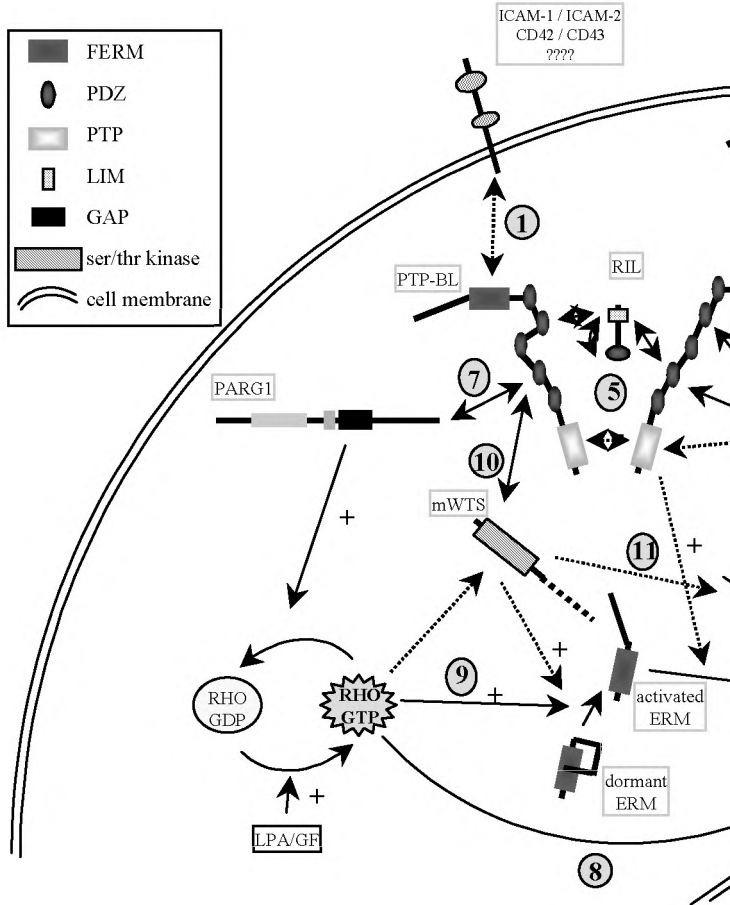
Although these associations form strong indirect evidence for a scaffolding function for PTP-BL, it remains speculative until now whether the protein forms indeed a core element in a multi-protein complex and also the function of such a complex remains elusive. Nevertheless, based upon our findings and data from the literature describing proteins with similar domains, we can propose a working model for PTP-BL function as shown in Fig. 1 (numbers between parentheses in text below refer to the numbers in this figure).

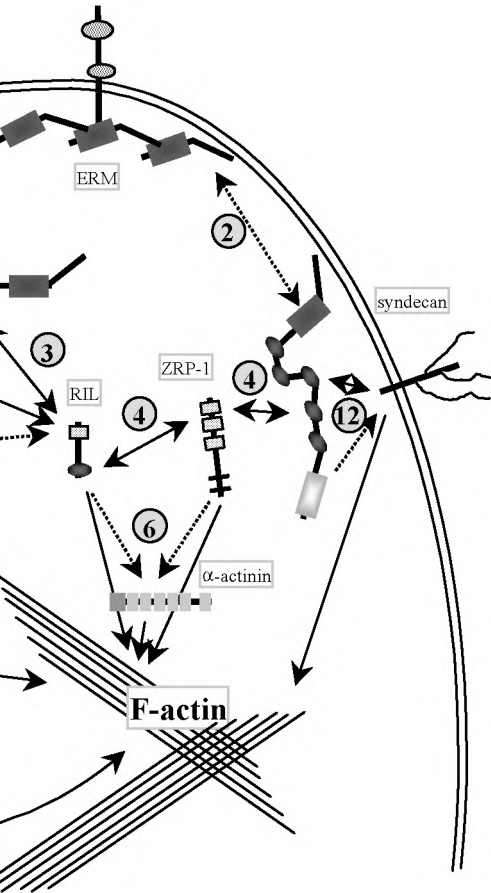
The FERM domain in PTP-BL targets the protein to its restricted subcellular microdomain, the apical submembranous region, by an unknown but dynamic mechanism. Thus far, no proteins have been identified that interact with the FERM domain and also our own efforts to identify such proteins by two-hybrid screenings remained unsuccessful. It is however, tempting to speculate that analogous to other members of the FERM protein family, this

domain may interact with transmembrane proteins like ICAM-1, ICAM-2, CD42 or CD43, or other as yet unidentified apical transmembrane proteins (1). Alternatively, the FERM domain of PTP-BL may participate in concatemerization as has been described for the actin-binding ERM proteins (2). Although we found no evidence for an interaction of the FERM domain of PTP-BL with ezrin in transfected MDCK cells, it is quite well possible that this domain may interact with other known or unknown members of the ERM subfamily, like radixin, moesin or merlin.

The PDZ motifs in PTP-BL form the most clearcut example of domains that can function as anchoring sites for various proteins. Motifs II and IV interact strongly with the LIM domain containing proteins RIL (3) and ZRP-1 (4). In turn, these proteins may function as adapter proteins, as they can mediate additional interactions via their LIM and PDZ domains. Also, the proline-rich N-terminus of ZRP-1 may recruit SH3, WW/WWP or EVH1 domain-containing proteins into a larger complex. In addition, RIL potentially is involved in regulating di- or multi-merization of PTP-BL by forming inter- and intra-molecular interactions. Interestingly, this may result in dimerization of the catalytic phosphatase domain of PTP-BL, which by itself can engage in a weak but specific homotypic interaction in a two-hybrid assay (5). It is of note here that ligand-induced dimerization has been demonstrated to regulate catalytic activity for some transmembrane PTPs, thus RIL-induced dimerization may reflect such a mechanism for PTP-BL. Moreover it is important to emphasize that RIL can exist in a tyrosine phosphorylated state and thus may represent a genuine substrate for PTP-BL. If true, this would add regulatory potential to the multimerization processes involving both proteins.

Both RIL and ZRP-1 colocalize with actin-rich structures suggesting a direct or indirect interaction with F-actin (6). Analogous to the situation for their closest homologues ALP-1 (Xia et al., 1997) and zyxin (Crawford et al., 1992), this may be mediated via an interaction with the actin crosslinking protein α -actinin. The observation of binding of PTP-BL to PARG1 and mWTS, further substantiates the relationship between PTP-BL and the actin cytoskeleton. The 150 kDa PARG1 protein (7) contains a GTPase-activating protein (GAP) domain as found in several proteins that modulate the action of Rho-like GTPases. In vitro, PARG1 displays strong GAP activity on Rho, and to a lesser extent on Rac and Cdc42 (Saras et al., 1997). Rho family members are well known effectors for remodeling of the actin cytoskeleton (8). Moreover, Rho also regulates the activation of dormant ERM family members (9). For example, ezrin is activated by phosphorylation on both tyrosine and serine residues and subsequently relocates to the apical plasma membrane where it forms concatamers and binds certain transmembrane proteins and F-actin. Several serine/threonine kinases that act downstream of Rho and that are implicated in such processes have been identified (Hall, 1998; Tapon and Hall, 1997). Most interestingly, mWTS (10) is a close relative of this Rho kinase family. Absence of WTS in *Drosophila*





causes apical hypertrophy in imaginal disc epithelial cells (Justice et al., 1995), indeed suggesting an important role in apical cytoskeleton remodeling and morphogenesis. Thus, although Rho-dependence and substrate specificity for mWTS still have to be demonstrated, there is the contention that the scaffolding function of PTP-BL may result in the recruitment of a potential Rho effector and a Rho inactivating component in the same complex, providing an intriguing example of 'hard-wiring' or 'channeling' of a signaling circuitry.

Another interesting observation concerns the rapid tyrosine dephosphorylation of ezrin, following translocation of this membrane-cytoskeletal linker protein to the apical membrane (Berryman et al., 1995). Since PTP-BL is localized in the same micro-compartment, it may be that its phosphatase activity mediates this process (11). Syndecans, the binding partner for the third PTP-BL PDZ motif, may also play a role as they can function as coreceptors for tyrosine kinases and are implicated in cell adhesion (Couchman and Woods, 1996; Woods and Couchman, 1998). Their highly conserved cytoplasmic domain is phosphorylated on tyrosines, binds PIP2 and PKC, and interacts with the actin cytoskeleton (12), potentially via the PDZ-containing CASK/LIN-2 protein, or via protein 4.1. By extrapolating these observations, one may conclude that phosphorylation on tyrosine residues is a necessary event promoting mobility and translocation of proteins in the submembranous cell cortex. Their relocation is stopped and properties are changed by dephosphorylation once they reach their ultimate destination, in a highly specific microdomain. Indeed, the importance of reversible tyrosine phosphorylation in remodeling of cellular structures, like for example cell-cell and cell-substratum contacts, is convincingly demonstrated in many studies using PTK and PTP inhibitors.

Taken together, our findings and those of others suggest that PTP-BL may be important for shaping the apical microenvironment, by recruiting proteins that interact directly or indirectly with filamentous actin, like RIL, ZRP-1 and syndecan-4, and/or remodel the actin-based cytoskeleton, like mWTS and PARG1. Although many oncogenic and tumor suppressor proteins have been found to participate in (sub)membranous signaling and cytoskeletal organization, there is no direct indication that PTP-BL itself functions as a classical tumor suppressor, as might be suspected based on its structural similarities (see Chapter 1 of this thesis). Rather, remodeling of the apical compartment may be crucial for developmental processes and dynamic events during tissue homeostasis at the adult stage. Surprisingly, mice lacking the complete catalytic domain of PTP-BL do not show obvious

Figure 1: (facing page) Working model for PTP-BL function. Structural and functional connections between the potential multi-protein complex coordinated by PTP-BL and the actin-based cytoskeleton are outlined schematically. For detailed explanation see text. Solid and dashed arrows indicate proven and hypothetical interactions or links, respectively.

phenotypic consequences; they develop normal, are fertile and do not (yet) develop tumors (Thomas et al., 1998; D.G. Wansink, personal communication). From this unanticipated feature, one may conclude that PTP-BL function is redundant, or that cellular plasticity allows alternative scenarios to compensate the loss of PTP-BL activity. This model is, however, somewhat in contrast to our finding that it is impossible to obtain epithelial cell lines that overexpress functional PTP-BL, or to generate cell lines stably expressing catalytic mutants (Chapter 2). Perhaps, the apparent discrepancy in biological effects that catalytic PTP-BL (point)mutants and a deletion mutation, involving the complete catalytic domain as well as the last four PDZ motifs of PTP-BL (Thomas et al., 1998), have on normal cell survival, may be caused by the ability of the point mutants to 'trap' its normal tyrosine-phosphorylated substrate (Flint et al., 1997). Trapping of substrates thus prohibits these proteins to participate in cellular processes and protects them from dephosphorylation by other PTPs, whereas absence of the complete catalytic segment of PTP-BL may still enable the substrate to interact with other (apical) PTPs. Different gene lesions may thus be categorized as (dominant negative) gain-of-function or loss-of-function mutations, respectively.

Future experiments should address the potential value of the proposed (hypothetical) structural and functional arrangement(s), and test the involvement of PTP-BL in apical processes as diverse as phagocytosis, pathogen entry, and synapse formation. Once an appropriate read-out has been found for PTP-BL function, the role for the different associated proteins can subsequently be tested using interaction defective or catalytically inactive mutants. The scheme proposed here can be considered a working model that may help in directing future experiments aimed at the biological significance of the PTP-BL-containing multi-protein complex.

References

- Berryman, M., Gary, R., and Bretscher, A. (1995). Ezrin oligomers are major cytoskeletal components of placental microvilli: a proposal for their involvement in cortical morphogenesis. *J. Cell Biol.* *131*, 1231-1242.
- Couchman, J. R., and Woods, A. (1996). Syndecans, signaling, and cell adhesion. *J. Cell. Biochem.* *61*, 578-584.
- Crawford, A. W., Michelsen, J. W., and Beckerle, M. C. (1992). An interaction between zyxin and actinin. *J. Cell Biol.* *116*, 1381-1393.
- Flint, A. J., Tiganis, T., Barford, D., and Tonks, N. K. (1997). Development of substrate trapping mutants to identify physiological substrates of protein tyrosine phosphatases. *Proc. Natl. Acad. Sci. USA* *94*, 1680-1685.
- Hall, A. (1998). Rho GTPases and the Actin Cytoskeleton. *Science* *279*, 509-514.
- Hendriks, W., Schepens, J., Bachner, D., Rijss, J., Zeeuwen, P., Zechner, U., Hameister, H., and Wieringa, B. (1995). Molecular cloning of a mouse epithelial protein-tyrosine phosphatase with similarities to submembranous proteins. *J. Cell. Biochem.* *59*, 418-430.
- Justice, R. W., Zilian, O., Woods, D. F., Noll, M., and Bryant, P. J. (1995). The *Drosophila* tumor

The PTP-BL multiprotein complex: All actin' together?

- suppressor gene warts encodes a homolog of human myotonic dystrophy kinase and is required for the control of cell shape and proliferation. *Genes Dev.* *9*, 534-546.
- Saras, J., Franzen, P., Aspenstrom, P., Hellman, U., Gonez, L. J., and Heldin, C. (1997). A novel GTPase-activating protein for Rho interacts with a PDZ domain of the protein-tyrosine phosphatase PTPL1. *J. Biol. Chem.* *272*, 24333-24338.
- Tapon, N., and Hall, A. (1997). Rho, Rac and Cdc42 GTPases regulate the organization of the actin cytoskeleton. *Curr. Opin. Cell Biol.* *9*, 86-92.
- Thomas, T., Voss, A. K., and Gruss, P. (1998). Distribution of a murine protein tyrosine phosphatase BL-beta-galactosidase fusion protein suggests a role in neurite outgrowth. *Dev. Dynamics* *212*, 250-257.
- Woods, A., and Couchman, J. R. (1998). Syndecans: Synergistic activators of cell adhesion. *Trends in Cell Biol.* *8*, 189-192.
- Xia, H., Winokur, S. T., Kuo, W.-L., Altherr, M. R., and Brecht, D. S. (1997). Actinin-associated LIM Protein: Identification of a Domain Interaction between PDZ and Spectrin-like Repeat Motifs. *J. Cell Biol.* *139*, 507-515.

Summary / Samenvatting

Summary

Phosphorylation on tyrosine residues in particular proteins is an important mechanism for signal transduction within eukaryotic cells. As such this posttranslational modification principle plays a critical role in the regulation of many cellular events, including cell proliferation, differentiation, metabolism, and cytoskeletal function. The overall cellular phosphotyrosine levels are controlled by the dynamic balance of the activities of protein tyrosine kinases (PTKs) and protein tyrosine phosphatases (PTPs). Here, we present our efforts to elucidate the biological function of one member of the family of PTPs, PTP-BL, which is predominantly expressed in epithelia. This 250 kDa cytosolic protein harbors several interesting modular protein domains that are also found in several submembranous and tumor suppressor proteins (see **Chapter 1**). To learn more about PTP-BL's function we have chosen to study the properties of its different domains and to characterize its molecular environment.

In **Chapter 2** we focus on the mechanisms that regulate PTP-BL's catalytic activity and substrate specificity. We show, by transient expression of modular protein domains of PTP-BL in epithelial MDCK cells, that presence of the FERM domain in the protein is both necessary and sufficient for its targeting to the apical side of epithelial cells. Furthermore, we describe an EGFP-based cell sorting protocol to obtain stable expressing cell pools for specific proteins, for which conventional approaches failed. Immuno-electron microscopical studies revealed that PTP-BL FERM domain-containing fusion proteins are enriched in villi and have a typical submembranous location at about 10-15 nm from the plasma membrane. In addition, fluorescence recovery after photobleaching (FRAP) experiments showed that PTP-BL confinement is based on a dynamic steady state and that complete redistribution of the protein in the cell is mediated via a cytosolic pool, rather than by lateral movement. Finally, we show that PTP-BL phosphatase domains are involved in homotypic interactions. Together with its highly restricted subcellular compartmentalization this may regulate the substrate specificity and catalytic activity of PTP-BL.

In **Chapter 3** we followed up on observations published by Sato et al. (*Science*, 1995, 268:411-415), that implicate PTP-BL as a negative regulator of Fas-mediated apoptotic signaling. Indeed, a direct interaction between the human Fas receptor C-terminus and the second PDZ motif in PTP-BL could be confirmed. However, we show that this interaction is not conserved for the mouse Fas receptor. In addition, using transfected T lymphoma cell lines we found no inhibitory effect of PTP-BL upon triggering apoptosis with mouse or human Fas-activating antibodies. Together with the markedly different tissue expression patterns for PTP-BL and Fas receptor, these findings rule out a key role for protein tyrosine phosphatase PTP-BL in the Fas-mediated death pathway.

Next, the yeast two-hybrid interaction assay was used to characterize the binding partners for the different modules in PTP-BL. Our search for proteins that can interact with the five PDZ motifs in PTP-BL led to the identification and characterization of RIL (**Chapter 4**), a small adaptor-like protein consisting of an N-terminal PDZ motif and a C-terminal LIM domain. The RIL LIM domain was found to be important for binding to the PDZ motif of RIL itself and the second and fourth PDZ motif in PTP-BL. Immunohistochemical studies revealed a submembranous colocalization of PTP-BL and RIL in epithelial cells. In addition, we found the RIL LIM domain to be phosphorylated on tyrosine *in vitro* and *in vivo*. In turn, the phosphorylated domain can be dephosphorylated *in vitro* by the PTP domain of PTP-BL. Our data point to the presence of a double PDZ-binding interface on the RIL LIM domain and suggest tyrosine phosphorylation as a regulatory mechanism for LIM-PDZ associations in the assembly of multiprotein complexes.

In **Chapter 5** we provide another example of PDZ-mediated interactions with a LIM-domain containing protein, namely zyxin-related protein-1 (ZRP-1). The second out of three LIM domains in ZRP-1 is sufficient for a strong interaction with RIL. Also an interaction with the third LIM domain is evident, provided the segment still contains its proper C-terminus. ZRP-1 also interacts with the second PDZ motif in PTP-BL. For this interaction to occur both the third LIM domain and its C-terminus are necessary. RNA expression profiles for ZRP-1, RIL and PTP-BL are overlapping, most notably in tissues of epithelial origin. Furthermore, we show that ZRP-1 can be co-precipitated with RIL and PTP-BL PDZ polypeptides and finally, using transfection experiments in epithelial cells we demonstrate a striking co-localization of ZRP-1 and RIL with F-actin structures.

In **Chapter 6** we describe a novel bromodomain-containing protein, BP75, that interacts uniquely with the first PDZ domain in PTP-BL via its C-terminal half. BP75 displays overall homology to a hypothetical protein in *C. elegans* and a putative DNA binding factor in yeast, and is ubiquitously expressed, with thymus, lung, liver, colon and spinal cord as high expression sites. Transient transfection studies show that BP75 is located mainly in the nucleus, excluding the nucleoli, but also cytoplasmic localization is evident. PTP-BL, on the contrary, is predominantly localized in the cytoplasm, although some basal nuclear staining is observed. Perhaps the molecular interaction described in this chapter reflects a mechanism of coupling submembranous signaling events and nuclear events, but additional experiments are necessary to further test this conception.

In **Chapter 7** we describe the identification and characterization of the mammalian orthologue of the *Drosophila* tumor suppressor warts, mWTS, that interacts specifically with the fourth PDZ motif in PTP-BL. The short C-terminal peptide stretch flanking the putative serine/threonine kinase domain of mWTS is sufficient for interaction, both in two-hybrid and co-immunoprecipitation experiments. Deletion of the last three residues completely abolishes any detectable interaction, clearly illustrating C-terminal peptide recognition by the fourth PDZ motif of PTP-BL. The mWTS kinase domain is highly

Summary

homologous to several cAMP dependent serine/threonine kinases, including kinases that are implicated in Rho-mediated signaling. Immunodetection of mWTS protein reveals peptides of 80 and 175 kDa and shows that mWTS, like PTP-BL, localizes predominantly to the apical side of epithelial cells.

Finally, in **Chapter 8**, all information on PTP-BL and its molecular environment that is gathered in this thesis work is presented in the context of literature data on submembranous signaling webs, and fitted into a working model. We propose that the different components that bind and surround PTP-BL may form a dynamic supramolecular assembly with a role in the (re-)modeling of the apical submembranous actin cytoskeleton.

Samenvatting

Fosforylering van tyrosine residuen in bepaalde eiwitten vormt een belangrijk mechanisme voor de overdracht van signalen in eukaryote cellen. Diverse cellulaire processen, zoals cel deling, cel differentiatie, metabolisme en cytoskeletaire functies, worden gereguleerd door middel van deze post-translationele modificatie. De totale cellulaire fosfotyrosine niveau's worden gecontroleerd door de dynamische balans tussen de activiteiten van proteïne tyrosine kinases (PTKs) en proteïne tyrosine fosfatases (PTPs). In dit proefschrift presenteren we onze inspanningen om de biologische functie van een lid van de familie van PTPs, PTP-BL, op te helderen. PTP-BL komt voornamelijk tot expressie in epitheliale celtypes en het ongeveer 250 kDa grote cytosolische eiwit bevat verschillende interessante modulaire eiwit domeinen, die ook voorkomen in diverse submembrane eiwitten en tumor suppressoren (zie **Hoofdstuk 1**). Om meer te weten te komen over de functie van PTP-BL is er voor gekozen om de eigenschappen van deze modulaire domeinen te bestuderen en om de moleculaire omgeving van het eiwit in kaart te brengen.

In **Hoofdstuk 2** focuseren we op het mechanisme dat de katalytische activiteit en substraat specificiteit van PTP-BL bepaalt. Door de verschillende modulaire eiwitdomeinen van PTP-BL transiënt tot expressie te brengen in gekweekte cellen van epitheliale oorsprong (MDCK), laten we zien dat aanwezigheid van het FERM domein in het eiwit zowel noodzakelijk als voldoende is voor het bepalen van de specifieke subcellulaire lokalisatie aan de apicale kant van epitheliale cellen. Verder beschrijven we een cel-sorteringsmethode voor het genereren van celpopulaties, die een bepaald eiwit stabiel tot expressie brengen. Deze methode is gebaseerd op het gebruik van eiwitten die gefuseerd zijn met het 'Green-Fluorescent-Protein' (EGFP) en kan als alternatief dienen indien conventionele benaderingen falen. Immuno-electronen microscopie op stabiel expreserende MDCK cellen, die met behulp van deze methode zijn verkregen, laten zien dat fusie-eiwitten welke het FERM domein van PTP-BL bevatten, zich op een afstand van ongeveer 10 tot 15 nanometer van de plasma membraan bevinden en verrijkt aanwezig zijn in de villi. Door middel van 'Fluorescence Recovery After Photobleaching' (FRAP) experimenten laten we zien dat deze specifieke subcellulaire lokalisatie dynamisch is en dat complete redistributie van PTP-BL in levende cellen plaatsvindt binnen 20 tot 30 minuten. Onze waarnemingen suggereren dat deze redistributie wordt gemedieerd via een cytosolische pool en niet door laterale beweging. Tenslotte laten we zien dat het katalytische fosfatase domein van PTP-BL een homotypische interactie kan aangaan. Samen met de zeer specifieke compartimentalizing van het eiwit, zou dit het mechanisme kunnen vormen dat de substraatspecificiteit en de katalytische activiteit van PTP-BL bepaalt.

In **Hoofdstuk 3** beschrijven we de experimenten die we uitgevoerd hebben naar aanleiding van observaties gedaan door Sato et al. (Science, 1995, 268:411-415), welke een rol voor PTP-BL impliceren als negatieve regulator van Fas-gemedieerde apoptose (gereguleerde cel dood). Hoewel we de directe interactie tussen de humane Fas receptor en het tweede PDZ motief in PTP-BL kunnen bevestigen, blijkt dat deze interactie niet geconserveerd is voor de muizen Fas receptor. Verder laten we zien dat overexpressie van PTP-BL in T-lymphoma cellijnen geen inhibiterend effect heeft op apoptose via de muizen of humane Fas receptor. Gecombineerd met de duidelijk verschillende weefsel expressie patronen voor PTP-BL en de Fas receptor, sluiten deze bevindingen een centrale rol voor PTP-BL in de Fas-gemedieerde celdood signalering uit.

Vervolgens hebben we de gist 'two-hybrid interaction trap' gebruikt om eiwitten te identificeren die kunnen associëren met de verschillende modules in PTP-BL. Een screening naar interacterende eiwitten met de vijf PDZ motieven van PTP-BL leidde tot de identificatie en karakterisatie van RIL (**Hoofdstuk 4**), een klein adapter eiwit dat bestaat uit een N-terminaal PDZ motief en een C-terminaal LIM domein. Het RIL LIM domein is belangrijk voor associatie met het PDZ motief van RIL zelf en met het tweede en vierde PDZ motief in PTP-BL. Immunohistochemie laat zien dat zowel PTP-BL als RIL submembraan gelokaliseerd zijn in epithelia. Verder laten we zien dat het RIL LIM domein gefosforyleerd kan worden op tyrosines, zowel in vitro als in vivo en dat het fosfatase domein van PTP-BL het gefosforyleerde domein kan defosforyleren in vitro. Onze waarnemingen geven indicaties dat er een dubbele PDZ-bindende interface is op het RIL LIM domein en suggereren dat tyrosine fosforylering een rol kan spelen in de regulering van LIM-PDZ gemedieerde interacties bij de opbouw van multi-eiwit complexen.

In **Hoofdstuk 5** beschrijven we een ander voorbeeld van PDZ-gemedieerde interacties met een LIM-domein bevattend eiwit, genaamd ZRP-1 (zyxin-related protein-1). Het tweede van de drie LIM domeinen in ZRP-1 is voldoende voor een sterke interactie met RIL. Ook het derde LIM domein interacteert met RIL, echter alleen als de normale C-terminus volledig aanwezig is. Hetzelfde domein in ZRP-1 kan ook interacteren met het tweede PDZ motief van PTP-BL. RNA expressieprofielen voor ZRP-1, RIL en PTP-BL laten zien dat er overlap is in expressie, met name in weefsels van epitheliale oorsprong. Verder laten we zien dat ZRP-1 gecoprecipiteerd kan worden met PDZ-bevattende segmenten van RIL en PTP-BL en dat ZRP-1 en RIL colocaliseren met F-actine-rijke structuren in epitheliale cellen.

In **Hoofdstuk 6** beschrijven we een nieuw bromodomein-bevattend eiwit, BP75, waarvan de C-terminale helft exclusief interacteert met het eerste PDZ motief van PTP-BL. BP75 is over de volledige lengte homoloog aan een hypothetisch eiwit van *C.elegans* en bevat verdere enkele domeinen, die homoloog zijn aan een mogelijk DNA bindende factor uit gist. BP75 komt in vele weefsels voor, met hoge expressie niveaus in thymus, long, lever, darm en ruggenmerg. Transiënte expressie studies laten zien dat BP75 voornamelijk in de

celkern is gelokaliseerd, met uitzondering van de nucleoli, hoewel ook cytoplasmatische lokalisatie kan worden waargenomen. In tegenstelling hiermee wordt PTP-BL met name in het cytoplasma terug gevonden, met slechts een zeer lage expressie in de celkern. Mogelijk reflecteert de hier beschreven moleculaire interactie een mechanisme dat submembrane signaaltransductie koppelt met nucleaire gebeurtenissen, echter additionele experimenten zijn noodzakelijk om dit concept verder te testen.

In **Hoofdstuk 7** beschrijven we de identificatie en karakterisatie van de vertebrate ortholoog van de *Drosophila* tumor suppressor warts, mWTS, welke specifiek interacteert met het vierde PDZ motief van PTP-BL. Het korte C-terminale peptide dat flankiert aan het voorspelde serine/threonine kinase domein van mWTS, is voldoende voor een sterke interactie, zowel in two-hybrid als co-immunoprecipitatie experimenten. Deze interactie kan volledig ongedaan gemaakt worden door deletie van de laatste drie aminozuur residuen van mWTS, hetgeen duidelijk een PDZ-gemedieerde interactie met een C-terminaal peptide illustreert. Het kinase domein van mWTS is sterk homoloog aan verschillende cAMP-afhankelijke serine/threonine kinases, inclusief kinases welke betrokken zijn bij Rho-gemedieerde signaaltransductie. Immunodetectie van mWTS eiwit toont peptiden van 80 en 175 kDa groot aan en immunohistochemie laat zien dat mWTS, net als PTP-BL, voornamelijk aan de apicale kant van epitheliale cellen is gelokaliseerd.

In **Hoofdstuk 8**, tenslotte, wordt alle informatie met betrekking tot PTP-BL en haar moleculaire omgeving, welke beschreven is in dit proefschrift, geplaatst in de context van data uit de literatuur en samengevat in een hypothetisch werkmodel. Hierin stellen we voor dat de verschillende componenten die PTP-BL binden en omgeven een dynamisch multi-eiwit complex vormen dat betrokken is bij het (re-) modelleren van het apicale submembrane actine-cytoskelet.

Acknowledgments

*I would like to express my gratitude to all
who have contributed to this thesis.*

Curriculum vitae

De schrijver van dit proefschrift werd geboren op 11 augustus 1970 te Boxmeer. In 1988 behaalde hij het VWO diploma aan het Merletcollege te Cuijk, waarna hij aan de studie Moleculaire Wetenschappen aan de Landbouw Universiteit Wageningen begon. Na de propaedeuse (1989) liep hij tijdens de doctoraal fase stages bij de vakgroep Moleculaire Biologie van de Landbouw Universiteit Wageningen (Prof. Dr. A. van Kammen en Dr. P. Zabel) en de vakgroep Celbiologie en Histologie van de Katholieke Universiteit Nijmegen (Prof. Dr. B. Wieringa). Tevens vervulde hij tijdens deze periode een buitenlandse stage aan het Whitehead Institute for Biomedical Research (Prof. Dr. R. Jaenisch en Dr. P.W. Laird) dat verbonden is aan het Massachussets Institute of Technology in Cambridge, MA, USA. In augustus 1994 slaagde hij met lof voor het doctoraal examen. In september 1994 trad hij in dienst bij de afdeling Celbiologie en Histologie, Faculteit der Medische Wetenschappen van de Katholieke Universiteit Nijmegen (o.l.v. Prof. Dr. B. Wieringa) waar hij enige maanden bijgedragen heeft aan een samenwerkingsproject voor het maken van een 'knock-out' muismodel. Bij dezelfde vakgroep begon hij in januari 1995 als assistent in opleiding, onder leiding van Dr. W.J.A.J. Hendriks, met het onderzoek dat in dit proefschrift werd beschreven. Vanaf januari 1999 is hij als post-doctoraal medewerker werkzaam bij de afdeling Moleculaire Biologie (Prof. Dr. R.H.A. Plasterk) van Het Nederlands Kanker Instituut/Antoni van Leeuwenhoekziekenhuis te Amsterdam, alwaar hij onderzoek verricht naar G-eiwit gekoppelde signaal transductie in *C.elegans*.

Publications

- Schepens, J., **Cuppen, E.** and Hendriks, W. (1997). The neuronal nitric oxide synthase PDZ motif binds to -GD XV* carboxyterminal sequences. *FEBS Lett.* *409*, 53-56.
- Cuppen, E.**, Nagata, S., Wieringa, B. and Hendriks, W. (1997). No evidence for involvement of mouse protein tyrosine phosphatase-BAS-like / Fas-associated phosphatase-1 in Fas-mediated apoptosis. *J. Biol. Chem.* *272*, 30215-30220.
- Cuppen, E.**, Gerrits, H., Pepers, B., Wieringa, B. and Hendriks, W. (1998). PDZ motifs in PTP-BL and RIL bind to internal protein segments in the LIM domain protein RIL. *Mol. Biol. Cell* *9*, 671-683.
- Cuppen, E.**, Van Ham, M., Pepers, B., Wieringa, B. and Hendriks, W. Identification and molecular characterization of BP75, a novel bromodomain-containing protein. Manuscript submitted.
- Cuppen, E.**, Leeuw, A. de, Wieringa, B. and Hendriks, W. Zyxin-Related Protein-1 (ZRP-1) interacts with PDZ motifs in the adaptor protein RIL and the protein tyrosine phosphatase PTP-BL. Manuscript submitted.
- Cuppen, E.**, Wijers, M., Schepens, J., Fransen, J., Wieringa, B. and Hendriks, W. A FERM domain governs apical, villi-like, confinement of PTP-BL in apical cells. Manuscript submitted.
- Cuppen, E.**, Wieringa, B., and Hendriks, W. The mouse orthologue of the *Drosophila* tumor suppressor and Rho-kinase homologue Warts interacts with protein tyrosine phosphatase PTP-BL. Manuscript to be submitted.

